Intelligent Decision Support for Dynamic Carbon Finance Management

A thesis submitted in fulfillment of the requirements
for the degree of

Doctor of Philosophy
in
Analytics

by

Charles Z. Liu

to

School of Computer Science
Faculty of Engineering and Information Technology
University of Technology Sydney
NSW - 2007, Australia

Jan. 2025

CERTIFICATE OF ORIGINAL AUTHORSHIP

I, Charles Zhenzhong Liu, declare that this thesis is submitted in fulfilment of the requirements for the award of PhD. In Analytics, in the UTS Faculty of Engineering and IT (FEIT) at the University of Technology Sydney.

This thesis is wholly my own work unless otherwise referenced or acknowledged. In addition, I certify that all information sources and literature used are indicated in the thesis.

This document has not been submitted for qualifications at any other academic institution.

This research was supported by an Australian Government Research Training Program (RTP) Scholarship doi.org/10.82133/C42F-K220.

SIGNATURE: Production Note: Signature removed prior to publication.

Charles Z. Liu

DATE: 31st January, 2025

PLACE: Sydney, Australia

Abstract

The increasing urgency of addressing climate change and promoting sustainable development has elevated the significance of carbon finance as a critical component of environmental economics. The complexity of carbon finance is inherently linked to the multifaceted nature of carbon credits, which traverse various domains, including environmental science, economics, social dynamics, and financial systems. This doctoral research focuses on developing a comprehensive intelligent knowledge assembly decision support system aimed at facilitating the dynamic management of carbon finance within the framework of a sustainable environmental economy.

At the core of this research lie several pressing scientific problems. Firstly, the integration of disparate fields necessitates a thorough understanding of the various factors that influence decision-making processes. This raises essential questions regarding the coordination and management of these influences. For instance, how do environmental factors, market dynamics, and societal influences interact to affect carbon credit valuation and trading? A comprehensive decision-making framework must account for these variables to effectively manage carbon credits and ensure their sustainable utilization.

Secondly, the heterogeneity and complexity of data across these disciplines present substantial challenges. Establishing an effective sorting and management mechanism is critical for the successful implementation of carbon finance strategies. Here, the challenge is to discern which supporting elements are required to construct a robust decision-making apparatus that can navigate the intricacies of mixed data content and derive meaningful insights.

Furthermore, carbon credits are not static; they represent a dynamic process influenced by both environmental and financial factors. This necessitates a decision support system capable of adapting to the ongoing changes within these domains. Understanding the interactions between these heterogeneous dynamics is vital for informed decision-making, particularly in a context where rapid shifts can have significant implications for carbon management strategies.

In response to these challenges, this research delves into the systematic solution of an intelligent knowledge assembly system. This involves addressing several technological issues: How can machine learning and intelligent computing be employed to provide decision support when data is mixed? When data scarcity is a concern, what strategies can be employed to leverage existing knowledge and experience effectively? Moreover, in scenarios where computing resources are constrained, how can we ensure that high-performance computing is accessible for intelligent decision-making processes? Lastly,

how do we tackle the biases inherent in knowledge and decision-making, ensuring an objective framework that defines optimal consistency across various stakeholder perspectives?

As this research unfolds, it aims to answer these critical questions while providing a comprehensive solution that integrates diverse knowledge, experiences, and data into a coherent decision support system. This system is envisioned to serve as a technical foundation for the sustainable development of carbon finance and its dynamic management.

Through rigorous analysis, this research elucidates the intricate relationships between carbon finance and sustainable environmental economics, identifying key factors that influence decision-making across cross-disciplinary domains. It also addresses the problems of knowledge sparsity, data dispersion, and decision bias, advocating for an intelligent integration of knowledge and data that enhances decision support and reduces biases.

The findings presented herein underscore the necessity of a high-performance computing framework that accommodates the assembly of comprehensive heterogeneous knowledge, facilitating dynamic management decision support. The development of the dynamic management system with knowledge informed orchestration based machine learning and knowledge support exemplifies innovative approaches to transforming knowledge into computable models, thereby addressing the dual challenges of data scarcity and complexity.

In conclusion, this doctoral research contributes to the understanding of carbon finance dynamics and provides actionable insights for sustainable environmental economic management. By advancing the discourse on intelligent decision support systems, this work aims to promote a more integrated approach to managing carbon credits, ultimately contributing to the long-term goals of sustainable development and climate resilience.

Dedication

This thesis is dedicated with profound gratitude to Professor Zhang Ying, my principal supervisor, whose exceptional guidance, unwavering support, and insightful mentorship have been pivotal to the completion of this research. His dedication and belief in my work have been a constant source of inspiration. Sincere thanks to Associate Professor Lu Qin, Dr. Dong Wen, and Dr. Dawei Cheng for their support, constructive feedback, and contributions throughout this journey.

I would also like to express my deepest thanks to Professor Farookh Hussain for his generous support in research and development. His valuable insights, encouragement, and technical guidance have greatly enriched this work. . . .

ACKNOWLEDGMENTS

I would like to express my heartfelt gratitude to those who have supported me throughout the journey of this research. First and foremost, I am deeply thankful to Prof. Ying Zhang, Prof. Lu Qin, and Prof. Farookh Hussain. Your unwavering guidance, insightful discussions, and invaluable feedback have been instrumental in shaping my work. Your concern for my academic and personal growth has inspired me to strive for excellence.

I extend my sincere appreciation to Dr. Dong Wen, Dr. Dawei Cheng, and Dr. Zhengyi Yang for their support and discussion. Your expertise and constructive critiques have greatly enriched my research and provided me with a clearer understanding of complex concepts.

I am also grateful to Maria T. Gambino, Linda Y. Dong, and Lanlan Lee for their collaboration in industry applications and scenario discussions. Your assistance with data services and practical insights into real-world challenges have significantly enhanced the relevance of my research.

To all of you, thank you for your encouragement and for believing in my potential. Your contributions have made a lasting impact on both my academic journey and my personal development. I am truly fortunate to have had the opportunity to work with such remarkable individuals.

List of Publications

Related to the Thesis :

1. Liu, C.Z., Zhang, Y. and Qin, L., Hussain, F., 2025. Kolmogorov-Arnold Carbon Informed Network Orchestration. Applied Intelligences, 55, no. 11 (2025): 790.

2. Liu, C.Z., Zhang, Y., Qin, L. and Liu, Y., 2024. Kolmogorov-Arnold Finance-Informed Neural Network in Option Pricing. Applied Sciences, 14(24), p.11618.

3. Liu, C.Z., Hussain, F., Zhang, Y. and Qin, L., 2024. Kolmogorov-Arnold Representation Based Informed Orchestration in Solving Partial Differential Equations for Carbon Balance Sustainability. Contemporary Mathematics, pp.5036-5061.

4. Liu, C.Z., Xiang, S., Cheng, D., Liu, J., Zhang, Y. and Qin, L., 2023, August. Transformed Graph Attention for Credit Rating. In 2023 IEEE 18th Conference on Industrial Electronics and Applications (ICIEA) (pp. 1011-1016). IEEE.

5. Liu, C.Z., Cheng, D., Zhang, Y. and Qin, L., 2025, August. Adversarial Backdoor Attacks on Machine Learning with Covert False Data Injection - Part A: Modeling. In 2025 IEEE 20th Conference on Industrial Electronics and Applications (ICIEA). IEEE. DOI: 10.1109/ICIEA65512.2025.11149199

6. Liu, C.Z., Cheng D., Zhang, Y. and Qin, L., 2025, August. Adversarial Backdoor Attacks on Machine Learning with Covert False Data Injection - Part B: Tests. In 2025 IEEE 20th Conference on Industrial Electronics and Applications (ICIEA). DOI: 10.1109/ICIEA65512.2025.11149083

7. Liu, C.Z., Zhang, Y. and Qin, L., 2025, August. Adaptive Bias Fusion Using Kappa-Ordered Weight to Address Multi-Expert Disparity. In 2025 IEEE 20th Conference on Industrial Electronics and Applications (ICIEA). IEEE. DOI: 10.1109/ICIEA65512.2025.11148450

OTHERS :

8. Liu, C.Z., Deng, R., Zhang, Y. and Qin, L., 2025, August. Hadamard Conversion Representation Based Feature Impact Quantification. In 2025 IEEE 20th Conference on Industrial Electronics and Applications (ICIEA). IEEE. DOI: 10.1109/ICIEA65512.2025.11148812

TABLE OF CONTENTS

List of Figures

Figure **Page**

List of Tables

Table **Page**

CHAPTER 1

INTRODUCTION

1.1 Background

The urgency of addressing climate change and promoting sustainable development has led to the emergence of carbon finance as a pivotal element in environmental economics [84, 131, 227]. Carbon finance primarily revolves around the trading of carbon credits, which serve as a market mechanism for mitigating greenhouse gas emissions [11, 230, 246]. As nations and organizations strive to meet increasingly stringent climate targets, the significance of carbon finance is underscored by its capacity to integrate economic incentives with environmental stewardship [56, 63, 144].

The dynamic nature of carbon credits necessitates a comprehensive understanding of multiple interrelated domains [147, 231, 291]. Specifically, the intersection of environmental science, economics, social considerations, and financial systems presents a complex landscape that must be navigated effectively. This complexity gives rise to several scientific challenges that are critical to the successful management of carbon finance. For instance, decision-makers must grapple with the intricate relationships between various influencing factors, such as carbon sequestration rates, market demand, pricing mechanisms, and regulatory frameworks.

Moreover, the heterogeneity of process and data across these domains complicates the decision-making process [162, 271, 277]. The diverse sources of data and processes, involved in spatial policies, trading schemes, environmental metrics, economic indicators, and social feedbacks, often result in a mixed context that is challenging to analyze. As a

consequence, there is an urgent need for robust technical support mechanisms that can sort, integrate, and manage this information effectively. Without such frameworks, the potential for decision-making to be hindered by data dispersion and information silos increases, thereby undermining the effectiveness of carbon finance strategies.

In recognizing the dynamic interplay between environmental and financial factors, it becomes evident that carbon credit management is not a static endeavor. Rather, it involves continual adjustments and responsive strategies that account for real-time changes in both environmental conditions and market dynamics [23, 297]. Thus, decision support systems must be designed to accommodate these fluctuating dynamics while providing actionable insights that facilitate coordinated management.

Given the complexity and dynamic nature of the current carbon finance landscape, our research focuses on the development of a comprehensive Intelligent Knowledge Orchestration Decision Support System (IKODSS). The primary objective of this system is to provide an Intelligent Decision Support for Dynamic Carbon Finance Management with effective Knowledge Orchestration Machine Learning framework by systematically integrating knowledge, expertise, and data from diverse sources, thereby enhancing decision-making processes and enabling customized optimization within the carbon finance sector.

1.2 Research Issues

1.2.1 Challenges

In the course of our research, we target several key technical challenges, formulating solutions to each.

The first challenge pertains to data integration and aggregation. In the domain of carbon finance, the diversity and heterogeneity of carbon finance process and data represent a significant challenge. The central question is how to effectively integrate and implement machine learning and intelligent computing technologies to support decision-making in a mixed data environment. Addressing this issue is critical for enhancing both the accuracy and efficiency of decision-making processes.

The second challenge concerns data scarcity, particularly in situations where reliable, domain-specific data is unavailable. In such cases, the question arises as to how existing knowledge and expert experience can be leveraged to provide reliable decision support. Optimizing the utilization of available knowledge resources and applying them effectively

to the decision-making process becomes a key focus of the research in this context.

The third challenge is computational efficiency, especially in environments with limited resources. We focus on how to achieve efficient deep computation within such resource-constrained settings. Many small and medium-sized institutions in the carbon finance sector face significant constraints in terms of real-time computational resources. Therefore, it is crucial to explore how high-performance deep computing can be effectively utilized in intelligent decision-making processes under these limitations.

Finally, the issue of bias and decision consistency is a core aspect of this study. The diversity of knowledge sources, coupled with varying expert preferences and decision-maker focuses, can lead to biases in the decision-making process. To address this challenge, we investigate how to integrate differing knowledge perspectives and decision viewpoints into a coherent framework, objectively define the optimal consistency, and design a computational framework that supports unbiased intelligent decision-making, thereby ensuring fairness and rationality in the decision-making process.

Our research presents an innovative approach to intelligent decision support in carbon finance, tackling critical issues such as data integration, knowledge utilization, computational efficiency, and bias in decision-support. The proposed system offers a robust and adaptable solution for addressing the challenges faced by institutions operating in this dynamic field, with significant potential for enhancing decision-making and optimizing outcomes.

Through our research, we address these critical issues and provide a comprehensive solution that enhances decision-support capabilities in carbon finance. By integrating advanced computational techniques, we develop a framework that not only improves performance in computing but also facilitates the dynamic adaptation with knowledge orchestration and decision fusion required for effective carbon credit management.

This research aims at contributing to the sustainable development of carbon finance, fostering an environment where intelligent decision-making is at the forefront of managing environmental economic challenges. Through innovative frameworks and systematic knowledge assembly, we aim to support the long-term goals of a sustainable environmental economy, thus positioning carbon finance as a vital component in the global response to climate change.

1.2.2 Solution Framework

The research questions outlined in this study naturally map to the core technical challenges and corresponding objectives of the proposed intelligent decision support system.

1.2.2.1 Data Integration and Aggregation

The first challenge involves managing heterogeneous and multi-source carbon finance data to enable accurate and efficient decision-making. This challenge is addressed through the knowledge-informed orchestration mechanisms presented in Chapter 3. This chapter describes the integration of the Data Engine, Market Operations, and Decision Support Intelligence (DSI) with advanced feature assembly techniques under graph structures, time-series models, and dynamic mechanisms. These sections provide the methodological foundation for achieving seamless data integration and supporting system-level decision-making.

1.2.2.2 Data Scarcity

The second challenge pertains to scenarios where domain-specific data is limited or unreliable. To tackle this, we employ a multi-domain knowledge assembly strategy and expert system approach, as elaborated in Chapter 4, in which the sections describe the construction of a comprehensive knowledge base and the application of a rule engine, enabling the system to leverage prior knowledge and expert experience to provide reliable decision support, even in data-sparse environments.

1.2.2.3 Computational Efficiency

The third challenge addresses computational constraints common in small- to medium-sized carbon finance institutions. Chapter 4 introduces the Kolmogorov-Arnold Representation (KAR)-based knowledge assembly computing framework integrated with neural networks. This framework allows for efficient reasoning and learning with limited resources, enabling faster and more accurate decision-making while reducing computational overhead.

1.2.2.4 Bias and Decision Consistency

The fourth challenge focuses on mitigating the impact of diverse expert preferences and cognitive biases on decision-making. Chapter 6 presents an adaptive decision fusion framework, which uses statistical consistency mechanisms to integrate differing expert perspectives. This ensures that decision outputs maintain a high degree of rationality and fairness, even in the presence of heterogeneous opinions and conflicting priorities.

1.2.2.5 Summary

The integrated framework described in Chapters 3 - 6 not only addresses these challenges but also provides a robust platform for intelligent decision-making in carbon finance, combining data-driven computation, knowledge-informed orchestration, and adaptive bias mitigation. Each research question is directly linked to the objectives and contributions of the study. This systematic alignment of research questions, challenges, methods, and chapters clarifies the scope and impact of the contributions throughout the work.

1.3 Research Objectives

The primary objective of this study is to develop a comprehensive decision support system (DSS) that effectively manages the dynamics of carbon finance through intelligent knowledge assembly. This system is designed to address the multifaceted challenges presented by the interplay between environmental, economic, social, and financial factors in the context of carbon credits.

To achieve this overarching goal, the research will focus on the following specific objectives:

- Integration of Diverse Knowledge: To create a framework that integrates heterogeneous knowledge sources, including scientific data, economic models, and social insights, ensuring a holistic understanding of carbon finance dynamics.

- Dynamic Data Management: To develop methodologies for assembling and managing mixed data types, facilitating real-time analysis and decision-making in the face of evolving environmental and market conditions.

- Application of Advanced Computing Techniques: To leverage advanced machine learning and artificial intelligence techniques, including the KAFIN and KACINO frameworks, for transforming existing knowledge into computable models that can provide robust decision support.

- Bias Mitigation and Decision Consistency: To establish strategies for identifying and mitigating biases in decision-making processes, enabling the system to define optimal decisions based on a consistent and objective framework.

- High-Performance Computing Support: To ensure that the decision support system operates efficiently under limited computing resources, utilizing high-performance computing techniques to enhance the scalability and effectiveness of the system.

- Practical Implementation: To provide a comprehensive implementation plan for the proposed decision support system, including case studies and pilot projects that demonstrate its effectiveness in real-world scenarios related to carbon finance.

By addressing these objectives, the study aims to contribute significantly to the field of sustainable environmental economics, facilitating better decision-making in carbon finance and supporting the transition towards a more sustainable future.

1.4 Main Contributions

This research makes several significant contributions to the field of carbon finance and sustainable environmental economics. These contributions are as follows:

- Development of a Comprehensive Decision Support System: This study introduces a novel decision support system (DSS) specifically designed for the dynamic management of carbon finance. The system integrates diverse knowledge sources and data types, facilitating informed decision-making across multiple interconnected fields.

- Innovative Knowledge Assembly Framework: We propose the Knowledge Informed Orchestration with KAR (KIOKAR) framework, which effectively assembles heterogeneous knowledge, experience, and data. This framework enhances the capability to derive actionable insights and supports sustainable decision-making in carbon finance.

- Advanced Machine Learning Techniques: The research presents the KAFIN and KACINO frameworks, which transform existing knowledge into computable partial differential equation (PDE) models. These models enable dynamic analysis and decision support for carbon credit management, illustrating the potential of machine learning in this domain.

- Strategies for Bias Mitigation: This study addresses the challenge of biases in decision-making processes. By developing methodologies to identify and mitigate

such biases, the research ensures that decisions made within the framework are objective and consistent, thereby enhancing the reliability of the outcomes.

- Knowledge Orchestration Based Computing Solutions: We provide insights into achieving computing support for intelligent decision-support under constraints of limited computational resources and data. This contribution is critical for the practical implementation of the decision support system in real-world scenarios.
- Integration of Multi-Disciplinary Insights: By synthesizing knowledge from environmental science, economics, finance, and social sciences, the research establishes a holistic approach to carbon finance dynamics. This multi-disciplinary perspective enriches the analysis and enhances the robustness of the decision-making framework.
- Practical Applications and Case Studies: The research includes practical applications and case studies that demonstrate the effectiveness of the proposed system. These examples provide valuable insights into how the system can be implemented in real-world settings, showcasing its potential to support sustainable development in carbon finance.

Overall, the contributions of this research not only advance the academic understanding of carbon finance dynamics but also offer practical solutions to pressing challenges in sustainable environmental economics.

1.5 Organization of the Thesis

This thesis is structured to address the research issues, objectives, and the contributions made in the area of intelligent decision-making frameworks for carbon finance.

Chapter 1 Introduction provides an overview of the background, research issues, objectives, and the main contributions of this study. It sets the context for the entire research, outlining the importance of addressing challenges in carbon finance and the proposed innovative solutions.

Chapter 2 Literature Review presents an in-depth review of the existing body of work related to carbon finance, sustainable economics, carbon credit option finance, and decision-making challenges. It also covers the interdisciplinary influences and highlights the gaps in current methodologies, focusing on computational techniques such as deep learning and their applications in carbon finance.

Chapter 3 Integrated Carbon Dynamics Management System introduces the system for managing carbon dynamics and integrates key components like data engines, market operations, and decision support intelligence. This chapter also discusses the knowledge-informed orchestration of machine learning algorithms and time series data for supporting carbon credit management and dynamic decision-making.

Chapter 4 Comprehensive Intelligent Decision Support System with Knowledge-Informed Orchestration explores computational knowledge modeling for carbon emissions, sequestration, and credit pricing. It highlights advanced computational techniques, including Kolmogorov-Arnold Representation (KAR), to facilitate knowledge orchestration, and discusses the applications of these models in carbon finance.

Chapter 5 Graph Information Orchestration with Transformed Graph Attention Computing focuses on transformed graph attention computing methods, including feature representation and graph fusion. This chapter delves into the development and application of graph-based models to enhance decision-making in the carbon finance domain.

Chapter 6 Adaptive Fusion for Consistency to Bias Disparity addresses the challenges of bias and disparity in decision-making systems, proposing adaptive fusion techniques for optimal decision outcomes. The chapter discusses how to manage false data, cognitive bias, and consistency in machine learning models, ensuring high-quality decision support.

Chapter 7 Case Studies and Empirical Analysis presents real-world case studies and experiments, evaluating the effectiveness of the proposed technical frameworks. This chapter includes detailed results from tests and analysis on carbon dynamics, sequestration, and option pricing, as well as discussions on the application of graph-informed orchestration and the impact of adversarial attacks on decision-making.

Chapter 8 Discussion and Conclusion concludes the thesis by summarizing the research contributions and discussing the findings. It provides answers to the research questions, highlights the limitations of the study, and suggests directions for future research in the area of intelligent decision support systems for carbon finance.

CHAPTER 2

LITERATURE REVIEW

2.1 Carbon Finance and Sustainable Economics

The pervasive threat of climate change poses significant risks to both global ecosystems and human societies, necessitating the development of robust and scalable emission reduction strategies [161]. In this context, carbon credits have emerged as a fundamental instrument in mitigating the adverse impacts of greenhouse gas emissions. These tradable units, each equivalent to one metric ton of CO2 or its greenhouse gas equivalent, function within market-based frameworks to enable emission reductions at both the national and corporate levels. By providing a flexible, cost-effective mechanism, carbon credits incentivize emission reductions across diverse sectors and regions [192].

Carbon credits not only facilitate compliance with regulatory targets but also allow for the financing of projects dedicated to reducing emissions. Through these financial instruments, organizations and individuals can offset their carbon footprints by investing in emission-reducing initiatives, thus contributing to the global effort to combat climate change. Moreover, the increasing recognition of carbon credits as financial assets has expanded their role within the global market. This has opened new avenues for trading, investment, and the scaling of sustainable practices, thereby enhancing the overall efficiency and impact of carbon markets [17]. In this way, carbon credits are integral to fostering both the economic and environmental transitions needed to achieve long-term sustainability goals.

Besides the environment physics, carbon credits also possess significant financial at-

tributes that manifest in their characteristics as tradable financial assets with inherent value and liquidity [20, 60, 83, 201]. These credits can serve as hedging tools, enabling companies to manage financial risks associated with carbon emissions [56, 104, 239]. The market dynamics of carbon credits are influenced by various factors, including carbon balance, supply and demand dynamics, policy changes, and market sentiment, resulting in observable price volatility. By leveraging their financial attributes, carbon credits function as a market mechanism that effectively incentivizes emission reduction initiatives and sustainable investments, thereby advancing both environmental protection and economic development.

In this context, carbon credits can be associated with financial instruments such as options and futures, offering diversified trading strategies and investment opportunities [56, 147, 220]. Through options, companies can lock in future carbon credit prices, effectively mitigating the uncertainties associated with price fluctuations. Thus, the significance of option pricing of carbon credit becomes particularly evident, which necessitates rigorous standards and transparency in the carbon credit system concerning about verification reliability and the risk of greenwashing in terms of both the environment physics and finance dynamics [1, 53, 126].

Greenwashing refers to the practice of misleading or deceiving consumers about the environmental merits of a product, service, or corporate operations. It typically involves the manipulation of sustainability claims, either by exaggerating the positive environmental impact or fabricating such claims entirely, in an attempt to create a false narrative of environmental responsibility [205, 276]. This can take various forms, such as the use of ambiguous terminology, the presentation of unsupported claims, or the promotion of minor, superficial eco-friendly actions while simultaneously overlooking or concealing larger, more significant environmental harm [4].

The prevalence of greenwashing is particularly problematic as it undermines genuine efforts toward sustainability. It not only distorts consumer perceptions of environmental performance but also diverts attention away from companies that are genuinely making substantial efforts to reduce their ecological footprint. In addition, greenwashing can attract regulatory scrutiny, as it raises concerns about the accuracy and transparency of environmental claims within the market. As such, the potential for regulatory backlash, coupled with the erosion of consumer trust, highlights the importance of addressing this issue.

To combat greenwashing, it is imperative to establish stringent and enforceable standards that promote transparency in environmental marketing and corporate reporting.

Clear guidelines for the communication of sustainability claims, supported by independent verification and robust accountability mechanisms, are essential to ensure that consumers can make informed decisions based on reliable and accurate information [126]. By instituting such measures, the integrity of sustainability efforts can be protected, and the broader goals of environmental responsibility can be advanced.

What is more, research on carbon credit systems, particularly in the context of integrating diverse knowledge from environmental physics and financial dynamics, remains underdeveloped, especially in the application of advanced modeling and computational techniques. This gap is evident when attempting to combine the complexities of environmental physics with the intricacies of financial mechanisms in carbon credit markets.

From the environmental physics perspective, understanding the carbon balance dynamics, specifically the relationship between carbon emissions and sequestration, is crucial for the effective management and credibility of carbon credit systems [223, 274]. Accurate modeling of this relationship enhances transparency, allowing stakeholders to verify the authenticity of emission reductions by clarifying the factors influencing carbon sequestration [66, 138, 259]. Such detailed models are essential for establishing trust in carbon credits as legitimate tools for mitigating climate change.

Despite considerable progress in the development of measurement models for emissions [44, 74, 110], sequestration [61, 160, 299], and integrated carbon models [188, 275], the intricate interactions between carbon emissions and sequestration remain a significant challenge. Current models are often limited by their static nature, relying on simplified linear approaches that assume constant parameters. These assumptions fail to capture the complex, dynamic feedback mechanisms inherent in the carbon cycle, including the temporal variations and decay processes affecting both emissions and sequestration. Consequently, such models are unable to provide accurate predictions of long-term trends or assess the true effectiveness of policies intended to mitigate carbon emissions.

From a financial perspective, existing models often assume market stability; however, the carbon credit market is influenced by a myriad of complex factors, including regional environment, engineering solutions, and the effects of climate change [7, 8, 33, 270]. This complexity necessitates the development of reliable dynamic models that can accurately reflect the multifaceted impacts of these factors. For instance, option pricing for carbon credits requires a thorough evaluation of the rights associated with buying and selling these credits, encompassing both environmental dimensions (such as carbon emissions and sequestration) and financial elements (including exercise price, expiration date,

and volatility). Despite the critical need for such comprehensive assessments, current research lacks an integrated model and computational framework that consolidates diverse knowledge, standards, and experiences into a cohesive approach.

Therefore, a comprehensive understanding of the interactions between carbon credit finance and environmental factors is essential for formulating more precise policies, ensuring the achievement of emission reduction targets, and minimizing the risks of finance [185, 218, 230], however, interdisciplinary research must draw upon knowledge from environmental science, finance, and economics, though collaboration across these fields may encounter communication and methodological challenges. Although data driven solutions provide a key to carbon credit dynamics modeling and computations, data often suffers from incompleteness or a lack of standardization, quality and understanding on environment and finance, complicating the establishment and verification of models [5, 33, 257, 258].

2.2 Carbon Credit Option Finance

Carbon Credit Option Finance represents an innovative convergence of environmental sustainability and financial markets, offering a novel approach to addressing climate change through market-driven solutions [56, 147, 220]. As global recognition of climate change intensifies, carbon credits have evolved into essential instruments for reducing greenhouse gas emissions. These credits, which signify the right to emit one metric ton of carbon dioxide or its equivalent, provide a framework that aligns environmental responsibility with economic incentives. Carbon Credit Options, as a financial derivative, extend this framework by granting holders the right, without the obligation,Äîto purchase (call option) or sell (put option) carbon credits at a pre-determined price within a specified timeframe.

The pricing of these options is a critical component of their functioning, as it determines the theoretical value of the underlying carbon credits. Option pricing theory, initially developed in the context of financial derivatives, is crucial in this regard [24, 73, 166, 222]. It provides the foundation for understanding how the value of these instruments is derived based on factors such as market volatility, time to expiration, and the underlying asset's price dynamics. A rational approach to option pricing [27, 166] is essential to ensure that these financial instruments are fairly valued, allowing for the effective allocation of capital and risk.

Furthermore, sound option pricing practices facilitate robust risk management strate-

gies by enabling market participants to accurately assess potential returns and risks. By providing a transparent and methodologically sound valuation framework, these practices help prevent arbitrage opportunities, thus ensuring the stability and integrity of carbon credit markets. In turn, this supports the broader objective of integrating financial markets with environmental goals, allowing carbon credits and their associated options to become effective tools in the global effort to combat climate change.

Carbon credit option pricing represents an innovative approach to valuing carbon credits as financial derivatives, akin to traditional options. This method enables stakeholders to manage risks associated with the volatility of carbon credit prices, which is crucial given the market's susceptibility to regulatory changes and public policy shifts aimed at mitigating climate change. The recognition of carbon credits as valuable financial assets has heightened the demand for this pricing strategy, allowing organizations to better anticipate future values and hedge against potential losses.

Integrating option pricing principles into the carbon credit market fosters a resilient framework for environmental sustainability, supporting global climate efforts and promoting sustainable investments. However, the implementation of Carbon Credit Option Finance involves complexities stemming from regulatory frameworks, market dynamics, pricing mechanisms, risk assessment, and operational challenges. Regulatory changes significantly impact credit generation and trading, while market forces introduce additional volatility. Accurate pricing and effective risk management strategies are necessary, often requiring advanced modeling techniques and collaboration among stakeholders. Overall, addressing these complexities is essential for developing a responsive market that supports climate objectives and facilitates the transition to a low-carbon economy.

Carbon credit option pricing represents an innovative approach to valuing carbon credits as financial derivatives, paralleling traditional options that enable risk management against price volatility in underlying assets. This method is particularly relevant in a market shaped by regulatory changes and public policies aimed at mitigating climate change, as it allows stakeholders to manage risks associated with fluctuating carbon credit prices effectively. As carbon credits gain recognition as valuable financial assets, the demand for option pricing has surged, facilitating more accurate forecasting of their future value and enabling organizations to hedge against potential market losses. This approach not only promotes investments in sustainable practices but also enhances the precision with which companies can manage their carbon liabilities.

Furthermore, carbon credit options contribute to increased market participation by offering flexible financial instruments that optimize emissions reduction strategies. This

flexibility enhances market liquidity and encourages a proactive approach to achieving emissions reduction targets. By incorporating option pricing principles into the carbon credit market, stakeholders benefit from improved risk management and decision-making frameworks that support global climate initiatives and sustainable investments. As organizations increasingly grasp the financial ramifications of their carbon footprints, robust carbon credit options become essential for harmonizing economic incentives with environmental goals.

The complexity of Carbon Credit Option Finance arises from various interrelated factors, including regulatory frameworks, market dynamics, pricing mechanisms, risk assessment, and operational challenges. Regulatory frameworks are pivotal, as the carbon market is influenced by evolving international agreements and national policies that dictate the generation and trading of credits. Stakeholders must remain agile in response to these changes to effectively navigate credit availability and pricing.

Market dynamics further complicate the landscape, with supply and demand pressures driven by economic conditions, technological advancements, and societal attitudes toward climate change introducing volatility. Accurate modeling of these factors necessitates advanced quantitative methods that combine historical data with predictive analytics.

Additionally, the pricing mechanisms for carbon credits are intricate, influenced by regulatory compliance costs and future emission reduction targets. Traditional pricing models, such as the Black-Scholes model, often require adaptation to accommodate the unique regulatory risks and non-linear movements of the carbon market, underscoring the need for tailored approaches.

Risk assessment is crucial, as the integration of options introduces further complexities related to price volatility and regulatory shifts. Developing effective risk management strategies, such as dynamic hedging and employing advanced techniques like Monte Carlo simulations, is essential for navigating this intricate risk landscape.

Operational challenges also pose significant hurdles, necessitating reliable systems for credit verification, transaction management, and compliance monitoring. Successful implementation of Carbon Credit Option Finance demands collaboration among stakeholders, including governments, NGOs, and financial institutions, to ensure adherence to regulatory standards and the effective tracking of carbon credits.

In conclusion, the multifaceted complexity of Carbon Credit Option Finance requires innovative modeling techniques and cooperative strategies among various stakeholders to create a responsive market capable of supporting climate goals effectively. This integrated

approach is vital for advancing sustainable investment strategies and facilitating the transition to a low-carbon economy.

2.3 Interdisciplinary Influences and Challenges

Carbon credits serve as vital financial instruments in the global effort to reduce greenhouse gas emissions. By enhancing trading capabilities and investment opportunities, carbon credits promote sustainable practices [17]. Their financial attributes as tradable assets contribute significantly to their value and liquidity [20, 60, 83, 201]. Companies can utilize these credits as hedging tools, effectively managing financial risks associated with carbon emissions [56, 104, 239].

Market dynamics affecting carbon credits are influenced by various factors, including carbon balance, supply and demand, policy shifts, and market sentiment. This complexity leads to observable price volatility, wherein carbon credits incentivize emission reduction initiatives and sustainable investments, supporting both environmental protection and economic growth. Furthermore, carbon credits can be associated with financial derivatives such as options and futures, enabling diversified trading strategies [56, 147, 220]. This integration improves liquidity and transparency within the carbon market, facilitating better risk assessment and management.

However, the success of carbon credit systems relies heavily on stringent standards and transparency to combat greenwashing and ensure the credibility of these credits [1, 53, 126]. Despite these advancements, research on carbon credits remains limited, particularly regarding modeling and computational methodologies that integrate environmental physics with financial dynamics.

From an environmental physics perspective, understanding carbon balance, the relationship between emissions and sequestration, is critical for effective management of carbon credits [223, 274]. Enhanced transparency regarding factors influencing carbon sequestration is essential for verifying legitimate emission reductions [66, 138, 259]. Although substantial efforts have been made to develop robust models for emissions [44, 74, 110] and sequestration [61, 160, 299], existing models often remain static and linear, failing to account for the dynamic interactions between emissions and sequestration, as well as the temporal variations involved. This static approach limits the ability to predict long-term trends and the effectiveness of related policies.

From a financial standpoint, current models typically assume market stability; yet the carbon credit market is subject to various complex influences, including regional

environmental conditions and the broader impacts of climate change [7, 8, 33, 270]. Consequently, there is a pressing need for dynamic models that accurately reflect these multifaceted influences. For instance, option pricing of carbon credits necessitates a comprehensive evaluation of associated rights and financial parameters, yet current research lacks an integrated framework that synthesizes diverse knowledge across environmental science and finance.

A thorough understanding of the interplay between financial factors and environmental dynamics is essential for developing precise policies aimed at achieving emission reduction targets while mitigating financial risks [185, 218, 230]. Interdisciplinary collaboration is vital; however, it often faces challenges in communication and methodology. Data-driven solutions are pivotal for modeling carbon credit dynamics; however, data integrity issues, including incompleteness and lack of standardization, complicate model establishment and verification [5, 33, 257, 258].

Moreover, interpretability remains a significant challenge in data-driven modeling, particularly with advanced machine learning approaches often characterized as "black boxes." This opacity undermines trust and understanding, especially in critical domains like carbon credit finance [7, 100, 176]. Although methods such as LIME and SHAP exist to enhance interpretability [40, 137, 152, 203], their effectiveness can vary and may fail to provide comprehensive insights. Additionally, data biases pose risks of unfair outcomes, and the lack of transparency complicates the identification of these biases [89, 234, 281, 287]. Regulators in carbon finance emphasize the importance of transparency and adherence to compliance standards, asserting that models lacking interpretability will not meet industry requirements [10, 55, 243]. Thus, limitations in interpretability, credibility, and reliability impede broader acceptance of these methodologies within the industry.

To address the multifaceted challenges associated with carbon credit management, we propose an integrated knowledge management framework that encompasses diverse objectives, including environmental, financial, socio-economic, and health considerations. The theoretical foundations and mechanisms of this integrated knowledge system management play a pivotal role in the interplay between carbon credits, comprehensive environmental governance, and human socio-economic development. This framework is designed to mitigate the fragmentation and complexity inherent in local knowledge, thereby fostering interdisciplinary collaboration and integration. As a result, it enhances the scientific rigor and efficacy of policy formulation and implementation. By improving the understanding of interactions among various physical, financial, and related

dynamics tied to carbon credits, the framework aims to bolster the reliability of forecasts.

Leveraging knowledge from diverse fields is essential for strengthening the carbon credit system and refining modeling efforts that account for carbon balance. This is not only critical for enhancing economic efficiency but also for effectively addressing climate change and promoting environmental protection. A comprehensive understanding of carbon dynamics will ultimately reinforce the role of carbon credits in advancing global sustainable development objectives. In this context, the integrated knowledge management framework serves as a tool to synthesize various knowledge domains, facilitating a holistic understanding of the interactions among ecosystems, human activities, and economic systems. By promoting interdisciplinary approaches, this framework can significantly improve the formulation and implementation of policies that effectively govern carbon credits within the broader context of environmental sustainability. This article explores the interconnectedness of carbon credits, environmental science, and human society, focusing on the significance of integrated dynamic knowledge system management in total environmental contexts.

2.4 Computing on Intricate Carbon Dynamics

The complex interactions between carbon emissions and sequestration present significant challenges in developing a unified, comprehensive model for carbon cycle dynamics. Despite substantial advancements in the development of measurement models for emissions [44, 74, 110] and sequestration [61, 160, 299], as well as integrated models that attempt to capture the entire carbon exchange process [188, 275], existing approaches remain inadequate in addressing the dynamic nature of these processes. The majority of current models rely on static, linear methodologies that assume constant rates of emission and sequestration, which fails to account for the nonlinear and evolving interactions between these two processes. These models typically neglect the essential physical laws that govern carbon dynamics, such as feedback loops, temporal variations, and the decay characteristics of emissions and sequestration. As a result, predictions made by these models often fall short in accurately forecasting long-term trends or assessing the effectiveness of policies designed to mitigate carbon emissions.

In response to these limitations, the Physical Information Neural Network (PINN) represents a promising alternative for improving the modeling of carbon emissions and sequestration. By embedding physical laws directly into the neural network training process, PINNs ensure greater consistency with established scientific principles, which

enhances the model accuracy and reliability [190]. This approach is particularly valuable when dealing with complex, multi-physics interactions or nonlinear phenomena, as it enables the integration of boundary and initial conditions, critical for capturing the full range of dynamics involved in carbon exchange systems [117]. Moreover, PINNs are less reliant on large datasets compared to traditional models, as they can effectively generate accurate predictions even in the absence of extensive empirical data. This capacity for handling sparse data makes PINNs an attractive tool for improving the understanding and prediction of carbon cycles, and by extension, advancing the development of more effective carbon management strategies.

Physics-Informed Neural Networks (PINNs) offer a significant advancement over traditional numerical methods, particularly in terms of computational efficiency and model interpretability. By incorporating physical laws directly into the neural network architecture, PINNs ensure that their predictions remain consistent with fundamental physical principles, thereby enhancing the reliability and accuracy of the model's outputs [190]. This integration of physical knowledge not only preserves the statistical integrity of the model but also guarantees its physical relevance, making PINNs an invaluable tool for solving complex, real-world problems that require a deep understanding of the underlying physical phenomena [117].

In contrast, traditional numerical techniques, such as the finite element method (FEM)[64, 79, 212] and spectral methods[92, 285], have been widely used to solve partial differential equations (PDEs) with considerable success. These methods, while well-established, face significant challenges in addressing high-dimensional problems. One of the most prominent of these challenges is the "curse of dimensionality"[111, 124], where the computational cost increases exponentially as the number of dimensions in the problem grows. For complex applications that require solving high-dimensional PDEs, conventional numerical methods demand enormous computational resources and large mesh sizes, which can quickly escalate into computationally prohibitive tasks[105, 128].

On the other hand, PINNs leverage the flexibility of neural networks, which are inherently capable of approximating high-dimensional functions efficiently [87]. This ability allows PINNs to handle complex high-dimensional problems with relatively lower increases in computational cost compared to traditional methods [88]. The efficiency of PINNs in managing high-dimensional spaces without the need for extensive computational resources offers a compelling advantage in fields requiring real-time or large-scale simulations. By reducing the reliance on massive computational grids and overcoming the curse of dimensionality, PINNs provide an effective and scalable alternative to classi-

cal numerical techniques, particularly for problems involving complex physical systems or large datasets.

Traditional numerical methods, such as finite element and finite difference approaches, rely heavily on structured meshes to discretize the computational domain [21, 237]. This dependency on mesh generation poses significant challenges, particularly when dealing with complex geometries and intricate boundary conditions. The process of mesh creation is not only time-consuming but also susceptible to errors, which can lead to inaccuracies in simulations, especially in problems with irregular or dynamic domains [149, 151]. In contrast, Physics-Informed Neural Networks (PINNs) offer a distinct advantage by bypassing the need for predefined meshes. Rather than requiring discretization into structured grids, PINNs learn directly over the continuous domain, adapting to the geometry without the constraints imposed by mesh-based methods [108, 215]. This mesh-free nature simplifies the computational process and significantly improves the efficiency of solving complex problems, particularly in geometrically challenging domains.

Another fundamental limitation of classical numerical techniques lies in their treatment of physical laws and boundary conditions. Traditional methods often require extensive preprocessing to properly define and apply boundary conditions, which introduces additional complexity and increases the potential for error [175, 183, 293]. Moreover, these methods can struggle with enforcing physical constraints consistently across the entire solution domain, leading to a lack of physical fidelity in the results. In contrast, PINNs seamlessly integrate physical laws into the model training process, allowing them to enforce these constraints directly while approximating the solution. This enables a more cohesive and accurate representation of the underlying physics [229, 264]. The inherent capability of PINNs to incorporate physical laws throughout the learning process allows for more efficient and reliable modeling, even in the absence of large, labeled datasets. This end-to-end learning framework enhances both the computational performance and the accuracy of predictions, making PINNs a powerful tool for tackling complex, physics-driven problems.

In domains where rapid computation is essential, such as real-time simulations or optimization tasks, Physics-Informed Neural Networks (PINNs) offer substantial advantages over traditional computational methods. PINNs exploit underlying physical knowledge during the training process, allowing them to converge to accurate solutions more efficiently, requiring fewer iterations than conventional approaches. Traditional methods, by contrast, often demand significant computational resources and numerous

iterations to achieve comparable results. The ability of PINNs to integrate physical information allows for faster convergence, making them particularly well-suited for scenarios that require quick decision-making or high-frequency calculations [173, 247].

In addition to improving computational efficiency, the incorporation of physical principles directly into the PINN framework enhances both the model's predictive accuracy and its interpretability [30, 191, 273]. In applications spanning fields such as engineering, finance, and healthcare, where the transparency and explainability of model predictions are essential, PINNs provide a clear and justifiable foundation for decision-making. This is because the solutions generated by PINNs are inherently consistent with the governing physical laws, making them not only more reliable but also easier to validate and verify. Such interpretability is crucial in these high-stakes domains, where understanding the rationale behind a model's output can be as important as the accuracy of the output itself. Therefore, PINNs not only offer computational benefits but also provide a more robust framework for model validation and trust, fostering their adoption in critical real-world applications.

It can be seen that Classical numerical methods, such as the Finite Element Method (FEM) and spectral methods, are widely recognized for their high accuracy when applied to well-defined, lower-dimensional problems. However, these methods face significant challenges when dealing with high-dimensional spaces, complex geometries, and real-time applications. The need for extensive computational resources, particularly when addressing large-scale problems or dynamically changing environments, can severely limit the scalability and efficiency of these traditional techniques. In contrast, Physics-Informed Neural Networks (PINNs) provide a flexible and efficient alternative that overcomes many of these limitations. By directly incorporating physical laws into the learning process, PINNs offer superior performance in scenarios that require rapid computations or involve intricate physical systems. Their ability to adapt seamlessly to complex geometries and high-dimensional problems positions them as a promising tool for tackling emerging computational challenges. As the demand for more sophisticated simulations and real-time solutions continues to grow, integrating PINNs into the field of numerical computing presents an exciting avenue for future research and practical applications.

Despite their advantages, PINNs are not without limitations. One of the primary challenges associated with PINNs lies in the optimization process, which involves minimizing a loss function that encompasses both the governing partial differential equations (PDEs) and the relevant boundary conditions [50]. In complex settings, such as anisotropic or

spatially varying environments, the optimization landscape becomes more intricate, which can complicate the training process [49, 88]. These complexities may lead to issues such as slow convergence or the inability of the algorithm to reach an optimal solution that accurately reflects the underlying physical dynamics of the problem. This variability in performance can be particularly problematic in applications requiring precise and consistent results. Therefore, while PINNs offer significant potential for solving complex, real-world problems, further research is needed to enhance their robustness and reliability, particularly in challenging or highly variable conditions.

The field of carbon credit research, particularly in relation to the dynamic interactions between various influencing factors, remains underexplored. While there has been increasing interest in applying machine learning techniques to model and predict carbon credit dynamics, the majority of existing studies primarily focus on specific methodologies. For instance, Gated Recurrent Units (GRUs) have been utilized for temporal forecasting of carbon credit trends [43, 134, 145, 153], while other approaches, such as Feedforward Neural Networks (FNNs)[93, 94], Residual Gain Strategy (REG)[58, 62, 102], Deep Neural Networks (DNN)[112, 244], and Multilayer Perceptron (MLP) networks[127, 206], have also been explored for carbon credit valuation and prediction.

Despite the growing adoption of these techniques, there remains a noticeable gap in comparative studies that evaluate the relative performance and applicability of these various methodologies. A comprehensive analysis that contrasts these models across different dimensions, such as accuracy, computational efficiency, and their ability to capture the complexities of carbon credit systems, is notably absent in the current literature. This lack of comparison limits the ability to identify the most effective techniques for modeling the intricate dynamics of carbon credit markets, an essential step in advancing research and practical applications in this area.

In this study, we investigate the application of Physics-Informed Neural Networks (PINNs) and introduce a novel framework termed Carbon Informed Neural Networks (CINNs) to address the unique challenges associated with modeling carbon-related physical systems. Our comparative analysis of various PINN-based approaches reveals that, while these methods offer promising solutions, they often require intricate network structures, which in turn lead to extended training times and computational overheads to achieve both convergence and the desired level of accuracy. This challenge is particularly pronounced in complex systems where multiple interacting factors must be modeled simultaneously.

To mitigate these issues, we systematically review and compare existing methodolo-

gies and identify areas where improvements can be made. Based on this analysis, we propose a new framework that leverages the Kolmogorov-Arnold Representation (KAR) to better organize and represent the data. By applying the KAR to the data structure, we aim to simplify the architecture of the neural network, thereby reducing the overall complexity of the model and potentially enhancing training efficiency. This approach not only streamlines the network design but also holds the potential to decrease the time required for training, offering a more efficient path toward achieving accurate solutions in the modeling of complex carbon systems.

2.5 Bias and Disparity in Decision Making

Bias in expert judgment is a key issue in the decision-making process. Because of various things that the expert has imperfect knowledge of, when experts' judgments are influenced by biases or differing methodologies, the resulting disparities can create confusion and uncertainty in the decision-making process [69, 178]. Because decision-making is often complex and multifaceted, necessitating input from various domains of expertise [174, 232], the presence of diverse perspectives can be beneficial [85, 119, 180].

Multi-expert decision-making involves aggregating diverse opinions from multiple experts to enhance the quality and reliability of decisions, and corresponding systems play a pivotal role in this context by integrating diverse perspectives and insights from specialists in areas such as risk assessment, market analysis, investment strategies, and regulatory compliance [67, 286]. These systems harness the collective intelligence of multiple experts to enhance the robustness and reliability of decisions. By mitigating the limitations inherent in individual expert judgments [139, 156, 228], such as cognitive biases and knowledge gaps [29, 65, 121], multi-expert systems foster a more holistic understanding. This collaborative approach not only enriches the decision-making process but also promotes greater transparency and accountability, as it allows stakeholders to consider a wider array of factors and potential outcomes. Consequently, the incorporation of multi-expert systems is crucial for organizations aiming to navigate the complexities of financial markets and to make informed, strategic decisions that align with their long-term objectives [158, 241].

Although the use of diversity in multi-expert systems can reduce monotonous bias through diversity, the multi-expert system also introduces diversity of bias thus disparity from various sources, which may cause confusion and contradiction in evaluation [2, 118]. This disparity can significantly impact decision quality, as differing opinions may lead

to conflicting conclusions and strategies [129, 198]. This inconsistency can dilute the credibility of the analysis and may result in suboptimal choices that do not align with the organization's goals.

Disparity caused by divergent biases among experts present significant challenges in financial decision-making, as they can lead to inconsistencies and misalignments in judgment and recommendations [25, 78, 86]. Each expert brings a unique set of experiences, knowledge, and cognitive predispositions, which can result in varying interpretations of data and divergent conclusions. Such biases may stem from personal experiences, industry backgrounds, or even the psychological heuristics that influence decision-making processes [182]. When these biases manifest within a multi-expert system, they can create conflicts that complicate consensus-building and obscure the true nature of the financial landscape. Moreover, divergent biases can introduce substantial risk, as they may lead to the neglect of critical information or the overemphasis of certain factors, skewing the final decision [77, 221, 226]. This not only hampers the effectiveness of collaborative decision-making but also raises concerns about accountability and trust in the outcomes produced. As financial markets become increasingly volatile and interconnected, addressing the challenges posed by divergent biases is essential for ensuring that decisions are well-informed, coherent, and aligned with strategic objectives [217, 219].

It can be seen that biases inherent in individual expert judgments can distort analyses and lead to inconsistent recommendations, ultimately compromising the effectiveness of financial strategies. Stakeholders may struggle to reconcile these differing viewpoints, leading to delays in decision-making and a potential loss of competitive advantage in rapidly changing [165, 252]. Ultimately, the presence of multi-expert disparity can undermine the reliability of forecasts and risk assessments, emphasizing the need for effective integration and synthesis of expert opinions to enhance overall decision quality.

Therefore, it is necessary to mitigate bias in multi-expert systems, enhancing the quality and reliability of decision-making processes, particularly in complex fields such as finance. To tackle the challenges of divergent biases in multi-expert systems, we present an Adaptive Kappa-Ordered Weight Averaging (KOWA) fusion for multi-expert decision-making. By employing ordered weighting principles, KOWA systematically integrates expert judgments, assigning weights based on consensus and reliability. The framework begins by identifying biases and outlier opinions through a kappa statistic, facilitating a nuanced weighting system that enhances decision quality by mitigating extreme biases. By addressing and reducing these biases, we aim to create a more cohesive and accurate synthesis of expert opinions.

We aim to obtain a reliable decision-fusion, improving assessment consistency with less disparity for risk management and overall organizational credibility in analyses. This involves employing systematic approaches to identify, quantify, and integrate diverse viewpoints, thereby fostering a more balanced representation of knowledge. Ultimately, the objective is to ensure that decisions are grounded in a robust, objective framework that reflects a comprehensive understanding of the financial landscape, thus enabling organizations to navigate uncertainties and capitalize on opportunities more effectively.

2.6 Bias by False Data

Bias can be critical in decision making For example, Decision Makings in quantification of creditworthiness are important in finance as they indicate a borrower's risk of meeting financial obligations and serve as a reference for risk prevention and credit pricing for lenders, investors, and other financial institutions [12, 36, 46]. Since data processing requires a lot of resources, more and more institutions have gradually introduced automation in financial information systems with data pipelines to perform data processing in recent years to improve business efficiency and increase the objectivity of the rating while reducing the cost of the labor force and time elapsed.

Most of the current automation approaches to credit evaluation can be broadly classified into two categories, rule-based models and machine-learning model-based approaches. A rule-based model analysis is one of the methods for estimating and predicting changes [15, 150, 187], which provides inferences about the dynamic laws based on the mechanics of the financial system. This type of approach requires reliance on experience and understanding of the market system with assumption. Without proper assumptions about the mechanism, specialized rule systems will not work and may lead to unobjective rating results due to subjective assumptions of the model and an incomplete understanding of the mechanism. In addition, due to the handcrafted nature of these methods, these rules are usually not publicly available and are difficult to be very generalized.

Machine learning (ML) techniques, in contrast to traditional rule-based methods, make fewer assumptions about the underlying mechanisms of the systems they model. These methods can leverage data-driven learning processes, bypassing the need for explicit rules or prior knowledge regarding system dynamics. This flexibility makes machine learning particularly useful in complex and dynamic environments where the mechanisms are not fully understood or are too intricate to capture through prede-

fined rules. Several widely-used machine learning strategies have been applied across various industries, each offering distinct advantages for predictive modeling and decision-making.

For instance, Regression Analysis is frequently employed in scenarios involving multivariate relationships or classification tasks, such as predicting financial outcomes or assessing creditworthiness [98, 99, 101]. Decision Tree Models, which structure data into a tree-like diagram, are utilized for classification and regression tasks, providing interpretable and explainable models [39, 80, 255]. Random Forests, an ensemble technique built upon multiple decision trees, are particularly valued for their robustness and accuracy, especially in high-dimensional settings [164, 194, 204, 248].

Gradient Boosting Decision Trees (GBDT) are another powerful ensemble method that constructs models by sequentially improving upon the errors of previous models, often yielding high predictive performance [57, 262, 295]. AdaBoost, another boosting method, focuses on improving weak learners by emphasizing misclassified instances [125, 193]. In addition, Multilayer Perceptron (MLP) neural networks, which are capable of learning complex, nonlinear relationships, have been successfully applied in various domains including credit risk assessment [14, 107, 109].

Furthermore, Statistical Learning techniques, which combine elements of machine learning with statistical theory, have been extensively used in modeling and forecasting tasks [106, 179, 181, 225, 233]. These methods are widely applied in decision-making contexts such as assessing the likelihood of a borrower ability to meet financial obligations, thus improving the accuracy of credit risk assessments and other financial predictions. Overall, these diverse machine learning strategies offer significant flexibility and power in modeling complex systems, providing critical insights for decision-making across various sectors.

In addition to the convenience and efficiency savings brought about by the popularity of machine learning in the financial world, there have been attendant malicious attacks against machine learning that have been creeping into the industry. Adversarial machine learning can be a particular concern in the context of FinTech, as misleading decisions made by corrupted machine learning models can have significant financial consequences with a risk of incorrect or malicious results [72, 81, 263]. Adversarial attacks involve intentional manipulation of input data in a way that causes machine learning models to be wrong or produce undesirable results, especially for data processing services.

2.7 Related Works

This section reviews the literature relevant to computational and modeling approaches in carbon finance. Due to the diversity of research topics, including classical quantitative models such as the Black-Scholes model, machine learning techniques like deep neural networks (DNNs) and feed-forward networks (FFNs), physics-informed neural networks (PINNs), finance-informed neural networks (FINNs), and the Kolmogorov-Arnold representation.

The reviewed works illustrate the spectrum from classical quantitative models to modern machine learning and knowledge-informed approaches. Integrating domain knowledge with data-driven models improves robustness, interpretability, and generalization. Structuring the review in this way is necessary to clarify the methodological foundations of the proposed system, identify gaps in existing models that motivate multi-domain knowledge assembly and adaptive decision frameworks, and demonstrate interdisciplinary connections between finance, machine learning, and domain expertise. This approach also justifies the choice of methods for robust, bias-aware carbon finance decision support. By organizing the literature this way, the study ensures that it builds on prior knowledge while addressing limitations, highlighting the need for integrated computational and domain-informed approaches.

2.7.1 Black Scholes Model

The Black-Scholes (BS) model has long been a cornerstone of financial mathematics, providing a systematic framework for valuing European options based on the dynamics of the underlying asset price [3, 19, 130, 154, 155]. By calculating the theoretical price of options, the BS model reflects the probabilities of various asset price paths at maturity, offering valuable insights for decision-making in financial markets. Despite its widespread use and foundational status in modern finance, the BS model operates under several simplifying assumptions, such as constant volatility and the absence of market frictions, which may limit its accuracy in real-world applications.

Recent advancements in Financial-Informed Neural Networks (FINNs) seek to extend the capabilities of traditional models like Black-Scholes by incorporating more complex financial systems and accounting for nonlinear relationships within the data. Unlike the BS model, which assumes linearity and fixed parameters, FINNs are designed to better capture the dynamic and multifaceted nature of financial markets, integrating empirical data and adapting to changing market conditions [58, 94, 112, 206, 244]. This approach

holds the potential to refine option pricing models, making them more responsive to real-world complexities and improving their reliability and predictive accuracy. By moving beyond the static assumptions of traditional models, FINNs offer a promising direction for enhancing the adaptability and precision of financial models, ultimately supporting more informed and effective decision-making in volatile markets.

2.7.2 Computing Multiple Layer Perceptron (MLP)

A fundamental method for neural network design involves the use of multi-layer perceptrons (MLPs), which introduce nonlinearity through activation functions. This allows MLPs to effectively capture and model complex patterns within financial data, mapping inputs to outputs in a manner that can accommodate the intricate dynamics of financial systems [127, 206]. While MLPs offer a straightforward and effective approach, they face challenges when applied to more complex financial scenarios. In such cases, careful design of loss functions and learning strategies becomes essential to ensure efficient training and prevent issues such as underfitting or slow convergence.

One notable application of MLPs in finance is the work by Santos et al. [206], who explored the use of neural networks to address the valuation of stock options, specifically applying the Black-Scholes equation, a cornerstone of financial mathematics. In this context, the authors proposed an innovative approach where neural networks were employed to solve the parabolic partial differential equation that underpins the Black-Scholes model. They utilized real-world data from call options of major Brazilian companies, such as Petrobras and Vale, to train their models. Their results demonstrated the effectiveness of the neural network-based method in predicting short-term call option prices, particularly within the context of the Brazilian options market. This case study underscores the potential of neural networks, particularly MLPs, in enhancing the accuracy and applicability of financial models in real-world settings, offering an alternative to traditional analytical methods for option pricing.

2.7.3 Computing with Deep Neural Networks (DNNs)

To improve the capacity of machine learning models for analyzing complex financial systems, many recent studies have incorporated deep neural networks (DNNs) into Financial-Informed Neural Networks (FINNs), leveraging their hierarchical layers to capture intricate patterns in financial data [112, 244]. By embedding regulatory frameworks and constraints within the architecture of these networks, researchers aim to

enhance the learning process and make the models more responsive to the underlying financial dynamics. However, while the addition of DNNs improves model performance, it also introduces significant challenges related to system complexity and computational demands, as these models require substantial computational resources to effectively train and execute.

In a notable study, Ibrahim et al. [112] applied a DNN-based FINN approach to improve the efficiency of solving time-dependent differential equations, particularly in the context of computational finance. They replaced traditional coarse integrators in parallel time algorithms, such as Parareal, with deep learning models to accelerate the integration process. This method demonstrated significant improvements in computational speed by exploiting concurrency, but it still required considerable computational time and resources to maintain the performance of deep learning-based frameworks, highlighting the trade-off between efficiency gains and resource expenditure.

Similarly, Villarino et al. [244] focused on addressing specific challenges related to training loss functions and boundary conditions in multi-dimensional nonlinear parabolic partial differential equations. They proposed a novel method for deriving boundary losses directly from the partial differential equations, which were adjusted by substituting the boundary conditions into the model equation. This approach aimed to rigorously constrain counterparty credit risk by enforcing boundary conditions within the modeling process, improving the precision and reliability of the financial model. While these methods contribute valuable insights into optimizing the performance of FINNs, they also underscore the ongoing need for advanced computational resources to handle the increased complexity of financial systems modeled by deep learning techniques.

2.7.4 Computing with Feed-Forward Networks (FFNs)

To further enhance the performance of Financial-Informed Neural Networks (FINNs), another promising approach is the utilization of Feed-Forward Neural Networks (FFNs). FFNs, as foundational neural architectures, consist of a straightforward data flow mechanism in which information progresses from input nodes through hidden layers to output nodes. The hierarchical structure of FFNs enables them to capture complex relationships and constraint patterns, which is particularly beneficial for financial applications [93, 94]. This structure allows FFNs to effectively model financial systems, where intricate dependencies between variables must be identified and learned.

Despite their advantages, the training of deep FFNs can pose significant challenges, particularly in terms of optimization. A common issue encountered during the training

process is the vanishing or exploding gradient problem. This issue arises when gradients become either too small or too large as they propagate back through the network during training, causing instability or impeding the learning process. To address these challenges, several strategies are employed, including gradient clipping, which limits the size of gradients during backpropagation, and more sophisticated initialization techniques that ensure the network begins with appropriate weights to facilitate stable learning. These techniques are crucial for ensuring that FFNs can be effectively trained, especially as the depth of the network increases, allowing them to unlock their full potential in complex financial modeling tasks.

2.7.5 Computing with Residual Gain Strategy (REGs)

To improve learning efficiency while avoiding the expansion of network dimensions, recent studies have explored the integration of residual gain (REG) strategies within neural network frameworks, demonstrating their effectiveness in enhancing performance without significantly increasing network complexity [58, 102]. The REG strategy involves augmenting the traditional Multi-Layer Perceptron (MLP) architecture by incorporating residual connections between layers. These residual connections allow each hidden layer's output to serve as a corrective signal, refining the network final output through a series of correctional gains.

This residual learning mechanism effectively enables the network to focus on learning the differences, or residuals, between predicted and actual outputs, rather than learning the entire mapping from input to output. Empirical studies have shown that the integration of residual gain within MLPs enhances the model's learning efficiency, achieving improved performance without the need for deeper networks. The ability to improve learning outcomes while keeping the network structure relatively shallow makes this approach particularly valuable for situations where computational resources are constrained or when model simplicity is desired, offering a balanced solution between complexity and efficiency.

2.7.6 Quantitative Approaches in Financial Analysis

Model-based methods had been widely used in risk control and financial contagion in banking and loan services. With mechanism models, features such as loan provision rate, macroeconomic factors can be introduced to predict rating and rating transitions [150, 187]. However, these models need to rely strongly on prior knowledge and

expert experience, which is hard to acquire especially for the latest ones. The reliability of the model requires a strong hypothetical basis, so it is inevitable to introduce certain subjective prior assumptions in the evaluation.

As a quantitative supervised learning solution to quantitative analysis, regression methods are also popular in quantitative risk management [97, 116], and ridge classification [59, 99, 146] is widely used to transform the classification problem into a regression problem with Tikhonov regularization [31, 82], especially for ill-posed problem and noisy data. These methods need to work with the assumption of discrete ratings as increasing and continuous numerical quantities and ignores the non-linearity and non-uniformity of rating classification after quantification. The ambiguous value between the two categories is projected through a priori hypothetical quantization mapping to obtain the differentiated value, which may not completely conform to the original discrete classification.

As for unsupervised learning, Nearest Neighbors Analysis [113] is also commonly applied as a method of numerical regression and classification based on the K Nearest Neighbours analysis method. It is simple to calculate, and can be used for both regression and classification. However, it relies heavily on data. Due to the lack of a adaptive mechanism, it only performs proximity analysis based on the data itself to classify and store the data. Therefore, it needs to wait for new data (test data) to come in before it starts learning.

Tree-based learning methods, such as Dcsion Tree Model [39, 80, 255], Random Forest[164, 194, 204, 248], gradient boosting decision tree (GBDT) [57, 262, 295] AdaBoost (Adaptive Boosting [125, 193]), are usually applied in financial prediction to handle high-dimensional data without dimensionality reduction, no feature selection. These methods need the support from many weaker classifiers, which lacks standardization for the design, both for the number and structure of the classifiers. Meanwhile, overfitting is also a common problem take place in these models.

Most statistical learning methods [106, 179, 181, 225, 233] have good model interpretability, and can further perform confidence interval analysis and hypothesis testing, but require a prior assumption based on a probability distribution or event independence. However, these assumptions are uncertain and introduce subjective factors. Meanwhile, such methods are often sensitive to input data and are not easy to generalize. The performance is low if the prior hypothesis does not hold or the feature dimension is high and the sample is incomplete.

A neural network model is a model that learns and fits through a nonlinear method [14,

107, 109], implicitly finding the required high-order feature items through such a network structure. The advantage of a neural network is its powerful nonlinear fitting ability despite its complexity of the model, while it is easily affected by outliers and prone to overfitting when the data is insufficient, so it has higher requirements for training data.

The graph convolution network (GCN) [120, 261] is a type of neural networks that can take a graph as input, process it through a neural network, and output a label. By integrating the information of the graph as the learning element, the possibility of information loss due to uncertain empirical priori hypothetical bias is reduced.

2.7.7 Physic Informed Neural Network (PINN)

The Physical Information Neural Network (PINN) is a powerful tool designed to address the complexities of physical systems by embedding physical laws directly into the neural network training framework. This integration significantly enhances the physical consistency and reliability of the model, enabling it to produce predictions that are not only statistically accurate but also physically plausible [190]. Unlike traditional machine learning methods that typically rely heavily on large datasets, PINNs reduce this dependency by leveraging existing physical knowledge, making them particularly useful in scenarios where data is sparse or difficult to obtain.

PINNs are especially effective in solving complex scientific and engineering problems that involve interactions between multiple physical processes or nonlinear phenomena. In such cases, they can naturally incorporate boundary conditions and initial states, ensuring that the model adheres to the governing laws of physics throughout the training and inference process [117]. This ability to integrate physical constraints into the model's architecture allows PINNs to handle multi-physics scenarios more efficiently and accurately, making them an invaluable tool in fields such as climate modeling, material science, and complex system simulations. By directly imposing the laws of physics, PINNs provide a framework for generating highly accurate predictions with minimal reliance on large, high-dimensional datasets, which is a significant advantage in many real-world applications.

Moreover, PINNs offer a compelling advantage over traditional numerical methods, primarily through their ability to enhance computational efficiency and model interpretability. Unlike conventional techniques that rely heavily on discretization methods such as finite element analysis (FEM), which can be computationally intensive, PINNs reduce the need for extensive mesh generation and allow for direct learning from the

governing physical equations. This reduction in computational demand not only accelerates the solution process but also provides a more efficient framework for addressing high-dimensional, complex systems.

A key strength of PINNs lies in their inherent alignment with physical laws, which ensures that the predictions generated by the model remain consistent with well-established principles of physics [190]. By embedding these physical constraints directly into the network architecture, PINNs are able to produce solutions that are not only accurate but also robust in terms of physical realism. This is particularly important in fields involving multi-physics interactions or non-linear phenomena, where traditional machine learning methods may lack the capacity to accurately capture the underlying dynamics.

Furthermore, the integration of physical knowledge into the PINN training process enhances both the statistical validity of the model and its physical relevance. This dual integration of empirical data and physical laws ensures that the resulting model can reliably predict outcomes even in scenarios with limited data. In doing so, PINNs offer a powerful tool for tackling complex scientific and engineering problems, where conventional methods may struggle to accommodate the intricate and dynamic nature of the systems being modeled [117]. Consequently, PINNs provide a flexible, computationally efficient, and physically consistent approach to solving a wide array of challenges across various domains.

While there has been significant progress in research involving Physics-Informed Neural Networks (PINNs), there remains a noticeable gap in studies specifically targeting their application to carbon credits and the intricate dynamics governing them. Existing research on PINNs has primarily focused on various neural network architectures, such as Gated Recurrent Units (GRUs), Feedforward Neural Networks (FNNs), Residual Gain Strategy (REG), Deep Neural Networks (DNNs), and Multilayer Perceptrons (MLPs). These methodologies have been explored across a wide range of applications, but their specific utilization in the context of carbon credits and the multifaceted interactions between carbon emission and sequestration processes is relatively underexplored.

For instance, GRUs have been widely utilized for temporal forecasting tasks, such as predicting future emissions or market behavior over time, with notable works in this domain by Li et al.[134], Liu et al.[145], and Chen et al.[43]. Similarly, FNNs have been applied in various domains, including financial modeling and option pricing[93, 94], yet their application in carbon-related systems is still limited. The Residual Gain Strategy (REG), which augments standard neural network architectures by incorporating residual

connections to enhance learning efficiency, has been explored for improving model performance in complex systems [58, 62, 102], but its use in environmental modeling remains scarce. DNNs and MLPs have shown promise in solving high-dimensional problems, including those involving physical processes [112, 206, 244], but their specific integration with carbon credit systems requires further investigation.

Despite these developments, there is a distinct lack of comprehensive studies that examine how these advanced PINN architectures can be tailored to model the nuanced and dynamic interactions within carbon credit systems. Such systems are characterized by complex temporal dynamics, intricate regulatory frameworks, and nonlinear relationships that may benefit from more robust, physics-constrained learning techniques. The integration of PINNs into the modeling of carbon credits represents an area ripe for further exploration, where advancements in machine learning could lead to improved understanding and management of carbon markets and sustainability efforts.

2.7.8 Finance Informed Neural Network (FINN)

The application of Physics-Informed Neural Networks (PINNs) in the financial sector has recently gained attention as an innovative approach that merges advanced computational techniques with complex financial modeling. This evolving field sits at the intersection of computational methodologies and financial applications, with the potential to enhance decision-making across various areas such as risk assessment, asset pricing, and portfolio optimization [18, 58, 76, 94, 112, 206, 250]. When these networks are specifically tailored to incorporate financial knowledge, constraints, and theories, they are referred to as Finance-Informed Neural Networks (FINNs). The application of FINNs aims to refine the accuracy and efficiency of financial modeling within regulated environments, improving traditional methods of asset pricing, risk management, and investment strategies.

The core of FINNs lies in the integration of financial theories with neural network architectures, enabling them to solve complex differential equations that represent real-world financial dynamics. For example, by utilizing financial models such as the Black-Scholes equation for option pricing [32, 38, 154], these networks can provide more reliable predictions and optimal solutions. A key component of the FINN framework is the use of a composite loss function, which incorporates both data-driven terms and the relevant financial equations. This loss function guides the training process, ensuring that the network outputs are consistent with established financial knowledge while capturing the intricacies of market behaviors. Tasks such as derivative pricing, risk

management, and investment strategy optimization become more robust and reliable through the integration of these financial principles [93, 244].

Despite the promising potential of FINNs, their implementation is not without challenges. The incorporation of financial theories and constraints adds a layer of complexity to the training process compared to traditional neural networks. Specifically, the complex nature of the loss functions, which must account for both empirical data and theoretical financial models, increases the computational burden and can affect the efficiency of the learning process. The need for larger network architectures and extensive training cycles further exacerbates the demands on computational resources. Additionally, ensuring interpretability of the models remains a significant hurdle, as the integration of financial constraints complicates the transparency of the network's decision-making process [41, 288]. Thus, while FINNs offer great promise, their successful deployment requires careful attention to computational efficiency, model interpretability, and the management of complex training procedures.

2.7.9 Kolmogorov-Arnold Representation

The application of the Kolmogorov-Arnold Representation (KAR) in machine learning presents a promising avenue for addressing the challenges of complexity reduction, model interpretability, and enhanced performance in scientific computations. The KAR theorem, which stems from multivariate function theory, asserts that any continuous multivariate function can be decomposed into a superposition of continuous functions of several variables [210, 245]. This decomposition, known as the Kolmogorov superposition representation, offers a novel way to break down complex functions into simpler, more manageable components, providing an interpretable framework for understanding intricate relationships within the data.

Several studies have explored the integration of the KAR theorem into machine learning models, with the goal of simplifying the underlying structures and improving both model interpretability and efficiency [122, 148, 186]. By leveraging the decomposition of complex functions into KAR components, these approaches map the representation directly onto the neurons of the network. This mapping allows the neural network to learn and represent intricate relationships in the target function throughout the learning process, thus facilitating a more transparent and interpretable model.

The potential benefits of incorporating the KAR mechanism into machine learning models are manifold. The ability to break down complex relationships into simpler components allows for a reduction in the complexity of the model's structure, improving

both computational efficiency and generalization capabilities. Furthermore, the interpretability of the learned models is significantly enhanced, as the decomposition provides insights into the contributions of individual components to the overall function. These attributes make the KAR approach particularly valuable in domains where model transparency and performance are critical, such as in scientific computations and applications involving complex, high-dimensional data.

The integration of the Kolmogorov-Arnold Representation into machine learning offers significant promise for overcoming some of the most persistent challenges in computational modeling. By simplifying model structures and enhancing interpretability, this approach could lead to more efficient and transparent machine learning models, particularly in the context of scientific applications requiring the analysis of complex, multivariate functions.

CHAPTER 3

INTEGRATED CARBON DYNAMICS MANAGEMENT SYSTEM

3.1 Carbon Dynamics Management

The preceding analysis demonstrates that the dynamic management of carbon credits constitutes a complex and interdisciplinary domain. Carbon credits are not merely instruments of environmental management; they also serve as valuable financial assets, significantly enhancing the trading capacity and investment potential within the carbon market. This transformation has been driven primarily by advancements in financial technology, which leverages real-time data analysis and efficient transaction processing to broaden market participation.

However, the effective management of carbon credits necessitates a profound understanding of their environmental impacts to fully realize their potential as tools for sustainable development. Establishing a robust quantitative assessment framework is essential. This framework should encompass asset valuation, pricing strategies, and a comprehensive understanding of relevant trading rights while considering a range of interconnected environmental, financial, market, and social factors. Current methodologies often fall short of providing a unified analytical and computational framework capable of addressing these multifaceted challenges.

In practical applications, the sustainability of carbon credit management must account for the social dimensions of environmental policies. An effective carbon credit

system should consider community impacts, fairness in resource allocation, and the socio-economic implications of carbon trading. Therefore, it is imperative to develop a system framework that integrates knowledge and data across various fields related to carbon credits. This integration will enable relevant managers to enhance their understanding of the dynamic interactions among carbon physics, environmental finance, and social economics, ultimately fostering positive interactions and impacts of strategies and policies across these domains.

Particularly in contexts characterized by data scarcity and information silos, the combination of domain-specific knowledge with principles of environmental sustainability can mitigate data dependency and model bias. This approach facilitates the development of reliable and reasonable decision support systems, even in the face of limited data availability.

To address this gap, this study presents an innovative methodological framework exemplified by the Integrated Environmental Governance Carbon Credit Knowledge Integration and Management System. The figure 3.1 illustrates an integrated management system with comprehensive sensing for carbon dynamics specifically designed to monitor and manage carbon dynamics. It encompasses various interconnected elements that contribute to effective carbon management and trading. This framework aims to

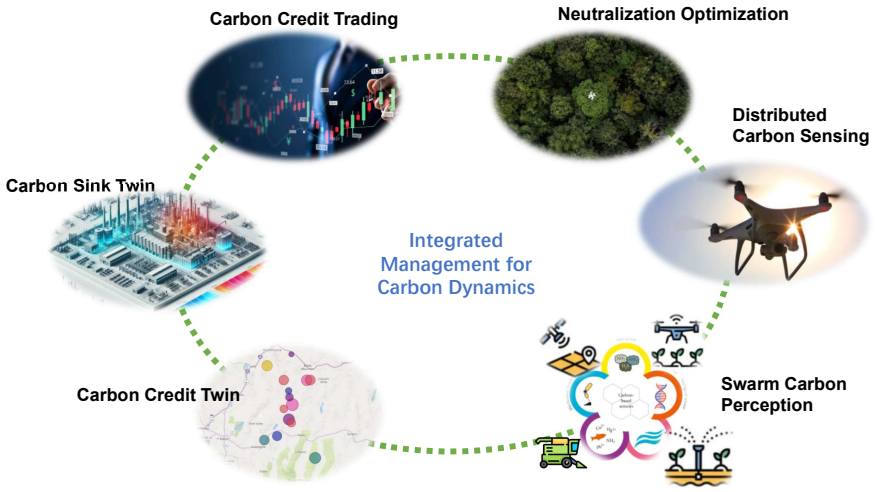

Figure 3.1: Integrated Management with Sensing for Carbon Dynamics

establish a novel and impactful research approach within the realms of environmental

science and engineering. It emphasizes the multidimensional integration of environmental components and their interrelationships with human activities, highlighting the vital role of scientific research within the broader environmental context.

The comprehensive knowledge system encompasses dynamic knowledge across several domains, including the atmosphere, hydrosphere, biosphere, and human sphere. By creating independent foundational knowledge systems and fostering interconnectivity among these fields, a large-scale, integrated knowledge system is developed. This system not only deepens the understanding of the dynamic relationships among various knowledge areas but also provides effective solutions to challenges such as knowledge silos and inadequate inter-field connections.

Moreover, the framework synthesizes empirical knowledge with physical models within a knowledge information network paradigm, enabling the cross-referencing of insights from diverse financial standards and fields, including environmental engineering. By clarifying the interconnections between ecosystems, human activities, and economic systems, it achieves a holistic approach to carbon credit management. This approach effectively addresses the limitations of existing methodologies, which often lack a cohesive analytical and computational framework necessary for tackling these complex challenges.

3.2 Dynamic Management for Sustainable Carbon Credit

Figure 3.2 shows a logic framework of the Integrated Dynamic Management System. The system comprises several key modules, including Decision Support Intelligence (DSI), Knowledge Information Orchestration with Machine Learning and Knowledge Support (KIO-MLAKS, or MLAK), a Data Engine (DE), actuators, and operational modules. Actuators encompass devices such as agricultural drones, machinery, and irrigation systems, which execute environmental tasks. Operational modules facilitate transactions, policy formulation, and compliance throughout the operational process. The Data Engine is responsible for gathering and processing essential data, including environmental and market information.

Decision Support Intelligence (DSI) functions as a comprehensive information processing system, designed to assist decision-makers in making informed choices by integrating and analyzing diverse data, models, and knowledge. Meanwhile, MLAKS synthesizes various forms of data, information, and experiences to generate new knowledge and advanced features, enabling complex analyses that support the decision-making process.

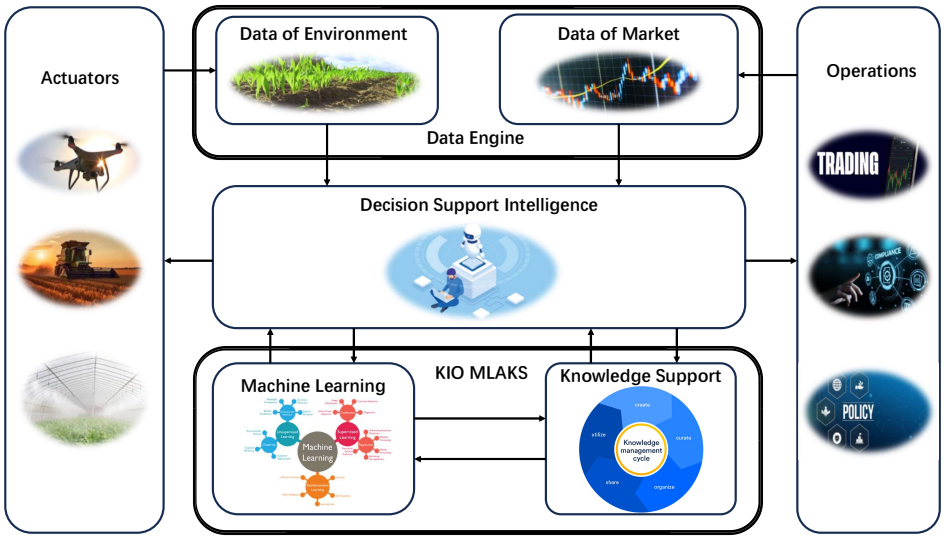

Figure 3.2: System Framework of Dynamic Management for Sustainable Carbon Credit

The integrated carbon credit management system, centered around Decision Support Intelligence (DSI), establishes a robust framework for enhancing decision-making processes within the realm of carbon credits. The DSI functions as the central hub for collecting and processing data, primarily sourced from the Data Engine (DE). This module is essential for aggregating diverse datasets, including environmental metrics, market conditions, and regulatory frameworks, which are crucial for informed decision-making in carbon credit transactions.

Figure 3.3 shows the procedure of the system. In this integrated system, DSI collects data from the DE, deriving decision analysis results and evidence with the assistance of MLAKS. This analysis aids decision-makers in engaging with the carbon credit market and environmental conditions through actuators and operational modules. Consequently, the system enables dynamic coordination and sustainable management of carbon credits, highlighting the interconnectedness of data-driven decision-making and practical execution in environmental governance.

The DSI leverages the data gathered by the DE to derive decision analysis results with the support of the Machine Learning and Knowledge Support (MLAKS) module. By utilizing advanced analytical techniques, MLAKS synthesizes various data inputs to generate insights that are pivotal for understanding market dynamics and environmental conditions. This integration of machine learning capabilities allows the DSI to identify

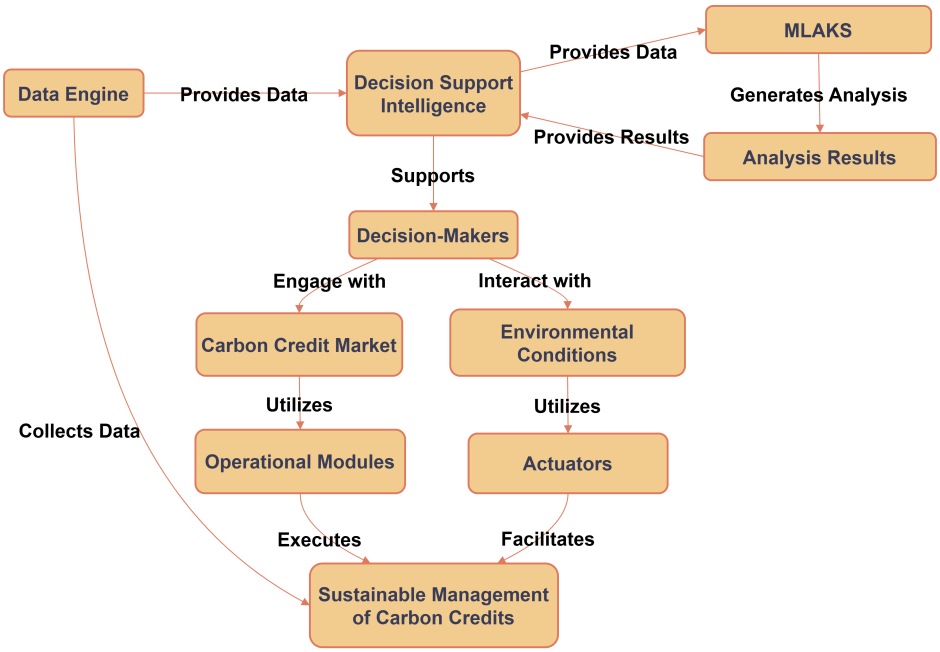

Figure 3.3: System Framework of Dynamic Management for Sustainable Carbon Credit

trends, assess risks, and forecast future scenarios, providing decision-makers with a solid evidence base for their actions.

The decision analysis results produced by the DSI play a critical role in guiding decision-makers as they navigate the complexities of the carbon credit market. This engagement is facilitated through a two-pronged approach: interacting with the carbon credit market and monitoring environmental conditions. By fostering this dual engagement, the system enables decision-makers to make informed choices that are aligned with both market opportunities and ecological sustainability.

Furthermore, the integrated system emphasizes the importance of actuators and operational modules in executing decisions. Actuators, such as automated systems for emissions monitoring and carbon credit transactions, play a vital role in translating analytical insights into practical actions. Operational modules support various tasks, including policy compliance, market transactions, and environmental assessments. Together, these components facilitate dynamic coordination within the system, ensuring that decisions are not only data-driven but also effectively implemented in real-time.

Ultimately, the strength of this integrated system lies in its ability to link data-driven decision-making with practical execution in the sphere of environmental governance. By creating a cohesive architecture that connects DSI, DE, MLAKS, and the various operational components, the system enhances the sustainable management of carbon credits.

This interconnected approach not only addresses immediate operational challenges but also fosters a culture of continuous learning and adaptation, essential for thriving in the ever-evolving landscape of carbon credit management.

3.2.1 Data Engine

The Data Engine System serves as a foundational component for carbon credit management, designed to efficiently collect, process, store, and analyze data from various environmental and market sources. Its architecture is built around the integration of diverse data streams, which enhances the comprehensiveness and accuracy of insights related to carbon credits.

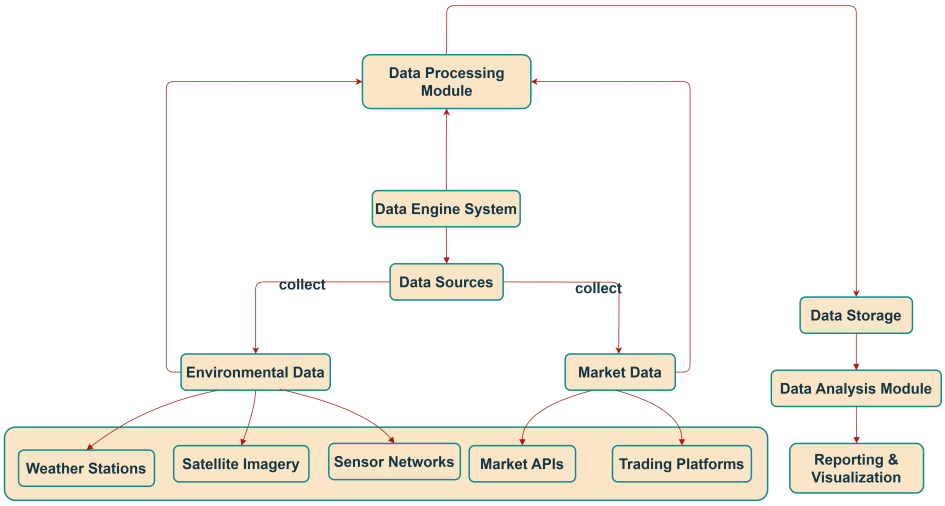

Figure 3.4: Data Engine For Carbon Credit Dynamic Management

As shown in Figure 3.4, at the core of the system are the Data Sources, which encompass two primary categories: Environmental Data and Market Data. Environmental data is gathered from multiple sources, including weather stations, satellite imagery, and sensor networks. These sources provide critical information on atmospheric conditions, land use, and carbon sequestration potential. By integrating these varied data points, the Data Engine ensures a robust understanding of the environmental factors influencing carbon credit generation and valuation.

In parallel, the system collects Market Data from APIs and trading platforms. This data is essential for tracking real-time market dynamics, including pricing fluctuations, demand-supply relationships, and regulatory developments. The interplay between environmental and market data is crucial, as it allows stakeholders to assess the economic

viability of carbon credit projects and make informed decisions regarding investments and compliance.

The Data Processing Module is a vital intermediary that transforms raw data into actionable intelligence. This module implements advanced algorithms for data cleaning, filtering, and aggregation, ensuring that the output is reliable and relevant. By systematically processing incoming data, the engine enhances the quality of information available for subsequent analysis.

Following processing, the Data Storage component securely archives the refined data, creating a centralized repository that facilitates easy access for analysis. This organized structure is crucial for maintaining data integrity and ensuring that stakeholders can retrieve historical datasets for longitudinal studies or trend analysis.

The Data Analysis Module then leverages this stored information to derive insights, employing statistical techniques and machine learning algorithms to identify patterns and predict future trends in carbon credit markets. This analytical capability is fundamental to understanding the complexities of carbon credit trading and optimizing decision-making processes.

The Reporting & Visualization module presents the analyzed data in user-friendly formats, such as dashboards and visual graphs. This function is particularly important, as it enables stakeholders, from policymakers to corporate decision-makers, to quickly grasp the implications of data and make strategic choices based on the insights generated.

It can be seen that the Data Engine System is meticulously designed to facilitate the comprehensive management of carbon credits. By integrating environmental and market data, implementing sophisticated processing techniques, and providing clear analytical outputs, this system empowers stakeholders to navigate the complexities of carbon credit management effectively. Its architecture not only enhances operational efficiency but also supports sustainable practices by promoting informed decision-making based on a robust evidence base.

The Data Engine constitutes a central pillar of the carbon credit management system, enabling the systematic collection, storage, and provision of high-quality data to the computational modules. By integrating heterogeneous environmental and market data streams, the system not only enhances the accuracy and comprehensiveness of insights but also establishes a robust foundation for subsequent analytical processes. Data processing is carried out through ETL pipelines applied to both static and dynamic storage systems, ensuring that raw information is transformed into structured, reliable, and actionable datasets. The processed data is then made accessible to downstream

modules via database APIs, facilitating seamless retrieval for statistical analysis, trend prediction, and decision support. This design reflects a professional balance between operational efficiency and analytical rigor, in which it allows the system to accommodate complex, multi-source data while maintaining flexibility for adaptive analysis. Moreover, by structuring data flow and accessibility in this way, the Data Engine supports evidence-based decision-making, strengthens model reliability, and provides a scalable framework that can evolve alongside emerging carbon finance methodologies.

3.2.2 Market Operations

3.2.2.1 Market Interaction

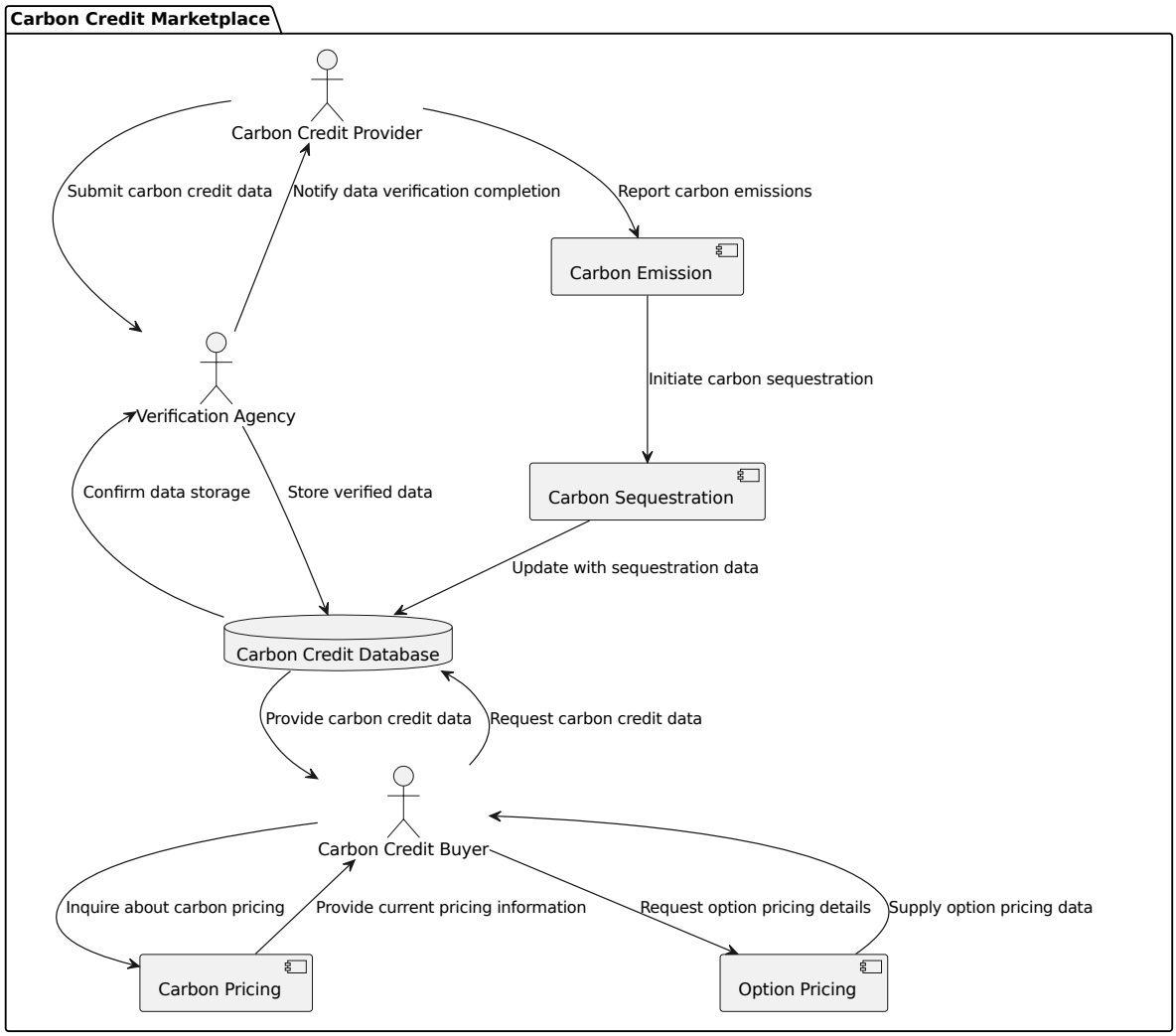

Figure 3.5: Component Interaction Logic in Carbon Credit

Figure 3.5 illustrates the package structure of the carbon credit marketplace, showcasing the interactions between key actors such as the **Carbon Credit Provider (CCP)**, **Carbon Credit Buyer (CCB)**, **Verification Agency (VA)**, and the **Carbon Credit Database (CCD)**. Additionally, it incorporates components such as **Carbon Emission (CE)**, **Carbon Sequestration (CS)**, **Carbon Pricing (CP)**, and **Option Pricing (OP)**, thereby highlighting their roles within the ecosystem.

Figure 3.6 elaborates on the existing carbon credit data flow by integrating additional components that encompass interactions related to carbon emissions, carbon sequestration, carbon pricing, and option pricing. This expansion illustrates a comprehensive framework for the management and exchange of carbon credits, which is essential in addressing climate change through market-based mechanisms.

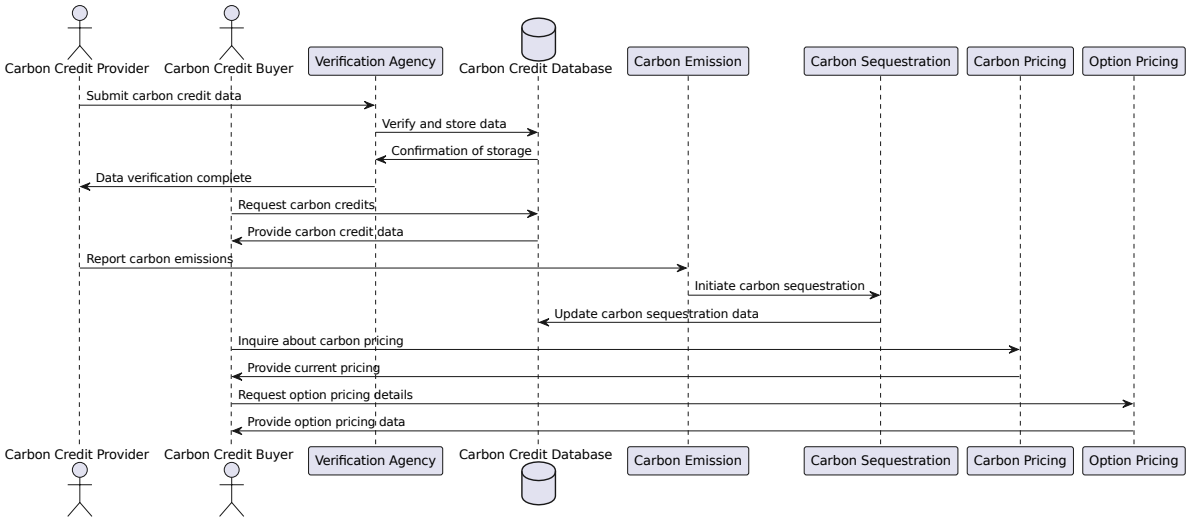

Figure 3.6: Carbon Credit Data Interaction Logic

The actors involved include the **Carbon Credit Provider (CCP)** and the **Carbon Credit Buyer (CCB)**, who are critical stakeholders in the carbon credit marketplace. The **Verification Agency (VA)** serves a pivotal role in ensuring the integrity of the data associated with carbon credits. The **Carbon Credit Database (CCD)** functions as a centralized repository for storing verified carbon credit data, thereby facilitating data accessibility and traceability.

The diagram delineates several key interactions. First, the **CCP** submits carbon credit data to the **VA** for verification. This step ensures that the data provided is accurate and complies with regulatory standards. Upon receipt of the data, the **VA** verifies and subsequently stores it in the **CCD**. This process includes a confirmation step, where the **CCD** communicates back to the **VA**, affirming that the data has been successfully stored.

The **VA** then informs the **CCP** that the data verification process has been completed, closing the feedback loop.

Concurrent with these foundational interactions, the **CCB** requests access to the carbon credits from the **CCD**, which responds by providing the requested carbon credit data. In addition to these interactions, the diagram introduces new participants that enhance the carbon credit ecosystem. The **Carbon Emission (CE)** component allows the **CCP** to report carbon emissions, establishing a direct link between emissions data and credit generation. Following the reporting, the **CE** initiates the **Carbon Sequestration (CS)** process, emphasizing the importance of sequestering carbon to offset emissions effectively. The **CS** then updates the **CCD** with relevant sequestration data, which is critical for tracking the effectiveness of carbon offset strategies.

Furthermore, the **CCB** engages with the **Carbon Pricing (CP)** mechanism to inquire about current carbon pricing. This interaction is crucial for buyers to make informed purchasing decisions based on market conditions. In response, the **CP** provides the **CCB** with up-to-date pricing information, ensuring transparency in the carbon credit market. Finally, the **CCB** seeks details regarding option pricing from the **Option Pricing (OP)** component, which is essential for evaluating financial instruments related to carbon credits. The **OP** then supplies the requested option pricing data to the **CCB**.

3.2.2.2 Carbon Credit Activities

Figure 3.7 delineates the activity flow for the carbon credit management process, providing a comprehensive overview of the actions undertaken by the various stakeholders involved in this domain. This activity flow is critical for understanding the sequential operations that facilitate the effective management of carbon credits, which are essential for mitigating climate change through market-based mechanisms.

The process initiates with the submission of carbon credit data, wherein stakeholders, presumably the Carbon Credit Providers, provide necessary information regarding their carbon credits. Following this submission, the data undergoes a verification process to ensure its accuracy and compliance with established regulatory standards. Upon successful verification, the data is stored in a designated repository, leading to a confirmation of storage. This step is vital as it ensures that the verified data is retrievable for future transactions and audits.

Subsequently, stakeholders complete the data verification process, after which they may proceed to request carbon credits. This request initiates a feedback loop, wherein the system provides the requested carbon credit data back to the stakeholders. In parallel,

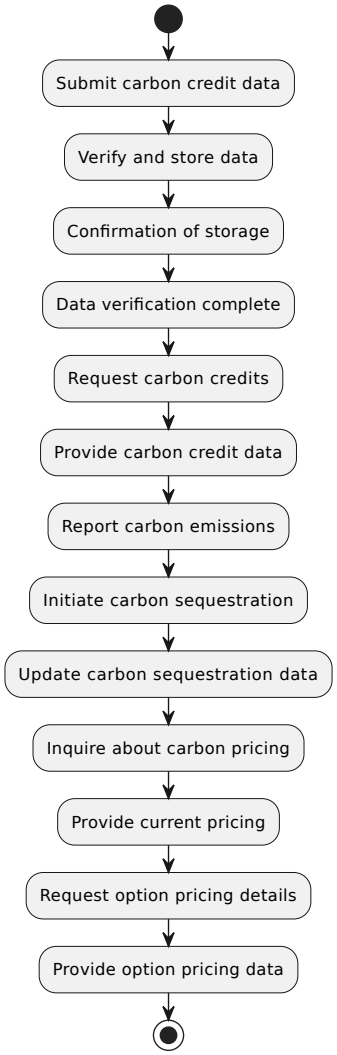

Figure 3.7: Carbon Credit Activityes Interaction Logic

carbon credit providers are required to report their carbon emissions, which is a crucial action that establishes a direct correlation between emissions and the credits generated.

The diagram further illustrates the initiation of carbon sequestration following the reporting of emissions. This process emphasizes the importance of carbon sequestration as a strategy for offsetting emissions effectively. The system subsequently updates the carbon sequestration data, ensuring that accurate records are maintained for future reference.

Moreover, stakeholders engage with the carbon pricing mechanism to inquire about current carbon pricing. This inquiry is instrumental in enabling stakeholders to make informed purchasing decisions based on prevailing market conditions. The system re-

sponds by providing the current pricing information, thereby enhancing transparency in the carbon credit marketplace.

Stakeholders may request details regarding option pricing, which are essential for evaluating the financial instruments associated with carbon credits. The system concludes this flow by supplying the relevant option pricing data to the stakeholders.

3.2.3 Decision Support Intelligence (DSI)

The Decision Support Intelligence (DSI) system serves as a vital framework for enhancing decision-making processes within carbon credit management. Functioning as a comprehensive information processing system, DSI integrates and analyzes a multitude of diverse data sources, models, and knowledge frameworks. This multifaceted approach is essential for navigating the complexities inherent in carbon credit markets, where decisions must be informed by real-time environmental, regulatory, and market dynamics. It can be seen in Figure 3.8, DSI system aggregates critical information from various

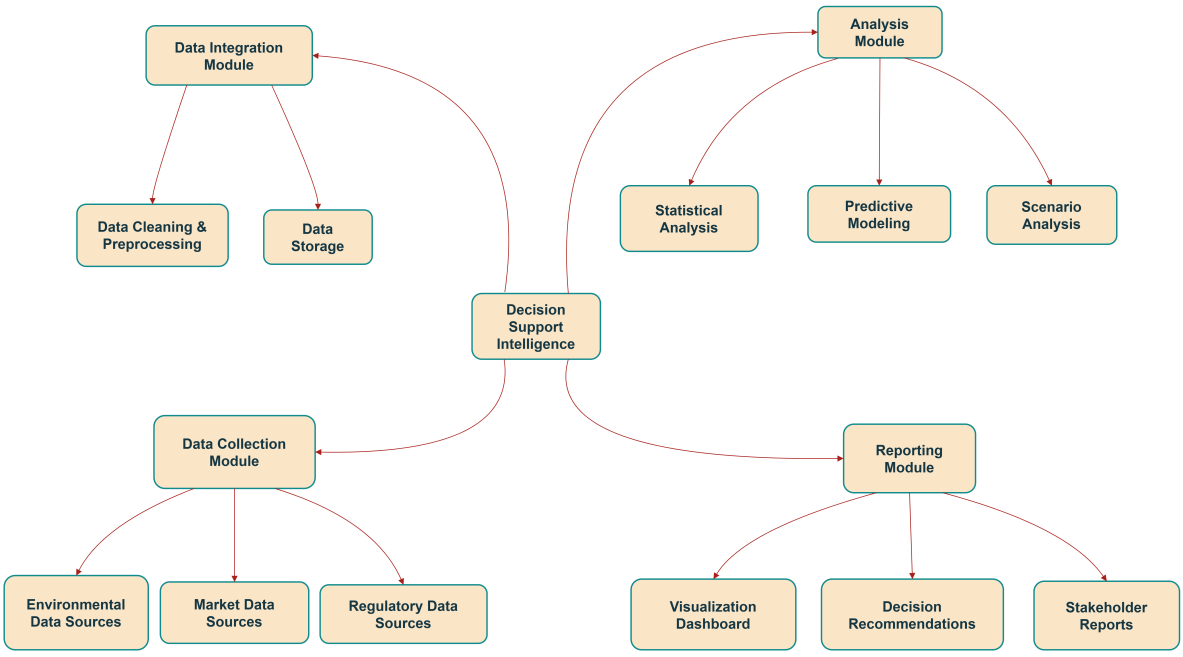

Figure 3.8: Decision Support Intelligence For Carbon Credit Dynamic Management

sources. This module is subdivided into specific areas focusing on environmental, market, and regulatory data. Environmental data sources provide insights into conditions that directly affect carbon credits, such as emissions levels, air quality metrics, and ecological assessments. Market data sources are indispensable, offering details about carbon credit

prices, trading volumes, and market trends that inform economic viability. Regulatory data sources ensure compliance with existing policies, capturing changes in legislation and regulatory frameworks that impact carbon credit transactions. By synthesizing these diverse datasets, the DSI establishes a robust foundation for informed decision-making.

The Data Integration Module plays a crucial role in the DSI system by ensuring the collected data is accurate and readily analyzable. It includes processes for data cleaning and preprocessing, which eliminate inconsistencies and enhance data quality. This is followed by data storage strategies that organize the information in a manner conducive to efficient retrieval and analysis. The integrity of this data is paramount, as it directly influences the outcomes generated by subsequent analytical processes.

The Analysis Module is where the transformative power of DSI is fully realized. By employing statistical analysis, predictive modeling, and scenario analysis, this module derives actionable insights from the integrated data. Statistical analysis identifies historical trends and relationships, enabling stakeholders to understand past performance and its implications for future actions. Predictive modeling employs advanced algorithms to forecast future scenarios based on current and historical data, providing stakeholders with foresight into potential market movements. Scenario analysis evaluates various policy and market conditions, allowing decision-makers to assess the impacts of different strategies and make proactive adjustments.

The Reporting Module effectively communicates the findings generated by the DSI. Through an interactive visualization dashboard, stakeholders can engage with the data, viewing trends and insights in a user-friendly manner. The module also generates decision recommendations that translate complex analytical outcomes into clear, actionable steps. Additionally, tailored stakeholder reports provide a comprehensive summary of the DSI's findings, ensuring that all parties involved in carbon credit management are informed and equipped to act decisively.

The DSI system is not merely a collection of tools; it represents a cohesive framework that integrates advanced data analysis techniques with comprehensive information sourcing. This holistic approach empowers organizations to navigate the intricate landscape of carbon credit management, facilitating informed decision-making that is responsive to the evolving environmental and market conditions. By leveraging the strengths of each component within the system, DSI enhances operational efficiency, promotes compliance, and ultimately contributes to more sustainable management of carbon credits.

3.3 Knowledge Informed Orchestration with MLAKS

The framework of Knowledge-Informed Orchestration is designed to address the complex challenges posed by dynamic environmental elements and the need for a comprehensive integrated knowledge system. It serves as a structured approach to enhance decision-making and resource management in environmental contexts.

As shown in figure 3.9, the framework integrates Knowledge Informed Orchestration with kernels of Machine Learning and Knowledge Support (MLAKS), which is structured around several key components, including time series intelligence engine, computing intelligence engine, graph intelligence engine, bias fusion engine. Each contributing to a cohesive system designed to enhance decision-making and operational efficiency.

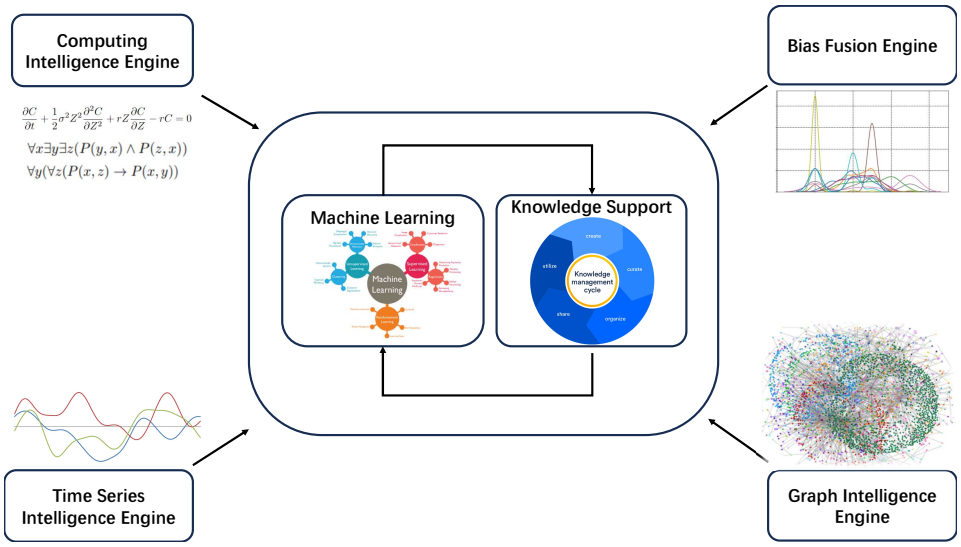

Figure 3.9: Knowledge Informed Orchestration Engine with (MLAKS)

3.3.1 Computing Intelligence Engine

The Computing Intelligence Engine is a sophisticated analytical framework designed to integrate the principles of carbon physics and financial dynamics, enhanced through PDE processing, knowledge orchestration, and intelligent computing with deep intelligence support. This multi-faceted system is aimed at optimizing decision-making in the carbon markets, enabling stakeholders to navigate the complexities of environmental sustainability and economic viability.

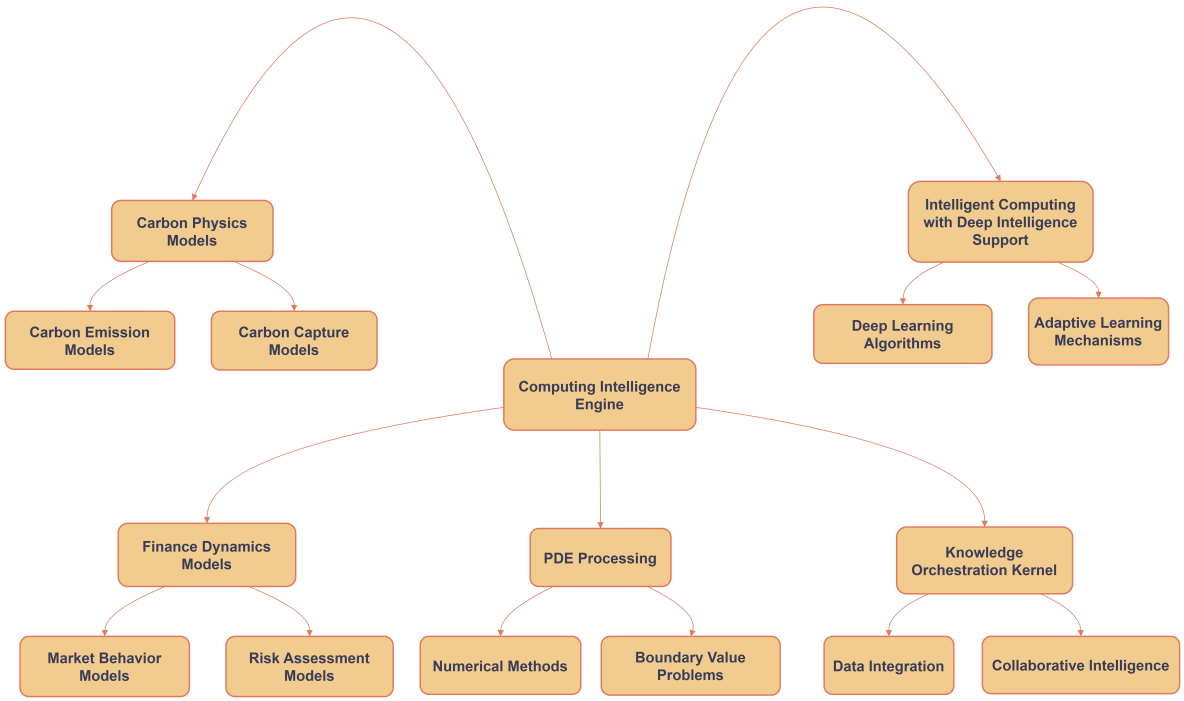

Figure 3.10: Computing Intelligence Engine

Figure 3.10 shows the structure of the engine, in which Carbon Physics Models utilize advanced computing algorithms to process the physical behaviors associated with carbon emissions and sequestration. The Carbon Emission Models quantify emissions across various sectors, providing crucial insights into sources and trends. They employ statistical analyses and empirical data to forecast future emission scenarios, which are essential for policy formulation and compliance monitoring. Complementing these are the Carbon Capture Models, which evaluate the effectiveness of carbon capture technologies by modeling the chemical and physical processes involved in sequestration. These models inform stakeholders about the potential impacts and feasibility of different technologies aimed at reducing carbon footprints.

The Finance Dynamics Models complement the physical models by assessing the economic factors influencing the carbon credit market. These models leverage financial theories to simulate pricing and trading behaviors. The Market Behavior Models analyze how market participants react to regulatory changes, technological innovations, and shifts in public attitudes toward climate action. By utilizing behavioral economics, these models provide insights into market volatility and potential pricing trends. Additionally, the Risk Assessment Models are critical for understanding exposure to financial risks. They integrate environmental and economic metrics to evaluate the risks associated with

carbon trading and investments in carbon-reducing technologies, enabling stakeholders to develop effective risk mitigation strategies.

The integration of PDE Processing significantly enhances the engine's capability to model complex systems where variables change continuously. This component employs a range of numerical techniques to solve the partial differential equations arising from the carbon physics and finance dynamics models. These methods enable detailed simulations that inform strategic decision-making in carbon management. Moreover, the aspect of Boundary Value Problems addresses specific mathematical challenges that are critical for forecasting outcomes of environmental and economic policies, ensuring accurate modeling of real-world scenarios.

Central to the engine's functionality is the Knowledge Orchestration Kernel, which manages and integrates diverse knowledge sources to produce actionable insights. This process ensures the seamless amalgamation of data from various models and external sources, enriching the analysis and enhancing the accuracy of the insights generated. This integrated data environment allows for more reliable forecasting and decision-making. Additionally, the Knowledge Orchestration Kernel facilitates collaboration among stakeholders, encouraging input from domain experts and enhancing the depth and applicability of the analyses. This collaborative approach fosters a richer understanding of the complexities of carbon management and financial dynamics.

The engine incorporates Intelligent Computing, utilizing deep learning and advanced analytics to bolster decision-making processes. Deep Learning Algorithms leverage neural networks to analyze large datasets, uncovering complex patterns and relationships that traditional methods may overlook. This capability enhances predictive accuracy and supports proactive decision-making. Furthermore, the engine's intelligent computing features enable continuous learning from new data and stakeholder interactions. This adaptive learning ensures that the models remain relevant and effective in responding to the evolving landscape of carbon markets.

The Computing Intelligence Engine represents a cutting-edge tool that synergizes carbon physics, financial dynamics, and advanced mathematical modeling through PDE processing, along with knowledge orchestration and intelligent computing. By integrating these diverse components, the engine offers a robust platform for analyzing and predicting the impact of carbon management strategies on both environmental sustainability and economic performance. This holistic approach enhances risk assessment and decision-making capabilities, facilitating a deeper understanding of the intricate relationships among carbon emissions, market dynamics, and policy effectiveness, ultimately

driving the transition to a sustainable low-carbon economy.

3.3.2 Time Series Intelligence Engine

The Time Series Intelligence Engine (TSIE) specializes in the analysis of temporal data, focusing on the identification of trends, seasonal patterns, and cyclical behaviors within datasets that evolve over time. This module is particularly adept at analyzing and forecasting based on historical time-related data, which is crucial in fields such as finance and carbon credit supply chain management within a sustainable carbon economy. By integrating advanced spatiotemporal analysis and hyper-feature processing, this engine enhances the capability to discern trend patterns, thereby enabling informed decision-making based on anticipated future states and optimizing operational planning.

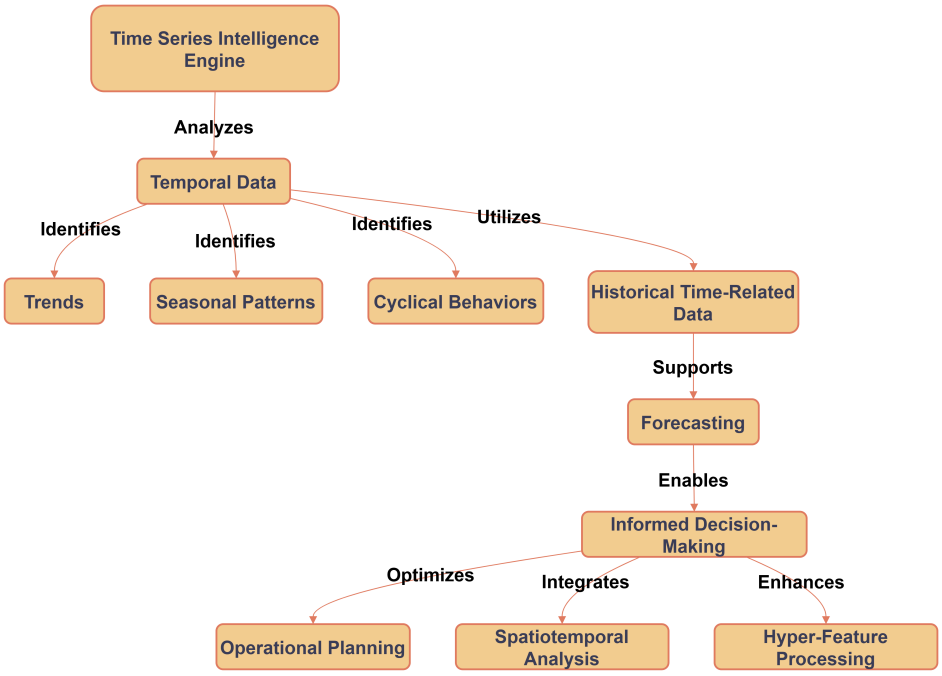

Figure 3.11: Time Series Intelligence Engine

As shown in Figure 3.11, central to the functionality of the TSIE is its ability to process historical time-related data. This capability allows the engine to discern long-term trends that can significantly impact the carbon credit market. For instance, by analyzing past carbon emissions data, the TSIE can identify patterns related to seasonal variations in emissions, thus enabling stakeholders to anticipate fluctuations in carbon credit prices and availability. Such insights are invaluable for optimizing strategies

around carbon credit purchasing and trading, ensuring that organizations are well-prepared to respond to market changes.

Moreover, the TSIE enhances its analytical capabilities through advanced spatiotemporal analysis and hyper-feature processing. Spatiotemporal analysis allows the engine to examine not only temporal changes but also geographical factors that may influence carbon credit markets. By integrating location-based data with temporal trends, decision-makers can gain a more nuanced understanding of how various factors interrelate over time. Hyper-feature processing further enriches this analysis by generating additional dimensions of data, leading to more comprehensive insights that support complex decision-making.

The implications of these capabilities extend to operational planning as well. With the insights derived from the TSIE, organizations can engage in informed decision-making that aligns with anticipated future states of the carbon market. This foresight enables more strategic operational planning, allowing companies to optimize their carbon credit portfolios and enhance compliance with regulatory requirements.

The Time Series Intelligence Engine is a critical asset in the carbon credit management framework, adept at analyzing temporal data to identify trends and patterns. Its ability to integrate advanced analytical techniques not only enhances the decision-making process but also supports the optimization of operational strategies within a sustainable carbon economy. By providing robust forecasting capabilities, the TSIE empowers organizations to navigate the complexities of the carbon credit market effectively, fostering more sustainable practices and compliance with environmental standards.

3.3.3 Graph Intelligence Engine

Specializing in the management and analysis of relational data through graph-based structures, the Graph Intelligence Engine excels at uncovering relationships and patterns within complex networks. This capability is particularly beneficial in areas such as social network analysis, fraud detection, and recommendation systems. By leveraging graph theory and algorithms, this engine enhances the framework's ability to visualize connections and dependencies, thereby fostering more informed and strategic decision-making.

One of the core functions of the GIE is its ability to analyze relational data, which often includes interdependencies among various stakeholders, regulatory frameworks, and environmental factors. As shown in Figure 3.12, by applying graph theory and advanced algorithms, the engine can identify and visualize intricate relationships within

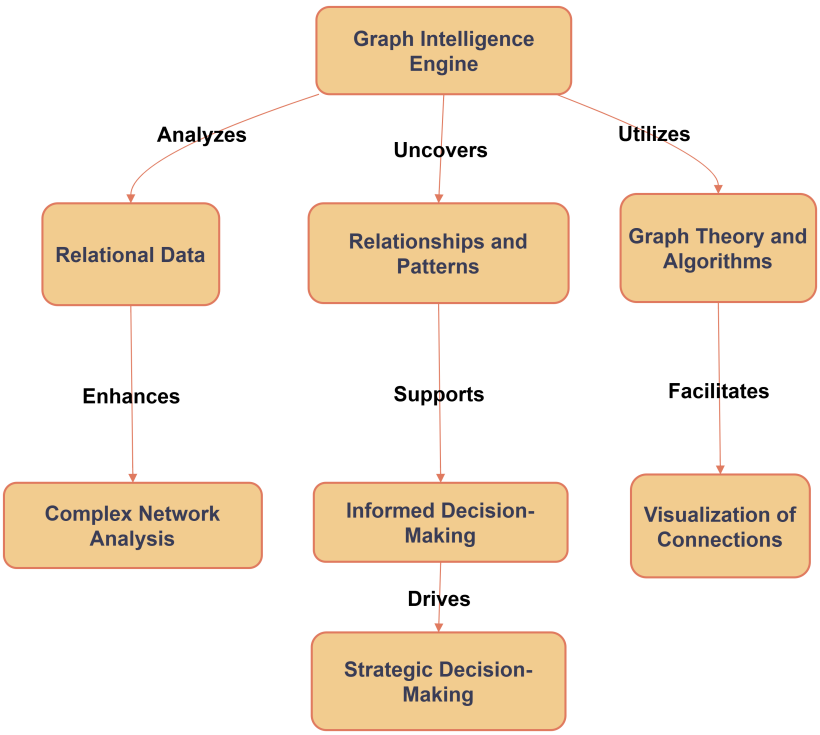

Figure 3.12: Graph Intelligence Engine

the data, allowing decision-makers to gain a clearer understanding of how different elements interact within the carbon credit ecosystem. This capability is particularly beneficial in scenarios where understanding the dynamics of stakeholder interactions can lead to more effective engagement and compliance strategies.

The GIE excels in uncovering significant relationships and patterns that may not be immediately apparent through traditional data analysis methods. For instance, in the context of carbon credit management, the engine can reveal connections between carbon credit prices and environmental indicators, or highlight relationships between market participants that may influence trading behavior. This insight is vital for stakeholders aiming to optimize their positions in the carbon market and make strategic decisions based on a comprehensive view of the underlying data.

By facilitating the visualization of connections and dependencies, the GIE enhances the overall analytical capability of the carbon credit management system. Visual representations of relational data allow users to explore complex networks intuitively, making it easier to identify potential opportunities and risks. This graphical insight can drive strategic decision-making by enabling stakeholders to anticipate changes in the market or shifts in regulatory landscapes.

The Graph Intelligence Engine (GIE) is a critical component of the carbon credit management system, offering advanced capabilities for analyzing relational data and uncovering complex patterns. By leveraging graph theory and algorithms, the GIE enhances the framework's ability to visualize connections and dependencies, thus fostering informed and strategic decision-making. The insights generated by the GIE not only aid in navigating the complexities of the carbon credit market but also empower organizations to align their strategies with sustainability goals effectively. As the carbon credit landscape continues to evolve, the GIE,Äôs contributions will be instrumental in ensuring that decision-makers are equipped with the knowledge necessary to thrive in this dynamic environment.

3.3.4 Bias Fusion Engine

The Bias Fusion Engine is a sophisticated analytical system designed to monitor bias and disparity while adaptively and optimally fusing various biases to achieve consistent and reliable decision support. This engine serves as a crucial tool for organizations aiming to enhance fairness and reduce the impact of biases in their decision-making processes.

As shown in Figure 3.13, Bias Monitoring Module in Bias Fusion Engine is responsible for systematically tracking various types of biases present in the data and decision-making processes. It begins with the Data Collection component, which gathers data from multiple sources, including historical records, user inputs, and algorithmic outputs. The collected data provides the foundation for identifying biases that may influence decisions. Once the data is collected, specialized Bias Detection Algorithms are employed to detect biases across different dimensions, such as gender, race, and socioeconomic status. These algorithms analyze patterns and anomalies within the data, facilitating the identification of potential biases that may affect decision outcomes.

Complementing the monitoring efforts is the Disparity Assessment Module, which evaluates the extent and implications of detected biases. This module employs various Disparity Metrics to quantify disparities resulting from biases. By calculating these metrics, it assesses how biases influence different groups and identifies areas where inequities may arise. Following the assessment of disparities, the Impact Analysis component analyzes the potential effects of identified biases on decision-making processes. Understanding the consequences of biases is essential for determining the necessary adjustments to mitigate their effects.

A critical component of the engine is the Adaptive Fusion Algorithm, which optimally fuses various biases to arrive at a balanced decision support output. This element

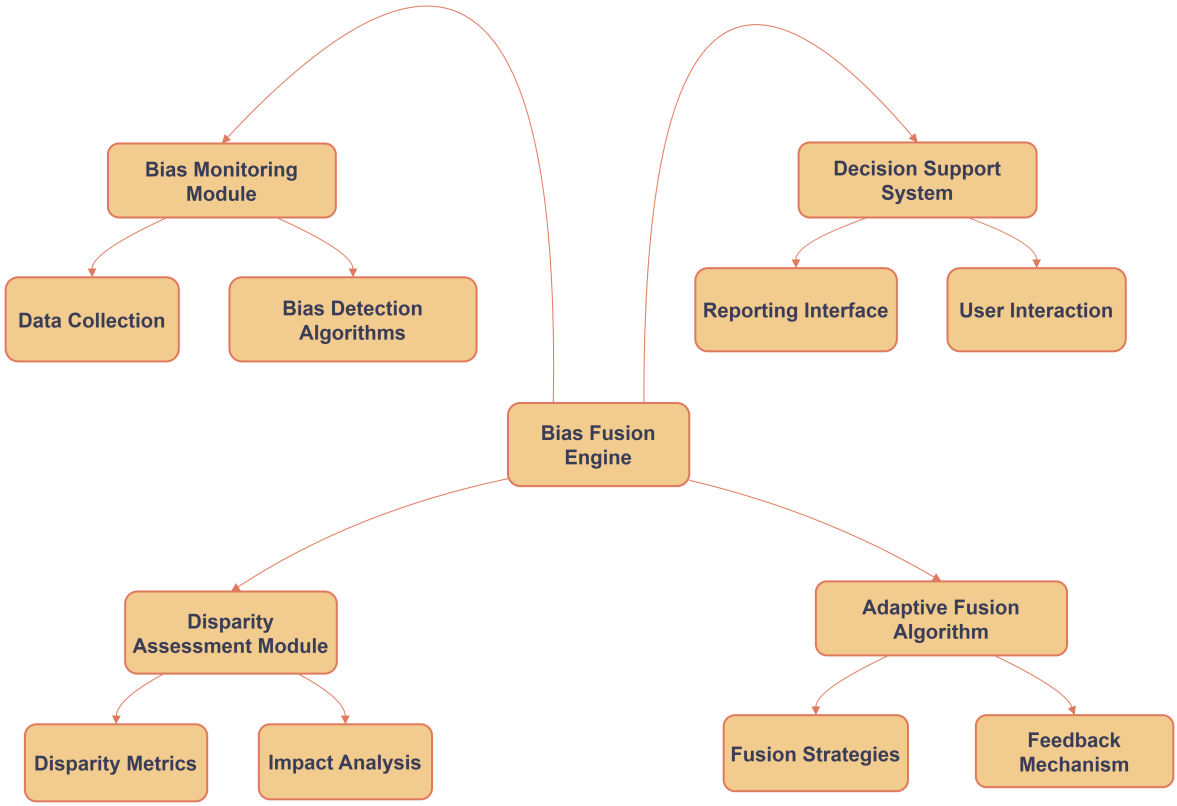

Figure 3.13: Bias Fusion Engine

involves the development of Fusion Strategies that intelligently combine different biases. By employing techniques such as weighted averaging and decision trees, the algorithm seeks to minimize the negative effects of biases while preserving the integrity of the decision-making process. Additionally, the Feedback Mechanism allows the engine to learn from past decisions and their outcomes. By continuously integrating feedback, the algorithm adapts its fusion strategies to enhance the reliability and fairness of future decisions.

One of the important components of the Bias Fusion Engine is the Decision Support System, which synthesizes information and outputs actionable insights for stakeholders. This system features a Reporting Interface that presents the results of the bias fusion process through a user-friendly format. It enables stakeholders to understand the implications of biases and the adjustments made to decisions, promoting transparency in the decision-making process. Furthermore, the system facilitates User Interaction, allowing stakeholders to input preferences and provide additional context that may influence decision-making. This interactivity ensures that the decision support system remains aligned with the needs and expectations of users.

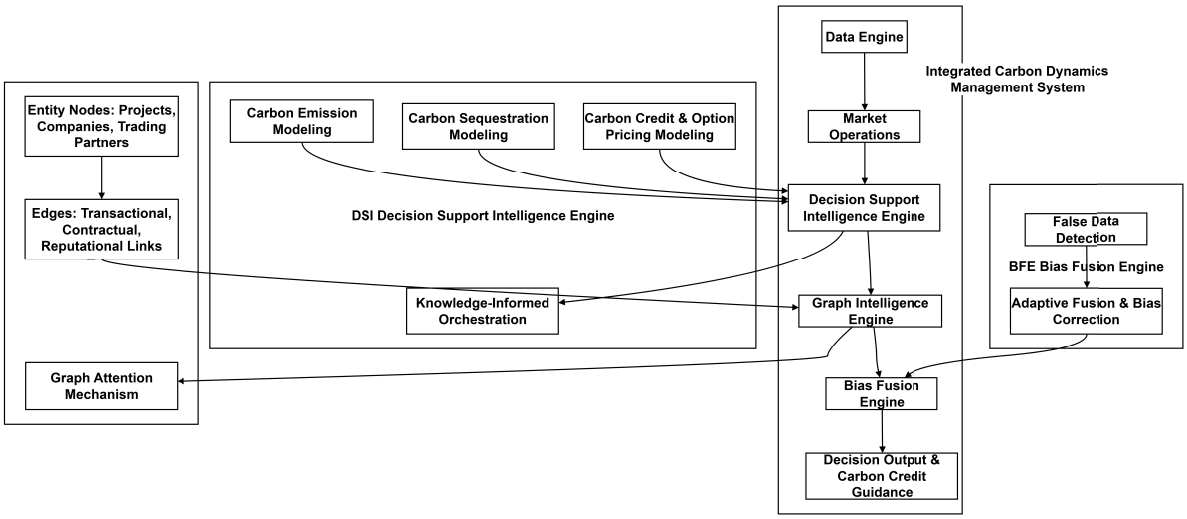

Figure 3.14: System Architecture

The Bias Fusion Engine is an analytical framework that integrates bias monitoring, disparity assessment, adaptive fusion algorithms, and decision support capabilities. By systematically addressing biases and their impacts, this engine empowers organizations to make more equitable and informed decisions. Its holistic approach not only enhances decision-making quality but also fosters trust and accountability in organizational practices, ultimately driving more effective and fair outcomes.

3.3.5 Architecture of the Integrated Carbon Dynamics Management System

The ICDMS is structured as a modular yet integrated system, where each engine contributes specialized functionality while maintaining seamless data and workflow connectivity. Figure 3.14 illustrates the architecture of the Integrated Carbon Dynamics Management System (ICDMS), depicting the relations between its core modules across Chapters 3 - 6.

At the foundational level, the *Data Engine* (DE) collects, validates, and preprocesses raw carbon-related data, which is then utilized by *Market Operations* (MO) to capture transactional and operational contexts relevant to carbon trading. These foundational modules provide the necessary inputs for the *Decision Support Intelligence* (DSI) engine, elaborated in Chapter 4. DSI operationalizes the theoretical framework presented in Chapter 3 by developing computational models for carbon emissions, carbon sequestration, carbon credits, and associated option pricing. Knowledge-Informed Orchestration

(KAR) within DSI ensures that dynamic dependencies, non-linear interactions, and systemic behaviors are faithfully represented, projecting them into actionable decision-making processes for carbon credit management and trading.

Building upon the outputs of DSI, the *Graph Intelligence Engine* (GIE), presented in Chapter 5, captures the relational dependencies among entities using graph-based representations. Nodes in the graph represent projects, companies, and trading partners, while edges encode transactional, contractual, and reputational links. The incorporation of attention mechanisms allows GIE to dynamically weight the influence of interconnected entities, thereby extending the predictive capabilities of DSI into a relational domain. This relational modeling enables the system to account for both local and global structural dependencies, reflecting how inter-entity correlations affect carbon credit flows and associated decisions.

The *Bias Fusion Engine* (BFE), discussed in Chapter 6, operates on the outputs of DSI and GIE to enhance system robustness. It addresses biases introduced by false data injection (FDI) or cognitive biases through preventive security measures and adaptive fusion techniques. By detecting compromised data and applying correction strategies, BFE ensures that decision outputs remain reliable and consistent even under adversarial or noisy conditions. Consequently, BFE preserves the integrity of both computational predictions and relational analyses, safeguarding the overall decision-making process.

The ICDMS follows a layered and sequential workflow, including data acquisition and preprocessing (DE, MO), predictive modeling and orchestration (DSI), relational enrichment (GIE), and bias mitigation and robustness (BFE). This modular design provides both specialization and scalability, allowing each engine to focus on its functional strengths while maintaining coherence through defined data flows. Modeling relational dependencies with attention mechanisms enhances prediction accuracy and system interpretability, while bias fusion mechanisms ensure resilience against corrupted inputs. The integrated architecture thus represents a comprehensive, reliable framework for carbon dynamics management, linking theoretical modeling, relational intelligence, and robust decision support in a unified system.

3.3.6 Summary

The integration of the diverse engines within the Knowledge Informed Orchestration with Machine Learning and Knowledge-Enabled (MLAKS) framework results in a comprehensive system capable of addressing complex carbon dynamics management challenges. Each module, ranging from the Data Engine and Market Operations to the Decision

Support Intelligence Engine (DSI), Graph Intelligence Engine (GIE), and Bias Fusion Engine (BFE), contributes specialized capabilities that collectively enhance system functionality and adaptability. The DSI operationalizes computational models for carbon emissions, sequestration, credits, and option pricing, incorporating Knowledge-Informed Orchestration (KAR) to capture dynamic dependencies and non-linear system behaviors. The GIE extends these models into a relational domain, representing entities and their interconnections as graphs and employing attention mechanisms to account for the influence of interconnected nodes. Meanwhile, the BFE ensures robustness against biases and false data injections, safeguarding the reliability of outputs under adversarial or noisy conditions.

This holistic integration not only improves operational efficiency but also fosters continuous learning and adaptive decision-making. The collaborative nature of the modules allows for dynamic, informed, and strategically aligned decision-making processes. At the core of the framework, the Machine Learning and Knowledge-Enabled Cores facilitate seamless data flow and orchestrated interaction among all modules, enabling collaborative processing, relational analysis, and bias mitigation. By providing this cohesive architecture, the framework supports the effective deployment of advanced machine learning algorithms and knowledge management practices, yielding real-time insights, enhancing predictive accuracy, and strengthening operational agility in complex, data-driven carbon management environments.

CHAPTER 4

COMPREHENSIVE INTELLIGENT DECISION SUPPORT SYSTEM WITH KNOWLEDGE INFORMED ORCHESTRATION

In this work, we introduce a novel computational framework, Knowledge Informed Orchestration with Kolmogorov-Arnold Representation (KIOKAR), designed to address the complexities of financial modeling, specifically in the context of carbon credit option pricing. The KIOKAR framework integrates the Kolmogorov-Arnold Representation (KAR) to decompose multivariate functions, facilitating a more efficient and interpretable representation of complex financial systems.

The KAR mechanism provides a mathematical foundation for breaking down intricate multivariate functions into simpler, more manageable components, offering a significant advantage in terms of model complexity reduction and interpretability [210, 245]. By incorporating KAR into our computational framework, we enhance the model ability to capture the dynamic interactions between various factors within carbon finance, which is characterized by complex, nonlinear relationships and multivariable dependencies.

To demonstrate the effectiveness of KIOKAR, we apply it to a case study involving carbon credit option pricing. This domain is particularly challenging due to the interplay between financial dynamics, regulatory constraints, and physical carbon market variables. The KIOKAR framework addresses this challenge by incorporating both carbon finance rules and physical constraints directly into the architecture of the model. This approach ensures that the model not only adheres to fundamental financial principles but also integrates critical domain-specific knowledge, which is essential for accurate pricing and decision-making within carbon markets.

Furthermore, the inclusion of these constraints within the KIOKAR framework significantly improves the model reliability and interpretability. By embedding domain-specific knowledge directly into the learning process, the framework enables the model to generate outputs that are both statistically sound and physically meaningful, thus providing more robust and actionable insights for stakeholders in the carbon market.

The KIOKAR framework represents a significant advancement in computational modeling for carbon finance. By leveraging the power of the Kolmogorov-Arnold Representation and incorporating domain-specific knowledge, the framework offers enhanced accuracy, efficiency, and interpretability, providing a more reliable tool for navigating the complexities of carbon credit option pricing. The proposed framework enables the integration of diverse knowledge into a customized system, facilitating synthesis through training. It incorporates factors such as original carbon emissions, carbon sequestration, decay rates, and their interactions, creating a unified system that dynamically coordinates these elements to enhance the framework. Additionally, the framework can construct a machine learning process using existing knowledge, even in the absence of data. By employing a meshless approach, it generates random solutions for knowledge evolution, thereby improving the efficiency of modeling and analyzing carbon dynamic systems.

4.1 Computational Knowledge Modeling

4.1.1 Carbon Emission Modeling

4.1.1.1 Carbon Emission Rate

The carbon emission rate, denoted as $P(t)$, represents the rate at which carbon dioxide (CO_2) or other greenhouse gases are released into the atmosphere over a specified period. This dynamic process can be effectively modeled using an exponential growth function, which captures the continuous and compounding nature of emissions over time. The general form of the model is given by

$$P(t) = P_0 \cdot e^{rt}, \tag{4.1}$$

where $P(t)$ is the emission rate at time t, P_0 is the initial emission rate at $t = 0$, r is the growth rate of emissions, e is the base of the natural logarithm, and t is time. This model describes how the emission rate evolves over time under the assumption of a constant growth rate r.

4.1.1.2 Accumulated Carbon Emission

The concept of accumulated carbon emissions refers to the total amount of carbon dioxide (CO_2) or its equivalent greenhouse gases released into the atmosphere over a designated period. This total is typically expressed in terms of metric tons of CO_2 or CO_2-equivalent gases. It is important to assess these emissions over various timescales, such as annually, over a specific project lifecycle, or for broader regional or global analyses.

The total accumulated carbon emission C over a period of time from $t = 0$ to $t = T$ can be represented as the integral of the emission rate function $P(t)$:

$$C(T) = \int_0^T P(t)\,dt, \tag{4.2}$$

where $C(T)$ denotes the accumulated emissions over T, and $P(t)$ is the emission rate as defined previously.

This integral formulation provides a cumulative measure of emissions, taking into account the varying rate over time. As described in equation (4.1), the exponential growth model suggests that emissions increase at a constant percentage rate over time, which is often used to reflect processes such as technological advancement or increasing consumption patterns. Under this assumption, the total accumulated emissions over a period from $t = 0$ to $t = T$ can be computed by substituting the exponential emission rate function into the integral expression for total emissions

$$C(T) = \int_0^T P_0 \cdot e^{rt}\,dt. \tag{4.3}$$

Solving this integral, we obtain

$$C(T) = P_0 \cdot \left[\frac{e^{rT} - 1}{r}\right]. \tag{4.4}$$

This formula represents the total carbon emissions accumulated over the time period T given an initial emission rate P_0, a growth rate r, and a time horizon T. It shows that the total accumulated emissions increase more rapidly as T and r increase, reflecting the compounding nature of exponential growth.

The derived equation for $C(T)$ under the exponential growth model highlights the relationship between initial emission rates, growth rates, and the time horizon in determining the total accumulated emissions. Notably, the growth rate r plays a crucial role in shaping the outcome; even a modest increase in r can lead to a significant rise in total emissions over time. This illustrates the importance of controlling emission growth rates in order to mitigate the long-term environmental impact.

Furthermore, the exponential model provides insights into the challenges associated with managing carbon emissions in scenarios where they grow rapidly over time. It is evident from the expression for $C(T)$ that interventions to reduce r or to limit the duration T of emissions would be critical in reducing the overall environmental impact.

The models in question serve as critical instruments in the analysis and evaluation of carbon emissions, offering a structured approach to understanding both the temporal dynamics of carbon release and its aggregate accumulation over defined time intervals. Specifically, these models differentiate between two key metrics: the carbon emission rate, which quantifies the speed at which carbon is emitted over a given period, and the total carbon emission, which represents the cumulative amount of carbon released across a specified timeframe. These analytical tools are indispensable for assessing the trajectory of emissions, forecasting their long-term environmental impact, and guiding the formulation of policies that aim to mitigate climate change and foster sustainable development.

By providing a means to track and project both the immediate and cumulative consequences of carbon emissions, these models support informed decision-making in the context of environmental regulation and climate action. They enable policymakers to evaluate current emission trends and anticipate future scenarios, facilitating the design of targeted strategies for emission reduction. In doing so, they contribute significantly to global efforts to combat climate change, reduce environmental degradation, and promote practices that enhance the long-term viability of ecosystems and human societies. Furthermore, the models' ability to offer quantitative predictions regarding future emissions plays a crucial role in developing effective mitigation policies, setting achievable emissions reduction targets, and monitoring progress towards global sustainability goals.

4.1.2 Carbon Sequestration Modeling

4.1.2.1 Carbon Sequestration Rate

Carbon sequestration is a crucial natural process in which carbon dioxide (CO_2) or its equivalent greenhouse gases are removed from the atmosphere and stored in carbon sinks, such as forests, oceans, and soil. The rate at which this process occurs is referred to as the carbon sequestration rate, denoted as $R(t)$. Accurately modeling this rate is essential for understanding the potential of natural systems to mitigate atmospheric CO_2 levels and contribute to climate change mitigation.

In many natural processes, the rate of sequestration increases initially but eventually

levels off as the system reaches its capacity to store carbon. This behavior is typically modeled using a logistic growth function, which is often employed to describe phenomena that exhibit growth that accelerates at first and then slows as the system approaches a maximum limit. The logistic growth model for carbon sequestration can be expressed as

$$R(t) = \frac{R_{\max}}{1 + e^{-k(t-t_0)}} \tag{4.5}$$

where $R(t)$ is the carbon sequestration rate at time t, $R_{\max}$ represents the maximum possible sequestration rate, or the upper limit of the system capacity to store carbon, k is the growth rate constant, which determines the rate at which sequestration increases over time, t_0 is the inflection point, which represents the time at which the rate of sequestration reaches half of its maximum value and begins to level off.

This model captures the logistic growth behavior of carbon sequestration, characterized by three key parameters, including the Maximum Sequestration Rate ($R_{\max}$), the Growth Rate Constant (k), and the Inflection Point (t_0). $R_{\max}$ represents the upper limit of carbon absorption, influenced by factors such as ecosystem health and environmental conditions. It provides frameworks for understanding how the carbon sequestration rate changes over time in various environmental and policy contexts.

The growth rate constant (k) governs the speed at which sequestration increases, with higher values indicating faster growth. The inflection point (t_0) marks the time when sequestration reaches half of its maximum potential, signaling the transition from rapid growth to stabilization. These parameters collectively describe the evolution of carbon sinks, particularly as they approach saturation. The model is widely used to assess the potential of carbon sinks, including forests and soils, in mitigating atmospheric CO_2.

4.1.2.2 Accumulated Carbon Sequestration

The concept of accumulated carbon sequestration $S(t)$ refers to the total amount of carbon dioxide (CO_2) or its equivalent greenhouse gases that have been sequestered by a natural system, such as forests, soils, or oceans, up to a given time t. This quantity is of significant importance in environmental sciences, as it allows for the assessment of the effectiveness of carbon sinks in mitigating atmospheric CO_2 levels over time. The rate of sequestration $R(t)$, which represents the instantaneous amount of carbon removed or stored in these systems, serves as the foundation for calculating the accumulated sequestration.

The total amount of carbon sequestered up to time (t) can be expressed as the integral of the sequestration rate $R(t)$ over the interval from (0) to (t):

$$S(t) = \int_0^t R(\tau), d\tau, \tag{4.6}$$

where (S(t)) represents the accumulated carbon sequestration at time (t), and $R(\tau)$ is the instantaneous sequestration rate. This formulation provides a general relationship between sequestration rate and accumulated sequestration. However, in real ecological systems, the sequestration rate does not grow indefinitely. Instead, it often follows a logistic growth pattern:

$$R(t) = \frac{R_{\max}}{1 + e^{-k(t-t_0)}}, \tag{4.7}$$

where $R_{\max}$ is the maximum sequestration rate, (k) is the growth constant, and t_0 is the inflection point when sequestration reaches half its maximum rate. This logistic function refines the general formulation by capturing the S-curve behavior typical of biological and ecological processes. Substituting the logistic expression for $R(t)$ into the accumulation formula yields:

$$S(t) = \int_0^t \frac{R_{\max}}{1 + e^{-k(\tau-t_0)}}, d\tau, \tag{4.8}$$

which describes accumulated sequestration as a function of time under realistic ecological dynamics. Although this integral is difficult to solve analytically for arbitrary parameter values, it can be evaluated using numerical methods or suitable approximations.

The model for accumulated carbon sequestration, described by an integral that generally lacks a closed-form solution, is often evaluated using numerical integration techniques such as the trapezoidal rule, Simpson rule, or more advanced methods like Runge-Kutta. These approaches allow for the practical approximation of sequestration dynamics based on model parameters $R_{\max}$, k, and t_0. The parameters play critical roles: $R_{\max}$ determines the maximum sequestration capacity, k influences the rate at which sequestration approaches $R_{\max}$, and t_0 marks the point where the sequestration rate begins to slow, signaling the system limitations. This model is particularly valuable for evaluating long-term sequestration projects such as reforestation or soil carbon storage, helping policymakers estimate sequestration potential and understand the time scales involved in carbon sink saturation. While the integral formulation captures the growth and eventual saturation behavior of carbon sinks, numerical methods provide a practical means to evaluate the accumulated sequestration, making the model an essential tool for both researchers and policymakers in climate change mitigation efforts.

4.1.3 Carbon Credit Modeling

The concept of carbon credits plays a crucial role in climate change mitigation by quantifying the reduction or removal of greenhouse gases (GHGs), typically expressed in metric tons of carbon dioxide equivalent (CO_2e). Carbon credits represent the amount of carbon removed from the atmosphere through various mitigation efforts, such as reforestation, carbon capture and storage, or renewable energy adoption. These credits are central to carbon markets, where entities can trade emissions reductions to meet regulatory or voluntary climate goals.

In parallel, carbon balance refers to the comparison between the amount of carbon stored in ecosystems and the amount released into the atmosphere through human activities. Carbon storage occurs in natural systems like forests, soils, and oceans, while carbon emissions result primarily from anthropogenic activities, particularly the combustion of fossil fuels. Maintaining a positive carbon balance, where sequestration exceeds emissions, is vital for mitigating the impacts of climate change.

The net carbon balance at a given time t is defined as the difference between carbon emissions and carbon sequestration. This balance is crucial for determining the surplus or deficit of carbon in the system, which directly impacts the issuance of carbon credits. Mathematically, the net carbon balance $B(t)$ at time t can be expressed as

$$B(t) = E(t) - S(t), \tag{4.9}$$

where $B(t)$ is the net carbon balance at time t, $E(t)$ represents the carbon emission rate at time t, $S(t)$ denotes the carbon sequestration rate at time t. A positive value of $B(t)$ indicates that emissions exceed sequestration, leading to a carbon deficit, while a negative value signifies that more carbon is being sequestered than emitted, resulting in a carbon surplus.

The carbon balance is a dynamic process, evolving over time as both emissions and sequestration rates change. To capture this dynamic nature, the carbon balance accumulation can be formulated as an integral over time, taking into account the emission and sequestration rates at each moment:

$$B(t) = \int_0^t (P(\tau) - R(\tau))\, d\tau, \tag{4.10}$$

where $B(t)$ is the cumulative net carbon balance at time t, $P(t)$ represents the carbon emission rate at time t, $R(t)$ is the carbon sequestration rate at time t.

This equation expresses the cumulative effect of carbon emissions and sequestration over time, where $P(t)$ and $R(t)$ are functions that describe the instantaneous rates of

emission and sequestration, respectively. The integral quantifies the net balance between these two processes, with the result determining the overall carbon status of the system.

The net carbon balance, as formulated above, provides the foundation for determining the amount of carbon credits an entity may earn or owe. If the system exhibits a net sequestration (negative $B(t)$), the entity has achieved a surplus, generating carbon credits. Conversely, if emissions exceed sequestration (positive $B(t)$), the entity faces a carbon deficit and may need to purchase carbon credits to offset the imbalance.

The carbon credit $\mathscr{C}(t)$ associated with the net carbon balance $B(t)$ at time t can be expressed as

$$\mathscr{C}(t) = S(t) - E(t), \tag{4.11}$$

where $\mathscr{C}(t)$ represents the carbon credit at time t, $S(t)$ is the carbon sequestration rate at time t, $E(t)$ is the carbon emission rate at time t.

A positive value of $\mathscr{C}(t)$ indicates that more carbon is being sequestered than emitted, resulting in the generation of carbon credits. Conversely, a negative value of $\mathscr{C}(t)$ implies that emissions exceed sequestration, and thus the entity would be liable for carbon debits.

The carbon credit system incentivizes entities to reduce emissions and enhance carbon sequestration by linking their net carbon balance to the issuance of carbon credits. A positive carbon balance, resulting in carbon credits, indicates that an entity has successfully sequestered more carbon than emitted, contributing to global climate goals and enabling participation in carbon trading markets. Conversely, a negative carbon balance signals the need for corrective actions, such as increasing sequestration or reducing emissions, to meet climate objectives.

This framework links emission reduction efforts to measurable outcomes, playing a critical role in facilitating the transition to a low-carbon economy. The modeling of carbon credits and carbon balance offers a rigorous method for quantifying the effectiveness of carbon mitigation strategies, determining whether entities are positively contributing to global carbon goals or need to address deficits. By using carbon credits as a tool to incentivize emission reductions, this system plays a crucial role in advancing global climate change mitigation efforts.

4.1.4 Carbon Credit Supplement Pricing Modeling

Carbon credits incentivize activities that reduce greenhouse gas emissions or enhance carbon removal, contributing to climate change mitigation by establishing a market

for carbon abatement. The price of carbon credits is determined by supply and demand dynamics, with supply driven by entities engaged in carbon sequestration or emissions reduction activities, such as reforestation or renewable energy projects. Demand comes primarily from corporations or governments aiming to meet emission reduction targets. The equilibrium price occurs when supply matches demand, though fluctuations can arise due to factors like regulatory changes, technological advances, or shifts in market sentiment. Key drivers of supply include innovations that improve carbon removal efficiency, while demand is influenced by policies such as stricter emission reduction goals or carbon pricing mechanisms.

Demand $\mathscr{C}$ signifies the market willingness to purchase carbon credits at a specific price level (Z). Typically, the demand for carbon credits increases as prices decline, largely driven by compliance needs and sustainability commitments from enterprises. Conversely, supply ($\mathscr{C}$) reflects the quantity of carbon credits that producers are prepared to offer, which generally rises with price increases. This supply is constrained by the number and quality of carbon emission reduction projects available.

A fundamental aspect of the supply and demand model is identifying the equilibrium point where supply equals demand. At this equilibrium, the market price stabilizes, fulfilling the condition

$$\mathscr{D}(Z) = \mathscr{C}(Z) \tag{4.12}$$

Demand and supply can typically be expressed as linear functions. The demand function is represented as

$$\mathscr{D}(Z) = \mathscr{D} - dZ \tag{4.13}$$

where D_0 denotes the initial level of demand, and d represents the price elasticity of demand. The supply function is expressed as:

$$\mathscr{C}(Z) = \mathscr{C} + cZ \tag{4.14}$$

where $\mathscr{C}$ indicates the initial level of supply, and c denotes the price elasticity of supply. To find the equilibrium price Z^*, the demand function is set equal to the supply function

$$\mathscr{D} - dZ^* = \mathscr{C} + cZ^* \tag{4.15}$$

Solving for Z^* yields

$$Z^* = \frac{\mathscr{D} - \mathscr{C}}{d + c} \tag{4.16}$$

which represents the optimal pricing for the equilibrium between demand and supply.

The supply-demand framework for carbon credits is essential for formulating climate policies, directing investments in carbon reduction technologies, and ensuring the efficient operation of carbon markets. By analyzing these dynamics, policymakers can better incentivize emissions reductions and facilitate the transition to a low-carbon economy. The equilibrium price, which is determined by the balance between supply and demand, plays a crucial role in climate change mitigation. It encourages the reduction of greenhouse gas emissions and promotes carbon sequestration activities, providing a rational pricing mechanism for carbon credits in a market-driven context. This pricing mechanism ensures that carbon credits reflect the true costs of emissions reductions and carbon sequestration efforts, aligning economic incentives with environmental goals.

4.1.5 Carbon Credit Option Pricing Modeling

Carbon credit options are financial derivatives with the underlying asset of carbon credits, each representing the right to emit one metric ton of carbon dioxide or its equivalent in other greenhouse gases at a predetermined price within a specified timeframe.

Based on the carbon credit pricing Z, the carbon credit option price C can be formulated by Black-Scholes model (BS model [154, 155]) as

$$C = ZN(d_1) - Ke^{-rT}N(d_2) \tag{4.17}$$

where

$$d_1 = \frac{\ln(Z/K) + (r + \sigma^2/2)T}{\sigma\sqrt{T}} \tag{4.18}$$

$$d_2 = d_1 - \sigma\sqrt{T} \tag{4.19}$$

in which C refers to the call option price, Z the current price of carbon credits, K the strike price, T the time to expiration, r is the risk-free interest rate, σ is the volatility of the underlying asset. The terms $N(d_1)$ and $N(d_2)$ refer to the cumulative distribution function (CDF) of the standard normal distribution evaluated at d_1 and d_2, respectively.

Therefore, the carbon credit option pricing can be obtained as vital instruments in carbon markets, providing participants with strategic opportunities to manage risk and speculate on price movements.

Based on the aforementioned knowledge, we can initially construct a computational knowledge system. However, this system exhibits a significant deficiency in its dynamic representation. Specifically, it fails to account for the dynamic processes and decay

associated with carbon emissions and carbon sequestration, which hinders its ability to accurately reflect the complexities of real-world dynamics. Furthermore, the effects of boundary conditions and initial conditions are not integrated into the model, thereby limiting its comprehensiveness.

In the option pricing model for carbon credits, while the adoption of an optimal equilibrium pricing strategy aims to minimize bias and achieve rational pricing, the model fails to adequately capture the inherent nonlinear characteristics of system dynamics, particularly with regard to temporal and state transitions. Furthermore, it relies on assumptions grounded in normal distribution, which do not fully align with real-world conditions. These discrepancies ultimately constrain the model applicability in practical scenarios.

In light of these limitations, we propose to advance our research by developing a computational knowledge orchestration that incorporates the dynamic characteristics of carbon credits.

4.2 Computational Knowledge of Dynamics

A comprehensive understanding of carbon credit evolution requires knowledge of the dynamics of carbon emissions, sequestration, and the accumulation of carbon balance over time. To accurately model this evolution, it is crucial to consider the impact of decay on both emissions and sequestration. The decay rate of carbon emissions refers to the change in emission intensity or overall emission levels over time, influenced by factors such as technological progress, policy interventions, and the transition to cleaner energy sources. These dynamics with decay are essential for managing emissions, implementing carbon offset programs, and ensuring compliance with emissions reduction targets. By understanding these interrelated factors, policymakers and stakeholders can develop more effective strategies to mitigate climate change.

4.2.1 Carbon Emission Dynamics

In the context of carbon emissions, natural systems that are free from human intervention typically exhibit emission dynamics that are directly related to the carbon emission rate, $P(t)$. In the absence of external factors or regulatory measures, the emission dynamics of such systems are governed by a simple dependence on the emission rate $P(t)$,

which quantifies the instantaneous rate of carbon release into the atmosphere at any given time t.

However, in real-world scenarios, external interventions such as carbon capture technologies, emissions reduction policies, or environmental changes (e.g., reforestation or changes in land use) can alter the emission dynamics. These interventions generally introduce a feedback mechanism, which modifies the system emissions based on the current levels of emitted carbon, and thus, the emission rate $P(t)$ is no longer the sole determinant of the system behavior. In these cases, the overall carbon emission dynamics are influenced by both the emission source and the mitigating factors that reduce or absorb the emitted carbon.

To capture the effect of such mitigating measures, the dynamics of carbon emissions $E(t)$, representing the cumulative amount of carbon released into the atmosphere up to time t, can be described by a differential equation. This equation incorporates the emission rate $P(t)$ and the mitigating effects, which are modeled through a decay or removal rate γ. The rate of change of carbon emissions over time is given by the following first-order linear differential equation

$$\frac{dE}{dt} = P(t) - \gamma E(t), \tag{4.20}$$

where $E(t)$ represents the accumulated amount of carbon emissions at time t, $P(t)$ is the instantaneous carbon emission rate at time t, γ is the decay rate or removal rate, which accounts for processes that reduce the amount of carbon emissions, such as carbon capture, natural absorption by ecosystems, or any other mitigation efforts implemented to lower the emissions over time.

The term $P(t)$ reflects the source of emissions, while $\gamma E(t)$ represents the removal or reduction of emissions due to natural or artificial sequestration processes. Thus, the equation models the combined effect of emissions generation and reduction, with the rate of emission change being determined by the difference between these two processes.

The differential equation (4.20) implies that the net rate of change of carbon emissions is the result of two opposing factors. The emission source, $P(t)$, which contributes to the increase in the total emissions; the decay or removal process, $\gamma E(t)$, which acts as a feedback mechanism to reduce the accumulated emissions over time.

The parameter γ represents the effectiveness of mitigation strategies, with larger values of γ indicating more effective carbon capture or absorption, leading to a faster reduction in emissions. Conversely, if γ is small or zero, the system will experience a slower reduction in emissions or even no reduction at all, causing the total carbon emissions to accumulate at a higher rate.

This model provides valuable insights into the management of carbon emissions in real-world scenarios by evaluating the impact of various mitigation strategies on emission trajectories over time. By adjusting the mitigation intensity parameter γ, we can explore how enhanced sequestration efforts or improvements in carbon capture technologies can influence long-term emission trends. The model also highlights the importance of a dual approach to climate policy, which not only focuses on reducing the carbon emission rate $P(t)$, but also on implementing measures to increase carbon sequestration or absorption. This combined strategy is crucial for meeting global climate targets. The dynamics of carbon emissions are shaped by both emission rates and the processes that mitigate or absorb these emissions.

The model captures the interaction between the carbon emission rate and the effectiveness of carbon mitigation processes, providing insights into how different levels of mitigation can influence long-term emissions behavior. The differential equation presented in (4.20) offers a comprehensive framework for modeling these interactions, enabling the analysis of factors that influence carbon emissions over time. Understanding these dynamics is essential for designing effective climate strategies, emphasizing the need for both emission reductions and enhanced sequestration to manage the long-term trajectory of global carbon emissions.

4.2.2 Carbon Sequestration Dynamics

Carbon sequestration plays a vital role in mitigating climate change by capturing and storing carbon dioxide (CO_2) from the atmosphere. This process occurs primarily through natural mechanisms such as photosynthesis in plants and trees, or through engineered solutions like carbon capture and storage (CCS) technologies. The efficiency of carbon sequestration is influenced by several factors, including environmental conditions, land use changes, and advancements in carbon capture technologies. Additionally, the effectiveness of sequestration efforts can diminish over time, as carbon may be released from storage or sequestration systems may degrade, necessitating the incorporation of a decay term in modeling the process.

The rate of carbon sequestration is typically dynamic and may change due to various external influences, such as shifts in land management practices, technological advancements, and environmental conditions that alter the capacity of carbon sinks. To model the dynamics of carbon sequestration over time, we define $S(t)$ as the cumulative amount of carbon that has been sequestered or stored up to time t.

The rate of change of carbon sequestration, $S(t)$, can be described by a differential equation similar to the emission dynamics. However, in this case, the dynamics are influenced by both the sequestration rate $R(t)$, which represents the rate at which carbon is being captured and stored, and a decay or loss rate λ, which accounts for processes that result in the release of stored carbon back into the atmosphere.

The rate of change of carbon sequestration can be expressed mathematically by the following first-order linear differential equation as

$$\frac{dS}{dt} = R(t) - \lambda S(t), \tag{4.21}$$

where $S(t)$ is the amount of carbon that has been sequestered at time t, $R(t)$ is the instantaneous carbon sequestration rate at time t, λ is the decay or loss rate, representing the rate at which carbon is released from sequestration or the storage systems.

In this equation, the sequestration rate $R(t)$ contributes to the increase in the amount of stored carbon, while the decay term $\lambda S(t)$ models the process by which carbon is lost from storage, either through natural processes such as decomposition or through human-induced actions such as land-use changes or storage system failure.

The differential equation (4.21) represents a dynamic system where the sequestration process is constantly being augmented by the influx of carbon from the atmosphere, as described by $R(t)$, but is simultaneously reduced by the release of stored carbon back into the atmosphere, modeled by the decay term $\lambda S(t)$. This model highlights the fact that the sequestration process is not permanent and that carbon can be re-released from storage, especially if environmental conditions change or the sequestration systems degrade over time.

The term λ represents the decay or loss rate of carbon sequestration, which may depend on several factors, including the type of sequestration system (e.g., natural vs. artificial), the stability of the storage medium (e.g., forests, soils, or underground reservoirs), and external factors such as climate change or land management practices. A higher value of λ indicates a more significant loss of stored carbon, while a lower λ suggests that the sequestration system is more stable and resistant to carbon release.

This model provides essential insights into the long-term effectiveness of carbon sequestration strategies, such as reforestation, soil carbon enhancement, and carbon capture and storage (CCS) technologies. By adjusting key parameters like the sequestration rate $R(t)$ and the decay rate λ, the model allows for the evaluation of various carbon removal scenarios and their sustainability over time. Increasing the sequestration rate through enhanced technologies or expanded natural sinks can significantly reduce atmospheric CO_2, while addressing the decay rate is crucial for ensuring the permanence of

carbon storage. The dynamics of carbon sequestration are influenced by both the capture rate and decay processes, which can lead to the release of stored carbon. The differential equation framework presented in (4.21) offers a comprehensive approach for assessing the interplay between sequestration and decay, aiding in the development of effective strategies to mitigate climate change through long-term carbon removal solutions.

4.2.3 Carbon Credit Option Pricing Dynamics

In the context of carbon markets, understanding the pricing dynamics of carbon credit options is crucial for stakeholders seeking to make informed financial decisions. The interaction between supply and demand for carbon credits, along with the intricacies of option pricing, reflects the complexity of the market and its role in addressing climate change through economic mechanisms. Carbon credit options provide a financial instrument that allows entities to hedge against the risk of fluctuating carbon credit prices, thus enabling more stable long-term planning and investment in emissions reduction projects.

To accurately model the pricing of carbon credit options, it is essential to apply established financial models. The Black-Scholes model (BS model) is a widely recognized and powerful tool for pricing options in financial markets, and it can also be adapted to model the pricing of carbon credit options. This model captures the evolution of the option price based on various factors, such as the underlying asset price, volatility, and time, and it forms the foundation of many financial instruments, including carbon credit options.

In the context of carbon credit options, the underlying asset price Z represents the price of carbon credits, and the model incorporates the time-dependent nature of option prices. The generalized form of the Black-Scholes PDE for carbon credit option pricing is given by

$$f_{BS} = \frac{\partial C}{\partial t} + \frac{1}{2}\sigma^2 Z^2 \frac{\partial^2 C}{\partial Z^2} + rZ\frac{\partial C}{\partial Z} - rC = 0, \tag{4.22}$$

where C represents the price of the carbon credit option, Z denotes the underlying asset price (i.e., the price of carbon credits), σ is the volatility of the carbon credit price, r is the risk-free interest rate, and t represents time. The equation (4.57) incorporates key elements of option pricing theory, including the time evolution of the option price ($\frac{\partial C}{\partial t}$), the effect of price volatility ($\frac{1}{2}\sigma^2 Z^2 \frac{\partial^2 C}{\partial Z^2}$), and the impact of the underlying asset price changes on the option value ($rZ\frac{\partial C}{\partial Z}$). The term $-rC$ represents the cost of carrying the option over time, which is discounted at the risk-free rate.

The application of the Black-Scholes model to carbon credit options pricing provides a valuable framework for analyzing financial dynamics within carbon markets. This model allows stakeholders to assess the value of carbon credits under varying market conditions, integrating factors such as price volatility and time-dependence. By doing so, it enables informed decision-making regarding carbon credit investments and hedging strategies. Additionally, the pricing of carbon credit options is essential for the efficient functioning of cap-and-trade systems, aiding in the management of emissions allowances and supporting climate change mitigation efforts. Through the use of a partial differential equation, the Black-Scholes model offers a robust method for understanding the factors driving carbon credit prices, ensuring that stakeholders can make strategic investments in emissions reduction projects. As carbon markets evolve, the incorporation of financial models like Black-Scholes will remain integral to enhancing the effectiveness of market-based climate policies.

4.3 Knowledge Informed Orchestration with KAR

4.3.1 Kolmogorov-Arnold Representation

The Kolmogorov-Arnold representation (KAR) theorem is a fundamental result in the theory of multivariate functions, particularly in the context of approximation theory. It asserts that any continuous multivariate function can be expressed as a superposition of univariate functions. This theorem provides a way to decompose complex functions of multiple variables into simpler, one-dimensional components, which can be beneficial in both theoretical analysis and practical applications.

For a given continuous function $f(x_1, x_2, \ldots, x_n)$, where $x_1, x_2, \ldots, x_n$ are the input variables, the Kolmogorov-Arnold representation asserts that this function can be written as a sum of simpler univariate functions. Specifically, the KAR representation is given by

$$f(x_1, x_2, \ldots, x_n) = \sum_{i=1}^{N} g_i(h_i(x_1), h_i(x_2), \ldots, h_i(x_n)), \tag{4.23}$$

where g_i are univariate functions, h_i are mappings that define how each univariate function interacts with the respective input variable $x_1, x_2, \ldots, x_n$, N is the number of terms in the superposition, which can be finite or infinite, depending on the function. This representation shows that a multivariate function $f(x_1, x_2, \ldots, x_n)$ can be expressed as a sum of simpler univariate functions g_i, each of which operates on a transformation of the original variables through the mappings h_i.

The Kolmogorov-Arnold representation (KAR) provides significant advantages in various fields by simplifying the analysis of complex multivariate functions. Through the principle of superposition, KAR decomposes multivariate functions into sums of simpler univariate components, facilitating their analysis and computation. This decomposition is particularly valuable in solving complex differential equations in high-dimensional spaces, as it reduces the problem complexity and allows for independent treatment of each component. KAR also enhances computational efficiency, particularly in machine learning, optimization, and simulation, by transforming high-dimensional problems into lower-dimensional ones. Additionally, it is highly effective for modeling nonlinear systems, where it provides an interpretable and efficient approach to approximating complex relationships. As a result, KAR is a powerful tool in approximation theory, control theory, nonlinear dynamics, and other areas of applied mathematics, offering a robust framework for understanding and solving complex mathematical problems.

4.3.2 Mnimal Viable KAR for Neural Computing

Consider a system characterized by a set of differential equations representing the dynamics of financial systems, such as option pricing models or portfolio optimization. The system can be formulated as

$$\mathscr{F}[\mathbf{u}(\mathbf{x},t);\lambda] = 0, \quad \mathbf{x} \in \Omega, \quad t \in [0,T], \tag{4.24}$$

where $\mathscr{F}$ denotes the financial differential operator, $\mathbf{u}(\mathbf{x},t)$ represents the financial variable of interest (such as option price or asset value), and λ encompasses the parameters of the financial model. The domain Ω represents the space of financial variables, and the interval $[0,T]$ corresponds to the time horizon of interest.

In the context of the Kolmogorov-Arnold representation (KAR), we approximate the solution $\mathbf{u}(\mathbf{x},t)$ using a neural network model $\mathbf{u}_\theta(\mathbf{x},t)$, constructed as a Kolmogorov-Arnold Network (KAN) with parameters θ. This network leverages the decomposition principle of KAR, where the solution can be expressed as

$$\mathbf{u}_\theta(\mathbf{x},t) = \sum_{i=1}^{L_2} g_{i,\theta}\left(\sum_{j=1}^{L_1} h_{ij,\theta}(x_j,t)\right), \tag{4.25}$$

where $g_{i,\theta}(\cdot)$ and $h_{ij,\theta}(\cdot)$ are the learned functions corresponding to the layers of the neural network, and L_1 and L_2 denote the number of units in the first and second layers, respectively. By learning the parameters θ, the neural network approximates the solution to the system, following the decomposition principle of KAR, which states

that any continuous multivariate function can be decomposed into the sum of univariate functions based on the linear combinations of the input variables.

To determine the optimal parameters θ, the network parameters $g_{i,\theta}(\cdot)$ and $h_{ij,\theta}(\cdot)$ are learned by minimizing the total loss function. The optimization problem can be formulated as:

$$\theta^* = \arg\min_{\theta} \mathscr{L}(\theta), \tag{4.26}$$

where $\mathscr{L}(\theta)$ is the total loss function that captures various components of the error in the model.

The loss function $\mathscr{L}(\theta)$ consists of several key components, each addressing different aspects of the problem as

$$\mathscr{L}(\theta) = \mathscr{L}_{\text{initial}}(\theta) + \mathscr{L}_{\text{boundary}}(\theta) + \mathscr{L}_{\text{governing}}(\theta), \tag{4.27}$$

where $\mathscr{L}_{\text{initial}}(\theta)$ ensures that the neural network prediction at the initial time $t = 0$ matches the given initial condition, $\mathscr{L}_{\text{boundary}}(\theta)$ ensures that the neural network solution satisfies the boundary conditions for the financial domain, $\mathscr{L}_{\text{governing}}(\theta)$ enforces that the network solution adheres to the financial governing equations and constraints.

The initial value loss $\mathscr{L}_{\text{initial}}(\theta)$ ensures that the neural network prediction at $t = 0$ matches the initial condition

$$\mathscr{L}_{\text{initial}}(\theta) = \frac{1}{N_{\text{init}}} \sum_{i=1}^{N_{\text{init}}} |\mathbf{u}_\theta(\mathbf{x}_i, 0) - \mathbf{u}_0(\mathbf{x}_i)|^2, \tag{4.28}$$

where $\mathbf{u}_\theta(\mathbf{x}_i, 0)$ is the neural network prediction at $t = 0$, $\mathbf{u}_0(\mathbf{x}_i)$ is the known initial condition at point $\mathbf{x}_i$, and N_{init} is the number of points used for the initial condition.

The boundary loss $\mathscr{L}_{\text{boundary}}(\theta)$ ensures that the solution satisfies the boundary conditions at the domain boundaries:

$$\mathscr{L}_{\text{boundary}}(\theta) = \frac{1}{N_{\text{b}}} \sum_{j=1}^{N_{\text{b}}} \left|\mathbf{u}_\theta(\mathbf{x}_j, t_j) - \mathbf{b}(\mathbf{x}_j, t_j)\right|^2, \tag{4.29}$$

where $\mathbf{u}_\theta(\mathbf{x}_j, t_j)$ is the neural network prediction at boundary point $(\mathbf{x}_j, t_j)$, $\mathbf{b}(\mathbf{x}_j, t_j)$ is the known boundary condition, and N_{b} is the number of boundary points.

The governing equation loss $\mathscr{L}_{\text{governing}}(\theta)$ ensures that the network solution adheres to the financial governing equation at each point in the domain

$$\mathscr{L}_{\text{governing}}(\theta) = \frac{1}{N_{\text{f}}} \sum_{k=1}^{N_{\text{f}}} |\mathscr{F}[\mathbf{u}_\theta(\mathbf{x}_k, t_k); \lambda]|^2, \tag{4.30}$$

where $\mathscr{F}$ is the financial differential operator, $\mathbf{u}_\theta(\mathbf{x}_k, t_k)$ represents the neural network prediction, and N_{f} is the number of points used to enforce the governing equation constraints.

4.3.3 Generalization of Deep KAR Neural Computing

We can further generalize the Kolmogorov-Arnold Representation (KAR) from its initial two-layer form to deeper architectures. In this generalized case, we define the first layer, $\Phi_1(\cdot)$, and the second layer, $\Phi_2(\cdot)$, as follows

$$\Phi_1(\cdot) = \sum g(\cdot), \quad \Phi_2(\cdot) = \sum h(\cdot).$$

Using this structure, we can represent the solution in the form of a deep architecture by expressing the model as

$$\mathbf{u}_\theta(\mathbf{x}, t) = \sum_{i=1}^{L_2} g_{i,\theta} \left(\sum_{j=1}^{L_1} h_{ij,\theta}(x_j, t) \right) = \Phi_2 \circ \Phi_1 z, \tag{4.31}$$

where

$$\Phi_2 = \left[g_1(\cdot), g_2(\cdot), \ldots, g_{L_2}(\cdot) \right],$$

$$\Phi_1 = \begin{bmatrix} h_{1,1}(\cdot) & h_{1,2}(\cdot) & \cdots & h_{1,L_1}(\cdot) \\ h_{2,1}(\cdot) & h_{2,2}(\cdot) & \cdots & h_{2,L_1}(\cdot) \\ \vdots & \vdots & \ddots & \vdots \\ h_{L_2,1}(\cdot) & h_{L_2,2}(\cdot) & \cdots & h_{L_2,L_1}(\cdot) \end{bmatrix},$$

$$z = \begin{bmatrix} (x_1, t) \\ (x_2, t) \\ \vdots \\ (x_{L_1}, t) \end{bmatrix}^T.$$

This formulation reflects the decomposition of the solution $\mathbf{u}_\theta(\mathbf{x}, t)$ into a sequence of simpler univariate functions, making use of a two-layer structure.

This approach can be extended further to deep architectures, where multiple layers are involved. For a general case, the solution can be expressed as a composition of functions across multiple layers, leading to the following deep Kolmogorov-Arnold Representation

$$\mathbf{u}_\theta(\mathbf{x}, t) = \Phi_L \circ \Phi_{L-1} \circ \cdots \circ \Phi_k \circ \cdots \circ \Phi_1 z, \tag{4.32}$$

where each layer Φ_k represents a transformation based on the previous layer output. Specifically, the k-th layer Φ_k is structured as

$$\Phi_k = \begin{bmatrix} \Phi_{1,1}(\cdot) & \Phi_{1,2}(\cdot) & \cdots & \Phi_{1,L_k}(\cdot) \\ \Phi_{2,1}(\cdot) & \Phi_{2,2}(\cdot) & \cdots & \Phi_{2,L_k}(\cdot) \\ \vdots & \vdots & \ddots & \vdots \\ \Phi_{L_{k+1},1}(\cdot) & \Phi_{L_{k+1},2}(\cdot) & \cdots & \Phi_{L_{k+1},L_k}(\cdot) \end{bmatrix}. \tag{4.33}$$

The network learns the decomposition at each level, with Φ_L being the final layer that outputs the desired solution $\mathbf{u}_\theta(\mathbf{x}, t)$.

To optimize the parameters of the deep Kolmogorov-Arnold Network, a general loss function is defined. This loss function is typically composed of a weighted sum of individual loss components, $\mathscr{L}_l(\theta)$, each corresponding to a specific aspect of the solution, such as initial conditions, boundary conditions, and adherence to governing equations. The general form of the loss function can be formulated as

$$\mathscr{L}(\theta) = \sum \lambda_l \mathscr{L}_l(\theta), \tag{4.34}$$

where λ_l are the weights assigned to each loss component, and $\mathscr{L}_l(\theta)$ represents the individual loss functions. The total loss function ensures that the network learns a solution that adheres to all necessary conditions and constraints.

The individual loss functions $\mathscr{L}_l(\theta)$ can include Initial condition loss, Boundary condition loss, Governing equation loss, and other related loss component that helps guide the learning process. The weighted sum in equation (4.34) allows the model to balance the importance of different constraints, thus ensuring that the final solution is both accurate and consistent with the physical, financial, or system dynamics.

4.4 Knowledge Informed Orchestration

The complexity inherent in carbon credit systems necessitates a structured and integrated approach to capture the dynamics of emissions, sequestration, and credit accumulation. This requires the synthesis of various interconnected processes, including carbon emission rates, sequestration rates, and credit accumulation rates, into a coherent framework that accurately reflects both environmental and financial aspects.

To model the carbon credit system effectively, we integrate the dynamics of carbon emissions, sequestration, and credit accumulation into a unified system of differential equations. These equations describe the evolution of the key variables in response to external factors and policy changes. The system is represented as

$$\begin{bmatrix} dE(t) \\ dS(t) \end{bmatrix} = \begin{bmatrix} 1 & -\gamma & 0 & 0 \\ 0 & 0 & 1 & -\lambda \end{bmatrix} \begin{bmatrix} P(t) \\ E(t) \\ R(t) \\ S(t) \end{bmatrix} dt \tag{4.35}$$

in which $P(t)$ represents the carbon emission rate at time t, $E(t)$ is the total carbon emissions at time t, $R(t)$ is the carbon sequestration rate at time t, $S(t)$ is the total

carbon sequestration at time t, γ is the decay rate of emissions due to natural processes or technological interventions, and λ is the decay rate of carbon sequestration due to processes like carbon release from storage. The matrix formulation of (4.35) captures the interdependencies between the emission and sequestration processes, enabling a comprehensive representation of the carbon dynamics.

Carbon credits, $\mathscr{C}(t)$, are defined as the difference between the amount of carbon sequestered and the amount emitted. Thus, the carbon credit accumulation at time t is given by

$$\mathscr{C}(t) = S(t) - E(t) \tag{4.36}$$

The price dynamics of carbon credits can be influenced by a variety of factors, including market forces and policy interventions. For a given price Z of carbon credits, the supply-demand balance is expressed as

$$Z = \frac{\mathscr{D} - \mathscr{C}}{d + c} \tag{4.37}$$

where $\mathscr{D}$ represents the demand for carbon credits, and d and c are constants representing supply factors and market dynamics, respectively.

Further, carbon credit options are typically priced using financial models, such as the Black-Scholes framework, which provides a partial differential equation (PDE) for option pricing. The pricing dynamics for carbon credit options are given by the following PDE as

$$\frac{\partial C}{\partial t} + \frac{1}{2}\sigma^2 Z^2 \frac{\partial^2 C}{\partial Z^2} + rZ\frac{\partial C}{\partial Z} - rC = 0 \tag{4.38}$$

in which C represents the price of the option, Z is the underlying asset price (carbon credit price), σ is the volatility of the carbon credit price, r is the risk-free interest rate, and t is time. This equation models the evolution of the carbon credit option price, accounting for both market volatility and the time decay of the option value.

The orchestration of carbon credit dynamics through the framework provided offers valuable insights into the intricate relationships between carbon emissions, sequestration, and credit accumulation. By modeling these interactions, the framework enables a deeper understanding of how various factors, such as policy interventions, technological advancements, and natural variability, influence the dynamics of carbon credits over time. By integrating environmental physics with financial modeling, the proposed framework offers a robust tool for assessing carbon credit systems. This is essential for the design of effective carbon markets, which play a critical role in addressing climate change and promoting sustainable environmental practices.

4.4.1 Knowledge Orchestration for Environment Physics

The complexity inherent in the modeling of carbon credit systems necessitates a sophisticated approach to integrate various dynamic processes such as carbon emissions, sequestration, and credit accumulation. A comprehensive understanding of these processes can be achieved through the application of a Knowledge Orchestration (KO) model, which enables the effective representation and analysis of the interactions between these variables.

The cornerstone of this framework is the differential operator, which serves as the foundation for the carbon orchestration (CO) model. This model is expressed as a system of partial differential equations (PDEs) that govern the carbon balance over time, encapsulating the dynamics of both emissions and sequestration. The CO equation for carbon balance is formulated as follows

$$f_{CO} = \begin{bmatrix} dE(t) \\ dS(t) \end{bmatrix} - \begin{bmatrix} 1 & -\gamma & & \\ & & 1 & -\lambda \end{bmatrix} \begin{bmatrix} P(t) \\ E(t) \\ R(t) \\ S(t) \end{bmatrix} dt = dD(t) - AG(t)dt = 0 \tag{4.39}$$

where $E(t)$ and $S(t)$ represent the carbon emissions and sequestration at time t, respectively, while $P(t)$ and $R(t)$ denote the rates of carbon emission and sequestration. The matrix of coefficients A incorporates the decay rates γ and λ, which account for losses in emissions and sequestration over time. Additionally, $D(t) = [E(t), S(t)]^T$ and $G(t) = [P(t), E(t), R(t), S(t)]^T$ represent the vector variables that capture the dynamics of emissions and sequestration, and d refers to the rate of change of the carbon credit accumulation.

The equation $f_{CO} = 0$ serves as the governing constraint of the system, ensuring that the changes in carbon emissions and sequestration adhere to the prescribed relationships. This equation represents the backbone of the carbon balance system, encapsulating the interplay of emission reduction strategies, sequestration efforts, and the accumulation of carbon credits.

To address the complexities of this system, the Knowledge Orchestration framework applies the Kolmogorov-Arnold Representation (KAR) theorem, which allows for the decomposition of the carbon orchestration dynamics into a series of simpler functions. This decomposition aids in simplifying the understanding and interpretation of the carbon balance by reducing the high-dimensional problem into univariate components.

Specifically, the solution to the carbon balance system $D(G,t)$ is approximated as

$$\mu_\theta(G,t) = \sum_{i=1}^{N} g_i(h_i(G),t) \approx D(G,t) \tag{4.40}$$

In this representation, g_i are univariate functions, and $h_i(x)$ are mappings that describe the interactions between the variables G and t, capturing the dynamics of carbon emissions and sequestration. By utilizing this decomposition, the knowledge orchestration model offers a more granular and interpretable representation of the carbon balance.

The neural network component of the orchestration model is designed to learn the parameters of these univariate functions and their interactions. The network is trained through the minimization of a composite loss function, which consists of three key components: the initial value loss, the boundary loss, and the carbon governing constraint loss.

The initial value loss $\mathscr{L}_{\text{initial}}(\theta)$ ensures that the neural network predictions align with the known initial conditions of the system at $t = 0$. This loss is formulated as

$$\mathscr{L}_{\text{initial}}(\theta) = \frac{1}{N_{\text{init}}} \sum_{i=1}^{N_{\text{init}}} |\mathbf{u}_\theta(\mathbf{x}_i, 0) - \mathbf{u}_0(\mathbf{x}_i)|^2 \tag{4.41}$$

where $\mathbf{u}_\theta(\mathbf{x}_i, 0)$ is the neural network prediction at the initial time $t = 0$, and $\mathbf{u}_0(\mathbf{x}_i)$ represents the known initial condition at the point $\mathbf{x}_i$.

The boundary loss $\mathscr{L}_{\text{boundary}}(\theta)$ ensures that the neural network predictions adhere to the boundary conditions of the system, which is given by

$$\mathscr{L}_{\text{boundary}}(\theta) = \frac{1}{N_{\text{b}}} \sum_{j=1}^{N_{\text{b}}} \left|\mathbf{u}_\theta(\mathbf{x}_j, t_j) - \mathbf{b}(\mathbf{x}_j, t_j)\right|^2 \tag{4.42}$$

where $\mathbf{u}_\theta(\mathbf{x}_j, t_j)$ is the neural network prediction at the boundary point $(\mathbf{x}_j, t_j)$, and $\mathbf{b}(\mathbf{x}_j, t_j)$ is the known boundary condition at that point.

Finally, the carbon governing constraint loss $\mathscr{L}_{\text{carbon}}(\theta)$ enforces the adherence of the neural network solution to the governing carbon balance equation, ensuring that the system satisfies the carbon emission and sequestration dynamics as described by the PDE in (4.39). This loss function is defined as

$$\mathscr{L}_{\text{carbon}}(\theta) = \frac{1}{N_{\text{f}}} \sum_{k=1}^{N_{\text{f}}} |\mathscr{F}[\mathbf{u}_\theta(\mathbf{x}_k, t_k); \lambda]|^2 \tag{4.43}$$

where $\mathscr{F}$ is the carbon differential operator, $\mathbf{u}_\theta(\mathbf{x}_k, t_k)$ represents the neural network prediction at the point $(\mathbf{x}_k, t_k)$, and λ includes the parameters of the carbon model. The term N_{f} refers to the number of points used to enforce the carbon constraints.

By minimizing the total loss function, which is the weighted sum of these individual loss components, the neural network learns the optimal parameters that accurately represent the carbon balance dynamics. This training process allows the knowledge orchestration framework to learn and predict the behavior of carbon credit systems under various scenarios and policy interventions, contributing to the development of more effective climate change mitigation strategies.

The integration of differential equations with neural networks through knowledge orchestration provides a robust framework for analyzing and forecasting carbon credit dynamics. It enables the effective modeling of complex environmental and financial interactions, offering valuable insights into the optimization of carbon credit trading mechanisms, policy decisions, and the long-term sustainability of carbon management strategies.

4.4.1.1 Governing Loss for Carbon Orchestration

In the context of carbon dynamics, accurate modeling of the system behavior is critical for enforcing the carbon balance dictated by the Carbon Orchestration (CO) model. To achieve this, we propose a framework where the neural network output is constrained by the governing differential equation of the CO model, ensuring that the predictions adhere to the underlying dynamics of carbon emissions, sequestration, and credit accumulation.

Let the neural network output for the carbon balance at any given point (G,t) be denoted as $u_\theta(G,t)$, where θ represents the learnable parameters of the network. The objective is to minimize the deviation between the network output and the carbon dynamics defined by the CO model. To enforce this, the governing loss function must penalize any discrepancies between the network predictions and the CO differential equation.

The carbon dynamics are governed by a differential equation that captures the time evolution of carbon emissions and sequestration. The residual $\mathscr{R}(G,t)$, representing the discrepancy between the time derivative of the network output and the right-hand side of the CO model, is defined as

$$\mathscr{R}(G,t) = \frac{du_\theta(G,t)}{dt} - AG(t), \tag{4.44}$$

where A is the matrix of coefficients governing the rate of change of the carbon variables, and $G(t)$ is the vector of carbon variables, including emissions, sequestration, and credit accumulation. The residual $\mathscr{R}(G,t)$ represents the error between the network output and the actual rate of change prescribed by the CO model at any given point (G,t).

To ensure that the neural network output aligns with the CO model across the entire domain, we define the carbon governing loss $\mathscr{L}_{\text{carbon}}$ as the mean squared error (MSE) of the residual over a set of sampled points (G_i, t_i) in the domain of interest. The carbon governing loss is formulated as

$$\mathscr{L}_{\text{carbon}} = \frac{1}{N}\sum_{i=1}^{N} \mathscr{R}^2(G_i, t_i), \tag{4.45}$$

where N is the total number of sampled points (G_i, t_i) used for training the network. This formulation ensures that the residual is minimized across the entire sampled domain, thereby forcing the neural network output to adhere to the governing dynamics dictated by the CO model.

By incorporating this carbon governing loss into the total loss function of the neural network, we guarantee that the network predictions respect the fundamental carbon balance dynamics. This loss term acts as a constraint that drives the neural network to generate solutions that are consistent with the carbon emission, sequestration, and credit accumulation processes as outlined in the CO model. Thus, the neural network is not only trained to fit the data but also to respect the physical and policy-driven constraints that govern the carbon system.

4.4.1.2 Initial Condition for carbon balance

In the context of carbon dynamics, ensuring that the neural network output adheres to the initial conditions is essential for accurate modeling. Specifically, for the carbon sequestration and carbon emission balances, the initial conditions are defined based on the system state at time $t = 0$, which is often determined by the payoff function at the time of issuance.

For carbon sequestration, the system ability to absorb carbon is bounded by an upper limit, S_K, which represents the maximum carbon storage capacity of the land. Once the carbon content in the land reaches this saturation point, the system is no longer able to absorb additional carbon, and the sequestration value is capped at S_K. Thus, the initial condition for carbon sequestration at $t = 0$ is expressed as

$$S(G, 0) = \min(S, S_K), \tag{4.46}$$

where $S(G, t)$ represents the carbon sequestration at time t, G is the underlying carbon dynamics, and S_K is the upper limit of sequestration dynamics.

Similarly, for carbon emissions, the system is typically constrained by an upper limit, E_K, which represents the maximum allowable emission in a given region. Once the

emission level reaches E_K, the system cannot emit beyond this threshold. Therefore, the initial condition for carbon emissions at $t = 0$ is given by

$$E(G,0) = \min(E, E_K), \tag{4.47}$$

where $E(G,t)$ denotes the carbon emission at time t, and E_K is the upper limit for emissions.

The objective of the initial value loss function, $\mathscr{L}_{\text{initial}}$, is to ensure that the neural network output at $t = 0$ accurately reflects these initial conditions. The initial value loss can be formulated as the mean squared error (MSE) between the network predicted carbon balances and the actual initial conditions over a set of sampled carbon dynamics G_i. Mathematically, the initial value loss function is expressed as

$$\mathscr{L}_{\text{initial}} = \frac{1}{M} \sum_{i=1}^{M} \left(u_\theta(G_i, 0) - \min(D_i(0), D_K) \right)^2, \tag{4.48}$$

where M is the number of sampled carbon points G_i, and $D_K = [E_K, S_K]^T$ represents the upper bounds for carbon emissions and sequestration. $D_i(t) = [E_i(t), S_i(t)]^T$ denotes the actual carbon balances at time t, and $u_\theta(G,t)$ is the output of the neural network with parameters θ, representing the predicted carbon balance at $t = 0$.

By minimizing this loss, the system is encouraged to produce predictions that match the expected initial conditions for both carbon sequestration and emissions, thereby ensuring that the network output is consistent with the physical constraints of the carbon system at the onset.

4.4.1.3 Boundary Loss for Carbon Dynamics

In order to mathematically model the boundary loss for carbon dynamics within the context of a neural network, it is crucial to ensure that the network output adheres to the boundary conditions defined by the underlying carbon balance model. These boundary conditions characterize the behavior of the carbon balance as the underlying carbon dynamics, G, approaches the extremes, namely, zero and infinity, and also at the expiration time.

For carbon dynamics, boundary conditions consist of the zero boundary and infinity boundary conditions. For the zero boundary condition, as the underlying carbon dynamics G approaches zero, the carbon balance should also approach zero. This can be mathematically expressed as

$$D(0,t) = 0 \quad \forall t, \tag{4.49}$$

where $D(0,t)$ represents the carbon balance at $G=0$, and t is the time variable.

For the infinity boundary condition, as the underlying carbon dynamics G approaches infinity, the carbon balance should asymptotically approach a value based on the dynamic behavior of the system during emission and sequestration processes. This is expressed as

$$\lim_{G\to\infty} D(G,t) = \min(D(t), D_K) \quad \forall t, \tag{4.50}$$

where $D(t)$ is the carbon balance at time t, and D_K is the upper bound for the emission and sequestration dynamics.

To enforce these boundary conditions in the neural network, the boundary loss function, $\mathscr{L}_{\text{boundary}}$, is introduced. The boundary loss ensures that the neural network output respects these boundary conditions. It can be formulated as the sum of the mean squared errors at the boundary points.

The zero boundary loss, $\mathscr{L}_{\text{boundary},0}$, is given by

$$\mathscr{L}_{\text{boundary},0} = \frac{1}{N_0}\sum_{i=1}^{N_0}(u_\theta(0,t_i))^2, \tag{4.51}$$

where N_0 is the number of sampled points t_i at the zero boundary condition.

The infinity boundary loss, $\mathscr{L}_{\text{boundary},\infty}$, is formulated as

$$\mathscr{L}_{\text{boundary},\infty} = \frac{1}{N_\infty}\sum_{i=1}^{N_\infty}(u_\theta(G_i,t) - \min(D_i, D_K))^2, \tag{4.52}$$

where N_∞ is the number of sampled points G_i at the infinity boundary condition.

The total boundary loss, $\mathscr{L}_{\text{boundary}}$, is the sum of the zero and infinity boundary losses as

$$\mathscr{L}_{\text{boundary}} = \mathscr{L}_{\text{boundary},0} + \mathscr{L}_{\text{boundary},\infty}. \tag{4.53}$$

4.4.1.4 Carbon Knowledge Orchestration in Loss

To optimize the neural network, the various loss functions are aggregated into a tensor, denoted as $\mathscr{L}_C$, which incorporates the initial value loss, boundary losses, and the carbon governing loss. This aggregation is mathematically expressed as

$$\mathscr{L}_C = \left[\mathscr{L}_{\text{initial}}, \mathscr{L}_{\text{boundary},0}, \mathscr{L}_{\text{boundary},\infty}, \mathscr{L}_{\text{carbon}}\right]. \tag{4.54}$$

Each of the individual loss components in $\mathscr{L}_C$ is weighted by its respective coefficient, stored in the tensor σ_C, as follows

$$\sigma_C = \left[\sigma_{\text{initial}}, \sigma_{\text{boundary},0}, \sigma_{\text{boundary},\infty}, \sigma_{\text{carbon}}\right]. \tag{4.55}$$

The total loss function, $\mathscr{L}_{\text{total}}$, is then computed as the weighted sum of the individual loss components

$$\mathscr{L}_{\text{total}} = \sigma_C \mathscr{L}_C^T. \tag{4.56}$$

This total loss function $\mathscr{L}_{\text{total}}$ serves as the objective function for training the neural network. It ensures that the network output adheres to the carbon balance model by satisfying the initial conditions, boundary conditions, and the governing carbon dynamics, thereby optimizing the overall learning process.

4.4.2 Knowledge Orchestration for Option Pricing

Knowledge Informed Orchestration with KAR (KIOKAR) integrates the foundational principles of the Black-Scholes (BS) model with data-driven neural network techniques, aiming to enhance prediction accuracy and model robustness. In this context, we explore how the KAR framework can be effectively employed to price European options, providing a case study for financial applications.

In the domain of European option pricing, the KAR model initiates by defining the financial differential operator based on the BS partial differential equation (PDE). The equation governing the financial dynamics is given by

$$\frac{\partial C(S,t)}{\partial t} + \frac{1}{2}\sigma^2 S^2 \frac{\partial^2 C(S,t)}{\partial S^2} + rS\frac{\partial C(S,t)}{\partial S} - rC(S,t) = 0, \tag{4.57}$$

where $C(S,t)$ represents the option price as a function of the asset price S and time t, σ is the volatility, and r denotes the risk-free interest rate. This PDE imposes the financial constraints governing the option price.

To further break down the complexities of option pricing, we apply the methodology outlined in equations (4.32) through (4.34). Specifically, we construct the Knowledge-Action-Response (KAR) model to decompose the option price $C(S,t)$ into a series of simpler, interpretable functions as

$$C(Z,t) = \sum_{i=1}^{N} g_i(h_i(Z),t), \tag{4.58}$$

where g_i are univariate functions, and $h_i(Z)$ represents the mappings of these functions with respect to the underlying asset price S and time t. This decomposition not only simplifies the complexity of the option pricing model but also enhances interpretability, facilitating a more granular understanding of the price dynamics.

The neural network component of the KAR framework is designed to learn the parameters of these univariate functions and their interactions. The training process is driven by a composite loss function that ensures the neural network output adheres to the financial constraints and boundary conditions dictated by the Black-Scholes model. This composite loss function includes several key terms: Initial Value Loss, Boundary Loss, and the Financial Governing Constraint Loss.

The financial governing constraint loss $\mathscr{L}_{\text{financial}}(\theta)$ is constructed by applying the PDE from equation (4.57). It enforces the Black-Scholes PDE constraints within the solution domain, ensuring that the network output remains consistent with the governing financial dynamics as

$$\mathscr{L}_{\text{financial}}(\theta) = \frac{1}{N}\sum_{i=1}^{N} |\mathscr{R}(S_i, t_i)|^2, \tag{4.59}$$

where $\mathscr{R}(S_i, t_i)$ denotes the residual of the Black-Scholes PDE when evaluated at the network predicted option prices. This residual term measures the deviation between the neural network output and the expected behavior dictated by the financial PDE.

By incorporating the financial governing constraint loss into the overall training framework, the KAR model ensures that the neural network predictions for European option prices are both accurate and consistent with the Black-Scholes model, while also providing a more interpretable and granular decomposition of the pricing dynamics.

4.4.2.1 Financial Governing Loss for Call Option Pricing

To mathematically model the financial governing loss for call option pricing using the Black-Scholes (BS) model within a neural network framework, we need to ensure that the network output adheres to the BS partial differential equation (PDE). The loss function should penalize deviations from the BS model, thereby enforcing the financial constraints.

Let the neural network output for the call option price be $u_\theta(S,t)$, where θ denotes the network parameters. The financial governing loss can be constructed by computing the residual of the BS PDE when applied to the network output. This residual should ideally be zero across the domain of interest. The residual $\mathscr{R}(S,t)$ is given by:

$$\mathscr{R}(S,t) = \frac{\partial u_\theta}{\partial t} + \frac{1}{2}\sigma^2 S^2 \frac{\partial^2 u_\theta}{\partial Z^2} + rZ\frac{\partial u_\theta}{\partial Z} - r u_\theta. \tag{4.60}$$

The financial governing loss $\mathscr{L}_{\text{financial}}$ can then be defined as the mean squared error

of the residual over the sampled points (Z_i, t_i) in the domain:

$$\mathscr{L}_{\text{financial}} = \frac{1}{N} \sum_{i=1}^{N} \mathscr{R}^2(Z_i, t_i), \tag{4.61}$$

where N is the number of sample points.

4.4.2.2 Initial Condition for European Call Option

In the context of European call option pricing using a neural network, the initial value loss function ensures that the network output satisfies the initial condition of the option pricing model at the time of issuance, specifically at time $t = 0$. For a European call option, this initial condition is determined by the payoff function, which dictates the value of the option at expiration. The payoff function for a European call option at $t = 0$ is given by

$$C(Z, 0) = \max(Z - K, 0), \tag{4.62}$$

where $C(Z, t)$ represents the option price at time t, Z is the underlying asset price, and K is the strike price of the option. This payoff function captures the fundamental pricing behavior of a European call option, where the option is exercised only if the asset price exceeds the strike price.

The initial value loss $\mathscr{L}_{\text{initial}}$ enforces that the neural network predicted option prices at $t = 0$ match the expected payoff at that time. Mathematically, this loss function is formulated as the mean squared error between the neural network predicted option prices and the true payoff function over a set of sampled asset prices Z_i

$$\mathscr{L}_{\text{initial}} = \frac{1}{M} \sum_{i=1}^{M} \left(u_\theta(Z_i, 0) - \max(Z_i - K, 0)\right)^2, \tag{4.63}$$

where $u_\theta(Z_i, 0)$ is the output of the neural network at time $t = 0$ for the input asset price Z_i, and M is the number of sampled asset prices Z_i used for training. The loss function minimizes the deviation between the neural network prediction and the actual payoff at the initial time, ensuring that the network accurately captures the option value at issuance.

This approach guarantees that the neural network adheres to the correct boundary conditions at the initial time, thus aligning its predictions with the expected pricing behavior of the European call option.

4.4.2.3 Boundary Loss for Call Option Pricing

In the context of European call option pricing using a neural network, the boundary loss function ensures that the network predictions respect the boundary conditions of the option pricing model. These boundary conditions are crucial in defining the behavior of the option price as the underlying asset price approaches extreme values, such as zero or infinity. Specifically, for a European call option, the boundary conditions are determined by the limiting behavior of the option price as the underlying asset price Z tends to zero, infinity, and at the expiration time.

For a European call option, the boundary conditions are characterized by the following. As the underlying asset price Z approaches zero, the option price should also tend to zero, reflecting the fact that a call option has no intrinsic value when the underlying asset is worthless. This is expressed as:

$$C(0,t) = 0 \quad \forall t, \tag{4.64}$$

where $C(Z,t)$ represents the option price at time t and underlying asset price Z.

As the underlying asset price Z increases without bound, the option price should asymptotically approach the intrinsic value of the call option, $Z-K$, where K is the strike price. This boundary condition ensures that the option price becomes equivalent to the intrinsic value when the asset price is sufficiently large. This can be written as:

$$\lim_{Z\to\infty} C(Z,t) = Z - K \quad \forall t. \tag{4.65}$$

The boundary loss function $\mathscr{L}_{\text{boundary}}$ is designed to enforce these boundary conditions within the neural network framework. It ensures that the predicted option prices approach zero as the asset price tends to zero and approach $Z-K$ as the asset price tends to infinity. To achieve this, the loss function is defined as the sum of the squared deviations from the boundary conditions at the respective points.

To implement the zero boundary condition, we compute the loss at sampled points where Z is close to zero. The corresponding loss, $\mathscr{L}_{\text{boundary},0}$, is formulated as

$$\mathscr{L}_{\text{boundary},0} = \frac{1}{N_0}\sum_{i=1}^{N_0}\left(u_\theta(0,t_i)\right)^2, \tag{4.66}$$

where $u_\theta(0,t_i)$ represents the neural network predicted option price at $Z=0$ and at time t_i, and N_0 is the number of sampled boundary points at $Z=0$.

Similarly, for the infinity boundary condition, we calculate the loss at points where Z is large, ensuring that the predicted option price approaches the intrinsic value $Z-K$ as

$Z \to \infty$. The corresponding loss function, $\mathscr{L}_{\text{boundary},\infty}$, is defined as

$$\mathscr{L}_{\text{boundary},\infty} = \frac{1}{N_\infty} \sum_{i=1}^{N_\infty} (u_\theta(Z_i, t) - (Z_i - K))^2, \tag{4.67}$$

where $u_\theta(Z_i, t)$ is the predicted option price at a sampled asset price Z_i, and N_∞ is the number of sampled boundary points at large Z_i.

The total boundary loss function, $\mathscr{L}_{\text{boundary}}$, is the sum of the individual losses at the zero and infinity boundaries. It ensures that the network output satisfies both boundary conditions and can be expressed as

$$\mathscr{L}_{\text{boundary}} = \mathscr{L}_{\text{boundary},0} + \mathscr{L}_{\text{boundary},\infty}. \tag{4.68}$$

This total boundary loss serves as an important component in the overall loss function, guiding the neural network to approximate the option pricing behavior accurately across the entire domain, while satisfying the fundamental boundary conditions of the European call option model.

4.4.2.4 Option Knowledge Orchestration in Loss

In the process of optimizing a neural network for European option pricing, various loss components are considered to ensure that the model accurately adheres to the initial conditions, boundary conditions, and financial constraints. These individual loss components are aggregated into a single tensor that represents the overall loss structure. The individual loss components include the initial value loss, boundary losses (for both zero and infinity), and the financial governing constraint loss.

Let the tensor $\mathscr{L}_Z$ represent the collection of all loss functions, which can be formally written as

$$\mathscr{L}_Z = \left[\mathscr{L}_{\text{initial}}, \mathscr{L}_{\text{boundary},0}, \mathscr{L}_{\text{boundary},\infty}, \mathscr{L}_{\text{financial}}\right]. \tag{4.69}$$

Each of these loss terms plays a distinct role in shaping the network output. The initial value loss ensures that the network output aligns with the option payoff at the time of issuance, while the boundary losses enforce the correct asymptotic behavior of the option price as the underlying asset price tends toward zero or infinity. The financial governing constraint loss guarantees that the neural network output satisfies the governing partial differential equation (PDE), which models the option pricing dynamics.

In order to control the contribution of each individual loss component to the total loss, corresponding weight factors are introduced. These weights are encapsulated in a tensor λ_Z, which is defined as

$$\lambda_Z = \left[\lambda_{\text{initial}}, \lambda_{\text{boundary},0}, \lambda_{\text{boundary},\infty}, \lambda_{\text{financial}}\right]. \tag{4.70}$$

The weight tensor λ_Z allows for the adjustment of the relative importance of each loss term during the training process. By modulating these weights, one can emphasize specific aspects of the option pricing problem, such as the accuracy of boundary conditions or adherence to the financial governing equation.

The total loss function $\mathscr{L}_{\text{total}}$ is obtained by computing the weighted sum of the individual loss components. This total loss serves as the objective function for the optimization of the neural network parameters. Mathematically, the total loss is expressed as the dot product of the weight tensor λ_Z and the loss tensor $\mathscr{L}_Z$, as follows

$$\mathscr{L}_{\text{total}} = \lambda_Z \mathscr{L}_Z^T. \tag{4.71}$$

The total loss function $\mathscr{L}_{\text{total}}$ is crucial in guiding the training process, as it incorporates all relevant constraints and ensures that the neural network learns a solution that respects the underlying option pricing dynamics, including the boundary conditions and the financial PDE.

4.4.3 Knowledge Orchestration of Carbon Credit and Option Pricing

To integrate the computational knowledge of carbon credit dynamics and European option pricing, we combine the respective loss functions into a unified framework. This approach allows the orchestration of both financial and environmental models within a single computational objective.

Let $\mathscr{L}_C$ represent the loss associated with the carbon credit model, as derived in equation (4.56), and $\mathscr{L}_Z$ represent the loss associated with the option pricing model, as defined in equation (4.71). The combined loss function tensor, $\mathscr{L}$, is then constructed as follows

$$\mathscr{L} = [\mathscr{L}_C \quad \mathscr{L}_Z]. \tag{4.72}$$

Each component of the combined loss function is weighted according to its relative importance. The corresponding weight tensor, ζ, incorporates the weight tensors for both

the carbon credit model and the option pricing model, denoted by σ_C and λ_Z, respectively. Thus, the weight tensor ζ is expressed as

$$\zeta = [\sigma_C \quad \lambda_Z]. \tag{4.73}$$

The total loss function, $\mathscr{L}_{\text{total}}$, is then computed as the weighted sum of the individual loss functions, resulting in

$$\mathscr{L}_{\text{total}} = \zeta \mathscr{L}^T. \tag{4.74}$$

This combined loss function incorporates the dynamics of both carbon credits and financial options, ensuring that the neural network output adheres to the relevant constraints and boundary conditions in both domains.

The total loss function, $\mathscr{L}_{\text{total}}$, is convex due to its quadratic nature. Specifically, it is a sum of squared terms, and it is well-established in optimization theory that quadratic functions are convex. Consequently, there exists at least one minimizer θ^* such that

$$\mathscr{L}(\theta^*) \leq \mathscr{L}(\theta), \quad \forall \theta \in \Theta,$$

where Θ represents the parameter space. The convexity of the loss function guarantees that the optimization problem has a global minimum, ensuring that the neural network parameters can be optimized effectively to minimize the loss function across both the carbon credit and option pricing models.

4.5 Summary

Extending the integration of environmental physics and carbon credit dynamics into the financial domain underscores that carbon credit option pricing serves as a natural and rigorous testbed for the Knowledge-Based Synergy (KIOKAR) framework grounded in the Kolmogorov-Arnold representation. Similar to environmental modeling, option pricing involves governing partial differential equations, boundary and initial conditions, and inherent market-driven uncertainties, making it an ideal application for assessing the framework capacity to capture complex, multi-domain dynamics. By applying KIOKAR to the Black-Scholes model, we illustrate how environmental and financial dynamics can be coherently unified under a consistent synergy paradigm, highlighting the versatility of the dual domain model and its potential to bridge climate-related markets with conventional financial derivatives.

In Chapter 7, we undertake an empirical evaluation of the KIOKAR (Kolmogorov-Arnold Financial Information Neural) model specifically within the context of carbon finance. Focusing on European call carbon options, which are central to both risk management and market valuation, the experiments are designed to rigorously assess the framework performance. Controlled simulations using benchmark parameters enable a systematic comparison of KIOKAR predictions against the analytical Black-Scholes solution as well as multiple established baseline models. This experimental approach not only validates the feasibility and accuracy of KIOKAR in modeling carbon credit options but also underscores its computational efficiency and interpretability, facilitated by the Kolmogorov-Arnold decomposition. Consequently, Section 7 bridges the theoretical foundations presented earlier with practical implementation, providing robust empirical evidence of KIOKAR potential to enhance carbon market analysis and financial risk assessment.

CHAPTER 5

GRAPH INFORMATION ORCHESTRATION WITH TRANSFORMED GRAPH ATTENTION COMPUTING

5.1 Introduction

Carbon finance inherits similar mechanisms. The credibility of emission reduction, carbon offset, and trading entities directly influences market stability and liquidity. For example, the credibility of carbon offset projects determines whether their credits are accepted by compliance mechanisms or valued in voluntary markets. Similarly, companies with a strong environmental compliance record can gain an advantageous position in trading and investment, while companies with a history of noncompliance face greater scrutiny and higher transaction costs. In this sense, the value of carbon credits functions similarly to financial credit ratings, embedding trust and accountability in carbon markets.

Thus, in financial markets underpinned by a credit system, similar credit ratings serve as a structured assessment of counterparty creditworthiness, influencing capital flows, determining risk premiums, and stabilizing the trading environment. Entities with higher ratings receive preferential financing at lower costs, while those with lower ratings represent higher risk and may trigger protective measures such as collateralization or regulatory intervention. This mechanism demonstrates how systemic trust and market efficiency are maintained through structured risk assessment.

In practice, domain-rule-based approaches for credit rating are developed by experts

who encode prior knowledge and industry heuristics into a set of tailored rules [95, 202, 224]. These rules are crafted to reflect the specific characteristics of the entities being evaluated and the mechanisms governing their interactions. While effective under well-understood conditions, such methods are inherently constrained by their reliance on assumptions and the subjective interpretation of mechanisms. Inaccurate assumptions or incomplete understanding of underlying processes can lead to biased or inconsistent credit assessments, limiting the robustness of rule-based evaluations.

In recent years, machine learning techniques have been increasingly applied to credit rating tasks, leveraging historical data to automatically infer patterns without explicit human-designed rules [99, 107, 193, 204, 255, 295]. These models, including regression-based, tree-based, and neural network architectures, offer a flexible and data-driven alternative. However, traditional machine learning models often treat entities as independent samples and fail to account for the relational dependencies that exist between institutions, projects, or market actors [143]. In credit and carbon finance contexts, the risk profile or credibility of one entity is often influenced by the status and behavior of interconnected entities. Ignoring these dependencies can reduce predictive accuracy and obscure systemic risk patterns.

To overcome this limitation, it is essential to incorporate the interconnections among entities into the modeling framework. Graph-based representations provide a natural way to encode such relationships, where nodes represent entities and edges encode transactional, contractual, or reputational links. Furthermore, attention mechanisms can be integrated into the graph framework to adaptively weight the influence of each connected entity based on context and relevance. By combining relational information with adaptive weighting, the model can more accurately capture the influence of interconnected entities on credit ratings, address systemic risk propagation, and provide a more nuanced, context-sensitive assessment.

This perspective motivates the development of a graph-based attention framework for credit rating, which leverages structural correlations and adaptive learning to improve both the interpretability and robustness of credit evaluations in complex financial.

5.2 Graph Learning with Transformed Graph Attention Representation (TGAR)

In this study, we propose a graph learning strategy based on the Transformed Graph Attention Representation (TGAR) framework, which is designed to enhance the knowledge

representation of each entity within a graph. The TGAR model leverages the principles of graph attention networks (GAT) and transformer-based architectures to better capture the intricate relationships between entities in a graph structure. This method is inspired by previous works, such as those by Ying et al. [279] and Yun et al. [283], which have successfully applied transformers to graph-based learning tasks.

TGAR enables a more sophisticated representation of the importance of each entity within the entire network by using attention mechanisms to weigh the influence of neighboring nodes. The graph attention mechanism is particularly effective for capturing the heterogeneous nature of relationships between entities, allowing the model to dynamically adjust the influence of each node in the graph based on its contextual relevance.

In the TGAR framework, the knowledge representation of each entity is learned through a series of transformations applied to the node features, where these transformations are influenced by the attention scores between nodes. The feature update for each entity is computed as the expected probability distribution of the transformations, taking into account the attention mechanism over all the neighboring nodes and the global network structure. This process allows the model to capture both local and global dependencies between entities, assigning higher importance to the nodes with stronger associations, while reducing the weight of less relevant connections.

The attention weights are learned iteratively through the network, which enables a dynamic adjustment of the node representations based on their contextual relationships with surrounding nodes. Thus, TGAR produces a more comprehensive and effective knowledge representation for each entity, incorporating both local structural features and global relational patterns from the entire graph. This approach significantly improves the ability of graph learning models to handle complex graph-structured data, making it a powerful tool for a variety of applications in graph-based machine learning tasks.

5.3 Hyper Feature and Context Representation

In this section, we introduce the design of the hyper feature unit and the hyper context unit, which are responsible for extracting feature knowledge in the form of tensors. These units are pivotal for the construction of a robust graph learning model, as they allow the representation of complex data structures through the use of hyper-features and contextual embeddings.

The hyper feature unit is designed to operate with two primary components: the

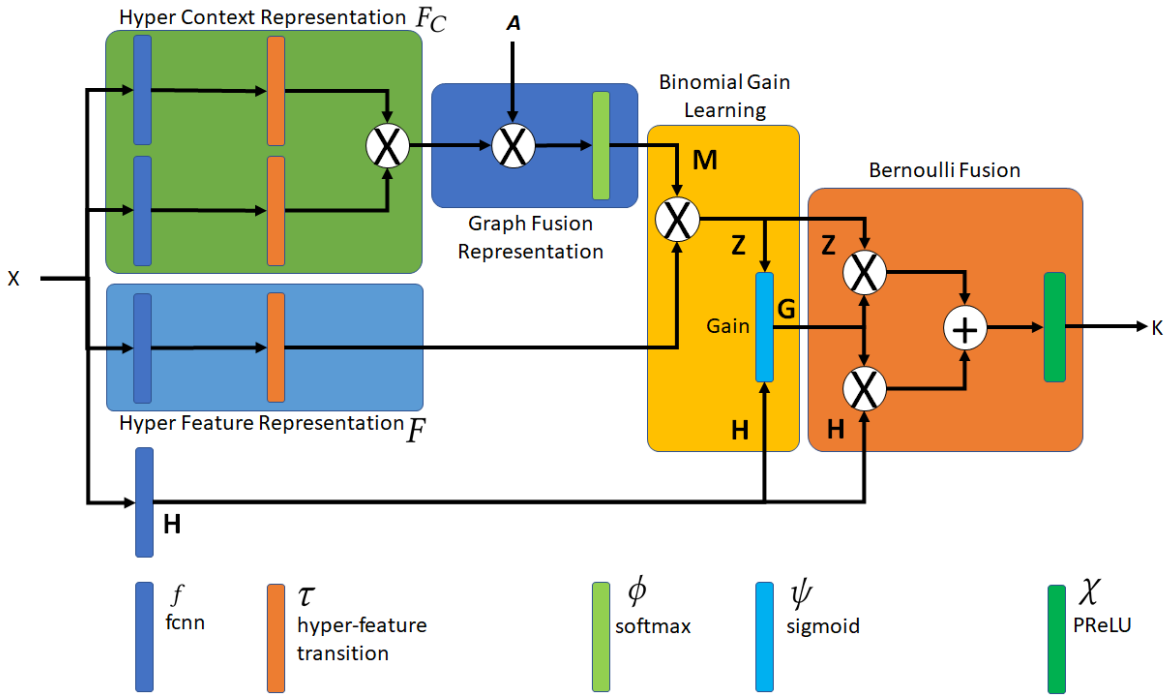

Figure 5.1: Context Knowledge Representation with TGAR

fully connected neural network (FCNN) operator, denoted by $f(\cdot)$, and the hyper-feature transition operator, denoted by $\tau(\cdot)$. These components work synergistically to map the input features to a higher-order tensor space.

The FCNN operator, $f(\cdot) = f_{\text{cnn}}(\cdot)$, establishes a linear mapping between the input features X and the output y, which can be formulated as:

$$y = WX + b \tag{5.1}$$

where X is the set of input features, W represents the learnable weights, and b is the bias term. This operator is fundamental for establishing the linear relationships between input and output variables in the feature space. In our design, the FCNN module is used to map elementary features X to functional projections, which are subsequently processed by other operators. The FCNN plays a central role in the learning process, as it allows the network to capture the underlying structure of the input data through the learned weights.

The hyper-feature transition operator $\tau(\cdot)$ is responsible for transforming the output of the FCNN into a tensor representation. This transition can be expressed as

$$\tau : \mathbb{R}_{n \times m} \longrightarrow \mathbb{R}_{k \times n \times \frac{m}{k}}, \tag{5.2}$$

where n and m represent the dimensions of the input matrix, and k denotes the number of hyper-feature tensors. This operator facilitates the mapping from a traditional feature space into a higher-dimensional tensor space, which enriches the feature representation by capturing more intricate relationships between the features.

Thus, the operation of the hyper feature unit can be expressed as the following composition of functions as

$$F(X) = \tau(f(X)), \tag{5.3}$$

This mapping process represents the transformation of input features X into the corresponding higher-order tensor space through the combination of the FCNN and the hyper-feature transition operator.

Building upon the hyper feature unit, the hyper context unit further refines the feature representation by incorporating multiple hyper-feature mappings. The operation of the hyper context unit can be described as the interaction of two independent hyper feature units, denoted by $F_1(\cdot)$ and $F_2(\cdot)$. These units operate in parallel, applying different transformations to the input feature set X.

The mapping of the hyper context unit is given by

$$F_C(X) = F_1(X) \times F_2(X) = \tau_1 \circ f_1(X) \times \tau_2 \circ f_2(X), \tag{5.4}$$

where $F_1(X)$ and $F_2(X)$ represent the feature transformations applied by two separate hyper feature units, $\circ$ denotes the composition of the operators, and $\times$ denotes the element-wise multiplication of the transformed features. The hyper context unit aggregates the information from these two distinct feature mappings, allowing the model to capture more comprehensive relationships between different aspects of the input data.

As illustrated in Figure 5.1, the hyper context unit plays a crucial role in capturing contextual dependencies within the data by combining multiple hyper-feature representations. This enables the model to learn more complex patterns by incorporating richer interactions between the features.

The mappings of the hyper feature unit and the hyper context unit are defined in (5.3) and (5.4). These mappings form the backbone of our knowledge extraction strategy, allowing the model to represent data in a higher-dimensional tensor space and capture complex relationships among features. The hyper feature and hyper context units, with their respective transformations, provide a powerful mechanism for encoding and learning intricate patterns in graph-based data.

5.4 Graph Fusion Representation

We incorporate the softmax operator for multi-class classification tasks within the framework of graph knowledge fusion. The softmax function, denoted as $\phi(\cdot)$, plays a crucial role in transforming numerical outputs into probabilities, which can then be used for classification. Specifically, when considering the correlation between entities represented by a graph A, the mapping for graph knowledge fusion can be expressed as:

$$M(A,X) = \phi(AX) \tag{5.5}$$

Here, the graph correlation is encapsulated in the adjacency matrix A, and X represents the feature matrix of the graph nodes. The softmax function, $\phi(\cdot)$, takes the linear combination of node features (given by AX) and maps them to a probability space. More formally, this function is defined as:

$$p_i = \frac{e^{c_i}}{\sum_{i=1}^{N_c} e^{c_i}} \tag{5.6}$$

In equation (5.6), $P = [p_1, p_2, \ldots]$ is the resulting probability vector corresponding to the vector of classification outputs $C = [c_1, c_2, \ldots]$, where c_i represents the output of the ith classifier. The total number of possible categories is denoted as N_C, and p_i gives the probability of the ith category. This transformation ensures that the output of the classification is a valid probability distribution, where each probability p_i is bounded between 0 and 1, and the sum of all probabilities equals 1.

5.5 Binomial Gain Learning

To further enhance the learning process, we introduce a unit for computing the binomial gain using two tensor inputs. This unit leverages differential aggregation and sigmoid operations to merge and map the tensors, ultimately calculating the gain. The sigmoid operator $\psi(\cdot)$ is used here to map the numerical space to a probability space. Specifically, the sigmoid function is defined as

$$\psi(x_i) = \frac{1}{1+e^{-x_i}}, \tag{5.7}$$

and when applied element-wise to a vector input, the operation can be expressed as

$$X = \begin{bmatrix} x_1 \\ \vdots \\ x_n \end{bmatrix} \qquad \Psi(X) = \begin{bmatrix} \psi(x_1) \\ \vdots \\ \psi(x_n) \end{bmatrix}. \tag{5.8}$$

The differential aggregation operator Υ is designed to aggregate two tensor inputs, X_1 and X_2, into a single tensor. This is achieved by concatenating the tensors X_1, X_2, and their element-wise difference $(X_1 - X_2)$, followed by a fully connected neural network (FCNN) with input size $3 \times n$ and output size 1. This operation is formally expressed as

$$\Upsilon(X_1, X_2) = f_{3\times n,1}([X_1, X_2, X_1 - X_2]^T), \tag{5.9}$$

where $f_{3\times n,1}$ denotes the FCNN operator. The output of this operation serves as the aggregated representation of the input tensors.

Finally, the binomial gain processing, $G(\cdot)$, is obtained by applying the sigmoid function to the aggregated tensor

$$G(X_1, X_2) = \Psi(\Upsilon(X_1, X_2)). \tag{5.10}$$

This final operation ensures that the binomial gain is mapped into the probability space, enabling the model to distinguish between the gains associated with the pair of input tensors.

Although both the softmax and sigmoid operators serve to map numerical values to a probability space, their applications in graph knowledge fusion and binomial gain learning differ significantly. The softmax operator, as used in equation (5.5), is primarily employed for multi-class classification, where it transforms the numerical outputs of multiple classifiers into a valid probability distribution across all classes.

In contrast, the sigmoid operator in binomial gain learning (equation (5.10)) is used to process the differential aggregation of two input tensors, distinguishing between the associated gains. While both operators map values to a probability space, the sigmoid function's role in binomial gain learning is to model binary relationships between inputs, as opposed to the softmax function, which is employed for multi-class classification tasks.

5.6 Bernoulli Fusion Processing

In the design of the Bernoulli Fusion processing, a parametric rectified linear unit (PReLU) [267] operator is employed to activate the output. The PReLU operator, denoted

as $\chi(\cdot)$, is applied to the resulting weighted combination of two input tensors, X_1 and X_2, where the weights are determined by the binomial gain G as defined in equation (5.10). The corresponding fusion operation is formulated as follows

$$Y = \chi(GX_1 + (1-G)X_2), \tag{5.11}$$

where $Y = [y_1, y_2, \ldots, y_n]$ represents the output of the Bernoulli fusion. The expression $\bar{X} = GX_1 + (1-G)X_2 = [\bar{x}_1, \bar{x}_2, \ldots, \bar{x}_n]$ defines the intermediate weighted combination of the input tensors. The PReLU activation function $\chi(\cdot)$ is then applied element-wise to $\bar{X}$ to produce the output vector Y. The output for each component is determined by the following piecewise function

$$y_i = \chi(\bar{x}_i) = \begin{cases} \bar{x}_i & \text{if } \bar{x}_i > 0, \\ a\bar{x}_i & \text{if } \bar{x}_i \leq 0, \end{cases} \tag{5.12}$$

where a is a parameter set to 0.25 as per the design choices in this work, and $\bar{x}_i$ and y_i represent the intermediate and final output values for each component, respectively.

The Bernoulli fusion operation can be interpreted as calculating the Bernoulli expectation of the feature knowledge under the classification probability domain. The role of the PReLU activation function in this context is crucial: by incorporating a generalized negative slope, the PReLU allows for the retention of more information, particularly from negative values of the weighted combination, which would otherwise be lost in a traditional ReLU activation. This feature is particularly beneficial for maintaining useful context and nuance in the learning process, especially when dealing with the intricate interactions between the inputs.

The use of this fusion mechanism ensures that both individual and correlated attention between the graph components are preserved and embedded into the system, effectively forming a contextual representation. This contextualized output can then be utilized in subsequent stages of the network, supporting further cascading extensions of the learned features. The overall effect of this design is to create a robust framework that integrates various forms of feature knowledge while maintaining the integrity of the relationships between different components of the graph.

5.7 Context Attention Representation Mapping

The systematic framework for context attention mapping integrates various units and operators, including the hyper context unit and graph knowledge fusion. The process

begins by applying the hyper context unit and graph fusion to the input feature matrix X and graph A. The output of the graph context learning can be derived by utilizing equations (5.4) and (5.5), leading to the following expression

$$M = \phi(A, F_C(X)), \tag{5.13}$$

where $\phi(\cdot)$ denotes the softmax operator, and $F_C(X)$ represents the output from the hyper context unit, as defined in equation (5.4). The output of the hyper feature unit, denoted by $F(X)$, is derived using equation (5.3). Subsequently, the tensor multiplication of M and $F(X)$ is computed, and the resulting product serves as one of the inputs for the binomial gain processing, which can be formulated as

$$Z = \phi(A, F_C(X))F(X). \tag{5.14}$$

Simultaneously, another hyper feature H is computed by applying the function $H = f_H(X)$, which serves as the second input to the binomial gain processing. Combining H and Z through differential aggregation, as outlined in equations (5.9) and (5.10), yields the binomial gain G, expressed as

$$G = \Psi(\Upsilon(H, Z)), \tag{5.15}$$

where $\Psi(\cdot)$ represents the sigmoid function, and $\Upsilon(H, Z)$ denotes the differential aggregation operation between H and Z. With G, H, and Z obtained, the fusion representation K can be derived by applying the Bernoulli fusion module. This fusion procedure is formulated as follows

$$K = \chi(GH + (1 - G)Z), \tag{5.16}$$

where $\chi(\cdot)$ represents the parametric ReLU (PReLU) activation function. The output K, which is the attention representation, encapsulates both the individual and correlated contextual information.

As the final output of the attention-based operations, the attention representation K can be further refined by using it as input for subsequent attention layers, thereby forming a cascaded context attention representation system. This cascading mechanism ensures the progressive enhancement of the learned features, preserving and refining the contextual relationships captured during the attention mapping process.

5.8 Summary

This chapter presents the Transformed Graph Attention Representation (TGAR) framework, which integrates advanced graph learning with hyper-feature extraction and

context-aware attention mechanisms to model complex relational structures. By embedding node attributes into higher-order tensor spaces through hyper feature and hyper context units, TGAR effectively captures multi-dimensional dependencies, while graph fusion, binomial gain learning, and Bernoulli fusion dynamically integrate local and global interactions. The resulting context-aware attention representations provide nuanced weighting of node influence, preserving both individual and correlated information. This modular and scalable architecture is applicable across diverse domains, including finance, social networks, and other graph-structured systems, highlighting the potential of attention-driven transformations to orchestrate heterogeneous data.

Building on this theoretical foundation, Chapter 7 transitions from methodological development to empirical validation, focusing on interbank financial networks, where dense interconnections amplify the risk of contagion and systemic crises. By combining historical financial metrics with the interbank relational graph, the section implements a graph-informed orchestration experiment to predict credit ratings and evaluate risk propagation. This experimental setup not only benchmarks TGAR against classical machine learning and graph-based models but also illustrates how attention-driven, context-aware representations capture intricate relational dependencies in dynamic financial systems. Through multi-year, multi-metric performance evaluation, the study establishes a rigorous framework for assessing TGAR predictive power and practical utility in high-stakes, networked environments.

CHAPTER 6

ADAPTIVE FUSION FOR CONSISTENCY TO BIAS DISPARITY

6.1 Bias in Machine Intelligence by False Data

False data can cause the bias in machine intelligence. In recent years, an attack pattern of false data injection (FDI) against machine learning-based financial information systems has gradually emerged in the industry, which corrupts the model of data processing systems by injecting false data into training or test data set. This data injection directly distorts the latent computations of processing, thus rendering it low-cost and well-concealed. This adversarial attack on a credit risk assessment model may involve altering input data in a way that causes the model to incorrectly predict low default risk, resulting in the approval of a loan that should have been rejected.

Meanwhile, to achieve better learning results, machine learning often uses massive amounts of data for training. However, while improving the generalizability of the model, massive data also brings the labor and time cost of data review, which is not easily checked frequently. Therefore, the false data injection against machine learning is often not easily detectable.

There are many works of false data injection in the power grid [249, 266] and cyber-physical systems [278, 296], as well as methods to detect and prevent them [171, 284]. Most methods are based on the stability principle of the control system to compare the data. Unlike data such as the power grid, financial data processing data does not have

the characteristics of the power grid system, and cannot be directly accomplished by methods similar to power grid steady-state analysis or filtering to detect and eliminate.

Nevertheless, there are not many studies on FDI for financial data, and there are no systematic tests on the rating responses of different machine learning strategies under the influence of FDI. To reduce the risk of adversarial attacks, it is important to carefully design and test machine learning models to defend against different kinds of attacks and to continuously monitor their performance to identify and resolve any potential problems. Therefore, we conduct research on adversarial attacks based on false data injection against machine learning for data processing services.

False data injection (FDI) in the financial system is the intentional introduction of false or misleading information into the financial system to disrupt normal operations or gain a financial advantage. FDI in financial systems is mainly used by attackers to manipulate financial data by hacking and taking over accounts through illegal means and injecting false data into the system under the condition of gaining access to the financial system. In Decision Making, attackers can tamper with financial data, such as financial reports, balance sheets, and other financial statements, through such attacks to present false information to investors and stakeholders, thus causing financial losses, reputational damage, and regulatory penalties for the attacked party. Although security measures such as encryption, firewalls, and intrusion detection systems are in place to prevent these types of attacks, a large number of financial data systems are still attacked each year, so the possibility of such attacks still cannot be completely ruled out [240].

Theoretically, data fraud attacks can be detected and prevented within financial institutions by means of regular audits, but this traditional data proofreading is labor-intensive and time-consuming. For the massive amount of machine learning data, traditional auditing methods can barely cope with such a huge proofreading workload manually, and even automatic line-by-line comparison by machines is often inefficient and infrequently implementable.

6.2 Covert FDI in Machine Intelligence

Covert false data injection refers to the malicious injection hiding in the area of thick data. The purpose of a covert attack is to accomplish an attack undetected, thus making the action unnoticeable or difficult to detect in such a way as to reduce the potential for alarm and defense. In this paper, we will first model the mechanism of various FDIs in terms of data processing in machine intelligence and introduce the actual mechanism of

the covert FDI model based on the analysis of these models with respect to the pattern and covert in the attack.

6.2.1 Adversarial Machine Learning in Decision Making

With the input X with n samples, the credit result Z can be obtained by using

$$Z = H(X) = [z_1, z_2, \ldots, z_n] = H([x_1, x_2, \ldots, x_n]) \tag{6.1}$$

in which $H(\cdot)$ refers to a specific rating function applied for Decision Making. In the machine learning scenario, X and Z are known and the $H(\cdot)$ operator can be formulated as a machine learning model determined by the parameter vector H. The task of system learning is to derive the parametric optimal solution H of the mapping rule based on the known X and Z. Its theoretical solution can be expressed as

$$H = T(X, Z) \tag{6.2}$$

The correspondence between $H(\cdot)$ and H can be formulated as $H(\cdot) = F(H)$. Once H is determined by $T(X, Z)$, the rating model $H(\cdot)$ can be determined correspondingly. To distinguish the data used for rating, the data used for training is defined as X_{Trn}, Z_{Trn}. Then the data processing system under machine learning can be simplified as shown in the figure 6.1.

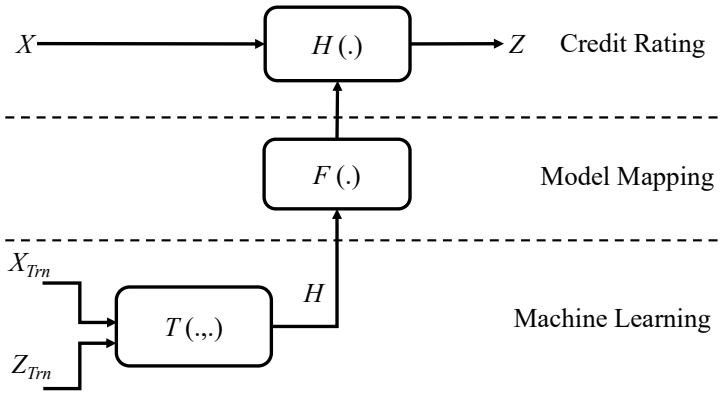

Figure 6.1: Machine Learning in Data Processing System

The symbol H is used to denote both the rating operator $H(\cdot)$ and its associated parameter vector H to highlight their one-to-one correspondence. Specifically, the operator

$H(\cdot)$ represents the functional mapping from input features to credit ratings, while H contains the parameters that fully determine this mapping. Formally, this relationship can be expressed as $H(\cdot) = F(H)$, where F defines how the parameters generate the function. Once the optimal parameters H are learned from the training data $(X_{\text{Trn}}, Z_{\text{Trn}})$ via $H = T(X_{\text{Trn}}, Z_{\text{Trn}})$, the operator $H(\cdot)$ is uniquely specified. Using the same symbol emphasizes that determining the parameters H is equivalent to defining the function $H(\cdot)$, simplifying notation and clarifying the mapping process in the machine learning credit rating system.

It can be seen that the adversarial attack against the data processing machine learning system can be developed for $F(\cdot), T(\cdot), X, Z$, and $H(\cdot)$ respectively. Directly targeting $F(\cdot), T(\cdot)$, and $H(\cdot)$, the cost of stealth attack and tampering is relatively high. In general, the tampering attack can only be successful if the specific structure of $F(\cdot), T(\cdot)$, and $H(\cdot)$ are known, otherwise, $F(\cdot)$ and $T(\cdot)$ systems will not work directly because the data or parameter structure is corrupted and the attack is found. As the data processing processing is usually a black box to external access, the cost of acquiring $F(\cdot), T(\cdot)$, and $H(\cdot)$ is relatively high, or even inaccessible to obtain directly due to the strict finance compliance. Even if they can be obtained and tampered with, it is not easy to redeploy them to the original system unnoticed.

In contrast, false data injection (FDI) is a cheaper attack. It can be used to corrupt machine learning models and ultimately affect ratings by changing data without hacking the black box system. Although the cost and difficulty of implementing such an attack under strict financial system standards remain high, this method is still cost-effective compared to obtaining a black-box model system for financial ratings. The modeling of this attack with corresponding analysis will be given in the next section to reveal the mechanism of how this type of attack affects the system.

6.2.2 Adversarial FDI Attack in Decision Making

6.2.2.1 Clandestine FDI Fraudulence

One of the most common ways to implement FDI is to plant a backdoor in the system data interface for input fraudulence(e.g., [136, 142]). This method is particularly common in schemes for network data pipelines. Modeling the backdoor with FDI as a function $B'(\cdot)$, the corrupted data $\tilde{X} = B'(X)$ after the attack, which has its impact on the data processing result as $\tilde{Z} = H(\tilde{X}) = H(B'_X(X))$. This attack is the most common type of attack. It is usually applied for data scrambling and fraud. In many cases, it is also used

as the first choice for adversarial probing attacks due to its low cost for implementation as only one backdoor is used.

6.2.2.2 Clean Label Attack

Another FDI-based covert attack with low detectability is the Clean Label Attack, whose main attack method is to apply a backdoor on the training data side to attack the training data while keeping the labels clean (e.g., [75, 142, 294]). The principle is to access the training component of the machine learning system by a backdoor and to influence the final model $H(\cdot)$ by corrupting the training data X_{Trn} with the corresponding backdoor $B_X(\cdot)$. Thus, $\tilde{X}_{Trn} = B_X(X_{Trn})$. Correspondingly, the effect of corruption on the learning outcome is $\tilde{H} = T(\tilde{X}_{Trn}, Z_{Trn})$, and $\tilde{H}(\cdot) = F(\tilde{H})$, which gives rise to $\tilde{Z} = \tilde{H}(X)$. This attack also requires only one backdoor to achieve the attack, which is cheap to implement and has a high cost-effectiveness in terms of stealth because the original labels are still correct and the corruption data is often covert due to the large scale of the training data.

6.2.2.3 Induced Model Attack

Induced Model Attack [48, 142] combines Clean Label Attack and Clandestine FDI Fraudulence with applying two backdoors simultaneously to the training component and data interface of the machine learning system, by purposefully corrupting the training data to guide the final model while further feeding the attribute data corresponding to the corrupted training to the data side through the data interface to make the system give the expected result in the guided state, i.e., $\tilde{Z} = \tilde{H}(\tilde{X})$. The attack is more stealthy and has strong anti-reconnaissance properties. In essence, the features of the fraudulent data are embedded in the machine learning system by this attack and can be repeatedly exploited and extended. However, relatively speaking, its attack is costly due to the need to use an additional backdoor.

6.2.2.4 Label-Flip Attack

Label-Flip corrupts only the labels without affecting other data [114, 133, 142]. Corrupt the training data Z_{Trn} by backdooring $B_Z(\cdot)$ against the label data, thus affecting the final model $H(\cdot)$ in the process of $F(\cdot)$, i.e, $\tilde{Z}_{Trn} = B_Z(Z_{Trn})$. Correspondingly, the effect of corruption on the learning outcome is $\tilde{H} = T(X_{Trn}, \tilde{Z}_{Trn})$, and $\tilde{H}(\cdot) = F(\tilde{H})$, which gives rise to $\tilde{Z} = \tilde{H}(X)$. The cost of this attack is also low, but its concealment is not as high because the number of tags is limited in practical applications and the tampering on the

tags is relatively easy to detect considering that the rating data of the organization is publicly available, so the concealment is not as good as the previous attacks.

6.2.2.5 FDI Model Corruption Attack

These attacks [251, 269] against machine learning are mainly based on the principle of data poisoning by corrupting the data X_{Trn} and Z_{Trn} used for training via $T(\cdot)$, and $F(\cdot)$ to affect the final model $H(\cdot)$ with the corresponding backdoor $B_X(\cdot), B_Z(\cdot)$. Therefore, $\tilde{X}_{Trn} = B_X(X_{Trn}), \tilde{Z}_{Trn} = B_Z(Z_{Trn})$. Correspondingly, the corruptions have their impacts on the learning result by $\tilde{H} = T(\tilde{X}_{Trn}, \tilde{Z}_{Trn})$, and $\tilde{H}(\cdot) = F(\tilde{H})$, which yields $\tilde{Z} = \tilde{H}(X)$. It can be seen that the main target of this attack is the training component of the machine learning system, which can be regarded as a full FDI attack against the input and output of the training component, and the damage is extremely high. If the attack is successful, the whole training component will be completely swayed. However, the cost of this attack is high, and not only two backdoors need to be applied, but also two backdoors need to be synchronized to achieve a successful model-induced corrosion attack, which leads to a significant decrease in its stealthiness.

6.2.2.6 Fraud Induced Label-Flip

Fraud Induced Label-Flip attack is also a bootstrap attack [142], the principle of which is similar to an Induced Model Attack, both are attacks against the training components, the difference is that Fraud Induced Label-Flip is to corrupt the labels in the training data to achieve a purposefully induced model, and then through the input data interface backdoor to feed the system with fraudulent data to influence the results. The procedure can be briefly formulated as $\tilde{H} = T(\tilde{X}_{Trn}, \tilde{Z}_{Trn})$, and $\tilde{H}(\cdot) = F(\tilde{H})$, and the result is $\tilde{Z} = \tilde{H}(\tilde{X})$. Again, due to the low concealment of label tampering, this attack has the risk of being easily detected and usually, the attacker needs to work with other auxiliary means to hide the attack.

6.2.2.7 Full Clandestine FDI Attacks

It can be seen that there are 3 accesses to applying this attack in machine learning subsystem, including the attacks on training data X_{Trn}, label Z_{Trn}, and the data to be rated X. When applying all these attacks against the system, the full adversarial machine learning model can be illustrated by Figure 6.2. When all the backdoors are activated at the same time and successfully attack the system, the rating process from

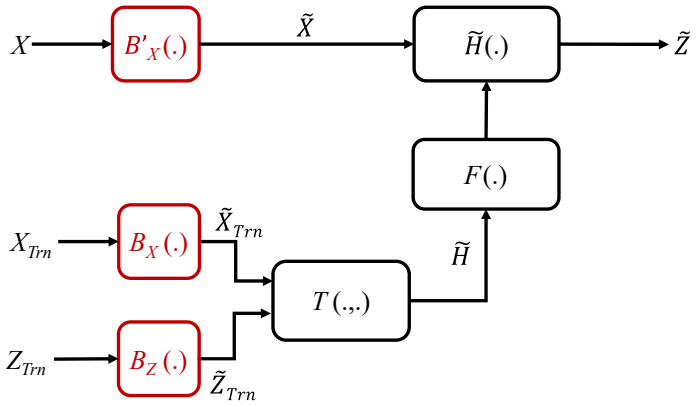

Figure 6.2: Adversarial FDI Machine Learning in Decision Making

Table 6.1: Combination Backdoor Attacks of Adversarial False Data Injection

Attack	B'_X	B_X	B_Z	Covert
Clandestine Fraudulence	Active	Inactive	Inactive	High
Clean Label Attack	Inactive	Active	Inactive	High
Induced Model Attack	Active	Active	Inactive	Mediate
Label-Flip Attack	Inactive	Inactive	Active	Mediate
Model Corruption Attack	Inactive	Active	Active	Low
Fraud Induced Label-Flip	Active	Inactive	Active	Low
Full Clandestine FDI	Active	Active	Active	Low

machine learning to the final result will be corrupted, but this attack does not affect the operation of the system, and there is not even a service interruption, so it has a high degree of stealth.

6.2.3 Covert FDI in Adversarial Backdoor Attacks

6.2.3.1 Covert False Data Injection

In practice, there are relatively few cases of full attacks on the system, and most of the cases are the effect of the attacks generated by the three accesses in different activation combinations. The combination pattern of different attacks is shown in Table 6.1.

Because only one backdoor is needed, Clandestine Fraudulence and Clean Label Attack has low cost and high concealment; for Label-Flip Attack although only one backdoor is used, it is more difficult to a certain extent, this is because for rating agencies the final result rating is often Strictly confidential, not easy to leak out, and the annual

rating results will be revised or different, the error allowed by the label is relatively small and easier to be found, so the concealment of Label-Flip Attack is not as high as imagined, not to mention that Fraud Induced Label-Flip also requires two backdoors. In contrast, other financial data of the organization can be obtained or estimated through public resources such as the company's annual report. Therefore, the Clandestine Fraudulence and Clean Label Attack is more cost-effective and highly concealable.

For the Induced Model Attack, although two backdoors are required because only the input data is attacked and there is no need to synchronize the two backdoors B'_X, B_X, the cost of the attack is still low and the stealthiness is also very high. However, for Model Corruption Attack and Full Clandestine FDI, both need to synchronize B_X, B_Z before the model can be guided with a certain intention. Since the synchronization process requires additional synchronization time communication data between the backdoor functions, which may alert the system to the failure of the attack by activating the defense, it is not as stealthy as the Induced Model Attacks with the covert FDI.

Since Clandestine Fraudulence, Clean Label Attacks, and Induced Model Attacks are better than other attacks in terms of stealthiness and cost-effectiveness, they are also commonly used by providers. The covert FDI attack model is often used by providers. In this paper, we will focus on these three covert FDI patterns for further in-depth study.

6.2.3.2 Adversarial Backdoor Attacks

In the process of adversarial backdoor attack implementation, the magnitude and scope of the data attack are usually also adjusted to further improve the concealment, in order to conceal as much as possible the attack traces without affecting the attack's effectiveness. For this reason, we parametrically model the magnitude and range to describe the pattern of such backdoor attacks. Therefore, the backdoor attack function can be formulated as

$$\tilde{X} = B(X, w, M) = X \odot (1 - M) + (1 \pm w) X \odot M \tag{6.3}$$

in which w refers to the attack magnitude as the error between the data after the attack and the original data, while M refers to the mask of the attack against the data sample.

To parameterize the attacks for the evaluation, we use relative error here to describe the attack magnitude w, which describes the percentage of the attacked data error to the original data, which can be formulated as

$$w = \frac{|x - \tilde{x}|}{x} \tag{6.4}$$

in which x refers to the original data record, and $\tilde{x}$ the corrupted data. Similarly, the attack mask M can be parameterized with the attack range r can be quantified as the number of attacked data records, i.e., how many data records have been tampered with. The attack range r is the ratio of the number m of contaminated data records to the number n of original data records, which can be formulated as $r = m/n$. The corresponding backdoor function $B(\cdot), B_X(\cdot), B_Z(\cdot)$ can be further parameterized as $B^{(w,r)}(\cdot), B_X^{(w,r)}(\cdot), B_Z^{(w,r)}(\cdot)$ to represent the diversity of the backdoor attacks.

Usually, when the amplitude and the range of the attack are smaller, the less detectable it is, but the effect of the attack is also limited by the constraint of the freedom of the attack. However, when the magnitude and range of the attack increase, the freedom and destructiveness of the attack increase at the same time, and the risk of the attack being detected also increases. Therefore, how accomplishing the attack expectation while ensuring the attack concealment is something that needs to be done by balancing concealment and freedom.

6.3 Countermeasures Against False Data Injection

False Data Injection (FDI) attacks represent a critical challenge in modern machine intelligence and cyber-physical systems, where adversaries attempt to manipulate sensor readings, control signals, or decision variables to introduce systematic bias. In this section, we provide an analytic discussion of both preventive mechanisms and remedial strategies when bias contamination has already occurred.

6.3.1 Preventive Security Mechanisms

The first line of defense against FDI attacks relies on proactive security enforcement at the data acquisition and transmission stages. Secure firewalls [6, 200], intrusion detection systems (IDS [123, 157, 169]), and role-based access control (RBAC [208, 209]) can effectively reduce the probability of unauthorized injections by external adversaries. Complementary to this, cryptographic techniques such as Transport Layer Security (TLS [168, 236]), Advanced Encryption Standard (AES [167]), and digital signatures ensure that transmitted data is protected from tampering and that its authenticity is verifiable [52, 216].

Beyond perimeter defense, redundancy and consistency play an essential role. Multi-source redundancy, where multiple independent sensors observe the same variable,

enables cross-validation checks to detect anomalous deviations that might indicate injected data [260, 268]. On the other hand, System-level design must embrace resilience principles. Fault-tolerant control ensures that even if a portion of the data pipeline is compromised, the overall decision-making process remains robust [22, 207, 265]. These strategies embody the notion of defense-in-depth, where multiple layers of complementary safeguards are deployed to collectively enhance security.

6.3.2 Mitigation After Bias Contamination

While preventive strategies are essential, they are not infallible. In practice, FDI attacks may succeed in partially contaminating data streams. Importantly, such contamination rarely affects all sources uniformly; typically, only a subset of data or expert agents is compromised. This leads to what we define as Disparity from Bias, where biased and unbiased data coexist within the system.

Under such conditions, mitigation strategies become indispensable. Instead of assuming data integrity, the system must adaptively recalibrate its decision-making process. Optimal decision-making frameworks allow the integration of both reliable and potentially contaminated inputs, using the trusted subset to counterbalance the distortion introduced by malicious injections. By designing fusion algorithms that assign dynamic weights based on reliability assessment, the system effectively compensates for bias, restoring fairness and decision reliability [135, 141].

The advantage of this approach lies in its resilience. Even when preventive defenses fail and adversarial bias is present, the system maintains robust decision quality. This two-pronged framework, comprising proactive prevention and adaptive mitigation, ensures that FDI-induced bias disparity does not critically impair system performance. The detailed implementation of the optimal fusion framework and adaptive weighting algorithms will be further elaborated in the subsequent sections.

It is therefore evident that a dual-layered defense paradigm is essential. While preventive mechanisms such as encryption, intrusion detection, and access control are indispensable for compliance and frontline protection, they cannot fully eliminate the possibility of compromise. In safety-critical domains, including financial information systems, power systems, intelligent transportation, and healthcare, partial data contamination remains an inevitable risk. This underscores the need for robust mitigation strategies capable of restoring reliability even under biased or adversarial inputs. To address this challenge, the following chapter introduces adaptive fusion methods, which

leverage decision-theoretic principles to reconcile conflicting signals, compensate for bias disparity, and safeguard the integrity of system-level decisions.

6.4 Disparity from Cognitive Bias

Bias in expert judgment is a key issue in the decision-making process. Because of various things that the expert has imperfect knowledge of, when experts' judgments are influenced by biases or differing methodologies, the resulting disparities can create confusion and uncertainty in the decision-making process [69, 178]. Because decision-making is often complex and multifaceted, necessitating input from various domains of expertise [174, 232], the presence of diverse perspectives can be beneficial [85, 119, 180].

Multi-expert decision-making involves aggregating diverse opinions from multiple experts to enhance the quality and reliability of decisions, and corresponding systems play a pivotal role in this context by integrating diverse perspectives and insights from specialists in areas such as risk assessment, market analysis, investment strategies, and regulatory compliance [67, 286]. These systems harness the collective intelligence of multiple experts to enhance the robustness and reliability of decisions. By mitigating the limitations inherent in individual expert judgments [139, 156, 228], such as cognitive biases and knowledge gaps [29, 65, 121], multi-expert systems foster a more holistic understanding. This collaborative approach not only enriches the decision-making process but also promotes greater transparency and accountability, as it allows stakeholders to consider a wider array of factors and potential outcomes. Consequently, the incorporation of multi-expert systems is crucial for organizations aiming to navigate the complexities of financial markets and to make informed, strategic decisions that align with their long-term objectives [158, 241].

Although the use of diversity in multi-expert systems can reduce monotonous bias through diversity, the multi-expert system also introduces diversity of bias thus disparity from various sources, which may cause confusion and contradiction in evaluation [2, 118]. This disparity can significantly impact decision quality, as differing opinions may lead to conflicting conclusions and strategies [129, 198]. This inconsistency can dilute the credibility of the analysis and may result in suboptimal choices that do not align with the organization goals.

Disparity caused by divergent biases among experts present significant challenges in financial decision-making, as they can lead to inconsistencies and misalignments in judgment and recommendations [25, 78, 86]. Each expert brings a unique set of experiences,

knowledge, and cognitive predispositions, which can result in varying interpretations of data and divergent conclusions. Such biases may stem from personal experiences, industry backgrounds, or even the psychological heuristics that influence decision-making processes [182]. When these biases manifest within a multi-expert system, they can create conflicts that complicate consensus-building and obscure the true nature of the financial landscape. Moreover, divergent biases can introduce substantial risk, as they may lead to the neglect of critical information or the overemphasis of certain factors, skewing the final decision [77, 221, 226]. This not only hampers the effectiveness of collaborative decision-making but also raises concerns about accountability and trust in the outcomes produced. As financial markets become increasingly volatile and interconnected, addressing the challenges posed by divergent biases is essential for ensuring that decisions are well-informed, coherent, and aligned with strategic objectives [217, 219].

It can be seen that biases inherent in individual expert judgments can distort analyses and lead to inconsistent recommendations, ultimately compromising the effectiveness of financial strategies. Stakeholders may struggle to reconcile these differing viewpoints, leading to delays in decision-making and a potential loss of competitive advantage in rapidly changing [165, 252]. Ultimately, the presence of multi-expert disparity can undermine the reliability of forecasts and risk assessments, emphasizing the need for effective integration and synthesis of expert opinions to enhance overall decision quality.

Therefore, it is necessary to mitigate bias in multi-expert systems, enhancing the quality and reliability of decision-making processes, particularly in complex fields such as finance. To tackle the challenges of divergent biases in multi-expert systems, we present an Adaptive Kappa-Ordered Weight Averaging (KOWA) fusion for multi-expert decision-making. By employing ordered weighting principles, KOWA systematically integrates expert judgments, assigning weights based on consensus and reliability. The framework begins by identifying biases and outlier opinions through a kappa statistic, facilitating a nuanced weighting system that enhances decision quality by mitigating extreme biases. By addressing and reducing these biases, we aim to create a more cohesive and accurate synthesis of expert opinions.

We aim to obtain a reliable decision-fusion, improving assessment consistency with less disparity for risk management and overall organizational credibility in analyses. This involves employing systematic approaches to identify, quantify, and integrate diverse viewpoints, thereby fostering a more balanced representation of knowledge. Ultimately, the objective is to ensure that decisions are grounded in a robust, objective framework that reflects a comprehensive understanding of the financial landscape, thus enabling

organizations to navigate uncertainties and capitalize on opportunities more effectively. Thus, we propose Adaptive Kappa Ordered Weighted Averaging (KOWA) method that integrates kappa statistics with its integration of ordered weighting principles with to address divergent biases in multi-expert systems. Unlike traditional methods, KOWA evaluates the reliability and consensus of expert opinions, allowing for dynamic weight adjustments based on input quality. This enhances decision-making robustness and effectively mitigates outlier influences. Its significance is especially relevant in financial decision-making, where varied expert opinions can introduce substantial risks. By promoting a consistent assessment framework, KOWA enables organizations to make informed, strategic decisions, thereby enhancing the credibility and trustworthiness of financial analyses and overall organizational resilience.

6.5 Optimal Decision-Making Under Bias

In multi-expert decision-making, various weighting methods have been developed to integrate diverse expert opinions effectively. Among these, the Ordered Weighted Averaging (OWA) method [70, 165, 272], the Analytic Hierarchy Process (AHP [90, 235, 238, 292]), and the Multi-Attribute Utility Theory (MAUT [163, 196, 253]), Preference Ranking Organization Method for Enrichment Evaluations (PROMETHEE [26, 37, 51, 170]) stand out as prominent techniques, each with distinct advantages and limitations.

The OWA method introduces an innovative approach to weighting by allowing decision-makers to assign different weights to expert opinions based on their significance and reliability. This technique emphasizes the importance of collective judgment, enabling a nuanced aggregation of expert evaluations. By utilizing ordered weights, OWA accommodates scenarios where the decision context favors consensus or dissent, making it versatile for various applications. However, its effectiveness largely depends on the accurate determination of weights, which can be subjective and challenging.

The AHP, on the other hand, is a structured technique that breaks down complex decision problems into a hierarchy of simpler, more manageable components. By conducting pairwise comparisons, AHP allows decision-makers to establish priorities among criteria and alternatives, ultimately leading to a comprehensive ranking. While AHP is beneficial for its systematic approach and ability to incorporate qualitative assessments, it can become cumbersome with an increasing number of experts or criteria, potentially leading to inconsistencies in judgments. Meanwhile, AHP relies heavily on pairwise comparisons, which may not adequately represent the nuances of expert judgments.

Multi-Attribute Utility Theory (MAUT) extends the evaluation framework by considering multiple attributes simultaneously, allowing for a holistic assessment of alternatives. This method employs utility functions to quantify preferences across various criteria, providing a clear framework for decision analysis. MAUT is particularly effective in capturing trade-offs between competing objectives; however, it requires detailed information about the decision-makers' preferences, which can be difficult to elicit accurately.

PROMETHEE (Preference Ranking Organization Method for Enrichment Evaluations) is a multi-criteria decision-making method that facilitates the ranking of alternatives based on multiple attributes. By comparing the performance of options across various criteria, PROMETHEE establishes preference relations that reflect decision-makers' priorities. This method incorporates weightings to account for the relative importance of each attribute, allowing for a nuanced evaluation of trade-offs among competing options. While PROMETHEE excels in providing a structured framework for complex decision problems, its effectiveness relies on the accurate determination of weights and preference thresholds, which can present challenges in practice.

While each of these techniques offers valuable tools for decision-making, they also exhibit limitations that can impact the overall quality of decisions. They struggle to account for divergent biases among experts, which can skew outcomes and lead to suboptimal decisions. Moreover, these techniques do not incorporate mechanisms for adaptive adjusting weights based on the consistency and disparity of expert input, resulting in a rigid framework that may fail to adapt to varying contexts. These limitations highlight the need for methods that can better manage biases and enhance the reliability with consistency and overall robustness of multi-expert decision-making.

6.6 Adaptive Kappa-Ordered Weight Averaging

The Kappa-Ordered Weight Fusion (KOWA) method aims to address these shortcomings by integrating the principles of ordered weighting with kappa statistics, providing a more dynamic and robust framework for managing biases and enhancing the decision-making process in multi-expert systems. The Kappa-Ordered Weight Fusion (KOWA) method addresses these challenges as a solution by synthesizing expert opinions to migrating biases, fostering a more balanced and reliable decision-making process.

Adaptive Kappa-Ordered Weight Averaging (KOWA) method serves as an adaptive fusion framework for decision-making that integrates the principles of ordered weighted averaging (OWA) with kappa statistics to effectively mitigate biases in multi-expert

systems. The methodology consists of several key steps: expert judgment collection, bias assessment, weight assignment using kappa statistics, and the final aggregation of expert opinions.

Ordered Weighted Averaging (OWA) is a mathematical aggregation method that combines individual expert opinions into a collective decision. It operates on the principle of ranking the inputs and applying different weights to these ranked values. The primary goal of OWA is to account for the varying degrees of optimism or pessimism in the decision-making process, allowing for a more nuanced aggregation of expert judgments.

Let $X = \{x_{ij}\}$ be a matrix of expert judgments, where i indexes the experts ($i = 1,2,\ldots,n$) and j indexes the objects ($j = 1,2,\ldots,m$). Each entry x_{ij} denotes the score given by expert i to object j. For each object j, the expert judgments are ranked in descending order. Let $x_{(1)j}, x_{(2)j}, \ldots, x_{(n)j}$ represent the ordered scores for object j, such that:

$$x_{(1)j} \geq x_{(2)j} \geq \ldots \geq x_{(n)j}$$

The OWA operator employs a weight vector $W = \{w_1, w_2, \ldots, w_n\}$ to assign different importance to the ranked scores. The weights must satisfy the following conditions:

1. $w_i \geq 0$ for all i. 2. $\sum_{i=1}^{n} w_i = 1$.

The weight vector can be determined using various methods, including uniform weighting, linear weighting, or exponential weighting, depending on the desired level of optimism or pessimism in the decision-making process.

The aggregation of expert opinions for object j using the OWA operator is defined as follows:

$$OWA_j = \sum_{i=1}^{n} w_i x_{(i)j}$$

This equation implies that the final decision OWA_j is a weighted sum of the ordered expert scores, where the weights reflect the relative importance assigned to each score.

OWA provides a flexible and robust framework for aggregating expert opinions by allowing decision-makers to express their attitude towards risk and uncertainty through the selection of appropriate weights. By ranking the expert judgments, OWA emphasizes the more favorable or relevant opinions while downplaying less critical inputs.

The choice of the weight vector W is particularly significant, as it directly influences the aggregation outcome. For instance, a weight vector that favors higher-ranked scores will result in a more optimistic decision, whereas one that emphasizes lower-ranked

scores may yield a more cautious assessment. This characteristic allows OWA to adapt to various decision-making contexts, making it suitable for a wide range of applications.

Moreover, the capacity of OWA to incorporate varying degrees of optimism or pessimism offers a significant advantage over traditional averaging methods, which treat all opinions equally. By doing so, OWA enhances the robustness and relevance of the aggregated decision, thus improving the quality of outcomes in multi-expert systems.

The Ordered Weighted Averaging method provides a powerful and flexible framework for aggregating expert opinions. Its mathematical rigor, combined with the ability to incorporate varying attitudes towards risk, makes OWA a valuable tool in decision-making processes across diverse fields. The structured approach of ranking and weighted aggregation positions OWA as a significant advancement in the methodology of multi-expert decision-making.

Based on it, let $X = \{x_{ij}\}$ denote a matrix of expert judgments, where i indexes the experts ($i = 1, 2, \ldots, n$) and j indexes the objects ($j = 1, 2, \ldots, m$). Each entry x_{ij} represents the score given by expert i to object j.

To identify biases among experts, we compute the pairwise kappa statistic, which measures the level of agreement among the expert judgments. The kappa statistic κ_{ij} between expert i and expert j is defined as

$$\kappa_{ij} = \frac{P_o - P_e}{1 - P_e}$$

where P_o is the observed agreement among experts, and P_e is the expected agreement by chance. The overall kappa statistic for expert i can be calculated as

$$\kappa_i = \frac{1}{n-1} \sum_{j \neq i} \kappa_{ij}$$

This statistic is crucial for determining the reliability of each expert judgment.

The weights assigned to each expert opinion are derived from their respective kappa statistics. The weight w_i for expert i is calculated as

$$w_i = \frac{\kappa_i}{\sum_{k=1}^{n} \kappa_k}$$

This ensures that the weights are normalized and sum to one

$$\sum_{i=1}^{n} w_i = 1$$

Once the weights have been established, the aggregation of expert opinions can be performed using the ordered weighted averaging (OWA) operator. The OWA operator for

a given object j is defined as

$$KOWA_j = \sum_{i=1}^{n} w_i f(x_{(i)j})$$

where f is a monotonic non-decreasing function, and $x_{(i)j}$ represents the i-th ranked score for object j.

The integration of kappa statistics within the KOWA framework serves to enhance the decision-making process by providing a nuanced weighting mechanism that reflects both the quality of individual expert inputs and the consensus among them. By systematically identifying outlier judgments through bias assessment, KOWA minimizes the impact of extreme scores that could distort the overall evaluation.

6.7 Summary

This chapter examines two critical sources of bias in decision-making, False Data Injection (FDI) in machine learning systems and disparities in multi-expert judgments. Both phenomena undermine the reliability, consistency, and accountability of financial analyses, albeit through distinct mechanisms.

False Data Injection (FDI) represents a covert and adversarial form of bias, wherein features or labels in financial datasets are deliberately manipulated to distort credit scoring or predictive outcomes without interrupting normal system operations. Unlike physical systems, financial data generally lack inherent invariants that enable straightforward anomaly detection, rendering conventional defenses largely ineffective. To systematically analyze FDI, a taxonomy of attacks is established based on target and stealth characteristics. Low-cost, highly covert attacks such as clandestine fraudulence, clean-label, and induced model attacks are practically significant, whereas label-flip and full-scale FDI attacks are easier to detect but more resource-intensive. Parameterizing attacks by magnitude (w) and range (r) provides a structured framework for evaluating the trade-off between impact and detectability, offering actionable insights into system vulnerabilities.

In parallel, multi-expert decision-making addresses bias arising from cognitive variability among human experts. Integrating diverse judgments in complex domains such as finance enhances robustness, accountability, and overall decision quality. However, expert diversity also introduces disparity: divergent biases, conflicting interpretations, and variable reliability can obscure consensus, dilute credibility, and elevate operational risk. Traditional aggregation methods, including Ordered Weighted Averaging

(OWA), Analytic Hierarchy Process (AHP), Multi-Attribute Utility Theory (MAUT), and PROMETHEE, provide structured frameworks for combining expert inputs but often fail to adapt to heterogeneous reliability or outlier judgments, limiting their effectiveness in practice.

To address these challenges, the Adaptive Kappa-Ordered Weighted Averaging (KOWA) method integrates OWA with kappa statistics, dynamically evaluating expert reliability and consensus. By identifying inconsistent or biased judgments, assigning weights proportional to agreement, and aggregating opinions using an ordered weighting scheme, KOWA mitigates the influence of extreme or conflicting inputs. This approach enhances coherence, accuracy, and robustness in multi-expert systems, providing a systematic mechanism that balances the benefits of expertise diversity with the need for consistent, high-quality financial decisions. Consequently, KOWA enables organizations to make informed, accountable, and strategically aligned choices under conditions of uncertainty and cognitive variability.

Building on these theoretical foundations, the chapter transitions to empirical evaluation. For FDI, robust training, secure data pipelines, anomaly detection, and layered auditing are examined through systematic experiments assessing model vulnerability. Machine learning-based credit rating systems are evaluated under diverse FDI scenarios using comprehensive metrics, accuracy, weighted precision, macro-averaged recall, and macro-averaged F1-score, aggregated across models and time periods. These experiments quantify the operational impact of adversarial interventions and provide guidance for designing resilient, defensible financial systems.

Similarly, the practical utility of KOWA in multi-expert decision-making is empirically tested through the investment evaluation of 924 Nasdaq-listed companies. Six anonymized experts from economics, finance, trading, business, and mathematics independently rated each company using standardized financial indicators and historical price data. This controlled experiment demonstrates how adaptive fusion of diverse expert assessments produces robust, unbiased ratings, illustrating the capacity of KOWA to enhance reliability, consistency, and overall decision quality. Collectively, these empirical studies underscore the critical importance of systematic bias mitigation, both algorithmic and cognitive, in strengthening financial decision-making processes, ensuring that predictions and judgments are not only accurate but also strategically actionable.

CHAPTER 7

CASE STUDIES AND EMPIRICAL ANALYSIS

7.1 KIO Experiment and Results

7.1.1 Test on KIOKAR for carbon

To demonstrate the feasibility and performance of the KIOKAR (Kolmogorov-Arnold Finance Informed Neural) network, an experiment is conducted to evaluate its effectiveness in modeling European call carbon options, a critical problem in carbon pricing and risk management. The experiment compares the predictions of KIOKAR with the analytical solution provided by the Black-Scholes (BS) model, which serves as the benchmark for this evaluation.

KIOKAR enhances computational efficiency and interpretability by leveraging the Kolmogorov-Arnold representation theorem, which decomposes complex multivariate functions into simpler univariate components. This decomposition improves both the model's performance and its interpretability, making KIOKAR a promising tool for financial and environmental modeling.

The experiment is designed to simulate carbon credit options pricing within a realistic market environment, incorporating common financial parameters. The strike price, set at 40, represents the price at which the holder of the option has the right to buy or sell carbon credits. The risk-free rate, set at 0.05, reflects the theoretical return on an investment with no risk, serving as a benchmark for comparing the carbon credit option performance. Volatility, assumed to be 0.2, measures the expected fluctuation in the

price of carbon credits, indicating the level of market uncertainty and risk. The maturity period of 1 year defines the time frame over which the option's value is assessed. These parameters, which mirror typical market conditions, enable the experiment to evaluate how fluctuations in carbon credit prices and market dynamics influence the valuation of carbon credit options.

The underlying asset prices range from 0 to 160, with time intervals spanning from the present to the maturity date. A total of 10,000 sample points are generated for the dataset, covering various combinations of asset prices and times to maturity.

By comparing the output of the KIOKAR model with the Black-Scholes pricing, we aim to highlight KIOKAR ability to capture the complex dynamics of European call carbon options. The results are expected to demonstrate KIOKAR accuracy in option pricing as well as its computational advantages over traditional methods. Furthermore, the interpretability of the model, enhanced by the Kolmogorov-Arnold decomposition, is expected to provide valuable insights for carbon analysis and risk management.

7.1.2 Experiment Setting and Implementation

This section presents the experimental setup utilized to assess the performance of the proposed KIOKAR framework in modeling carbon finance dynamics, particularly in the context of call credit option pricing. The key parameters and settings employed during the experiments are summarized in Table 7.1.

The evaluation primarily focuses on comparing the model loss using various performance metrics, such as the mean squared error (MSE), which are employed to assess both the accuracy and robustness of the model under the given governing rules. These metrics are crucial for understanding how effectively the KIOKAR framework captures the underlying dynamics of carbon markets and option pricing, with particular attention to carbon balance computations. The objective of this experimental setup is to validate the potential of KIOKAR in enhancing carbon modeling and risk management.

In order to further evaluate the effectiveness of the KIOKAR model, a comparative analysis is conducted against several baseline models that have demonstrated utility in similar fields. These baseline models include KIO REG as proposed by [58, 62, 102], KIO FNN developed in [35, 93, 94, 282], KIO DNN explored in [112, 195, 244], KIO MLP studied in [127, 159, 206], and KIO GRU introduced in [43, 134, 145, 153]. These models serve as performance baselines, offering a comparative framework to evaluate KIOKAR's advantages in terms of both accuracy and computational efficiency.

Parameter	**Value**
Emission Upper Bound (E_K)	200
Emission Growth Rate (r)	0.05
Emission Decay (γ)	0.05
Initial emission rate (P_0)	10
Sequestration Upper Bound (S_K)	700
Maximum sequestration rate (R_{max})	90
Sequestration growth rate (k)	0.1
Sequestration Decay (λ)	0.05
Emission Range (E)	$E \in [0, 100]$
Sequestration Range (S)	$S \in [0, 100]$
Strike Price (K)	60
Risk-Free Rate (r)	0.05
Volatility (σ)	0.2
Asset Price Range (Z)	$Z \in [0, 160]$
Time Range (t)	$t \in [0, T]$
Start time (t_0)	0
Expiration Maturity (T)	10
Number of Samples (N_{sample})	10000
Carbon Info Weight (σ_{carbon})	0.1
Initial Value Weight ($\sigma_{initial}$)	1
Zero Boundary Weight ($\sigma_{boundary,0}$)	1
Infinity Boundary Weight ($\sigma_{boundary,\infty}$)	1
Finance Info Weight ($\lambda_{financial}$)	0.1
Initial Value Weight ($\lambda_{initial}$)	1
Zero Boundary Weight ($\lambda_{initial}$)	1
Infinity Boundary Weight ($\lambda_{initial}$)	1

Table 7.1: Parameter Settings for Carbon Balance Test

All models are evaluated under identical experimental settings to ensure a fair comparison. This approach allows for a meaningful evaluation of KIOKAR performance in the context of carbon finance dynamics.

For each model, the training process is carried out over 2300 epochs. This configuration is selected to ensure adequate model convergence and stability. During training, the performance of the models is measured using the mean squared error (MSE) as the primary evaluation metric. The results of this evaluation will provide insight into how well each model can approximate the carbon market and option pricing behaviors while also accounting for generalization ability and computational efficiency.

7.1.3 Results

In this section, we present the results of our KIOKAR-based approach for modeling carbon dynamics. Figures 7.1 and 7.2 illustrate the solutions obtained by KIOKAR for emission and sequestration after 5000 epochs of training. Additionally, Figure 7.3 depicts the results for option pricing.

We also analyze the convergence behavior of the KIO models throughout the training process. To monitor the progress of the model, we track all loss function values over successive iterations. Figures 7.4 to 7.21 display the loss trajectories during training. The KIOKAR model demonstrates rapid convergence, as indicated by the stabilization of all loss functions. This result reflects the efficiency of the KIOKAR approach in training neural networks, specifically for carbon-related applications, where convergence is a critical factor in ensuring the model's effectiveness and accuracy.

Furthermore, Table 7.2 presents a comparative evaluation of six different methods,ÄîKIO DNN, KIO FFN, KIO GRU, KIO MLP, KIO REG, and KIOKAR,Äîover 5000 epochs. The analysis focuses on Total Loss and Sequestration, with the provided metrics including the mean, standard deviation (std), minimum (min), and maximum (max) values. This comparative analysis offers a comprehensive assessment of the performance of these methods based on these critical metrics, highlighting the strengths and weaknesses of each approach in the context of carbon modeling and risk management.

Table 7.2: Total Loss Stats with 5000 Epochs

Emission	KIO DNN	KIO FFN	KIO GRU	KIO MLP	KIO REG	KIOKAR
mean	9.01×10^{3}	9.41×10^{3}	1.07×10^{4}	1.03×10^{4}	3.82×10^{3}	2.68×10^{08}
std	7.84×10^{2}	7.66×10^{2}	4.08×10^{1}	3.30×10^{2}	3.26×10^{2}	1.77×10^{10}
min	7.96×10^{3}	8.30×10^{3}	1.05×10^{4}	9.74×10^{3}	3.31×10^{3}	4.82×10^{0}
max	1.11×10^{4}	1.11×10^{4}	1.08×10^{4}	1.10×10^{4}	4.67×10^{3}	1.26×10^{12}
Sequestration	KIO DNN	KIO FFN	KIO GRU	KIO MLP	KIO REG	KIOKAR
mean	7.93×10^{5}	7.67×10^{5}	8.39×10^{5}	8.26×10^{5}	7.83×10^{5}	1.67×10^{13}
std	3.40×10^{4}	4.97×10^{4}	3.79×10^{3}	1.08×10^{4}	4.00×10^{4}	1.17×10^{15}
min	7.21×10^{5}	6.88×10^{5}	8.22×10^{5}	7.95×10^{5}	7.03×10^{5}	5.09×10^{1}
max	8.51×10^{5}	8.52×10^{5}	8.53×10^{5}	8.51×10^{5}	8.48×10^{5}	8.32×10^{16}
Option	KIO DNN	KIO FFN	KIO GRU	KIO MLP	KIO REG	KIOKAR
mean	1.07×10^{4}	1.14×10^{4}	1.42×10^{4}	1.21×10^{4}	8.16×10^{3}	2.88×10^{1}
std	7.25×10^{2}	4.10×10^{2}	2.82×10^{2}	1.81×10^{2}	1.87×10^{3}	1.52×10^{2}
min	9.93×10^{3}	1.08×10^{4}	1.22×10^{4}	1.17×10^{4}	5.85×10^{3}	9.41×10^{-1}
max	1.25×10^{4}	1.23×10^{4}	1.57×10^{4}	1.25×10^{4}	1.29×10^{4}	5.93×10^{3}

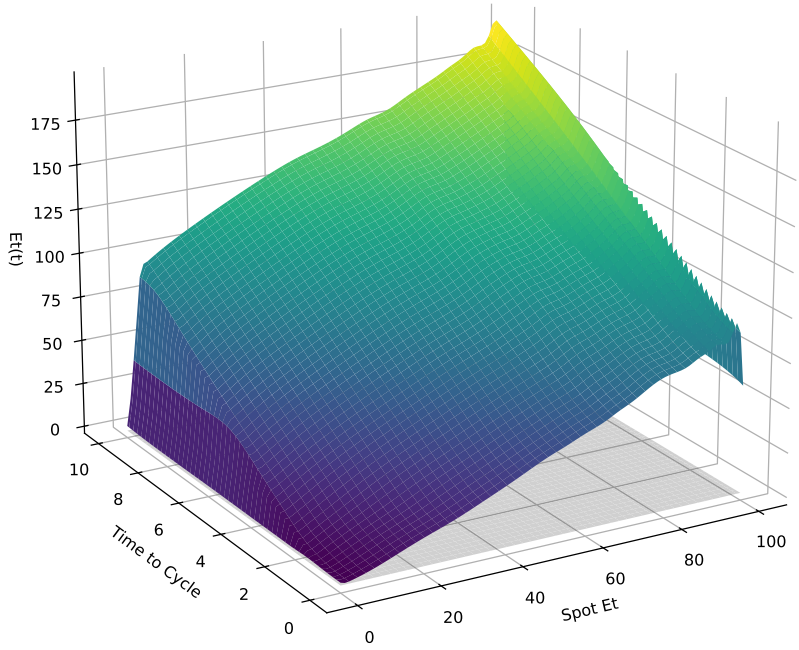

Figure 7.1: KIOKAR Et

7.1.4 Emission Analysis

The KIO REG model demonstrates the most favorable performance in terms of total loss minimization, achieving the lowest mean total loss of 3.82×10^3. This outcome highlights KIO REG's superior average performance relative to the other models evaluated. In contrast, KIO DNN and KIO FFN exhibit higher mean total losses of 9.01×10^3 and 9.41×10^3, respectively, indicating that, while competitive, these models are less efficient in minimizing total loss compared to KIO REG. On the other hand, the KIOKAR framework reports a significantly higher mean total loss of 2.68×10^8, which initially suggests a performance disparity and implies that KIOKAR may be less effective in terms of total loss minimization relative to the KIO models.

Despite this higher mean total loss, KIOKAR demonstrates exceptional convergence capabilities, which is a critical aspect of its performance. The observed high standard deviation (1.77×10^{10}) for KIOKAR, although indicating variability in its performance, also reflects its robustness in rapidly reducing loss values across epochs. This suggests that, despite the higher initial loss, KIOKAR is able to effectively recover from subopti-

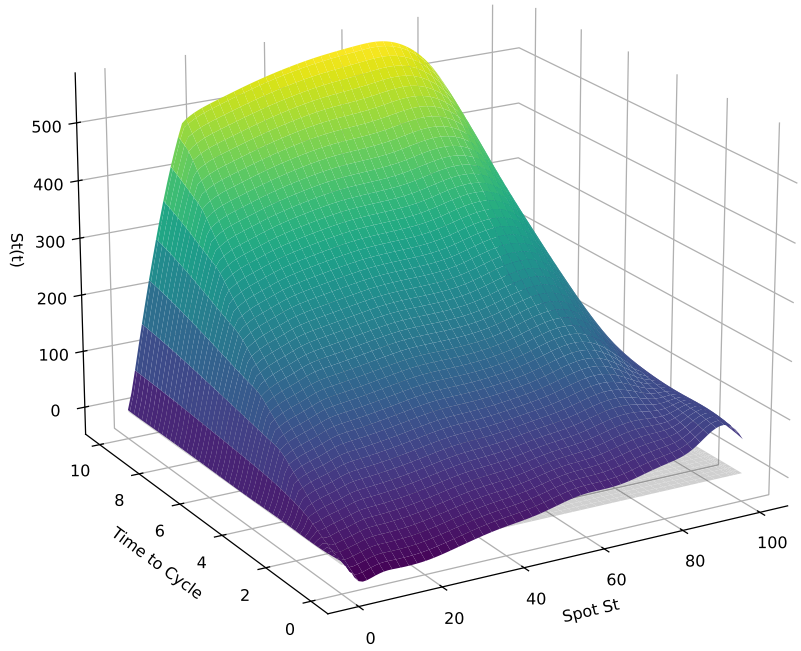

Figure 7.2: KIOKAR St

mal initialization conditions and converge to an optimal solution more efficiently than its counterparts. The model's ability to rapidly adjust and bring the loss toward zero indicates that, over time, it stabilizes and achieves minimal loss, showcasing its fast convergence ability.

In comparison, KIO GRU achieves the lowest standard deviation (4.08×10^1), demonstrating stable performance across epochs. This stability is advantageous for applications where consistent performance is required, as it ensures that the model delivers reliable results over time. Although KIO REG and KIO MLP report lower minimum total losses (3.31×10^3 and 9.74×10^3, respectively), their higher maximum total losses (4.67×10^3 for KIO REG and 1.10×10^4 for KIO MLP) suggest that, while these models can achieve low losses, they are more prone to significant fluctuations in performance.

KIOKAR, by contrast, exhibits a wide range of total loss values, with a minimum of 4.82×10^0 and a maximum of 1.26×10^{12}. This variability highlights the framework's dynamic nature and its ability to navigate through a broad spectrum of loss values. Despite this variability, KIOKAR's rapid convergence and its capacity to stabilize performance

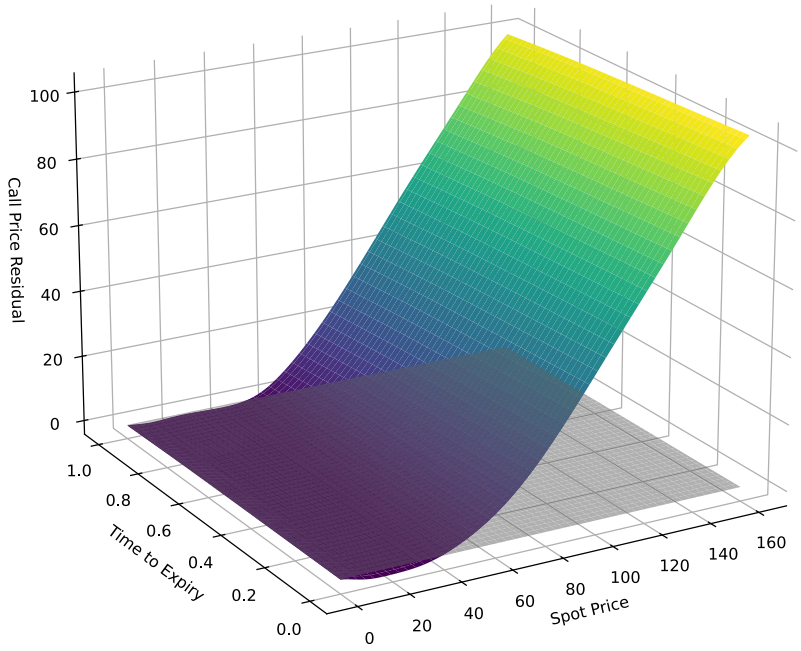

Figure 7.3: KIOKAR Option Price

quickly after initial fluctuations further underscore its potential. The model's ability to handle large variations and still converge to minimal loss levels efficiently sets it apart from the other methods in terms of long-term performance.

In conclusion, while KIOKAR initially demonstrates a higher mean total loss, its superior convergence speed and robustness make it a highly effective model for achieving optimal solutions in complex systems, even when faced with suboptimal starting conditions. The ability of KIOKAR to efficiently stabilize and minimize loss, despite initial performance challenges, positions it as a strong contender for applications in carbon dynamics and beyond.

.

7.1.5 Sequestration Analysis

The KIOKAR model outperforms other methods in terms of sequestration, demonstrating an exceptionally high mean sequestration value of 1.67×10^{13}. This remarkable performance positions KIOKAR as a leader in sequestration capacity, surpassing the other

models by a substantial margin. In comparison, the KIO methods such as KIO DNN and KIO FFN, while still competitive, exhibit slightly lower mean sequestration values. These methods, though effective, do not match the extensive sequestration capability demonstrated by KIOKAR, underscoring its superior performance in this particular metric.

However, the exceptional mean sequestration value of KIOKAR is accompanied by a significant degree of variability, as evidenced by the highest standard deviation observed in sequestration among all models, which is 1.17×10^{15}. This indicates considerable fluctuations in KIOKAR's performance across training epochs. Despite this variability, KIOKAR's ability to quickly converge to minimal loss values is noteworthy. The high standard deviation does not diminish its overall effectiveness but rather reflects its dynamic nature and the ability to recover from fluctuations during the training process.

In contrast, KIO GRU exhibits the lowest standard deviation in sequestration, with a value of 3.79×10^{3}, which signifies a more stable and consistent performance across training iterations. This stability is advantageous in applications where reliable and predictable results are crucial, particularly in real-time systems or situations demanding high consistency.

Further examination of the range of sequestration values reveals that KIOKAR exhibits the greatest variability among the models, with minimum and maximum values spanning from 5.09×10^{1} to 8.32×10^{16}. This broad range indicates a more dynamic behavior, suggesting that KIOKAR has a higher potential for exploring a wide variety of sequestration scenarios. Despite this variability, KIOKAR's rapid convergence towards minimal loss values over time demonstrates its robustness. On the other hand, models like KIO DNN, KIO FFN, and other KIO variants tend to show more narrow ranges and greater consistency in their sequestration outcomes. Notably, KIO GRU reaches the highest maximum sequestration value of 8.53×10^{5}, but the overall range remains smaller compared to KIOKAR.

While KIOKAR exhibits considerable variability in sequestration values, it distinguishes itself through its exceptional capacity for sequestration, rapid convergence, and effective stabilization over time. These characteristics underscore the model's potential for applications that require extensive sequestration capabilities, as well as its ability to improve performance through efficient convergence processes. Despite the variability, KIOKAR's overall effectiveness in sequestration, coupled with its dynamic nature, positions it as a highly competitive and promising model in carbon dynamics modeling and risk management.

7.1.6 Option Pricing Analysis

In this section, we present the results of KIOKAR's performance in option pricing after training for 2300 epochs. Figure 7.3 illustrates the learning outcomes, demonstrating that the KIOKAR model's predictions converge closely with the analytical benchmark solution. This alignment indicates that KIOKAR effectively captures the underlying dynamics of the option pricing problem.

To provide a more comprehensive comparison, we evaluate the performance of KIOKAR relative to several baseline models. Table 7.3 presents the statistics of the residuals between the predicted solutions from the various models and the analytical solution. The metrics include the mean, standard deviation (std), minimum, absolute minimum, maximum, and absolute maximum values, along with the mean squared error (MSE).

It can be seen in Table 7.3 that KIOKAR, with a mean of 2.88×10^1, demonstrates a remarkably lower performance metric when juxtaposed with alternative methods. For example, KIO GRU presents a mean value of 1.42×10^4, which is several orders of magnitude greater than that of KIOKAR. This significant disparity suggests that KIOKAR operates at a substantially lower output level. Such a characteristic may imply that KIOKAR is not only more efficient but also potentially more precise in the context of the metrics being assessed.

Further analysis of the standard deviation corroborates the findings regarding KIOKARs performance consistency. With a standard deviation of 1.52×10^2, KIOKAR exhibits a moderate variability when compared to KIO DNN, which has a standard deviation of 7.25×10^2, and KIO REG, with 1.87×10^3. This relatively lower standard deviation indicates that KIOKARs performance remains stable across different scenarios, suggesting reliability in its outputs compared to the greater variability observed in the other models.

Examining the minimum and maximum values provides additional insights into KIOKARs performance characteristics. The minimum output for KIOKAR, recorded at 9.41×10^{-1}, is considerably lower than the minimum values associated with all other methods. This observation indicates that, while KIOKAR may excel in certain scenarios, it is also capable of underperforming in others. Conversely, KIOKARs maximum value of 5.93×10^3 remains competitive when compared to the maximum outputs of the other models, which are higher. This duality suggests that KIOKAR can achieve favorable performance in specific instances, despite occasional low outputs.

Notably, KIOKAR demonstrates the smallest residuals across all measures, out-

performing the baselines by achieving lower values in every statistical category. This suggests that KIOKAR exhibits superior accuracy in its predictions, even after a relatively moderate number of epochs.

These results highlight the effectiveness of KIOKAR in the context of option pricing, demonstrating its ability to quickly converge to a solution that closely approximates the analytical benchmark. Furthermore, the comparative analysis underscores KIOKAR's robustness and efficiency relative to other models, providing strong evidence of its potential for practical applications in financial modeling and risk management.

Table 7.3: Residual Stats with 2300 Epochs

Residual	mean	std	min	abs min	max	abs max	MSE
KIOKAR	-0.2532	0.9578	-2.6867	0.0001	2.8779	2.8779	0.9814
KIO REG	-16.2222	23.7148	-73.0200	0.0002	15.1721	73.0200	825.4969
KIO FFN	-28.6290	32.1351	-97.0683	0.0003	4.1276	97.0683	1852.1833
KIO DNN	-22.9026	33.8007	-93.1510	0.0006	9.7752	93.1510	1666.8705
KIO MLP	-30.4478	33.8083	-100.7151	0.0040	2.1933	100.7151	2069.9526

7.1.7 Comparative Discussion

It can be seen that KIOKARs performance can be characterized by several noteworthy attributes. The model overwhelmingly lower mean performance compared to its counterparts may indicate a more efficient or accurate predictive capability. The moderate standard deviation reflects a level of consistency that is advantageous, particularly when contrasted with the greater variability seen in other methods. Moreover, while KIOKAR presents a rapid convergence to a lower minimum value among all, it also possesses competitive maximum performance, indicating its potential applicability in targeted scenarios.

KIOKAR shows impressive performance in sequestration but with substantial variability. This high performance in magnitude comes with significant unpredictability, implying that while KIOKAR would be effective in specific contexts, its overall reliability is questionable.

KIO REG stands out due to its low average total loss and stable performance with a relatively low standard deviation. However, its maximum total loss is higher than other KIO methods, suggesting that while it performs well on average, it may encounter higher loss in some cases. KIO GRU and KIO FFN offer more consistent performance in both total loss and sequestration. This stability makes them suitable for applications

Table 7.4: Loss Stats with 2300 Epoch Training

MEAN	$\mathscr{L}_{total}$	$\mathscr{L}_{initial}$	$\mathscr{L}_{financial}$	$\mathscr{L}_{boundary}$	$\mathscr{L}_{boundary,0}$	$\mathscr{L}_{boundary,\infty}$
KIOKAR	28.8352	18.6403	2.3630	7.8319	1.3675	6.4644
KIO REG	8156.2915	8156.1657	0.1257	1203.5108	0.0915	6952.5634
KIO FFN	11421.6493	11421.6481	0.0012	1861.5178	0.0004	9560.1299
KIO DNN	10732.5727	10732.5727	0.0000	1722.6049	0.1503	9009.8176
KIO MLP	12110.2974	12110.2974	0.0000	2020.4457	0.0017	10089.8499
STD	$\mathscr{L}_{total}$	$\mathscr{L}_{initial}$	$\mathscr{L}_{financial}$	$\mathscr{L}_{boundary}$	$\mathscr{L}_{boundary,0}$	$\mathscr{L}_{boundary,\infty}$
KIOKAR	151.5633	79.9292	2.4999	91.8692	5.0428	91.6668
KIO REG	1868.4424	1868.5568	0.1521	378.4857	0.0621	1490.7575
KIO FFN	410.3859	410.3870	0.0015	96.8601	0.0010	317.0152
KIO DNN	725.1539	725.1539	0.0001	157.5038	0.3906	569.4847
KIO MLP	180.6481	180.6481	0.0000	51.5401	0.0011	136.8783
MIN	$\mathscr{L}_{total}$	$\mathscr{L}_{initial}$	$\mathscr{L}_{financial}$	$\mathscr{L}_{boundary}$	$\mathscr{L}_{boundary,0}$	$\mathscr{L}_{boundary,\infty}$
KIOKAR	0.9411	0.4308	0.3437	0.0558	0.0066	0.0485
KIO REG	5849.0020	5848.5151	0.0003	727.2389	0.0287	5121.2471
KIO FFN	10825.3271	10825.3223	0.0000	1670.5862	0.0000	9140.9287
KIO DNN	9933.3311	9933.3311	0.0000	1481.9844	0.0001	8407.6611
KIO MLP	11744.3564	11744.3564	0.0000	1879.0813	0.0002	9850.9521
MAX	$\mathscr{L}_{total}$	$\mathscr{L}_{initial}$	$\mathscr{L}_{financial}$	$\mathscr{L}_{boundary}$	$\mathscr{L}_{boundary,0}$	$\mathscr{L}_{boundary,\infty}$
KIOKAR	5934.0322	1675.9518	10.5056	4255.2658	27.0373	4255.2524
KIO REG	12850.6650	12850.6641	0.5156	2249.6992	0.2395	10644.5205
KIO FFN	12270.0977	12270.0977	0.0055	2103.2632	0.0096	10183.2969
KIO DNN	12458.5586	12458.5586	0.0007	2175.2749	2.9416	10298.2354
KIO MLP	12493.1035	12493.1035	0.0000	2188.5798	0.0034	10312.2305

where dependable and predictable results are essential. KIO DNN and KIO MLP exhibit moderate performance, being outperformed by KIO REG in total loss and lagging behind KIOKAR in sequestration.

Overall, KIOKAR emerges as a formidable contender in the field, especially for objectives prioritizing reduced mean performance or the need for stable outputs.

.

7.1.8 Discussion

This paper emphasizes the pivotal role of carbon credits in mitigating greenhouse gas emissions through market mechanisms, facilitating cost-effective transactions between nations and companies. By recognizing carbon credits as financial assets, the study enhances trading capabilities and investment opportunities, further integrating financial technology to enable real-time data analysis and efficient transactions. This integration

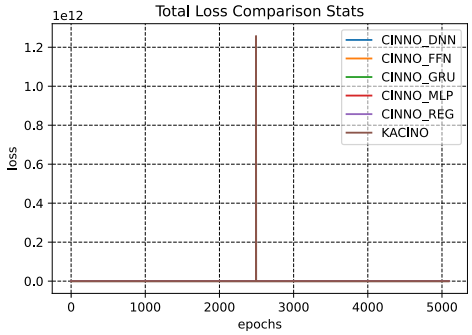

Figure 7.4: Total $\mathscr{L}_{initial}$ of E_t

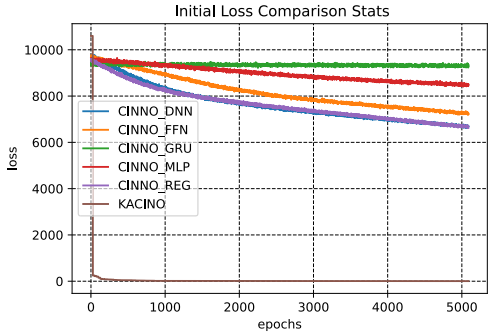

Figure 7.5: $\mathscr{L}_{initial}$ of E_t

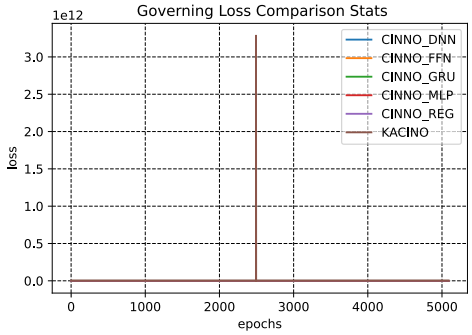

Figure 7.6: $\mathscr{L}_{carbon}$ of E_t

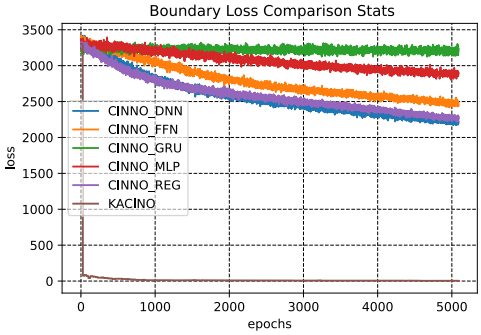

Figure 7.7: $\mathscr{L}_{boundary}$ of E_t

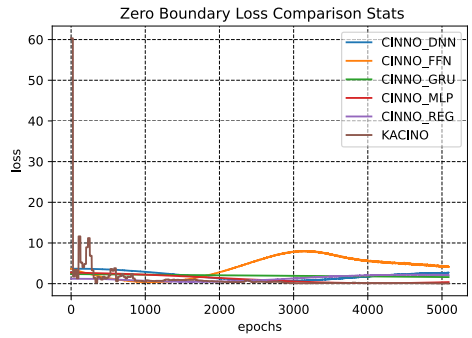

Figure 7.8: $\mathscr{L}_{boundary,0}$ of E_t

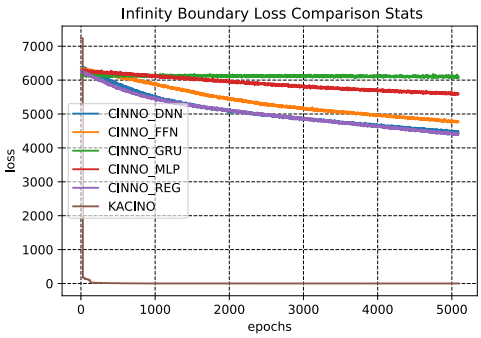

Figure 7.9: $\mathscr{L}_{boundary,\infty}$ of E_t

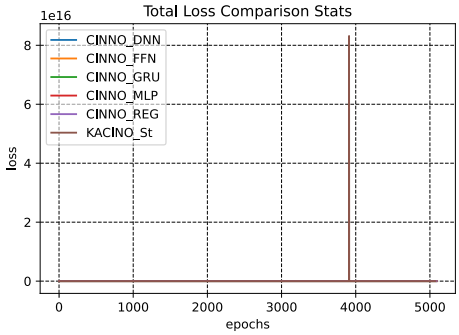

Figure 7.10: Total $\mathscr{L}_{initial}$ of S_t

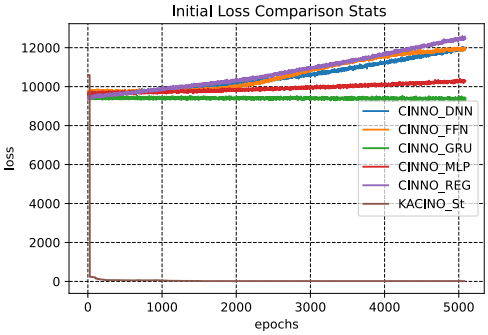

Figure 7.11: $\mathscr{L}_{initial}$ of S_t

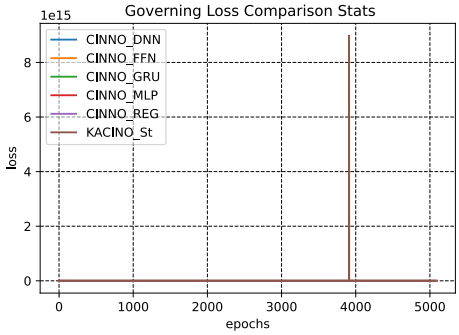

Figure 7.12: $\mathscr{L}_{carbon}$ of S_t

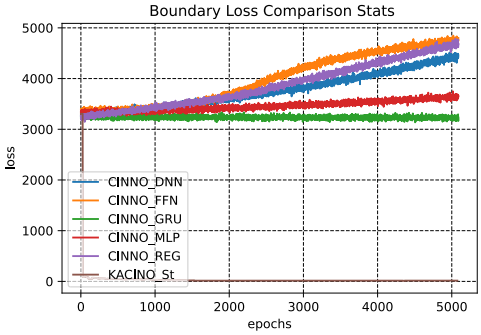

Figure 7.13: $\mathscr{L}_{boundary}$ of S_t

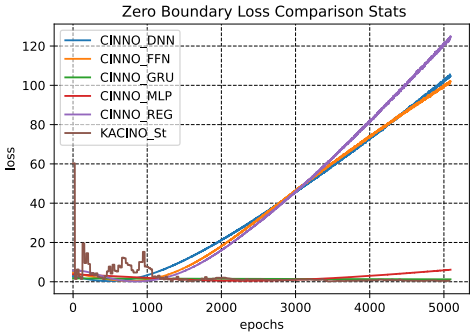

Figure 7.14: $\mathscr{L}_{boundary,0}$ of S_t

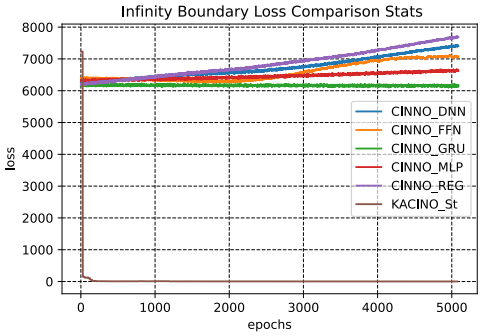

Figure 7.15: $\mathscr{L}_{boundary,\infty}$ of S_t

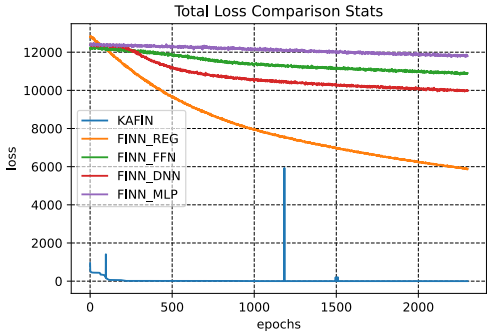

Figure 7.16: Total $\mathscr{L}_{initial}$ of Z_t

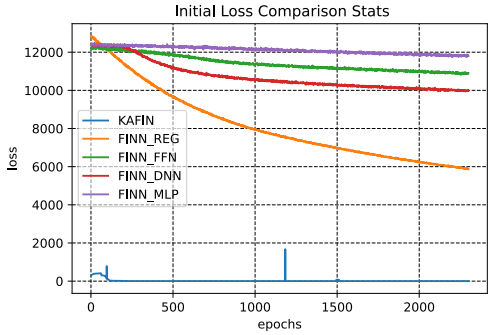

Figure 7.17: $\mathscr{L}_{initial}$ of Z_t

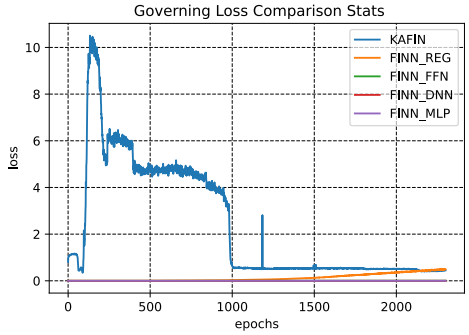

Figure 7.18: $\mathscr{L}_{carbon}$ of Z_t

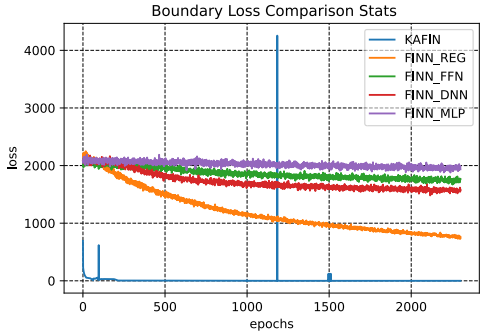

Figure 7.19: $\mathscr{L}_{boundary}$ of Z_t

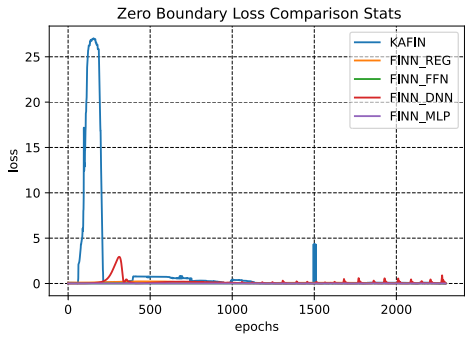

Figure 7.20: $\mathscr{L}_{boundary,0}$ of Z_t

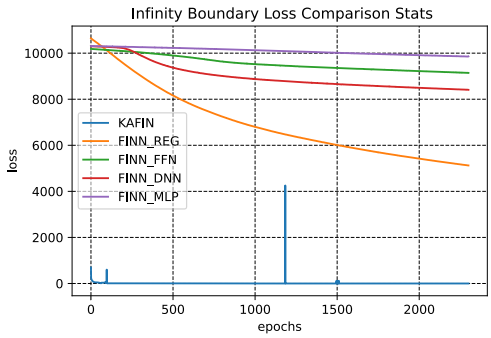

Figure 7.21: $\mathscr{L}_{boundary,\infty}$ of Z_t

Table 7.5: Governing Loss Stats with 5000 Epochs

Emission	KIO DNN	KIO FFN	KIO GRU	KIO MLP	KIO REG	KIOKAR
mean	1.35×10^3	1.23×10^3	1.32×10^3	1.33×10^3	1.22×10^3	6.97×10^8
std	1.35×10^1	6.95×10^1	1.19×10^1	1.17×10^1	7.84×10^1	4.62×10^{10}
min	1.30×10^3	1.08×10^3	1.27×10^3	1.30×10^3	1.08×10^3	9.43×10^0
max	1.39×10^3	1.36×10^3	1.36×10^3	1.39×10^3	1.37×10^3	3.29×10^{12}
Sequestration	KIO DNN	KIO FFN	KIO GRU	KIO MLP	KIO REG	KIOKAR
mean	7.82×10^5	7.56×10^5	8.30×10^5	8.16×10^5	7.72×10^5	1.80×10^{12}
std	3.47×10^4	5.05×10^4	3.79×10^3	1.10×10^4	4.09×10^4	1.26×10^{14}
min	7.09×10^5	6.76×10^5	8.12×10^5	7.84×10^5	6.91×10^5	3.44×10^2
max	8.41×10^5	8.42×10^5	8.43×10^5	8.42×10^5	8.39×10^5	8.98×10^{15}

fosters broader participation in the carbon market.

The research identifies a significant gap in existing methodologies, which fail to provide a unified computational framework for the complexities of carbon credit physics and financial option pricing. To address this gap, the paper proposes a methodological framework that synthesizes experiential knowledge with physical models, employing the Kolmogorov Arnold representation (KAR) for customizable knowledge orchestration.

The proposed approach effectively mitigates model bias by leveraging domain-specific knowledge, yielding reasonable predictions even in data-scarce scenarios,Äîan essential aspect of financial modeling. The findings also offer a theoretical foundation for advancing intelligent financial practices in environmental economics. This framework integrates various criteria and models from finance and environmental engineering, allowing for a comprehensive examination of carbon credit option pricing within the context of environmental economics.

7.2 Graph Informed Ochestration with TGAR

7.2.1 Scenario

In this section, we provide an example of graph-informed orchestration based on the TGAR (Temporal Graph Attention Networks) model and present the results of extensive experiments conducted to evaluate the effectiveness of various methods in the context of interbank financial networks.

An interbank network consists of a web of commercial banks engaged in lending and borrowing activities. The default of a single bank within such a network can create a domino effect, triggering defaults in other institutions and potentially leading to a

systemic financial crisis [12, 36, 46]. The interconnectedness of these banks highlights the risk of contagion, where financial shocks originating in one part of the system can rapidly propagate across the network, magnifying the overall threat to financial stability.

In this environment, credit ratings serve as an essential tool for assessing the financial health and reliability of banks. These ratings, which reflect the creditworthiness of institutions, are crucial for measuring the risk of default between interconnected entities in the network [199]. While credit ratings provide a straightforward and widely used measure of financial risk, they face inherent limitations in the context of interbank networks. Specifically, ratings lack timeliness and often fail to account for the evolving nature of financial shocks, which can range from small-scale contagion events to full-blown systemic crises. As a result, it is challenging for rating agencies and policymakers to detect emerging risks in time and formulate appropriate interventions to prevent crises.

To address these challenges, the introduction of rating outlooks with early warning mechanisms has gained prominence. Rating outlooks provide a forward-looking perspective on the potential direction of a credit rating, offering a mechanism to assess risks in the medium term [9, 68, 96]. These outlooks help identify latent risks before they materialize, enabling financial institutions and regulators to take preemptive action to mitigate the impact of potential crises.

In industrial practices, *domain rule-based approaches* are widely employed to predict the credit ratings of banks. These approaches are typically designed by financial experts who craft rules based on specific data features and the mechanics of the interbank system. While these rules are highly practical in real-world applications, as far as we are aware, the problem of credit rating prediction in the context of interbank networks has not been systematically addressed in the research literature.

However, in line with other finance-related studies, *classical machine learning models* can also be applied to the problem without requiring prior knowledge of the rules or underlying mechanisms. Several machine learning techniques have been successfully employed in financial prediction tasks, such as Regression Analysis [99], Decision Tree Models [255], Random Forests [204], Gradient Boosting Decision Trees (GBDT) [295], AdaBoost [193], Multilayer Perceptron (MLP) neural networks [107], and other Statistical Learning methods [106, 179, 181, 225, 233]. These methods can be applied directly to financial data without the need for expert-crafted rules, thus providing a flexible and automated approach to prediction.

In the test in this research, the independent variables consist of financial metrics

such as assets, liabilities, buffer, and weights, which serve as input features for the model. The target variable is the predicted credit rating of the bank for the next year. We utilize a variety of financial data sources, including Moody's Analytics BankFocus, Standard Poor's Rating, and Trading Economics Credit Rating, to gather a comprehensive dataset for training and evaluation. Specifically, we collect interbank data spanning a period of ten years, from 2011 to 2020. Each year, the dataset contains 14,245 records, corresponding to 14,245 unique entities (banks), each with associated financial attributes, such as bank ID, assets, liabilities, buffer, weights, and credit rating. A summary of the statistical features for the attributes, including assets, liabilities, buffer, and weights, is presented in Table 7.8.

Table 7.6: Annual Stats of Feature Data

Year	Avg Assets	Avg. Liabilities	Avg. Buffer	Avg. Weights
2011	10.1805	9.5426	326.8603	347.5834
2012	10.5614	9.8705	262.1356	283.5675
2013	10.7974	10.0724	498.7543	520.6241
2014	10.6820	9.9356	19795.6968	19817.3144
2015	10.4534	9.7032	27590.7611	27611.9178
2016	10.7571	9.9811	394.9608	416.6989
2017	11.8442	10.9607	1527.9176	1551.7226
2018	12.0645	11.1478	1981.3933	2005.6057
2019	12.2837	11.3360	1854.6793	1879.2990

The credit rank attribute consists of four rating categories, which are ordered from the lowest to the highest rank as D, C, B, and A. This categorization follows a similar approach to Moody's credit ranking methodology [16]. The distribution of these credit ranks across the dataset is visualized in Figure 7.34, providing a detailed breakdown of the frequency of each rating category.

In addition to the credit ranks, the interbank relationships are represented as a graph, where each bank is considered an entity (or node), and the connections between them (interbank lending relationships) are represented as edges. The graph contains a total of 46,416 edges, which reflects the interconnectedness between the banks in the system. A summary of the graph's key statistics, such as the number of nodes, edges, and other relevant metrics, is provided in Table 7.7.

7.2.2 Implementation and Evaluation

In this study, we introduce a novel 2-layer cascading context attention representation for the prediction of credit ratings in the interbank system. The proposed model leverages

Table 7.7: Annual Stats of the Entity Networks

year	2011	2012	2013	2014	2015	2016	2017	2018	2019	Average
max Degree	768	888	753	785	753	901	816	1047	717	825.3333
mean Degree	3.2924	3.2723	3.2659	3.2648	3.2778	3.2662	3.2669	3.2599	3.2529	3.2688
Mode Proportion%	85.0294	84.9054	84.9513	84.3824	83.9153	84.0003	83.4770	83.9515	83.8461	84.2732
avg clustering	0.4590	0.4715	0.4422	0.4576	0.4864	0.4691	0.4596	0.4331	0.4220	0.4556
transitivity	0.0534	0.0486	0.0535	0.0476	0.0415	0.0400	0.0404	0.0419	0.0433	0.0456
avg shortest path	3.0515	3.0328	3.0671	3.0441	3.0141	3.0298	3.0387	3.0567	3.0733	3.0453
degree centrality	0.0004	0.0004	0.0004	0.0004	0.0004	0.0004	0.0004	0.0004	0.0004	0.0004
betweenness centrality	0.0001	0.0001	0.0001	0.0001	0.0001	0.0001	0.0001	0.0001	0.0001	0.0001

a cascading architecture to enhance the efficiency and performance of the prediction process. To train the model, we employ the Adam optimizer with parameters $\beta_1 = 0.9$, $\beta_2 = 0.999$, and a learning rate of $\alpha = 0.02$. This configuration ensures effective optimization by adjusting the learning rate based on the training dynamics.

The core of our experimental setup involves utilizing the feature information from the preceding year to predict the credit rating for the following year. Specifically, the prediction is modeled as $y_{k+1} = h(X_t)$, where X_t represents the feature vector for year k, and $h(\cdot)$ denotes the prediction function applied to the input X_t to obtain the credit rating y_{t+1} for the subsequent year. For models incorporating graph-based computations, the prediction model is expanded to $y_{t+1} = h(X_t, A_t)$, where A_t denotes the graph-based adjacency matrix that encodes the relationships between entities within the interbank network, thereby enhancing the prediction model by incorporating structural dependencies among the banks.

In order to evaluate the effectiveness of the proposed context attention representation model, we perform a comparative analysis with several widely used models in the field of risk assessment and prediction tasks. These models include Ridge Classifier, Gradient Boosting Decision Trees (GBDT), Nearest Neighbors, Decision Trees, Random Forests, Neural Networks, AdaBoost, Naive Bayes (NB), Multinomial Naive Bayes, Bernoulli Naive Bayes, Gaussian Process, and Graph Convolution Networks (GCN) [120, 261]. The performance of these models is assessed across multiple metrics that provide insights into their predictive accuracy and reliability.

To ensure a comprehensive evaluation, we use four commonly adopted metrics in the context of credit rating prediction: accuracy, weighted precision, macro-averaged recall, and macro-averaged F1-score.

Let the set $\{I_i\}$ represent the aggregation of the performance indicators, which includes accuracy, average-weighted precision, macro-averaged recall, and macro-averaged F1-score. For each method $h_k(\cdot)$ and input at year t, the ith performance indicator can be denoted as $I_i(k,t)$, which refers to the value of the ith indicator for the kth method

at year t. To evaluate the expectation of these metrics both method-wise and yearly, we define three types of scores: the time-method-wise score $\bar{S}_k(t)$, the metric-method-wise score $\bar{S}_k(i)$, and the yearly score $\bar{S}_t(i)$.

The time-method-wise score $\bar{S}_k(t)$ represents the average performance of the kth method across all metrics for year t, and it can be expressed as

$$\bar{S}_k(t) = \frac{\sum_i I_i(k,t)}{M} \qquad \bar{S}_k(i) = \frac{\sum_k I_i(k,t)}{T} \qquad \bar{S}_t(i) = \frac{\sum_k I_i(k,t)}{K} \tag{7.1}$$

where M is the number of metrics, K is the number of methods, and T is the number of years. In the context of this study, we have $K = 13$, $M = 4$, and $T = 9$ years. These scores reflect the expected performance after aggregating the various t, k, or i factors.

To further synthesize the performance across different methods, the comprehensive method score $\bar{S}_k$ is introduced. This score evaluates the overall performance of the kth method by considering the average across all metrics and years that

$$\bar{S}_k = \frac{\sum_i \sum_t I_i(k,t)}{MT} \tag{7.2}$$

This metric is crucial for evaluating the performance of each method over the entire time period. Similarly, the annual comprehensive score $\bar{S}_t$ is introduced to reflect the synthesis of performance across different methods for a specific year that

$$\bar{S}_t = \frac{\sum_k \sum_i I_i(k,t)}{MK} \tag{7.3}$$

This score provides insight into the overall performance of all methods in a given year, summarizing the predictive accuracy for that specific period.

To assess the global performance across both time and method factors, we define the overall score $\bar{S}$, which provides a holistic view of the dataset‚Äôs prediction performance by combining all dimensions as

$$\bar{S} = \frac{\sum_i \sum_t \sum_k I_i(k,t)}{MTK} \tag{7.4}$$

This metric represents the global performance expectation for the prediction task, synthesized across all methods, metrics, and years, thus providing a comprehensive evaluation of the model's performance across the entire dataset and time period.

To clarify the references (7.1), (7.2), (7.3), and (7.4), these correspond to the evaluation scores designed to comprehensively assess the impact of FDI injection attacks. The **time-method-wise score** ($\bar{S}_k(t)$, (7.1)) evaluates the performance of a specific method k across all performance metrics‚Äîaccuracy, average-weighted precision, macro-averaged

recall, and macro-averaged F1-score,Äîfor a given year t. This score provides insight into how a particular method performs over time, aggregating multiple metrics for each year to identify temporal trends or vulnerabilities. The **metric-method-wise score** ($\bar{S}_k(i)$, (7.2)), on the other hand, assesses a method,Äôs performance for a specific metric i across all years, allowing a detailed comparison of methods according to each individual performance metric. This is particularly useful for understanding which methods excel or lag in terms of accuracy, precision, recall, or F1-score, independent of temporal effects. Finally, the **yearly score** ($\bar{S}_t(i)$,(7.4)) represents the average performance of all methods for a specific metric i in a particular year t, offering a snapshot of overall system performance for that year. Collectively, these three scores enable a multidimensional evaluation, across time for each method, across metrics for each method, and across methods for each year. By defining and using these scores, the study ensures a rigorous and systematic assessment of predictive performance, addressing potential questions about how different methods perform over time, across metrics, and in different yearly contexts, thereby providing a transparent and interpretable evaluation framework.

7.2.3 Main Results

To evaluate the performance of the proposed methods, the main results are presented in Figure 7.31. Specifically, Figure 7.35 shows the statistics for accuracy evaluation. From the results, it is evident that the context attention representation method outperforms all other methods. This superior performance can be attributed to the integration of both graph-based and feature-based information, allowing the model to extract richer feature representations through the attention mechanism. On the other hand, while the Graph Convolutional Network (GCN) also incorporates graph information, its lack of an attention mechanism hampers its performance. This results in GCN's performance being relatively unimpressive, even when compared to other methods that do not utilize graph information, such as Gradient Boosting Decision Trees (GBDT) and Random Forest. The addition of a multi-layer composite context attention mechanism significantly enhances the performance of the context attention representation method, as evidenced by the experimental results, particularly in terms of accuracy.

This advantage is further reflected in the precision metric. As shown in Figure 7.36, the context attention representation method consistently achieves high precision, with the highest value in 2019 reaching over 66%, which is significantly higher than the corresponding results for GCN. This observation underscores the fact that the mere introduction of graph features does not necessarily guarantee improved accuracy. Rather, the

effective use and integration of context through graph learning is crucial for enhancing model performance.

The same trend is observed in recall evaluation. As illustrated in Figure 7.37, the context attention representation method achieves the highest recall rate among all methods. It outperforms Random Forest, showing that the incorporation of graph-based context attention learning improves the model's classification accuracy without being adversely affected by the characteristics of different sample types. This enhances the reliability and robustness of the model's predictions, far surpassing the performance of both traditional neural network models and GCN.

To assess the trade-off between precision and recall, we also evaluated the F1 Score for each model, as shown in Figure 7.38. Although the context attention representation method ranks second behind AdaBoost with an F1 score of 0.5140, the difference is marginal. Moreover, the context attention representation method significantly outperforms both the neural network (0.2788) and GCN (0.4293) methods. This indicates that the context attention representation approach is successful in improving both precision and recall, minimizing the gap between the two and thus balancing the hit rate and coverage.

The overall results of various experimental comparisons and evaluations suggest that the context attention representation method, which integrates graph-based context learning, is highly effective in extracting additional features under the same conditions, thereby enhancing both the prediction hit rate and coverage.

Figure 7.32 presents a comparison of the metric comprehensive scores. The context attention representation model achieves the highest $\bar{S}_k$ score, followed by AdaBoost and Random Forest. Among the neural network methods, the context attention representation method also performs significantly better than GCN and MLP neural networks. This highlights the importance of the attention mechanism in improving the performance of neural network-based methods.

Finally, the overall metric score, $\bar{S}$, as defined in (7.4), is 0.4349. In comparison, the performance of the MLP neural network is lower than $\bar{S}$ due to the lack of correlation information. Although GCN benefits from the inclusion of graph data, the context attention representation method outperforms it further by incorporating both the graph and context attention mechanisms.

Figure 7.40 presents a yearly comparison between the synthesized metric scores $\bar{S}_k(t)$ and $\bar{S}_t$, illustrating the performance disparities among the different methods. In terms of forecast performance for each year, the expected performance of the Naive Bayes

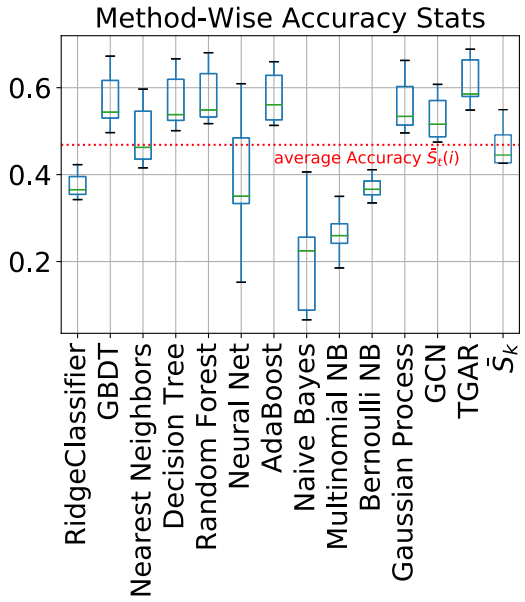

Figure 7.22: Method-Wise Accuracy

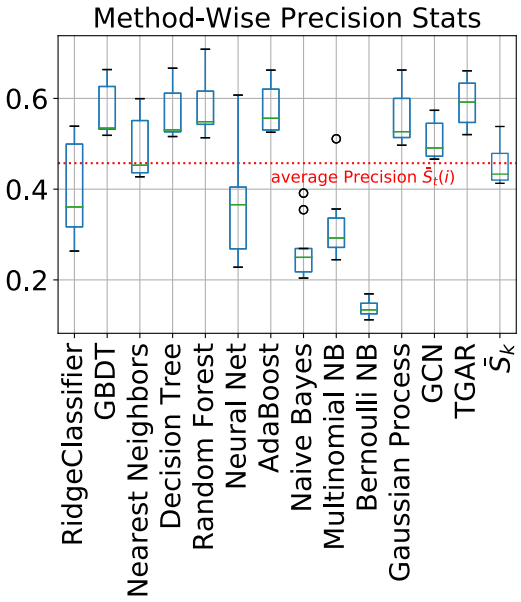

Figure 7.23: Method-Wise Precision

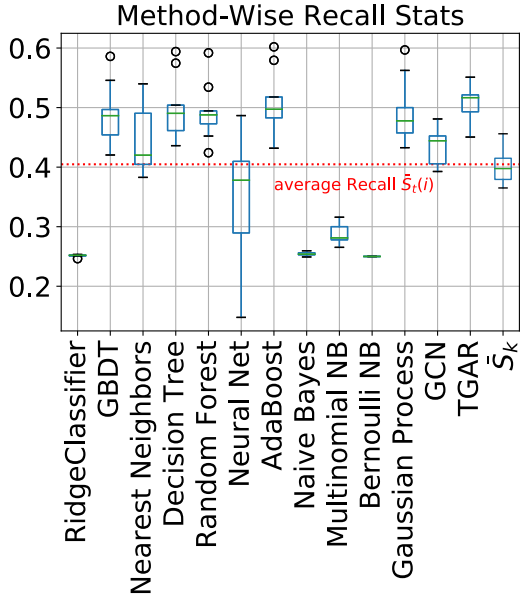

Figure 7.24: Method-Wise Recall

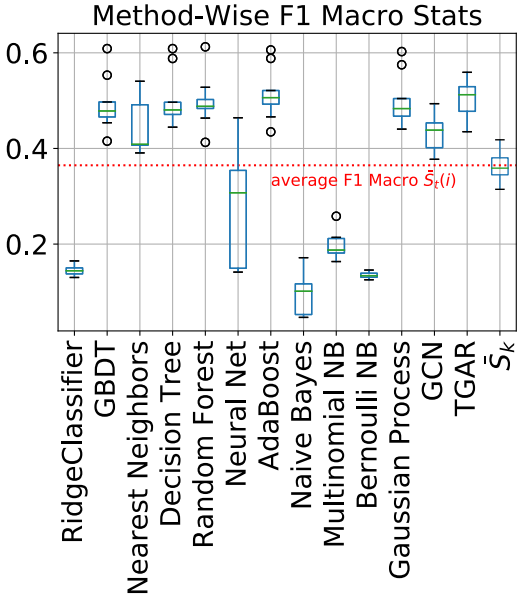

Figure 7.25: Method-Wise F1

Figure 7.26: Method-Wise Metric $\bar{S}_k(i)$ Comparison

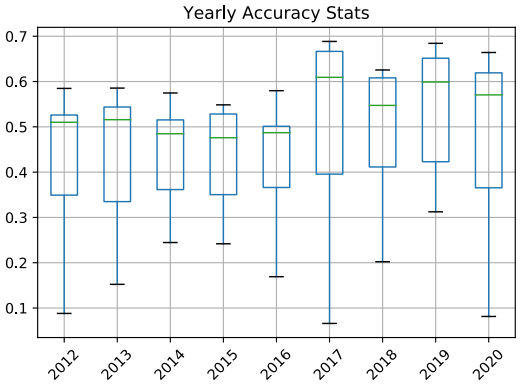

Figure 7.27: Yearly Accuracy Stats

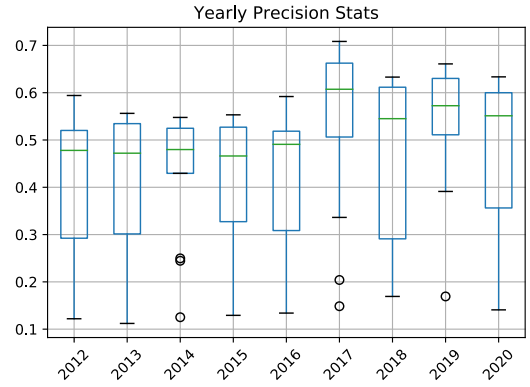

Figure 7.28: Yearly Precision Stats

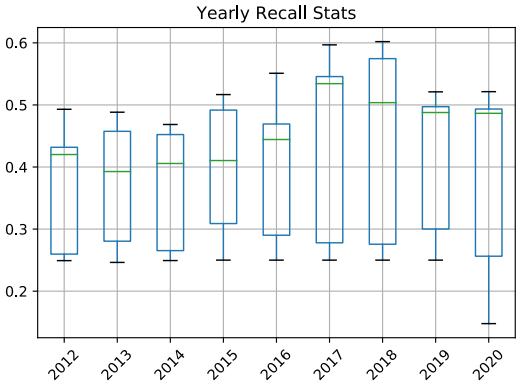

Figure 7.29: Yearly Recall Stats

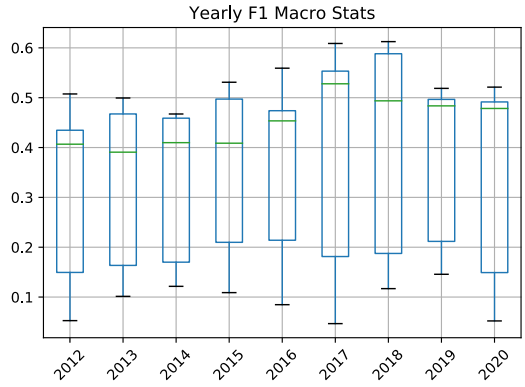

Figure 7.30: Yearly F1 Stats

Figure 7.31: Method-Wise Metric $\bar{S}_k(i)$ Comparison

method consistently falls below the annual average level. Conversely, methods such as TGAR, GCN, and GBDT consistently achieve performance expectations above the average level. Notably, the context attention representation method demonstrates the highest performance across all annual comparisons.

In contrast, the MLP neural network shows lower-than-average performance in most years, with the exception of 2014 and 2017, when it surpasses the annual average. This observation suggests that MLP, in the absence of graph information, is more sensitive to the influence of the feature data for the current year, resulting in relatively poor performance compared to tree-based methods. However, when graph features are incorporated, both GCN and context attention representation exhibit more stable performance across the years, with their performance expectations consistently exceeding the annual average. This indicates that the integration of graph-based learning significantly enhances the stability and predictive performance of these models in yearly predictions.

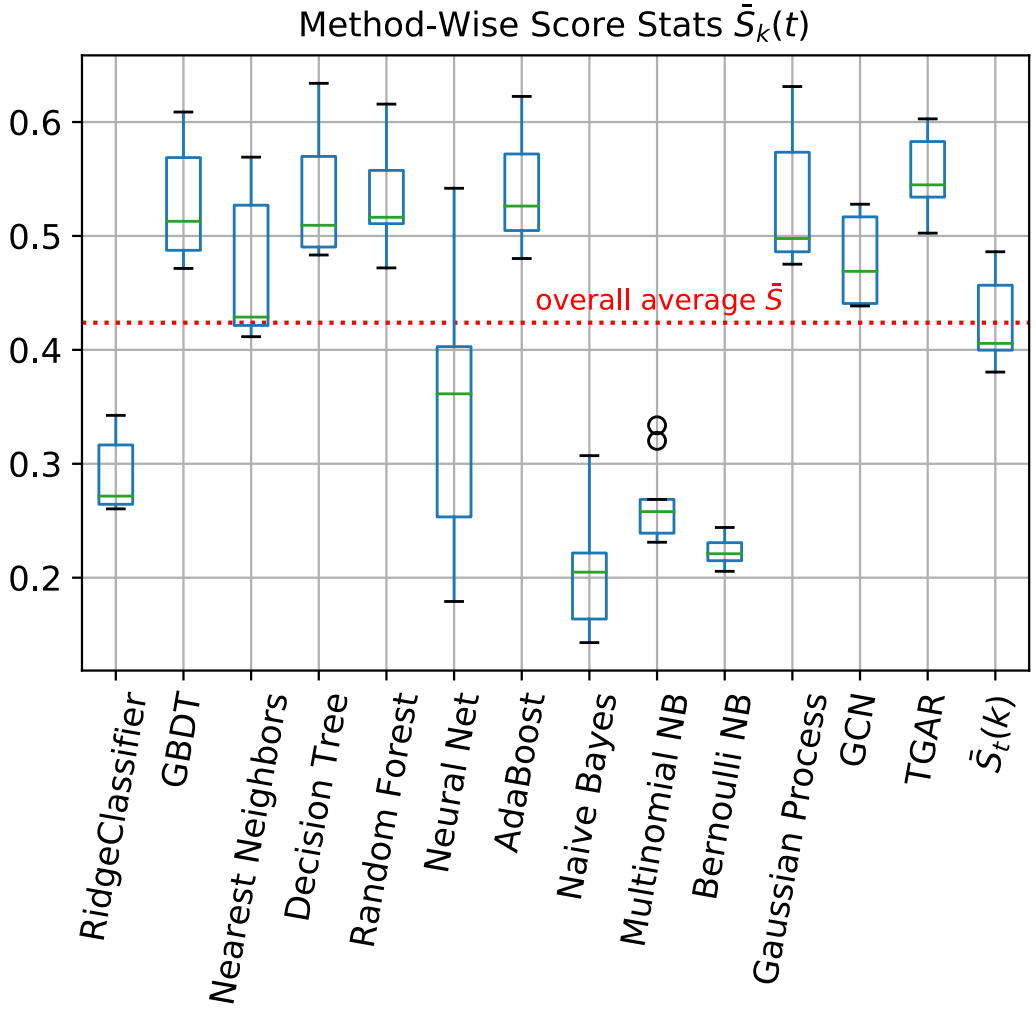

Figure 7.32: Method-Wise $\bar{S}_k$ Comparison

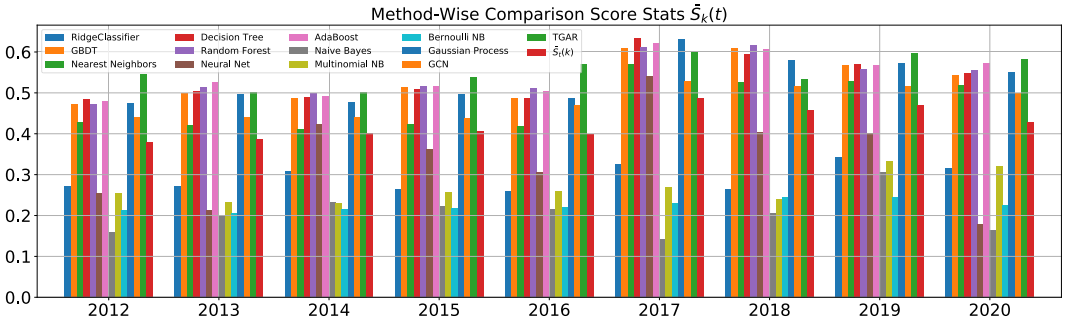

Figure 7.33: Yearly Stats Comparison between $\bar{S}_t$ and $\bar{S}_k(t)$ of Typical Methods

7.2.4 Discussion

The proposed TGAR approach addresses five major challenges in the financial risk assessment domain: the lack of comprehensive prior mechanisms, the difficulty in quantifying the interrelationships between financial entities, time-consuming feature extraction, incomplete historical data, and the heterogeneity between different data sources. The solution combines context graph computing, weight embedding, and efficient data pipeline management to enhance the performance and scalability of predictive models.

Through extensive experimentation with a real-world dataset, our approach was compared to twelve established baseline methods. The results consistently demonstrated that the proposed method outperforms the baselines across all evaluation metrics, particularly in terms of predicting numerical features such as expectations and variances. This indicates that the proposed context attention representation offers superior predictive accuracy and robustness.

The advantages of the proposed method are significant. First, the weight embedding technique reduces storage and computational costs by efficiently handling incomplete data and minimizing the need for extensive storage resources. Second, the context attention representation effectively integrates heterogeneous data sources while preserving the independence and correlation of individual features. This is crucial in ensuring that the model does not lose important information when fusing diverse types of data. Third, the ability to perform multiple learning on relational and feature-based data using Bernoulli fusion and binomial gain enhances the model's predictive power.

The test results suggest that the key to improving predictive performance is not just the use of graph structures but the effective extraction and utilization of context attention features. These features enable the model to capture high-level contextual patterns that are essential for accurate prediction in dynamic and complex financial systems.

The results of this study validate the efficacy of the proposed predictive rating method in addressing several critical challenges in interbank rating outlooks. By leveraging advanced data representation techniques and optimizing computational efficiency, our approach presents a promising solution for enhancing financial risk prediction models. Further research will continue to refine and extend the framework, with potential applications in broader financial risk management scenarios.

7.3 FDI Injection Attack

This study introduces a comprehensive set of evaluation metrics designed to assess the performance of various machine learning-based credit rating prediction methods, particularly in the context of FDI attacks. The goal is to provide a multi-dimensional perspective on the effectiveness and accuracy of these methods across different time periods and computational strategies. Four widely recognized performance metrics are used: accuracy, average weighted precision, macro-average recall, and macro-average F1-score. These metrics capture various aspects of model performance, such as overall prediction correctness and the ability to handle class imbalances, which are typical in credit rating tasks.

The evaluation framework incorporates several aggregate scores to assess method performance across different time periods and metrics. These include time-method scores (7.1), metric-method scores (7.2), and yearly scores (7.4). These aggregate scores offer insights into the performance of each method over specific time frames, for particular metrics, and across all methods in a given year. To synthesize these results, the study introduces a composite method score and a yearly composite score. These scores provide a holistic view of method performance across all metrics and time periods. Additionally, difference metrics are defined to track changes in evaluation scores before and after interventions, such as system modifications or external disruptions, allowing for a deeper understanding of performance shifts.

The system used for evaluation is based on widely-used machine learning methods, ensuring that the results are grounded in industry-standard practices. This provides a robust framework for testing and comparing different prediction methods under controlled conditions, particularly in the presence of potential FDI attacks.

7.3.1 Methods

We collect the related applicable methodologies to test for the evaluation on the impact of FDI on the interbank credit prediction, including Ridge Classifier, Gradient-Boosted Decision Trees (GBDT), Nearest Neighbors, Decision Tree, Random Forest, Neural Network, AdaBoost, Naive Bayes (NB), Multinomial Naive Bayes (Multinomial NB), Bernoulli Naive Bayes (Bernoulli NB), and Gaussian Process.

7.3.1.1 Ridge Classification

The essence of ridge classification method [54, 99, 146] is to transform the classification problem into a regression problem, and then use ridge regression to solve it. Its essence is a variant of least squares in linear regression for classification. It adds a penalty on the size of the coefficients to the objective function of ordinary least squares. The main task of ridge classification can be formulated as

$$\min_{w} \|Xw - y\| + \alpha\|w\| \tag{7.5}$$

where X refers to the input feature, y referes to the tag, and w refers to the weight for classifier to be solved.

7.3.1.2 Nearest Neighbors Analysis

Nearest Neighbors Analysis [289, 290] is a method of numerical regression and classification based on the K Nearest Neighbours analysis method. In the experiment of this paper, we choose the number of neighbours as 3, and all points in each neighborhood are weighted equally.

7.3.1.3 Random Forest

Random Forest [140, 213], is composed of many decision trees, and there is no correlation between different decision trees. It has been widely used in price regression and property classification in the business. In the experiments of this paper, we choose 200 trees in the forest and the maximum depth of the tree is 5.

7.3.1.4 AdaBoost

AdaBoost (Adaptive Boosting [47, 242]) is a two-classifier that uses a linear combination of weak classifiers to construct a strong classifier. In this paper, we apply the model that is combined linearly through the additive model, which can be formulated as

$$F(x) = \sum_{l} w f_l(x) \tag{7.6}$$

where x is the input vector, $F(x)$ is the strong classifier, $f(x)$ is the weak classifier, $0 \geq w \leq 1$ is the weight value of the weak classifier, which is a positive number. We set $l = 100$ and the learning rate as 1.0. The output value of the weak classifier is +1 or -1, corresponding to positive samples and negative samples, respectively.

7.3.1.5 Decision Tree

Decision tree [172] is a commonly used classification method and requires Supervised Learning. By calculating information entropy, gain rate, and Gini index as the information gain selection classification. In contrast, the attributes that can bring the highest information gain are usually selected based on information entropy In the experiments of this paper, we choose the maximum depth of the tree is 5 with Gini index criterion.

7.3.1.6 Gradient Boosting Decision Tree

GBDT (Gradient Boosting Decision Tree [254]) is an iterative decision tree algorithm, which uses weak classifiers for cascading and fully considers the weight of each classifier, enable it to flexibly handle continuous values and discrete values [71]. In the experiments of this paper, we choose the 20 trees with 31 leaves for base learners, and the learning rate is set as 0.05.

7.3.1.7 Naive Bayes

The Naive Bayesian [197] method is based on a basic premise, that is, after updating the original belief about something with objective new information, a new and improved belief will be obtained. The core of the idea of this method is that when the nature of an event cannot be accurately known, the probability of its essential attributes can be quantified by the number of evidences related to the specific nature of the event. Therefore, the more evidences that support a certain attribute, the greater the probability that the attribute will be established.

7.3.1.8 Bernoulli Naive Bayes

Unless otherwise specified, the default Naive Bayes is based on Gaussian distribution for probability calculation. It is applicable when the characteristic variable is a continuous variable conforming to the Gaussian distribution.

When the feature variable is a Boolean variable that conforms to the 0-1 distribution, the probability distribution of the feature event needs to be introduced into the Bernoulli distribution for Bayesian analysis, that is, the Bernoulli Naive Bayes method [211].

In the experiments of this paper, we adopt an additive Laplace smoothing to improve the performance [45].

7.3.1.9 Multinomial Naive Bayes

When the characteristic variable is a discrete variable and the distrubition of each feature conforms to multinomial distribution, the Gaussian distribution is no longer applicable. The multinomial distributions may be introduced to describe these features, and the naive Bayes under this distribution is Multinomial Naive Bayes [115]. In the experiments of this paper, we adopt an additive Laplace smoothing to improve the performance.

7.3.1.10 Gaussian Process (GP)

Gaussian Process (GP) classification is a supervised learning method based on the Gaussian distribution model [28, 189]. Its mechanism is to solve the probabilistic classification problem based on distributed regression analysis by analyzing the probability characteristics of the dependent variable and the independent variable in a closed probability space. In the experiments of this paper, we use RBF kernel as a stationary kernel for the training of Gaussian process [256].

7.3.1.11 Support Vector Machine

Support Vector Machine is another popular method used in credit rating services [42, 109, 132, 280], which attributes the rating to a classification problem and trains an optimal support vector structure based on datasets of credit history information to predict the likelihood of borrowers defaulting on their loans. Besides, it is also be used in financial applications, such as acquisition analysis [184], pricing [298], customer identification [13], etc.SVM overcomes difficulties such as "dimensional disaster" and "over-fitting" of traditional machine learning models.

7.3.1.12 Neural Networks

A neural network model is a model that learns and fits through a nonlinear method [91], which has been used widely in industrial application. In the experiments of this paper, we design a multiple layer preceptor with L2 penalty (regularization term) parameter $\alpha = 0.02$ and learning rate0.001. The hidden layer size is 100, using ADAM [34] as the optimizer and ReLU as activation.

7.3.2 Test with FDI-Based Covert Attacks

7.3.3 Data Materials

This study uses 10 years of financial data (2011-2020) from 14,245 institutions per year, totaling 142,450 records. Each institution is described by four attributes: assets, capabilities, buffers, and weights, with weights derived from historical data using data fusion. The dataset includes additional attributes such as liabilities, credit rank (categorized as D, C, B, and A), and other financial metrics. The credit rank distribution is visually represented, providing a foundation for credit rating prediction tasks. The stats of feature assets, liabilities, buffer, weights is shown in Table 7.8. The attribute credit rank include 4 rating categories, from the lower to the upper rank as D, C, B, A with the stats as shwon in figure 7.34.

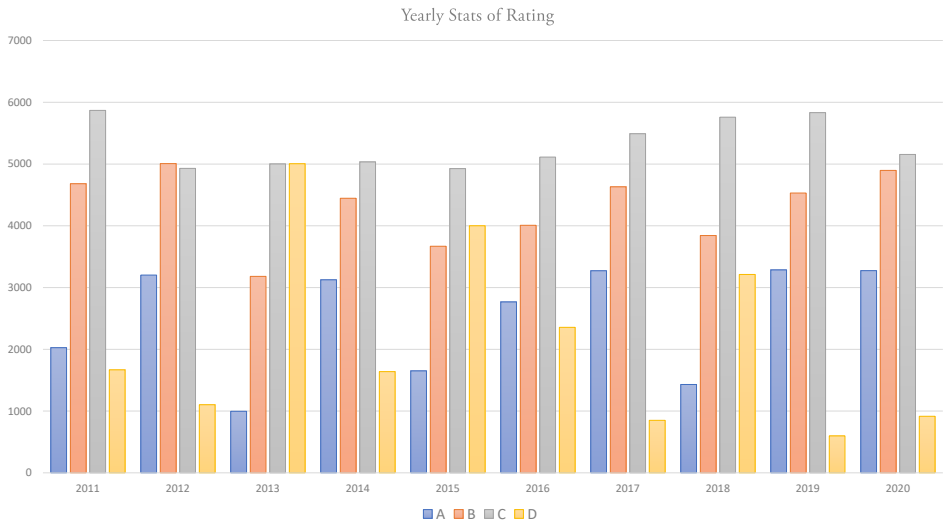

Figure 7.34: Stats of InterBank Rating

From these statistics, it can be seen that there is an imbalance in the data itself and that there is a wide variation in the distribution of the attribute values of the data. These are not friendly for machine learning training, not to mention that when considering attacks, the reliability of the financial credit rating results is an interesting issue to study, with many real business benefits at stake. Therefore, we perform attack tests on a real system to verify the extent to which induced attacks affect real financial operations and the response and robustness of each different machine learning strategy to the attacks.

Due to strict compliance with the requirements of data protection regulations as the top priority of financial institutions in the process of project implementation, we cannot

Table 7.8: Stats of Feature Data

2011	assets	liabilities	buffer	weights
mean	10.1805	9.5426	326.8603	347.5834
std	96.9511	92.1931	31035.2683	31036.0194
min	0.00001	0.00001	0.00001	0.00001
max	3174.5329	3014.9653	3702700	3702739.729
2012	assets	liabilities	buffer	weights
mean	10.5614	9.8705	262.1356	283.5675
std	98.05765937	92.88715675	22211.79067	22212.68955
min	0.000014	0.00001	0.05	1.210723
max	3201.861752	3016.656261	2645280	2645310.022
2013	assets	liabilities	buffer	weights
mean	10.79737279	10.07237788	498.7543012	520.6240518
std	101.7557002	96.36793646	32271.8614	32272.38741
min	0.000017	0.000014	0.08	1.230908
max	4024.149	3969.135	2932850	2932851.043
2014	assets	liabilities	buffer	weights
mean	10.68197114	9.935571096	19795.69681	19817.31435
std	103.0993167	97.44788745	2314829.194	2314829.103
min	0.00002	0.000016	0.00675078	1.243343
max	4497.774	4440.63	276260300	276260310
2015	assets	liabilities	buffer	weights
mean	10.45342349	9.703247864	27590.76113	27611.9178
std	101.8873977	96.2518487	3247903.656	3247903.531
min	0.000021	0.000017	0.02	1.342143
max	4484.765	4445.257	387633700	387633705.6
2016	assets	liabilities	buffer	weights
mean	10.75706062	9.981067975	394.9607666	416.6988952
std	105.1761954	99.49488251	26687.59307	26688.20089
min	0.000021	0.000015	0.03	1.660063
max	4453.337	4412.895	2320400	2320413.299
2017	assets	liabilities	buffer	weights
mean	11.84418906	10.96073941	1527.917635	1551.722564
std	115.2993319	108.830701	113996.632	113996.6152
min	0.000006	0.000004	0.001657715	1.076282715
max	4974.909663	4937.718474	12158982.19	12158984.45
2018	assets	liabilities	buffer	weights
mean	12.06450572	11.14783043	1981.39332	2005.605656
std	118.0244491	111.3820204	125166.2805	125166.1799
min	0.000019	0.000004	0.008940187	1.009021187
max	5575.974021	5534.308194	12510110	12510111.62
2019	assets	liabilities	buffer	weights
mean	12.28366596	11.3360237	1854.679286	1879.298976
std	119.5762523	112.5253804	122315.3848	122315.299
min	0.00002	0.000004	0.007573631	1.010846757
max	5561.036455	5519.202075	12861237.81	12861238.9

disclose the data source with specific raw elements and provide it to readers, but the necessary data characteristics that can be used to verify performance are retained in the data set.

7.3.3.1 Settings

To evaluate the performance of proposed method, we apply the covert attack based on FDI to the methods including Ridge Classifier, Gradient Boosting Decision Tree (GBDT), Nearest Neighbors, Decision Tree, Random Forest, Neural Network, AdaBoost, Naive Bayes (NB), Multinomial NB, Bernoulli NB, Gaussian Process.

- Ridge Classification [59, 99, 146] is to transform the classification into a regression with ridge regression. The main parameter is α for ridge fitting. In the experiment of this paper, $\alpha = 1$.

- Nearest Neighbors Analysis [113] is a method of numerical regression and classification based on the K Nearest Neighbours analysis method. In the experiment of this paper, we choose the number of neighbours as 3, and all points in each neighborhood are weighted equally.

- Random Forest[164, 194, 204, 248] is composed of many decision trees, and there is no correlation between different decision trees. In the experiments of this paper, we choose 200 trees in the forest and the maximum depth of the tree is 5.

- AdaBoost (Adaptive Boosting [125, 193]) is a two-classifier that uses a linear combination of weak classifiers to construct a strong classifier. In this paper, the model uses 100 classifiers with the learning rate as 1.0. The output value of the weak classifier is +1 or -1, corresponding to positive samples and negative samples, respectively.

- Decision tree [39, 80, 255] is a commonly used classification method and requires Supervised Learning. In the experiments of this paper, we choose the maximum depth of the tree is 5 with Gini index criterion.

- GBDT (gradient boosting decision tree [57, 262, 295]) is an iterative decision tree algorithm, which uses weak classifiers for cascading and fully considers the weight of each classifier, enable it to flexibly handle continuous values and discrete values [71]. In the experiments of this paper, we choose the 20 trees with 31 leaves for base learners, and the learning rate is set as 0.05.

- The Naive Bayesian [179, 225, 233] method is based on the idea that the probability of its essential attributes can be quantified by the number of evidences related to the specific nature of the event. In the experiments of this paper, we set the portion of the largest variance of features to update variances as 10^{-9}.
- Bernoulli Naive Bayes [225] method introduces the Bernoulli distribution for Bayesian analysis for Boolean variable modeling. In the experiments of this paper, we adopt an additive Laplace smoothing to improve the performance [45].
- Multinomial Naive Bayes [181, 233] introduces multinomial distributions to describe discrete features under the Bayes inference. Laplace smoothing is also adopted in the experiment of this paper.
- Gaussian Process (GP) [106, 189] classification is a supervised learning method based on the Gaussian distribution model. In the experiments of this paper, we use RBF kernel as a stationary kernel for the training of Gaussian process [256].
- A neural network model [14, 107, 109] is a model that learns and fits through a nonlinear method [91], which has been used widely in industrial application. In the experiments of this paper, we design a multiple layer preceptor with L2 penalty (regularization term) parameter $\alpha = 0.02$ and learning rate 0.001. The hidden layer size is 100, using Adam [34] as the optimizer and ReLU as activation.
- Support vector machine (SVM) [177] is a supervised learning algorithm for classification and regression analysis that classifies data through a hyperplane with maximum margin [214], and can handle both linear and nonlinear data by using appropriate kernel functions [103]. In this paper, the kernel function is selected as a linear kernel function and the penalty parameter is 0.025 by L2 regularization.

We test the above methods with and without the attacks to see the influence of the attacks. In the tests, we numbered the individual methods to represent them in the data analysis results. The table 7.9 provides a glossary of machine learning algorithms. It includes the full name of the algorithm (Method), a unique identifier (ID), and a brief name for each algorithm above. In the next section, we apply the proposed full and partial false data injection to covert adversarial backdoor attacks on the credit rating systems running under the above machine learning methods. We focus on the attack effects of Clandestine Fraudulence (CF), Clean Label Attack (CLA), and Induced Model Attack (IMA) and statistically analyze the results of the adversarial machine learning performance.

Table 7.9: Methods and ID

Method	ID	Breif Name
Ridge Classifier	M1	Ridge Classifier
Gradient Boosted decision Tree	M2	GBDT
Nearest Neighbors	M3	Nearest Neighbors
Decision Tree	M4	Decision Tree
Random Forest	M5	Random Forest
Neural Networks	M6	Neural Net
Adaptive Boosting	M7	AdaBoost
Naive Bayes	M8	Naive Bayes
Multinomial Naive Bayes	M9	Multinomial NB
Bernoulli Naive Bayes	M10	Bernoulli NB
Gaussian Process	M11	Gaussian Process
Linear Support Vector Machine	M12	Linear SVM

7.3.4 Main Results

7.3.4.1 Test Results without Attack

First, we evaluate the system performance based on each machine learning strategy under the original data without applying any attacks. Figure 7.39 shows the performance evaluation results for each method in terms of accuracy, precision, recall, and F1, respectively. It can be seen that several methods such as GBDT, Random Forest (RF), Decision Tree, AdaBoost, Nearest Neighbors and Gaussian Process generally have better markers than the average performance $\bar{S}_t(i)$, in which GBDT, Random Forest (RF), and AdaBoost have the most outstanding performance, especially in Accuracy and Precision, which show well-balanced stability in both mean and maximum values.

As a result of comprehensive performance evaluation, figure 7.40 shows that GBDT, Decision Tree, Random Forest, Adaboost and Gaussian Process are the top five strategies in each year $\bar{S}_k(t)$. Meanwhile, what is noticeable, the performance in 2017 and 2018 has the highest record.

Overall, the random forest and GBDT models performed well overall, maintaining high scores over the years. The ridge classifier, nearest neighbor, and decision tree also show relatively consistent performance. On the other hand, the performance of the Neural Net, AdaBoost, and Gaussian Process models is more variable, with some years showing better results than others. The Naive Bayes model scored relatively low compared to the other models, while Bernoulli NB and Multinomial NB showed similar performance. What is noticeable, the performance of these models may have changed

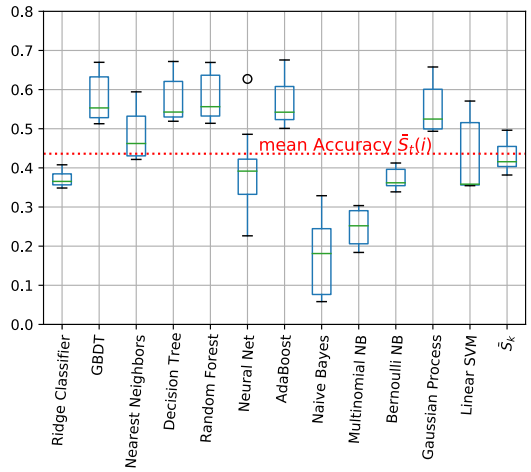

Figure 7.35: Accuracy Stats without Attack

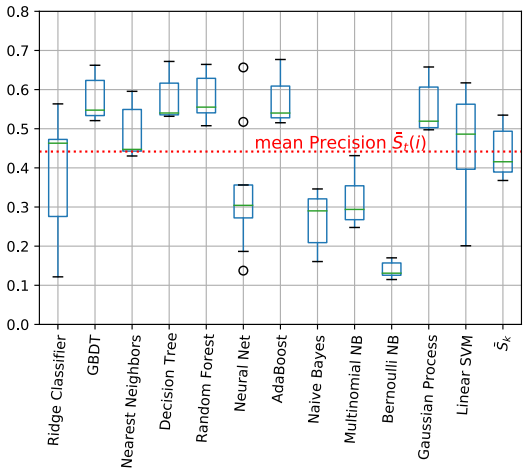

Figure 7.36: Precision Stats without Attack

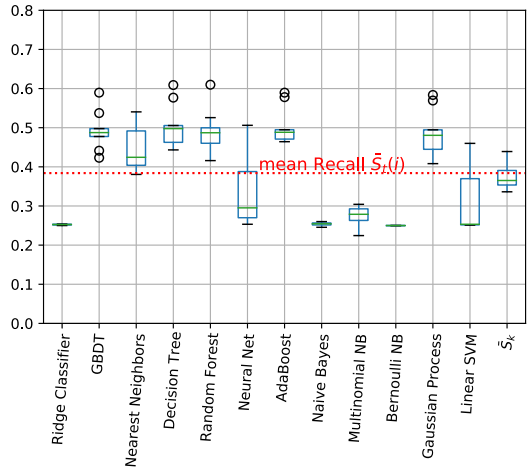

Figure 7.37: Recall Stats without Attack

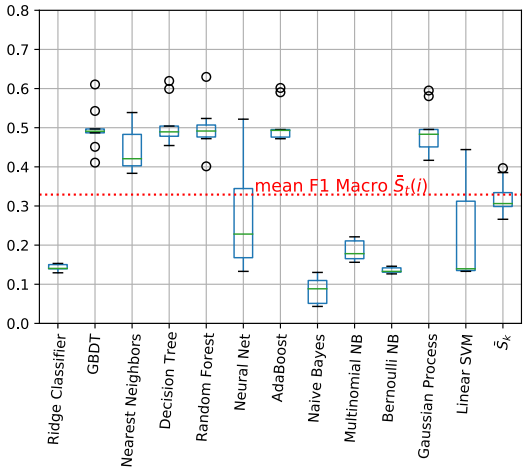

Figure 7.38: F1 Macro Stats without Attack

Figure 7.39: Method-Wise Metric $\bar{S}_k(i)$ without Attack

over time, which is also a more common feature in financial data learning.

7.3.4.2 Test Results under Covert FDI Partial Attacks

Under the adversarial backdoor attacks based on covert FDI with $w = 30\%, r = 30\%$, the figure 7.53 shows the stats of each method with performance evaluation. Under the attack of Clandestine Fraudulence, the Random Forest classifier performs well overall, with the highest median score for all years. The Ridge classifier, nearest neighbor, and linear SVM consistently score lower compared to the other models. the GBDT, decision tree, neural

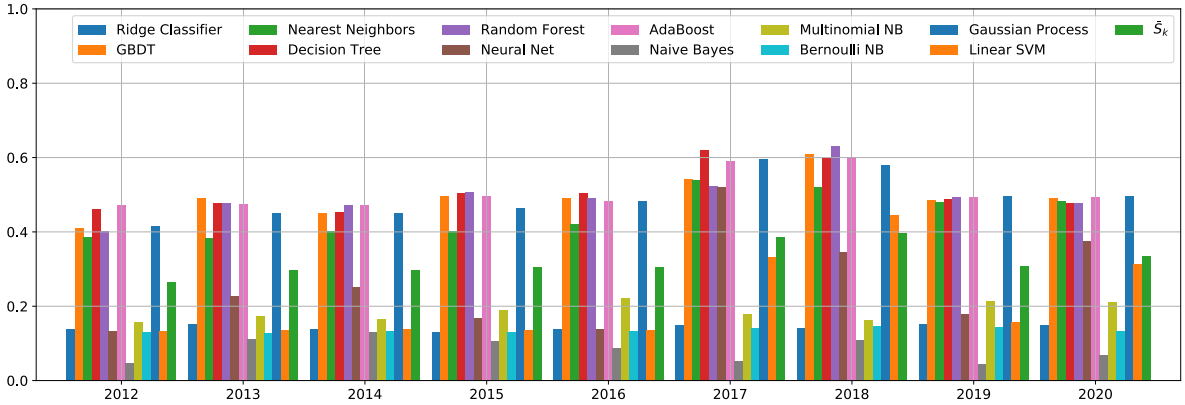

Figure 7.40: Yearly Stats Comparison between $\bar{S}_t$ and $\bar{S}_k(t)$ of Typical Methods

net, AdaBoost, Naive Bayes, Multinomial NB, Bernoulli NB, and Gaussian Process classifiers perform better, but not as well as the random forest. It is also noteworthy that in 2012, Ridge Classifier and Nearest Neighbors performed similarly, but in 2018, Ridge Classifier performed much lower than Nearest Neighbors.

Under the Clean Label Attack, Random Forest and GBDT algorithms performed well over the years. In contrast, decision trees, neural nets, and linear SVMs have lower accuracy scores. In contrast, the Ridge classifier, Nearest Neighbors, Bernoulli NB, and Gaussian Process have relatively low performance. AdaBoost and Naive Bayes has performed relatively consistently over the years.

Under the Induced Model Attack, the GBDT model performs the best in most years, especially in 2013, 2015, and 2017 with the highest performance values. The random forest and decision tree models also performed well in most years. the ridge classifier, linear SVM, and neural net models had the lowest performance values.

Figure 7.61 shows a comprehensive comparison of overall criteria. It can be seen that When applying $w = 30\%, r = 30\%$ adversarial backdoor attacks, under the influence of covert FDI, each partial backdoor attack succeeds in disrupting the comprehensive system performance of machine learning. Although the performance metrics of the Decision Tree represented by GBDT and Random Forest are still high, the overall performance is held below 60% overall.

7.3.4.3 Evaluation under Covert FDI Full Attacks

When Covert FDI Full Attack was employed to corrupt all data samples in the system, the destructiveness of the individual adversarial backdoor attacks on the system was further exacerbated. As shown in figure 7.74, the mean values of all the metrics are

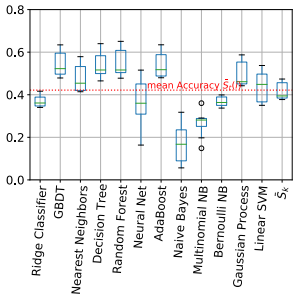

Figure 7.41: Accuracy under Clandestine Fraudulence

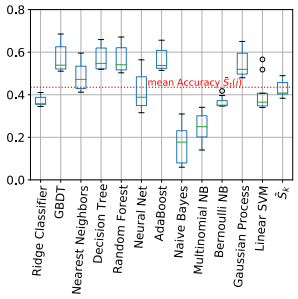

Figure 7.42: Accuracy under Clean Label Attack

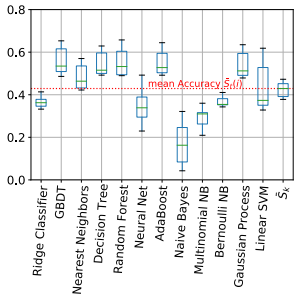

Figure 7.43: Accuracy under Induced Model Attack

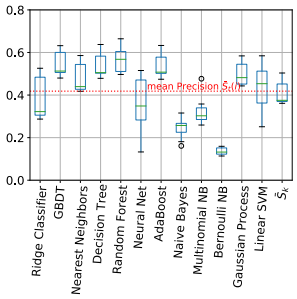

Figure 7.44: Precision under Clandestine Fraudulence

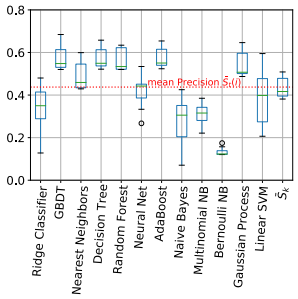

Figure 7.45: Precision under Clean Label Attack

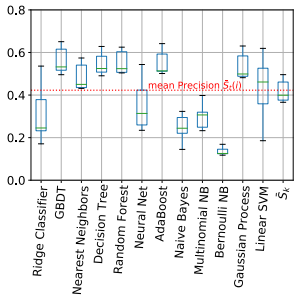

Figure 7.46: Precision under Induced Model Attack

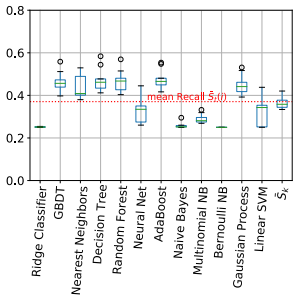

Figure 7.47: Recall under Clandestine Fraudulence

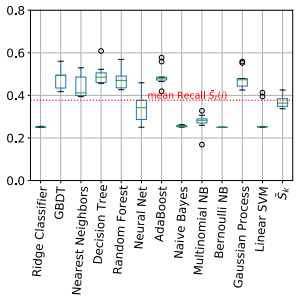

Figure 7.48: Recall under Clean Label Attack

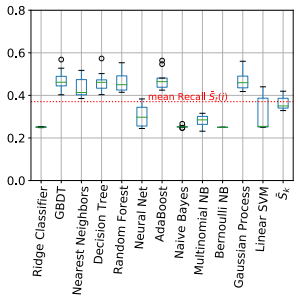

Figure 7.49: Recall under Induced Model Attack

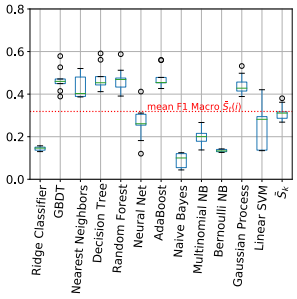

Figure 7.50: F1 Macro under Clandestine Fraudulence

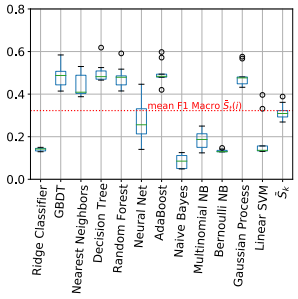

Figure 7.51: F1 Macro under Clean Label Attack

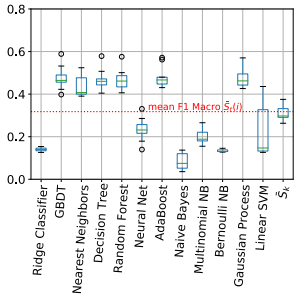

Figure 7.52: F1 Macro under Induced Model Attack

Figure 7.53: Method-Wise Metric $\bar{S}_k(i)$ Comparison Under Covert Attack Based on FDI ($w = 30\%, r = 30\%$)

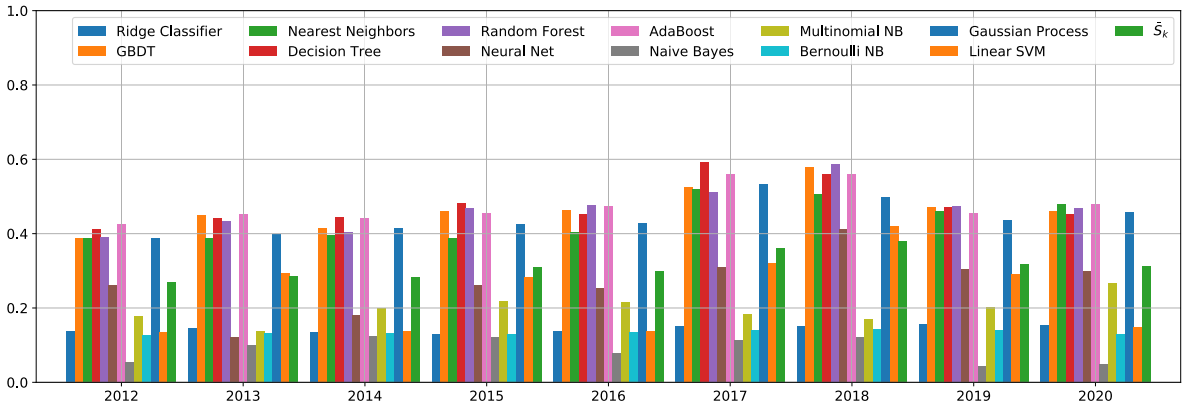

Figure 7.54: Yearly Comprehensive Stats under Clandestine Fraudulence

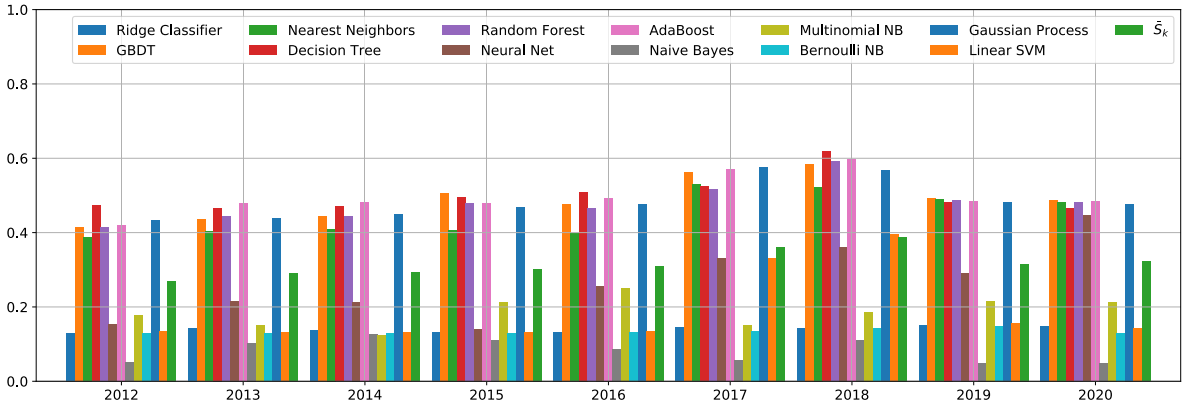

Figure 7.55: Yearly Comprehensive Stats under Clean Label Attack

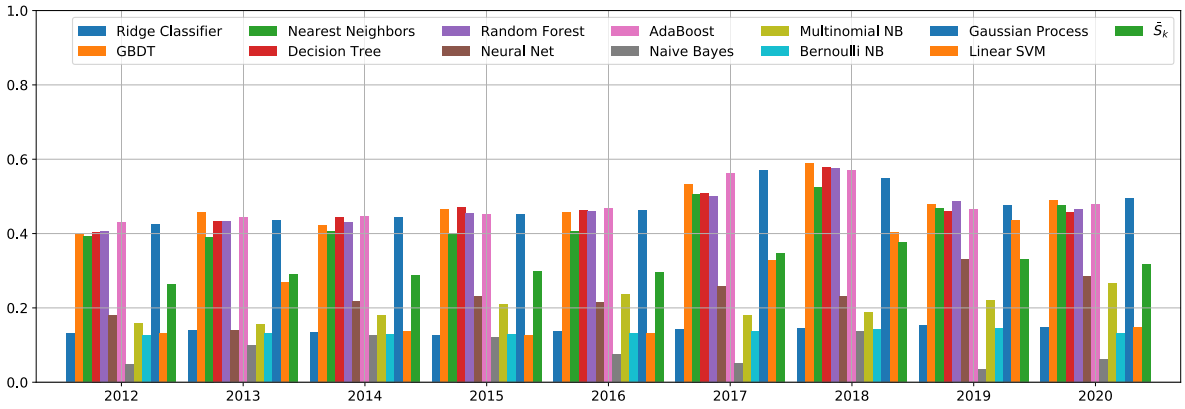

Figure 7.56: Yearly Comprehensive Stats under Induced Model Attack

Figure 7.57: Method-Wise Yearly Stats Comparison between $\bar{S}_t$ and $\bar{S}_k(t)$ with Covert Attacks Based on FDI (w=30%, r=30%)

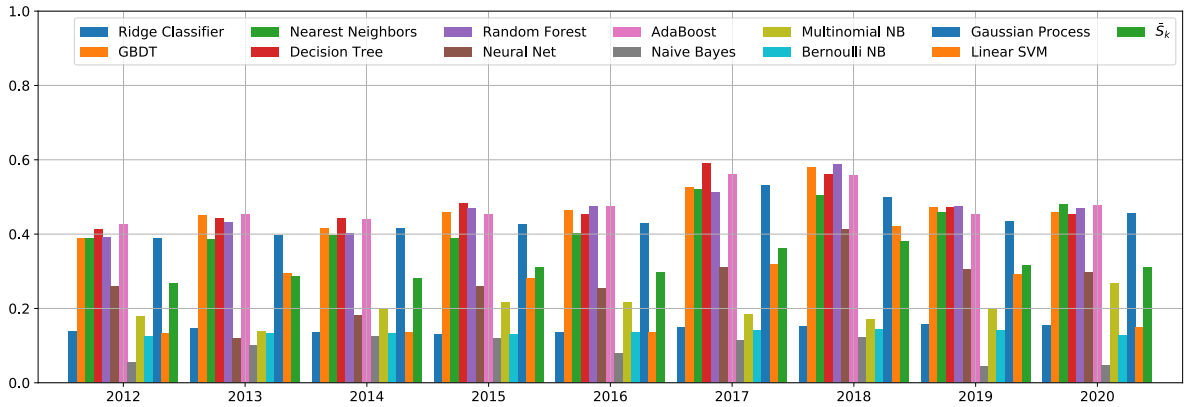

Figure 7.58: Yearly Comprehensive Stats under Clandestine Fraudulence

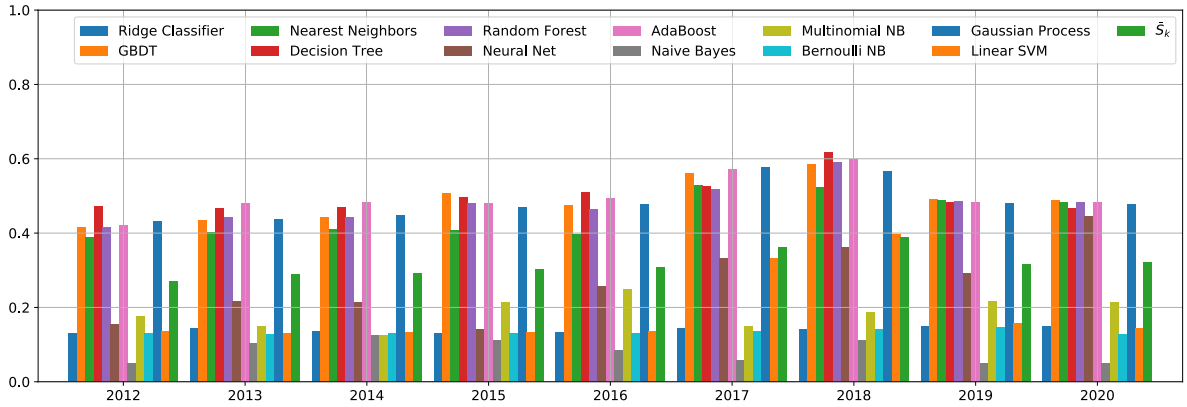

Figure 7.59: Yearly Comprehensive Stats under Clean Label Attack

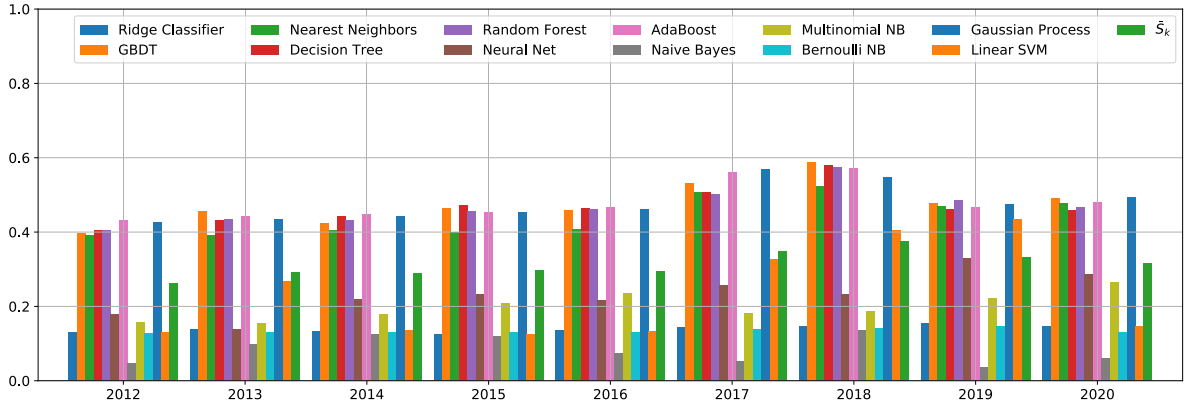

Figure 7.60: Yearly Comprehensive Stats under Induced Model Attack

Figure 7.61: Method-Wise Yearly Stats Comparison between $\bar{S}_t$ and $\bar{S}_k(t)$ with Covert Attacks Based on FDI (w=30%, r=30%)

pulled to nearly 50%, especially under Induced Model Attack, the model reliability of GBDT, Random Forest, Decision Tree, and AdaBoost systems which originally performed better are relocated to nearly 40%, and under Induced Model Attack attack reduces the F1 score performance by nearly 10%.

The phenomenon is also evident in the comprehensive performance evaluation statistics. As shown in figure 7.78, the comprehensive performance of all the machine learning methods is held below 50% under the covert FDI attacks with $w = 30\%, r = 100\%$, in which most of them do not exceed 40%. This result implies that the validity of the machine learning systems is almost destroyed, and their output rating results have almost no reliable credit reference value.

This indicates that the broader the attack on the data nodes, the more obvious the effect of the attack is, and even if the modification is not very large it can successfully destroy the reliability of the model.

7.4 Discussion on Attacks

7.4.1 Partial FDI Adversarial Backdoor Attacks

From the point of view of damage to the model, all three covert backdoor attacks succeeded in having an impact on the raw performance of the system, especially in accuracy and precision, the significant metrics in practical applications. Table 7.10-7.12 shows the accuracy before and after the attacks. Under the $w = 30\%, r = 30\%$ covert FDI CF attack, the largest decrease in average accuracy is in Gaussian Process with a decrease of 0.0580. followed by Decision Tree with a decrease of 0.0310, GBDT with an average decrease in accuracy of 0.0303, AdaBoost with a decrease of 0.0289, and We can see the difference statistics compared to the original performance without the attack, and the performance of the original high accuracy machine learning system is relatively affected. The most affected under Clean Label Attack is linear SVM which decreases by 0.0271, followed by Random Forest which decreases by 0.0086, GBDT, and Decision Tree which decreases by 0.0039 and 0.0033 respectively. It can be seen that SVM is more sensitive to label attacks. more sensitive. Under the Induced Model Attack, the accuracy of the neural network system is most affected by 0.0430, followed by Decision Tree with a decrease of 0.0299; GBDT and AdaBoost are affected by -0.0186 and -0.0213, respectively.

When comparing $\Delta\bar{S}_i$ together, the largest impact on accuracy is Clandestine Fraudulence (-0.0134), followed by Induced Model Attack (-0.0063), and finally Clean Label

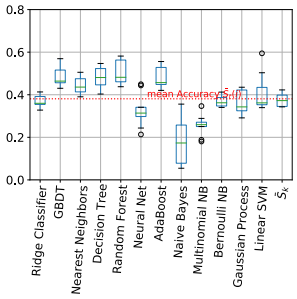

Figure 7.62: Accuracy under Clandestine Fraudulence

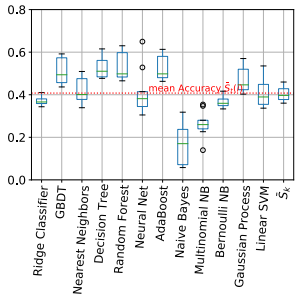

Figure 7.63: Accuracy under Clean Label Attack

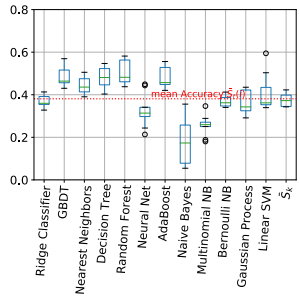

Figure 7.64: Accuracy under Induced Model Attack

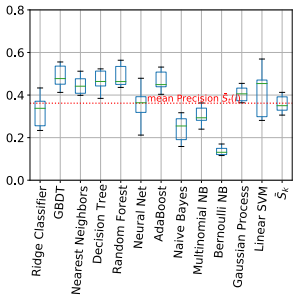

Figure 7.65: Precision under Clandestine Fraudulence

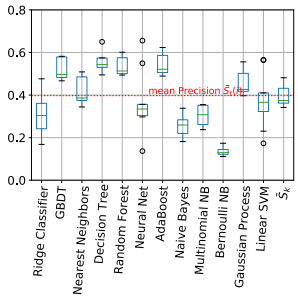

Figure 7.66: Precision under Clean Label Attack

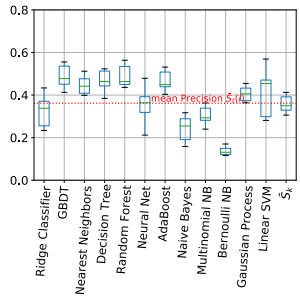

Figure 7.67: Precision under Induced Model Attack

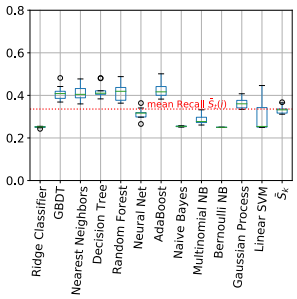

Figure 7.68: Recall under Clandestine Fraudulence

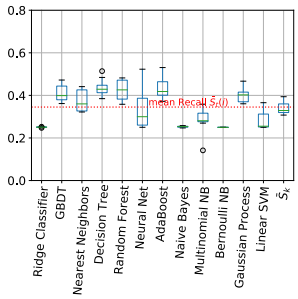

Figure 7.69: Recall under Clean Label Attack

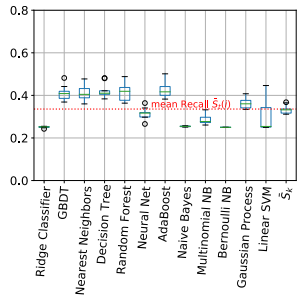

Figure 7.70: Recall under Induced Model Attack

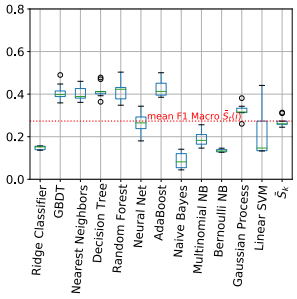

Figure 7.71: F1 Macro under Clandestine Fraudulence

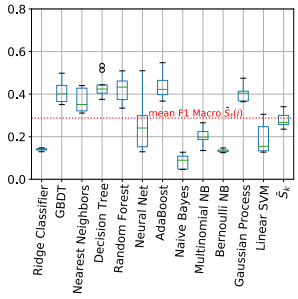

Figure 7.72: F1 Macro under Clean Label Attack

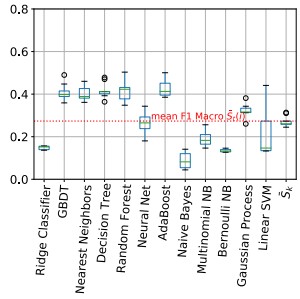

Figure 7.73: F1 Macro under Induced Model Attack

Figure 7.74: Method-Wise Metric $\bar{S}_k(i)$ Comparison Under Covert Attack Based on FDI ($w = 30\%, r = 100\%$)

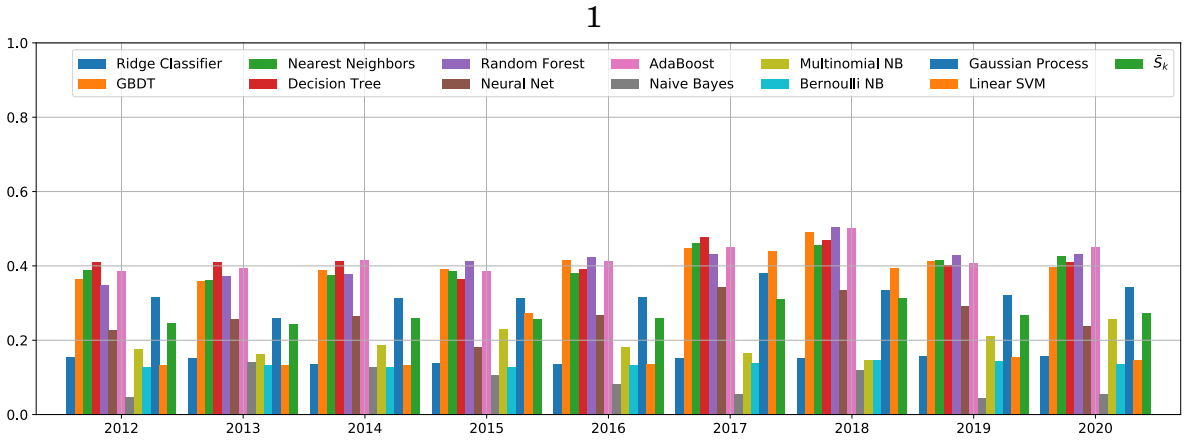

Figure 7.75: Yearly Comprehensive Stats under Clandestine Fraudulence

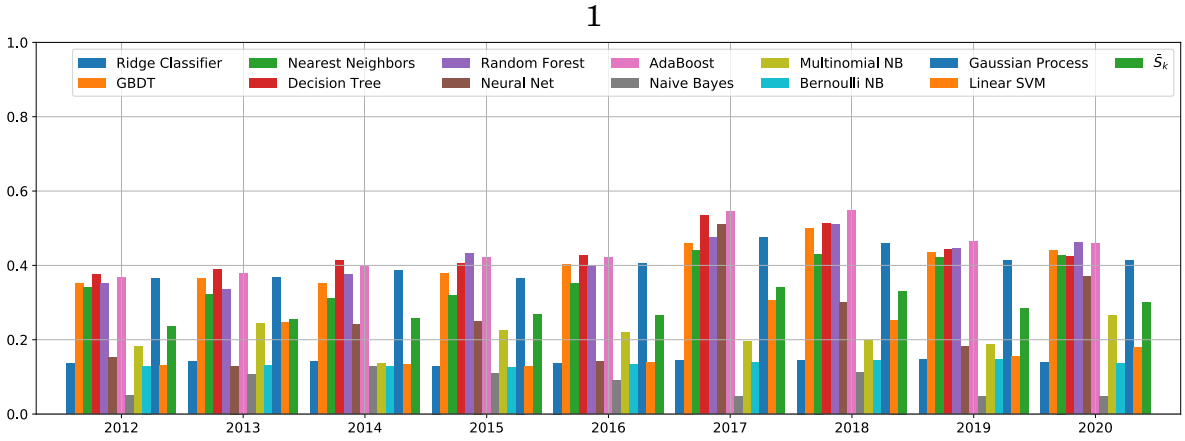

Figure 7.76: Yearly Comprehensive Stats under Clean Label Attack

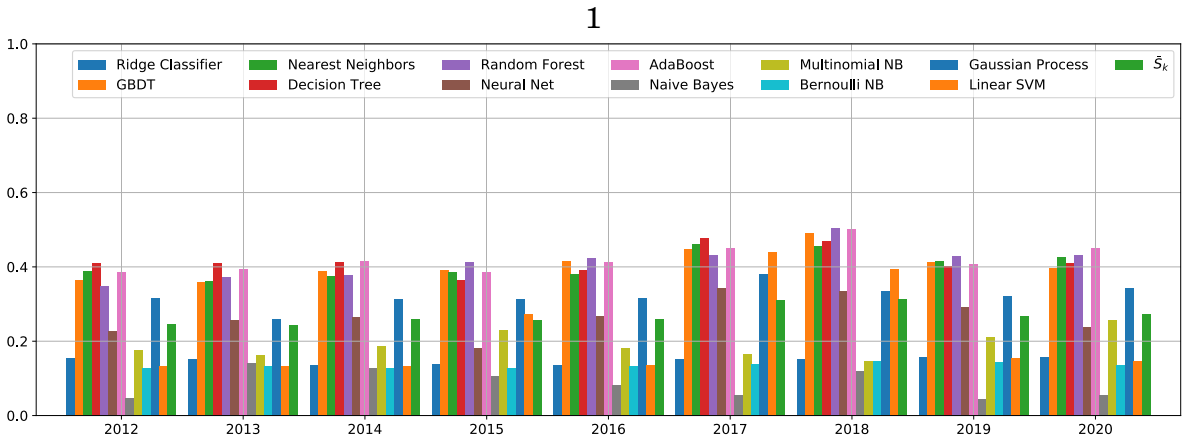

Figure 7.77: Yearly Comprehensive Stats under Induced Model Attack

Figure 7.78: Method-Wise Yearly Stats Comparison between $\bar{S}_t$ and $\bar{S}_k(t)$ with Covert Attacks Based on FDI (w=30%, r=100%)

Table 7.10: Accuracy Difference Stats under Clandestine Fraudulence (w=30%, r=30%)

Years	M1	M2	M3	M4	M5	M6	M7	M8	M9	M10	M11	M12	$\Delta\tilde{S}_k(t)$
2012	-0.0025	-0.0414	-0.0070	-0.0305	-0.0154	0.0818	-0.0246	0.0130	0.0028	-0.0172	-0.0386	-0.0042	-0.0043
2013	-0.0105	-0.0305	-0.0081	-0.0263	-0.0400	-0.2583	-0.0246	-0.0193	-0.0498	0.0249	-0.0635	0.1309	-0.0245
2014	-0.0183	-0.0340	-0.0028	-0.0239	-0.0548	-0.1151	-0.0253	-0.0112	0.0590	0.0004	-0.0509	0.0007	-0.0190
2015	-0.0081	-0.0232	-0.0154	-0.0249	-0.0316	-0.0274	-0.0435	0.0355	0.0453	0.0004	-0.0502	0.0902	-0.0110
2016	-0.0011	-0.0256	-0.0165	-0.0541	-0.0133	0.1337	-0.0130	-0.0137	0.0000	0.0109	-0.0569	0.0105	-0.0052
2017	0.0042	-0.0355	-0.0154	-0.0319	-0.0186	-0.1766	-0.0411	0.0769	0.0263	-0.0011	-0.0706	-0.0235	-0.0224
2018	0.0253	-0.0232	-0.0200	-0.0284	-0.0347	0.0849	-0.0316	0.0088	0.0137	-0.0133	-0.0863	-0.0347	-0.0164
2019	0.0088	-0.0225	-0.0214	-0.0211	-0.0260	0.2138	-0.0365	-0.0018	-0.0154	-0.0176	-0.0579	0.0779	0.0084
2020	0.0067	-0.0372	0.0004	-0.0376	-0.0077	-0.1288	-0.0197	-0.0084	0.0586	-0.0133	-0.0474	-0.1453	-0.0257
$\Delta\tilde{S}_k(i)$	0.0005	-0.0303	-0.0118	-0.0310	-0.0269	-0.0213	-0.0289	0.0089	0.0156	-0.0029	-0.0580	0.0114	-0.0134

Table 7.11: Accuracy Difference Stats under Clean Label Attack (w=30%, r=30%)

Years	M1	M2	M3	M4	M5	M6	M7	M8	M9	M10	M11	M12	$\Delta\tilde{S}_k(t)$
2012	-0.0098	-0.0077	0.0077	0.0042	0.0126	0.0168	-0.0028	0.0060	-0.0014	-0.0035	0.0088	-0.0070	0.0017
2013	-0.0116	-0.0323	0.0098	0.0046	-0.0154	-0.1064	-0.0049	-0.0137	-0.0369	0.0091	-0.0053	-0.0112	-0.0076
2014	-0.0084	-0.0021	-0.0007	-0.0011	-0.0295	-0.0161	0.0168	-0.0193	-0.0892	-0.0144	-0.0137	-0.0074	-0.0004
2015	0.0091	0.0105	-0.0021	-0.0109	-0.0190	-0.0011	-0.0088	0.0077	0.0372	0.0014	-0.0042	-0.0183	-0.0015
2016	-0.0074	-0.0070	-0.0186	0.0021	-0.0053	0.2032	0.0214	-0.0039	0.0502	-0.0067	-0.0081	0.0098	0.0157
2017	0.0032	0.0154	0.0014	-0.0126	0.0018	-0.0751	-0.0197	0.0067	-0.0049	-0.0239	-0.0074	0.0049	-0.0066
2018	0.0063	-0.0119	0.0032	0.0112	-0.0183	0.0621	0.0060	-0.0067	0.0176	-0.0161	-0.0053	-0.0527	-0.0027
2019	0.0025	0.0070	0.0000	-0.0112	-0.0091	0.0863	-0.0074	0.0014	-0.0004	0.0105	-0.0084	-0.0119	0.0032
2020	0.0021	-0.0070	0.0021	-0.0158	0.0049	0.0783	-0.0084	-0.0084	-0.0007	-0.0130	-0.0112	-0.1506	-0.0086
$\Delta\tilde{S}_k(i)$	-0.0016	-0.0039	0.0003	-0.0033	-0.0086	0.0276	-0.0009	-0.0034	-0.0032	-0.0063	-0.0061	-0.0271	-0.0008

Table 7.12: Accuracy Difference Stats under Induced Model Attack (w=30%, r=30%)

Years	M1	M2	M3	M4	M5	M6	M7	M8	M9	M10	M11	M12	$\Delta\tilde{S}_k(t)$
2012	-0.0154	-0.0235	0.0102	-0.0298	-0.0056	0.0211	-0.0235	0.0077	0.0586	-0.0116	-0.0014	-0.0102	-0.0013
2013	-0.0102	-0.0186	0.0014	-0.0274	-0.0239	-0.0832	-0.0147	-0.0200	0.1225	0.0158	-0.0126	0.1074	0.0134
2014	-0.0179	-0.0267	0.0000	-0.0295	-0.0397	-0.0646	-0.0137	-0.0074	0.0330	-0.0130	-0.0147	0.0014	-0.0028
2015	-0.0161	-0.0193	-0.0014	-0.0256	-0.0418	-0.0414	-0.0176	0.0221	0.0193	0.0032	-0.0102	-0.0302	-0.0140
2016	0.0004	-0.0242	-0.0084	-0.0204	-0.0242	0.0032	-0.0091	-0.0183	0.0253	-0.0046	-0.0158	-0.0053	-0.0088
2017	-0.0063	-0.0165	-0.0242	-0.0428	-0.0119	-0.2380	-0.0312	-0.0039	0.0137	-0.0147	-0.0228	0.0014	-0.0291
2018	0.0228	-0.0165	0.0056	-0.0221	-0.0414	-0.1348	-0.0295	0.0197	0.0256	-0.0183	-0.0298	-0.0428	-0.0209
2019	0.0053	-0.0049	-0.0165	-0.0467	-0.0084	0.1902	-0.0386	-0.0154	0.0063	0.0035	-0.0176	0.1994	0.0187
2020	-0.0007	-0.0168	0.0021	-0.0246	-0.0119	-0.0397	-0.0133	0.0046	0.0583	-0.0067	-0.0070	-0.1422	-0.0123
$\Delta\tilde{S}_k(i)$	-0.0043	-0.0186	-0.0035	-0.0299	-0.0232	-0.0430	-0.0213	-0.0012	0.0403	-0.0051	-0.0147	0.0088	-0.0063

Attack. it is worth noting that although Induced Model Attack does not have the greatest impact on the machine system, its correspondence reflects that the attack is the most confusing since it does not reflect significant fluctuations in accuracy even though both the input and the model are attacked at the same time.

From the accuracy point of view, the corresponding of each machine learning system for different parts of the FDI attack pattern is shown in Table 7.13-7.15. It can be seen that the Clandestine Fraudulence has the largest impact on Gaussian Process (-0.0548), followed by Decision Tree (-0.0374), AdaBoost (-0.0345), and GBDT (-0.0290), respectively. Under the Clean Label Attack, the top three affected are Ridge Classifier, Linear SVM, and Random Forest in descending order, while GBDT, Decision Tree, and AdaBoost are less affected; thus, in terms of accuracy, GBDT, Decision Tree, and AdaBoost are not sensitive to the label attack. Decision Tree is not sensitive to labeling attacks.

Under Induced Model Attack, the accuracy is most affected by Ridge Classifier (-0.0731), followed by Decision Tree (-0.0319); GBDT, Random Forest, and AdaBoost are affected by -0.0146, -0.0251, and -0.0251, respectively. 0.0251, -0.0222. From the statistics of comprehensive precision, Clandestine Fraudulence has the highest average damage to precision (-0.0224), while Clean Label Attack has the lowest in the partial FDI model. Similarly, Induced Model Attack is the most disorienting. The accuracy reflected by the experimental results can still be maintained at a comparable level when both the input data and the training attribute data are corrupted.

Table 7.13: Precision Difference Stats under Clandestine Fraudulence (w=30%, r=30%)

Years	M1	M2	M3	M4	M5	M6	M7	M8	M9	M10	M11	M12	$\Delta\bar{S}_k(t)$
2012	-0.1856	-0.0126	-0.0033	-0.0373	0.0603	0.2198	-0.0300	-0.0313	0.0176	-0.0119	-0.0461	-0.0445	-0.0149
2013	0.0307	-0.0348	-0.0076	-0.0352	-0.0444	-0.2213	-0.0325	-0.1091	-0.0914	0.0175	-0.0374	-0.0340	-0.0457
2014	-0.0889	-0.0526	-0.0122	-0.0265	-0.0499	-0.0194	-0.0380	-0.0941	0.0492	0.0003	-0.0597	0.0298	-0.0270
2015	0.2082	-0.0311	-0.0138	-0.0327	-0.0376	0.0006	-0.0495	0.0482	-0.0151	0.0002	-0.0335	0.1475	0.0075
2016	-0.1661	-0.0287	-0.0217	-0.0616	-0.0270	0.0964	-0.0134	0.0975	-0.0246	0.0080	-0.0603	-0.1187	-0.0281
2017	0.0305	-0.0302	-0.0100	-0.0344	0.0000	-0.1858	-0.0440	-0.0108	0.0138	-0.0008	-0.0737	-0.0328	-0.0311
2018	0.1407	-0.0275	-0.0182	-0.0337	-0.0354	0.1591	-0.0365	-0.0225	0.0549	-0.0108	-0.0707	-0.0503	-0.0014
2019	-0.0796	-0.0007	-0.0102	-0.0252	-0.0243	0.1886	-0.0509	-0.0305	0.1041	-0.0140	-0.0617	-0.0177	-0.0195
2020	0.0373	-0.0426	-0.0054	-0.0501	-0.0065	-0.1688	-0.0159	-0.0556	0.0037	-0.0094	-0.0497	-0.0451	-0.0416
$\Delta\bar{S}_k(i)$	-0.0081	-0.0290	-0.0114	-0.0374	-0.0183	0.0077	-0.0345	-0.0231	0.0125	-0.0023	-0.0548	-0.0184	-0.0224

Table 7.14: Precision Difference Stats under Clean Label Attack (w=30%, r=30%)

Years	M1	M2	M3	M4	M5	M6	M7	M8	M9	M10	M11	M12	$\Delta\bar{S}_k(t)$
2012	-0.1227	0.0257	0.0097	0.0082	0.0128	0.1297	0.0055	0.0587	0.0130	-0.0025	0.0095	-0.0214	0.0071
2013	0.0742	-0.0273	0.0119	0.0106	-0.0213	0.0322	-0.0055	-0.2196	-0.0888	0.0063	-0.0135	-0.1491	-0.0265
2014	-0.0942	-0.0023	-0.0107	0.0028	-0.0265	0.1790	0.0183	-0.1063	-0.0285	-0.0102	-0.0155	-0.0298	0.0038
2015	0.0064	0.0144	-0.0007	-0.0139	-0.0194	0.0311	-0.0001	-0.0722	0.0001	0.0010	0.0001	0.0056	0.0135
2016	-0.1827	-0.0074	-0.0136	-0.0034	-0.0107	0.2635	0.0352	0.1905	-0.0139	-0.0048	-0.0059	-0.0879	0.0273
2017	-0.0153	0.0222	0.0037	-0.0142	-0.0301	-0.2143	-0.0228	-0.0153	0.0107	-0.0183	-0.0114	-0.0223	-0.0262
2018	0.0057	-0.0143	0.0042	0.0047	-0.0195	0.1396	0.0060	0.0205	0.0679	-0.0131	-0.0101	-0.0123	0.0070
2019	-0.1492	0.0070	0.0062	-0.0094	-0.0062	0.1257	0.0041	0.0088	0.0123	0.0087	-0.0097	-0.1280	-0.0171
2020	-0.0360	-0.0178	-0.0037	-0.0335	0.0087	0.0167	-0.0141	0.1026	-0.0101	-0.0092	-0.0154	-0.0585	-0.0153
$\Delta\bar{S}_k(i)$	-0.0571	0.0000	0.0008	-0.0053	-0.0125	0.0781	0.0029	-0.0036	-0.0041	-0.0047	-0.0080	-0.0560	-0.0029

Table 7.15: Precision Difference Stats under Induced Model Attack (w=30%, r=30%)

Years	M1	M2	M3	M4	M5	M6	M7	M8	M9	M10	M11	M12	$\Delta\bar{S}_k(t)$
2012	-0.2273	-0.0042	0.0168	-0.0435	0.0163	0.1221	-0.0223	-0.0869	-0.0349	-0.0081	-0.0041	0.0527	-0.0120
2013	-0.0370	-0.0153	0.0029	-0.0309	-0.0312	-0.1197	-0.0265	-0.0696	-0.1825	0.0109	-0.0203	-0.0376	-0.0415
2014	-0.0762	-0.0368	-0.0097	-0.0322	-0.0400	0.2713	-0.0149	-0.0971	0.0041	-0.0093	-0.0210	-0.0201	0.0027
2015	0.1107	-0.0162	-0.0002	-0.0211	-0.0366	-0.0568	-0.0192	0.0928	0.0128	0.0022	-0.0111	-0.0153	-0.0017
2016	-0.2525	-0.0247	-0.0106	-0.0155	-0.0340	0.1272	-0.0141	-0.0159	-0.0348	-0.0033	-0.0188	0.0241	-0.0085
2017	-0.1167	-0.0114	-0.0215	-0.0436	-0.0394	-0.2972	-0.0353	-0.0310	-0.0045	-0.0115	-0.0273	-0.0534	-0.0557
2018	0.0183	-0.0192	0.0049	-0.0268	-0.0408	-0.0800	-0.0277	0.0606	0.0590	-0.0147	-0.0340	-0.0366	-0.0126
2019	-0.0275	-0.0079	-0.0072	-0.0487	-0.0052	0.1190	-0.0363	-0.0228	0.0254	0.0029	-0.0166	0.0555	-0.0017
2020	-0.0499	0.0043	-0.0085	-0.0249	-0.0148	-0.0518	-0.0036	-0.0280	-0.0007	-0.0048	-0.0105	-0.0745	-0.0324
$\Delta\bar{S}_k(i)$	-0.0731	-0.0146	-0.0037	-0.0319	-0.0251	0.0038	-0.0222	-0.0220	-0.0173	-0.0039	-0.0182	-0.0117	-0.0182

7.4.2 Full FDI Adversarial Backdoor Attacks

After further increasing the attack range, the corresponding different machine learning systems for different adversarial backdoor attacks in the full FDI mode with $w = 30\%, r = 100\%$ is shown in Table 7.16-7.21. Under the full FDI attack of Clandestine Fraudulence, the accuracy is most severely impaired by Gaussian Process, while the rest of Decision Tree (-0.0994), GBDT (-0.0910), AdaBoost (-0.0896), Random Forest (- 0.0771) are all affected to a large extent. These are all methods that are used to have outstanding accuracy performance in the absence of attacks. It is worth noting that the same situation occurs with Induced Model Attacks, which implies that when the attack range reaches 100%, the impact of the attack on the input side dominates the accuracy. The next most sensitive are GBDT (-0.0654) and Nearest Neighbors (-0.0665). In terms of the combined impact of each adversarial backdoor attack on the accuracy metric, Clandestine Fraudulence and Induced Model Attack have comparable destructive effects on the accuracy of the machine learning system, while Clean Label Attack is relatively weak but still degrades the accuracy of the system by 0.0276.

Table 7.16: Accuracy Difference Stats under Clandestine Fraudulence (w=30%, r=100%)

Years	M1	M2	M3	M4	M5	M6	M7	M8	M9	M10	M11	M12	$\Delta\tilde{S}_k(t)$
2012	-0.0288	-0.0786	0.0007	-0.0698	-0.0586	-0.0888	-0.0786	0.0032	0.0074	-0.0074	-0.1481	-0.0151	-0.0367
2013	0.0035	-0.0892	-0.0263	-0.0618	-0.0744	-0.1081	-0.0853	0.1113	-0.0102	0.0218	-0.2334	-0.0032	-0.0573
2014	-0.0214	-0.0565	-0.0376	-0.0751	-0.0948	-0.0516	-0.0583	-0.0183	0.0414	-0.0165	-0.1572	-0.0123	-0.0309
2015	0.0060	-0.0979	-0.0221	-0.1274	-0.0748	-0.1229	-0.1028	0.0028	0.0604	-0.0091	-0.1766	0.0762	-0.0624
2016	-0.0067	-0.0720	-0.0351	-0.1081	-0.0691	0.0713	-0.0702	-0.0077	-0.0376	0.0004	-0.1766	0.0007	-0.0423
2017	0.0070	-0.1229	-0.0888	-0.1488	-0.0944	-0.1836	-0.1474	-0.0014	-0.0042	-0.0095	-0.2289	0.0337	-0.0735
2018	0.0225	-0.1092	-0.0583	-0.1221	-0.1007	-0.1134	-0.0969	0.0084	-0.0035	0.0000	-0.2573	-0.0674	-0.0852
2019	-0.0088	-0.0765	-0.0769	-0.1028	-0.0741	0.1474	-0.0885	-0.0035	-0.0147	-0.0035	-0.2001	-0.0088	-0.0338
2020	0.0039	-0.1165	-0.0569	-0.0783	-0.0530	-0.1446	-0.0786	-0.0056	0.0449	0.0091	-0.1787	-0.1537	-0.0565
$\Delta\tilde{S}_k(i)$	-0.0025	-0.0910	-0.0446	-0.0994	-0.0771	-0.0660	-0.0896	0.0099	0.0093	-0.0016	-0.1952	-0.0167	-0.0532

Table 7.17: Accuracy Difference Stats under Clean Label Attack (w=30%, r=100%)

Years	M1	M2	M3	M4	M5	M6	M7	M8	M9	M10	M11	M12	$\Delta\tilde{S}_k(t)$
2012	0.0021	-0.0442	-0.0369	-0.0197	-0.0298	0.0183	-0.0463	0.0070	0.0077	-0.0056	-0.0642	-0.0070	-0.0213
2013	-0.0123	-0.0611	-0.0614	-0.0607	-0.0730	-0.0772	-0.0442	-0.0074	0.1492	0.0161	-0.0783	0.0923	-0.0188
2014	0.0049	-0.0639	-0.0888	-0.0323	-0.0586	0.0228	-0.0386	-0.0109	-0.0899	-0.0161	-0.0734	-0.0014	-0.0247
2015	-0.0049	-0.0916	-0.0765	-0.0467	-0.0432	0.0772	-0.0432	0.0084	0.0537	-0.0161	-0.0983	-0.0214	-0.0280
2016	0.0039	-0.0639	-0.0527	-0.0421	-0.0484	0.0786	-0.0379	-0.0109	-0.0509	-0.0021	-0.0755	0.0161	-0.0238
2017	-0.0042	-0.0927	-0.0874	-0.0565	-0.0393	0.0225	-0.0625	-0.0014	0.0253	-0.0165	-0.0878	-0.0256	-0.0365
2018	0.0193	-0.0579	-0.0776	-0.0576	-0.0804	-0.0407	-0.0253	0.0084	0.0425	-0.0074	-0.1057	-0.0892	-0.0402
2019	0.0007	-0.0541	-0.0611	-0.0449	-0.0495	0.0060	-0.0376	-0.0004	-0.0383	0.0095	-0.0874	-0.0133	-0.0256
2020	-0.0063	-0.0590	-0.0565	-0.0597	-0.0183	0.0425	-0.0277	-0.0133	0.0523	0.0095	-0.0811	-0.1260	-0.0293
$\Delta\tilde{S}_k(i)$	0.0004	-0.0654	-0.0665	-0.0467	-0.0489	0.0167	-0.0404	-0.0023	0.0168	-0.0032	-0.0835	-0.0195	-0.0276

From an accuracy perspective, the same attacks on the input still dominate when an adversarial backdoor attack with all FDI modes is used. As shown in Figure 7.19-7.21, the combined precision destructiveness under Clandestine Fraudulence reaches -0.0776,

Table 7.18: Accuracy Difference Stats under Induced Model Attack (w=30%, r=100%)

Years	M1	M2	M3	M4	M5	M6	M7	M8	M9	M10	M11	M12	$\Delta\tilde{S}_k(t)$
2012	-0.0288	-0.0786	0.0007	-0.0698	-0.0586	-0.0888	-0.0786	0.0032	0.0074	-0.0074	-0.1481	-0.0151	-0.0367
2013	0.0035	-0.0892	-0.0263	-0.0618	-0.0744	-0.1081	-0.0853	0.1113	-0.0102	0.0218	-0.2334	-0.0032	-0.0573
2014	-0.0214	-0.0565	-0.0376	-0.0751	-0.0948	-0.0516	-0.0583	-0.0183	0.0414	-0.0165	-0.1572	-0.0123	-0.0309
2015	0.0060	-0.0979	-0.0221	-0.1274	-0.0748	-0.1229	-0.1028	0.0028	0.0604	-0.0091	-0.1766	0.0762	-0.0624
2016	-0.0067	-0.0720	-0.0351	-0.1081	-0.0691	0.0713	-0.0702	-0.0077	-0.0376	0.0004	-0.1766	0.0007	-0.0423
2017	0.0070	-0.1229	-0.0888	-0.1488	-0.0944	-0.1836	-0.1474	-0.0014	-0.0042	-0.0095	-0.2289	0.0337	-0.0735
2018	0.0225	-0.1092	-0.0583	-0.1221	-0.1007	-0.1134	-0.0969	0.0084	-0.0035	0.0000	-0.2573	-0.0674	-0.0852
2019	-0.0088	-0.0765	-0.0769	-0.1028	-0.0741	0.1474	-0.0885	-0.0035	-0.0147	-0.0035	-0.2001	-0.0088	-0.0338
2020	0.0039	-0.1165	-0.0569	-0.0783	-0.0530	-0.1446	-0.0786	-0.0056	0.0449	0.0091	-0.1787	-0.1537	-0.0565
$\Delta\tilde{S}_k(i)$	-0.0025	-0.0910	-0.0446	-0.0994	-0.0771	-0.0660	-0.0896	0.0099	0.0093	-0.0016	-0.1952	-0.0167	-0.0532

which is much higher than the precision destructiveness of Clean Label Attack (-0.0029) and almost Induced Model Attack and almost twice as high. In terms of sensitivity to accuracy corruption, Gaussian Process has the highest sensitivity to Clandestine Fraudulence with an accuracy drop of 0.1491, followed by Decision Tree and AdaBoost with a drop of 0.1130 and 0.1033, respectively. Induced Model Attack is the most sensitive to Gaussian Process attack, followed by Ridge Classifier and Linear SVM, with a decrease of 0.0571 and 0.0560, respectively, while GBDT and AdaBoost have relatively small changes in accuracy and stable performance. GBDT and Random Forest are correspondingly more destructive to Induced Model Attack than Decision Tree and AdaBoost. In summary, Clandestine Fraudulence has the strongest accuracy destructiveness, while Clean Label Attack has the weakest, and Induced Model Attack has the best accuracy destructiveness concealment.

Table 7.19: Precision Difference Stats under Clandestine Fraudulence (w=30%, r=100%)

Years	M1	M2	M3	M4	M5	M6	M7	M8	M9	M10	M11	M12	$\Delta\tilde{S}_k(t)$
2012	-0.2063	-0.0433	0.0112	-0.0818	-0.0577	0.1383	-0.0923	-0.0163	0.0256	-0.0052	-0.1243	-0.0074	-0.0592
2013	0.0620	-0.1097	-0.0270	-0.0749	-0.0918	0.0382	-0.1011	-0.1082	-0.0926	0.0152	-0.1276	-0.1156	-0.0820
2014	-0.1554	-0.0815	-0.0420	-0.0891	-0.1108	0.0916	-0.0788	-0.0023	0.0317	-0.0117	-0.1365	0.0811	-0.0464
2015	0.1122	-0.1211	-0.0233	-0.1510	-0.0911	-0.0901	-0.1202	0.0775	-0.0040	-0.0063	-0.0916	0.0975	-0.0619
2016	-0.1006	-0.0837	-0.0442	-0.1337	-0.0877	0.1320	-0.0884	-0.0022	-0.0439	0.0003	-0.1432	-0.0313	-0.0620
2017	-0.1172	-0.1262	-0.0835	-0.1489	-0.1008	-0.1803	-0.1689	-0.0660	-0.0127	-0.0074	-0.2029	-0.0480	-0.1243
2018	0.0998	-0.1202	-0.0578	-0.1346	-0.1098	-0.0130	-0.1092	0.0070	0.0163	0.0000	-0.1763	-0.0921	-0.0752
2019	-0.1301	-0.0871	-0.0688	-0.1086	-0.0750	0.1746	-0.0975	-0.0373	-0.0098	-0.0028	-0.1778	-0.1097	-0.0850
2020	-0.0945	-0.0598	-0.0727	-0.0945	-0.0582	-0.1524	-0.0731	-0.0339	-0.0156	0.0067	-0.1617	-0.1261	-0.1019
$\Delta\tilde{S}_k(i)$	-0.0589	-0.0925	-0.0453	-0.1130	-0.0870	0.0154	-0.1033	-0.0202	-0.0117	-0.0013	-0.1491	-0.0390	-0.0776

7.4.3 Discussion

The results of the above experimental tests show that the proposed Clandestine Fraudulence is the most destructive to performance, while Clean Label Attack is the weakest, and the most confusing attack is the Induced Model Attack because it can be seen that although the difference in system performance is not obvious after the attack, the internal

Table 7.20: Precision Difference Stats under Clean Label Attack (w=30%, r=100%)

Years	M1	M2	M3	M4	M5	M6	M7	M8	M9	M10	M11	M12	$\Delta\bar{S}_k(t)$
2012	-0.1227	0.0257	0.0097	0.0082	0.0128	0.1297	0.0055	0.0587	0.0130	-0.0025	0.0095	-0.0214	0.0071
2013	0.0742	-0.0273	0.0119	0.0106	-0.0213	0.0322	-0.0055	-0.2196	-0.0888	0.0063	-0.0135	-0.1491	-0.0265
2014	-0.0942	-0.0023	-0.0107	0.0028	-0.0265	0.1790	0.0183	-0.1063	-0.0285	-0.0102	-0.0155	-0.0298	0.0038
2015	0.0064	0.0144	-0.0007	-0.0139	-0.0194	0.0311	-0.0001	-0.0722	0.0001	0.0010	0.0001	0.0056	0.0135
2016	-0.1827	-0.0074	-0.0136	-0.0034	-0.0107	0.2635	0.0352	0.1905	-0.0139	-0.0048	-0.0059	-0.0879	0.0273
2017	-0.0153	0.0222	0.0037	-0.0142	-0.0301	-0.2143	-0.0228	-0.0153	0.0107	-0.0183	-0.0114	-0.0223	-0.0262
2018	0.0057	-0.0143	0.0042	0.0047	-0.0195	0.1396	0.0060	0.0205	0.0679	-0.0131	-0.0101	-0.0123	0.0070
2019	-0.1492	0.0070	0.0062	-0.0094	-0.0062	0.1257	0.0041	0.0088	0.0123	0.0087	-0.0097	-0.1280	-0.0171
2020	-0.0360	-0.0178	-0.0037	-0.0335	0.0087	0.0167	-0.0141	0.1026	-0.0101	-0.0092	-0.0154	-0.0585	-0.0153
$\Delta\bar{S}_k(i)$	-0.0571	0.0000	0.0008	-0.0053	-0.0125	0.0781	0.0029	-0.0036	-0.0041	-0.0047	-0.0080	-0.0560	-0.0029

Table 7.21: Precision Difference Stats under Induced Model Attack (w=30%, r=100%)

Years	M1	M2	M3	M4	M5	M6	M7	M8	M9	M10	M11	M12	$\Delta\bar{S}_k(t)$
2012	-0.1686	-0.0244	-0.0442	0.0105	-0.0139	0.1971	-0.0275	0.0111	0.0401	-0.0040	-0.0719	-0.0653	-0.0206
2013	-0.0319	-0.0563	-0.0660	-0.0336	-0.0567	-0.2173	-0.0509	-0.0703	-0.0905	0.0112	-0.0930	-0.0689	-0.0619
2014	-0.0388	-0.0568	-0.1008	-0.0018	-0.0357	0.0691	-0.0067	-0.0353	-0.0122	-0.0115	-0.0894	-0.0136	-0.0224
2015	0.1142	-0.0666	-0.0831	-0.0407	-0.0275	0.0543	-0.0340	0.0504	-0.0320	-0.0110	-0.1004	-0.0277	-0.0259
2016	-0.1105	-0.0524	-0.0682	-0.0029	-0.0374	0.1110	-0.0095	0.0208	-0.0327	-0.0015	-0.0896	-0.0771	-0.0273
2017	-0.0189	-0.0802	-0.0920	-0.0218	-0.0632	-0.0008	-0.0536	-0.0317	0.0284	-0.0128	-0.1017	-0.0522	-0.0535
2018	0.0157	-0.0478	-0.0731	-0.0425	-0.0608	-0.0224	-0.0163	0.0061	0.0138	-0.0060	-0.1158	-0.2400	-0.0519
2019	-0.2195	-0.0539	-0.0569	-0.0478	-0.0534	-0.0008	-0.0427	-0.0880	-0.0175	0.0078	-0.0949	0.0006	-0.0495
2020	-0.2211	-0.0360	-0.0639	-0.0642	-0.0191	0.0318	-0.0236	0.0155	-0.0024	0.0069	-0.0926	-0.1699	-0.0619
$\Delta\bar{S}_k(i)$	-0.0755	-0.0527	-0.0720	-0.0272	-0.0408	0.0247	-0.0294	-0.0135	-0.0117	-0.0023	-0.0944	-0.0793	-0.0417

machine learning rules have been tampered with, i.e., this attack is not easily detectable from the performance check. Another reason why this attack is not easily detected is that there are a few attacks with a purpose. In other words, this attack does not necessarily require extensive data corruption to achieve its goal, but only requires targeted selection of data records that correspond to the expected rating to be induced, which is more undetectable than the attack tested in this paper, especially when the number of targets is small. The attacker selects only several target data entities, and after targeting their data features to be implanted into the training model through Induced Model Attacks, then selects data with the same features to be input into the system, and the system can give the expected results. Due to the small sample under attack, this type of covert attack is more stealthy if the magnitude of its attack is not large.

7.5 Adaptive Fusion

7.5.1 Introduction

This case study explores the investment value of 924 Nasdaq-listed companies through an expert rating system. We invited six experts from diverse fields,Äîeconomics, finance, trading, business, and mathematics,Äîto evaluate the stocks. To minimize bias, the names of the companies were withheld, allowing the experts to focus solely on stock

prices and fundamental financial data. Each expert rated the companies on a scale from 3 to 0, corresponding to the categories of “excellent, “good, “fair, and “poor.

The experts independently assessed each company based on the provided financial information, contributing to a robust and unbiased evaluation process. Each expert was given access to the information independently about financial indicators, historical price trends, and other relevant metrics. The anonymity of the companies aimed to eliminate any preconceived notions or biases that could arise from brand reputation or market perception. The diverse panel of experts provided a multifaceted perspective on stock valuation.

This case study underscores the effectiveness of employing a diverse panel of experts to evaluate the investment potential of Nasdaq-listed companies. By anonymizing company identities and concentrating on empirical data, the study minimizes biases, thereby yielding more accurate assessments of stock values. The integration of interdisciplinary collaboration enhances the comprehensiveness of investment analysis.

7.5.2 Disparity Analysis on Expert Evaluations

Despite the unbiased and independent process, preliminary analysis reveals variability in the scores assigned by different experts, reflecting their unique perspectives and areas of specialization. This variability highlights the importance of diverse expertise in enhancing the depth of financial analysis.

We analyze the disparities among the judgments of six experts (Exp1 to Exp6) using Tukeys Honestly Significant Difference (HSD) test. The test results in Table 7.22 provide insight into the pairwise comparisons of the mean scores assigned by each expert, highlighting significant differences that may indicate divergent biases in their assessments.

The Tukey HSD test revealed significant differences in expert judgments across all pairs of comparisons, with the exception of the comparison between Exp5 and Exp6. Specifically, the mean differences (meandiff) were found to be statistically significant (p-adj < 0.05) in 14 out of 15 comparisons. This suggests that the expert assessments exhibit substantial variability, with some experts consistently rating the objects higher or lower than others.

The analysis of mean differences shows that Exp1 consistently received lower ratings compared to the other experts. For example, the mean difference between Exp1 and Exp4 is -2.5952, indicating that Exp4s assessments were significantly more favorable.

group1	group2	meandiff	p-adj	lower	upper	reject
Exp1	Exp2	0.4394	0.0000	0.2553	0.6235	True
Exp1	Exp3	-0.2652	0.0006	-0.4492	-0.0811	True
Exp1	Exp4	-2.5952	0.0000	-2.7793	-2.4111	True
Exp1	Exp5	-1.3799	0.0000	-1.5640	-1.1958	True
Exp1	Exp6	-1.3387	0.0000	-1.5228	-1.1547	True
Exp2	Exp3	-0.7045	0.0000	-0.8886	-0.5205	True
Exp2	Exp4	-3.0346	0.0000	-3.2187	-2.8505	True
Exp2	Exp5	-1.8193	0.0000	-2.0034	-1.6352	True
Exp2	Exp6	-1.7781	0.0000	-1.9622	-1.5940	True
Exp3	Exp4	-2.3301	0.0000	-2.5142	-2.1460	True
Exp3	Exp5	-1.1147	0.0000	-1.2988	-0.9306	True
Exp3	Exp6	-1.0736	0.0000	-1.2577	-0.8895	True
Exp4	Exp5	1.2154	0.0000	1.0313	1.3995	True
Exp4	Exp6	1.2565	0.0000	1.0724	1.4406	True
Exp5	Exp6	0.0411	0.9882	-0.1430	0.2252	False

Table 7.22: Significant Pairwise Comparisons

Similarly, the mean differences between Exp1 and both Exp5 and Exp6 were -1.3799 and -1.3387, respectively, reinforcing the notion that Exp1s evaluations are less optimistic.

In contrast, Exp4 emerged as the most optimistic expert, with significant positive mean differences when compared to Exp5 (1.2154) and Exp6 (1.2565). This trend indicates that while Exp4 rates the objects higher, Exp5 and Exp6 tend to offer more conservative assessments, as seen from their lower scores.

Exp2 and Exp3 also display notable disparities when compared to Exp1. The mean difference between Exp1 and Exp2 is 0.4394, indicating that while Exp2 rated objects higher than Exp1, the difference was not as pronounced as that of Exp4. Similarly, Exp3s assessments were lower than those of Exp4, with a mean difference of -2.3301.

The consistent patterns of disagreement among the experts highlight critical implications for decision-making processes in multi-expert systems. The significant variability in assessments suggests that decisions made without accounting for these biases could lead to suboptimal outcomes. For instance, relying heavily on the assessments of an overly optimistic expert (like Exp4) could distort the overall evaluation, while the more conservative perspectives of Exp5 and Exp6 may underrepresent potential opportunities.

The only non-significant comparison was between Exp5 and Exp6, with a meandiff of 0.0411 (p-adj = 0.9882), suggesting a degree of alignment between these two experts. This alignment could provide a stabilizing influence in decision-making if their assessments

are considered jointly.

The disparities observed among the experts underscore the necessity of employing methods that can effectively reconcile these divergent judgments. The significant mean differences point to varying levels of optimism and caution among the experts, indicating a potential for bias that must be addressed in the decision-making framework. This implies the focus on integrating these expert judgments in a manner that minimizes the impact of extreme biases while maximizing the utility of their collective input.

7.5.3 Statistics in Expert Decision

Table 7.23 shows the stats for expert decision. As shown in the table, the mean scores

	Exp1	Exp2	Exp3	Exp4	Exp5	Exp6
Mean	2.7165	3.1558	2.4513	0.1212	1.3366	1.3777
Median	3.0000	5.0000	3.0000	0.0000	2.0000	2.0000
Variance	0.7811	4.4757	3.1567	0.4485	1.0393	1.6463
Standard Deviation	0.8838	2.1156	1.7767	0.6697	1.0195	1.2831
Mean Absolute Deviation	0.5174	1.9040	1.4784	0.2335	0.9547	1.2197
Interquartile Range	0.0000	5.0000	3.0000	0.0000	2.0000	3.0000
Coefficient of Variation	0.3253	0.6704	0.7248	5.5251	0.7627	0.9313
Skewness	-2.7170	-0.5362	-0.1052	6.0374	-0.4207	0.0172
Kurtosis	5.5582	-1.4071	-1.1122	37.4728	-1.4781	-1.7232
Gini Coefficient	0.0959	0.3529	0.3964	0.9710	0.3797	0.4988

Table 7.23: Statistical Summary for Experimental Groups

highlight marked differences among the experiments, with Exp2 achieving the highest mean of 3.1558, indicating a more favorable outcome. In stark contrast, Exp4 has a notably low mean of 0.1212, reflecting poor performance. The median values reinforce these trends, as Exp2 leads with a median of 5.0000, while Exp4s median of 0.0000 confirms its heavy skew toward lower values.

Variability metrics, including variance and standard deviation, reveal that Exp2 exhibits the highest variance (4.4757) and standard deviation (2.1156), suggesting substantial fluctuation in individual outcomes despite a high average score. Conversely, Exp4 shows the lowest variance (0.4485) and standard deviation (0.6697), indicating a consistent yet low performance. The mean absolute deviation further supports this, with Exp4 having the lowest deviation (0.2335) and Exp2 the highest (1.9040), pointing to unstable performances within the latter.

Skewness values indicate the asymmetry of score distributions. Exp4 has a highly positive skew (-2.7170), indicating a clustering of low scores with a few high outliers. In contrast, Exp1 shows a slight negative skew (-0.5362), suggesting a more balanced distribution. Kurtosis measures reveal that Exp4 possesses an extremely high kurtosis (37.4728), reflecting heavy tails and outliers, while Exp2 negative kurtosis (-1.4071) suggests a flatter distribution with fewer extremes.

The Gini coefficients illustrate disparities within the results. Exp4 has the highest Gini coefficient (0.9710), indicating significant inequality, as most scores are clustered at the lower end. In contrast, Exp1 has the lowest Gini coefficient (0.0959), suggesting a more equitable distribution of scores.

The range across most experiments is 5, indicating broad variability, except for Exp5 and Exp6, which have a range of 3, suggesting less spread within these groups. The interquartile range (IQR) for Exp2 (5.0000) and Exp3 (3.0000) indicates substantial variability in the central 50% of the data, particularly for Exp2, which correlates with its high mean and variance.

It can be seen that Exp2 demonstrates the best average outcomes, though accompanied by high variability and inequality. In contrast, Exp4 exhibits the lowest performance, characterized by significant skewness and inequality. The findings suggest that while some experiments yield favorable results, others face considerable challenges in achieving consistent and equitable outcomes. Further investigation into the methodologies and conditions of each experiment could elucidate the factors contributing to these differences.

7.5.4 Bias Fusion

Table 7.24 shows the statistical summary for the results of bias fusion by OWA, KOWA, AHP, MAUT, PROMETHEE. It can be seen in the table, the mean scores for each method indicate varying levels of performance. AHP achieves the highest mean score of 3.0096, followed closely by MAUT at 2.3158 and PROMETHEE at 2.3567. In contrast, OWA records the lowest mean score of 1.9639, suggesting its relative ineffectiveness compared to the other methods. Similarly, the median values corroborate this trend, with AHP leading again at 3.0761. The median scores for the remaining methods range from 1.9753 for OWA to 2.3810 for MAUT, indicating a more concentrated distribution of lower values, particularly for OWA.

Examining the variability, AHP exhibits the highest variance (1.3649) and standard deviation (1.1683), highlighting substantial fluctuations in its outcomes. This suggests

	OWA	KOWA	AHP	MAUT	PROMETHEE
Mean	1.9639	2.3874	3.0096	2.3158	2.3567
Median	1.9753	2.4638	3.0761	2.3810	2.3603
Variance	0.7449	0.5726	1.3649	0.8077	0.8618
Standard Deviation	0.8631	0.7567	1.1683	0.8987	0.9284
Mean Absolute Deviation	0.6928	0.6204	1.0054	0.7501	0.7820
Interquartile Range	1.2963	1.2100	2.0317	1.4286	1.4950
Coefficient of Variation	0.4395	0.3169	0.3882	0.3881	0.3939
Skewness	-0.0034	-0.3737	-0.3180	-0.1343	-0.0476
Kurtosis	-0.4599	0.0417	-0.9576	-0.6913	-0.7063
Gini Coefficient	0.2499	0.1778	0.2219	0.2217	0.2251

Table 7.24: Statistical Results for OWA, KOWA, AHP, MAUT, and PROMETHEE

that while AHP can achieve high scores, it also faces considerable variability. Conversely, KOWA shows the lowest variance (0.5726) and standard deviation (0.7567), indicating a more consistent performance across its data points. The mean absolute deviation further supports these findings; AHP has the highest deviation (1.0054), while KOWA maintains the lowest (0.6204), reinforcing its reliability.

The skewness values for all methods are relatively close to zero, indicating approximately symmetric distributions. OWA has a slight negative skew (-0.0034), suggesting a minimal tendency towards higher values. KOWA, AHP, MAUT, and PROMETHEE exhibit mild negative skewness, indicating a potential clustering of scores at the lower end. Regarding kurtosis, AHP negative kurtosis (-0.9576) implies a flatter distribution with fewer extreme values. OWA and MAUT also show negative kurtosis, reflecting similar characteristics, while KOWA near-zero kurtosis (0.0417) indicates a distribution that approximates normality.

The Gini coefficients reveal the degree of inequality among the scores. OWA has the highest Gini coefficient (0.2499), signifying a relatively higher inequality compared to other methods. In contrast, KOWA lower Gini coefficient (0.1778) suggests a more equitable distribution of outcomes.

All methods demonstrate a consistent range of 5, indicating that the maximum and minimum scores differ by the same amount across all methods, suggesting a comparable extent of variation. The interquartile range (IQR) further illustrates this variability; AHP has the highest IQR (2.0317), indicating significant variability within the middle 50% of its scores. OWAs IQR (1.2963) is lower, suggesting less variability among its central scores.

KOWA, while achieving lower average scores, demonstrates the most consistent performance with minimal variability. OWA, despite its lower scores, reveals the highest inequality in outcomes. This analysis suggests that while some methods can attain higher average scores, they may do so at the expense of consistency and equity. Further investigation into the specific contexts and criteria used for each method could provide valuable insights into the underlying causes of these performance differences. AHP emerges as the most effective method based on mean and median values, however, it also displays high variability, implying potential inconsistencies in results.

7.5.5 Disparity Analysis on Fusion Evaluations

Table 7.25 shows the results of disparity analysis fusion evaluations with Tukeys HSD Test to interpret the outcomes and their implications for the decision-making process. The test results reveal that the AHP group shows statistically significant mean differences when compared to all other groups, including KOWA, MAUT, OWA, and PROMETHEE. Specifically, the mean differences indicate that AHP scores significantly lower than KOWA with a mean difference of -0.6222 (p-adj = 0.0000). Similarly, AHP outperforms MAUT, with a mean difference of -0.6938 (p-adj = 0.0000).

The disparity is even more pronounced in the comparison between AHP and OWA, which shows a mean difference of -1.0456 (p-adj = 0.0000). Additionally, AHP is significantly lower than PROMETHEE, as evidenced by a mean difference of -0.6529 (p-adj = 0.0000). The comparison between OWA and PROMETHEE indicates a positive mean difference of 0.3928 (p-adj = 0.0000), suggesting that OWA significantly outperforms PROMETHEE.

In the comparisons involving KOWA, the results indicate its strong performance across different methodologies. Specifically, the comparison between KOWA and MAUT reveals a minimal mean difference of -0.0716 (p-adj = 0.4664), suggesting that these two groups perform similarly, which is indicative of KOWAs robustness. Similarly, the KOWA versus PROMETHEE comparison yields an even smaller mean difference of -0.0307 (p-adj = 0.9551), reinforcing the notion that KOWA is on par with PROMETHEE and exhibits minimal disparity.

Moreover, while the comparison between KOWA and OWA shows a significant mean difference of -0.4235 (p-adj = 0.0000), indicating that KOWA scores lower than OWA, this does not diminish KOWA overall effectiveness compared to other methods. In contrast, the analysis of MAUT versus OWA reveals a significant mean difference of -0.3519 (p-adj = 0.0000), illustrating that MAUT also underperforms relative to OWA.

These results position KOWA as the most balanced method, exhibiting the least mean differences with other approaches. This highlights KOWAs consistent performance in comparison to the AHP group, which shows marked underperformance. The findings suggest a hierarchy of effectiveness, with OWA generally leading, but KOWAs minimal differences establish it as a highly competitive alternative. These insights are crucial for strategic decision-making and further research, emphasizing the need to carefully consider the context of these methodologies.

Table 7.25: Tukeys HSD Test Results

group1	group2	meandiff	p-adj	lower	upper	reject
AHP	KOWA	-0.6222	0.0000	-0.7407	-0.5037	True
AHP	MAUT	-0.6938	0.0000	-0.8123	-0.5753	True
AHP	OWA	-1.0456	0.0000	-1.1641	-0.9271	True
AHP	PROMETHEE	-0.6529	0.0000	-0.7714	-0.5343	True
KOWA	MAUT	-0.0716	0.4664	-0.1901	0.0469	False
KOWA	OWA	-0.4235	0.0000	-0.5420	-0.3050	True
KOWA	PROMETHEE	-0.0307	0.9551	-0.1492	0.0878	False
MAUT	OWA	-0.3519	0.0000	-0.4704	-0.2334	True
MAUT	PROMETHEE	0.0409	0.8805	-0.0776	0.1594	False
OWA	PROMETHEE	0.3928	0.0000	0.2743	0.5113	True

7.5.6 Comparison Study

Figures 7.79 and 7.80 illustrate the distribution densities of expert evaluations and fusion evaluations, respectively. The analysis reveals that expert evaluations exhibit a sparse distribution characterized by considerable disparity among the evaluations. In contrast, fusion evaluations demonstrate a more concentrated Gaussian density. Notably, among the fusion evaluation methods, KOWA occupies a central position within the distribution range, exhibiting lower bias alongside higher consistency.

To further investigate the phenomenon of bias migration within the fusion evaluations, a detailed disparity test is presented in Figures 7.81 and 7.82. The results of these tests substantiate the findings regarding the relative performance of KOWA. Specifically, KOWA emerges as a significant contender when assessed against various other groups, highlighting its robustness and reliability within the evaluation framework. This analysis underscores the importance of examining the density and disparity of evaluations to better understand the implications for decision-making in expert and fusion contexts.

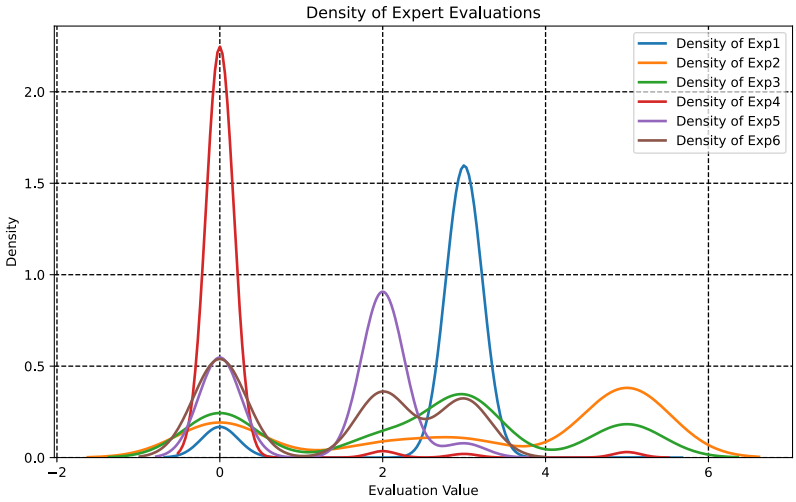

Figure 7.79: Density of Expert Evaluation

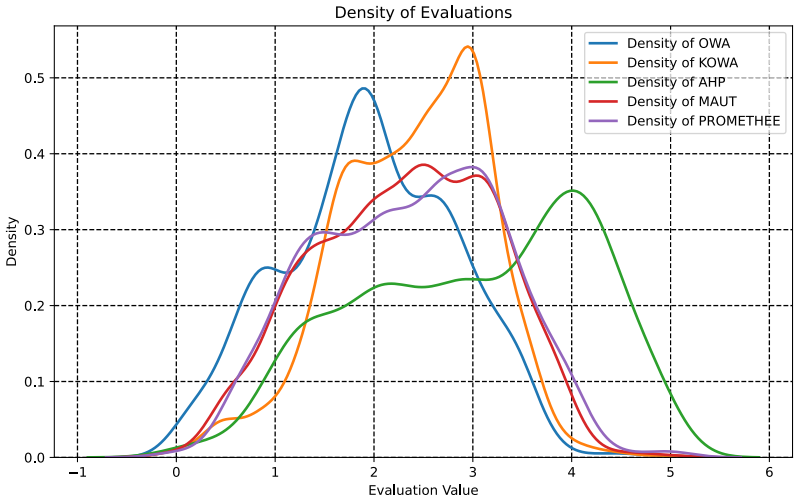

Figure 7.80: Density of Fusion Evaluation

As shown in Figure 7.82, KOWA has consistently shown favorable mean differences when compared to other groups. For instance, the comparison of KOWA vs. MAUT yields a mean difference of -0.0716 (not significant, p = 0.9724), while KOWA vs. OWA shows -0.4235 (significant, p = 0.0000) and KOWA vs. Exp5 results in 1.0508 (significant, p = 0.0000). These comparisons indicate that while KOWA is statistically comparable to MAUT, it performs significantly better than OWA and Exp5.

The p-values associated with KOWA comparisons are telling. For example, the p-

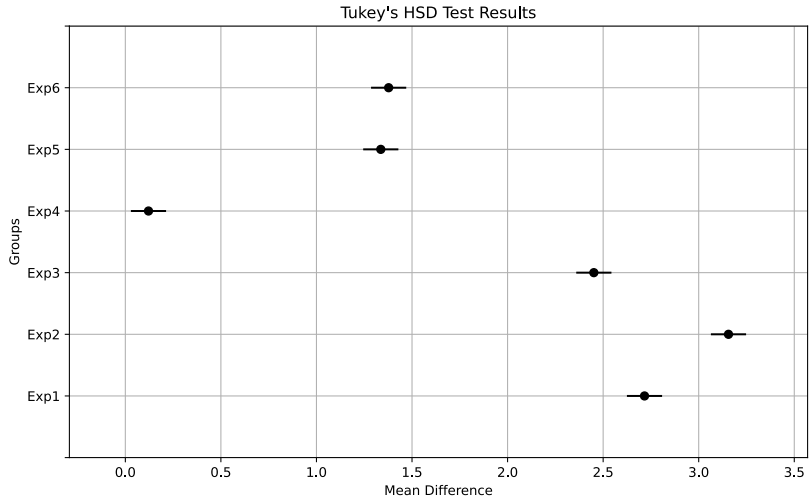

Figure 7.81: Tukeys HSD Test Results of Expert Evaluation

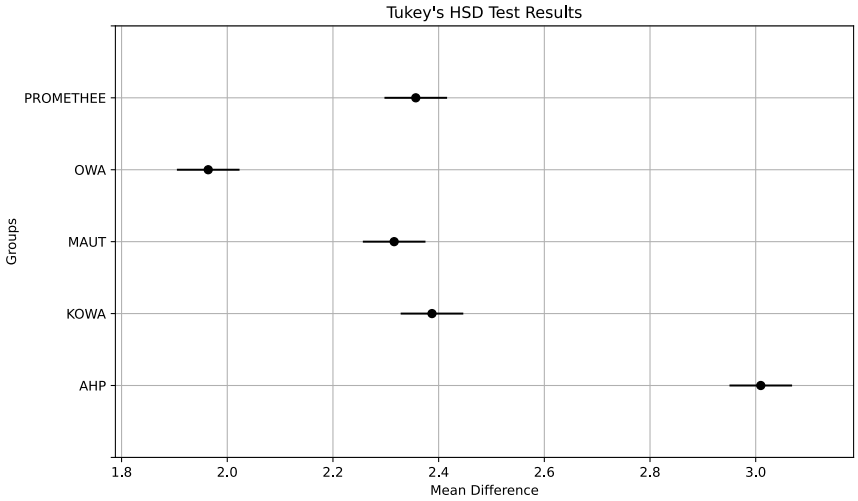

Figure 7.82: Tukeys HSD Test Results of Fusion Evaluation

values for KOWA against OWA and Exp5 are both 0.0000, indicating strong statistical significance. This suggests that KOWAs performance is superior to these groups with a high level of confidence.

The confidence intervals for KOWA mean differences further support its robustness. For KOWA vs. OWA, the interval (-0.6036, -0.2433) indicates a significant negative difference, reinforcing that KOWA outperforms OWA. In the case of KOWA vs. Exp5, the interval (0.8707, 1.2310) indicates a significant positive difference, suggesting KOWAs

superiority over Exp5.

In terms of practical implications, these findings suggest that KOWA approach is not only competitive but also versatile across different comparisons. This could make it an attractive option for various applications, from decision analysis to operational modeling. Given its strong performance metrics, adopting KOWA could lead to better outcomes in scenarios that require systematic and quantitative analysis. Its ability to produce significant results across various comparisons speaks to its strategic value.

It can be seen that KOWA stands out as a robust choice based on the comparative analysis of mean differences and significance levels. Its strong performance against competitors, combined with statistical backing, positions it as the best option in the provided dataset. This suggests that KOWA not only excels in theory but also holds practical advantages in application, making it a favorable model for decision-making processes.

7.5.7 Interpretation of Results

Determining the suitable method among OWA, KOWA, AHP, MAUT, and PROMETHEE is contingent on the criteria that are prioritized. A comparison of key metrics reveals distinct strengths and weaknesses among the methods.

In terms of average performance, AHP stands out with the highest mean (3.0096) and median (3.0761), suggesting it consistently outperforms the other methods. However, KOWA excels in producing consistent results, exhibiting the lowest variance and standard deviation. For contexts where consistency is paramount, KOWA may be the preferred choice.

On the other hand, the Gini coefficient indicates that OWA has the highest inequality in scores, which could be a disadvantage in scenarios where equitable outcomes are crucial. Additionally, AHPs high interquartile range points to significant variability within the central 50% of scores, raising concerns about its reliability in performance. For those prioritizing consistency and reliability, KOWA would be the more suitable option.

7.5.8 Discussion

In the case study, KOWA shows an effective aggregation of scores from six experts facilitates a more robust determination of overall investment value, mitigating individual biases and providing collective insights quantitatively. The findings of this study carry significant implications for investment strategies. By harnessing the varied perspectives

of experts, investors can attain a more nuanced understanding of potential investment opportunities. This successful mitigation of bias not only improves the precision of financial forecasts and risk assessments but also promotes greater stakeholder confidence in the decision-making process.

Moreover, the adaptive fusion ensures that the contributions of all experts are proportional to their reliability, fostering a more equitable aggregation process. This methodology not only improves the robustness of the resultant decision but also aligns the collective expert input with the strategic objectives of the organization.

The KOWA approach is notable for its adaptive weight adjustment mechanism, which responds to the dynamic contexts of expert judgments, effectively mitigating the challenges posed by divergent biases in multi-expert systems. By providing a comprehensive and mathematically rigorous framework for aggregating expert opinions, KOWA enhances decision quality in complex scenarios. Its integration of kappa statistics and ordered weighting principles positions it as a significant advancement in the field of multi-expert decision-making, offering a robust solution for improving the reliability of collective judgments.

CHAPTER 8

DISCUSSION AND CONCLUSION

8.1 Research Contributions

This thesis contributes to the fields of carbon finance and decision-making processes by integrating advanced computational methods and addressing the complexities of bias and disparity in decision support systems. The primary contributions are outlined as follows.

8.1.1 Development of an Integrated Carbon Dynamics Management System

This research presents a comprehensive framework for managing carbon dynamics that combines various disciplines such as economics, finance, and environmental science. The proposed system effectively integrates carbon emission modeling, sequestration analysis, and credit management, thereby providing a holistic approach to sustainable carbon finance. This contribution is significant as it addresses the pressing need for innovative solutions to climate change challenges through a structured and adaptive management system.

8.1.2 Innovative Decision Support Mechanisms

The thesis introduces the Multi-Level Adaptive Knowledge System (MLAKS), which employs knowledge-informed orchestration to enhance decision-making in carbon finance. By integrating various intelligence engines, including the Computing Intelligence Engine and Bias Fusion Engine, the framework allows for real-time adaptability and optimization of decisions based on dynamic data inputs. This innovation addresses existing gaps in decision support systems by providing a robust mechanism for dealing with uncertainties and biases inherent in data-driven environments.

8.1.3 Analytical Exploration of Bias and Disparity

A critical contribution of this thesis is the rigorous analysis of bias in machine intelligence, particularly in the context of false data and cognitive biases. The research elucidates how these biases affect decision-making processes and proposes methods such as adaptive kappa-ordered weight averaging to mitigate their impact. By exploring these themes, the thesis contributes to a deeper understanding of the psychological and technical challenges faced in decision-making frameworks, promoting more equitable and informed decision processes.

8.1.4 Application of Advanced Computational Techniques

The thesis effectively applies cutting-edge computational methodologies, such as transformed graph attention computing and Kolmogorov-Arnold representation, to the domain of carbon finance. These techniques enhance the analytical capabilities of the proposed systems, allowing for improved data representation and context-aware decision-making. This application is a significant step forward in utilizing machine learning and graph theory within environmental economics, illustrating the potential for interdisciplinary approaches to address complex global issues.

8.1.5 Empirical Validation through Case Studies

Empirical analyses presented in this thesis substantiate the theoretical frameworks developed. Through a series of case studies, the effectiveness of the proposed models and algorithms is demonstrated, providing real-world applicability to the theoretical constructs. This validation not only reinforces the contributions made but also highlights the practical implications for policymakers and practitioners in the field of carbon finance.

8.1.6 Framework for Future Research

Finally, this work lays a foundation for future research by identifying key areas where further investigation is warranted. The exploration of adaptive fusion techniques and their implications for risk detection and management presents a novel avenue for subsequent studies. By framing the challenges and solutions presented in this thesis, it invites ongoing discourse and exploration within the academic community and beyond.

8.1.7 Summary

The contributions of this thesis significantly advance the understanding of carbon finance and decision-making processes. By bridging theoretical insights with practical applications, this work not only addresses current challenges but also paves the way for innovative solutions in the face of climate change. The integration of advanced computational techniques with a keen awareness of bias and disparity enriches the discourse on sustainable decision support systems, ultimately fostering a more equitable approach to environmental and economic stewardship.

8.2 Answers to the Research Questions

To address the first challenge of data integration and aggregation, this study proposes a knowledge assembly method and mechanism tailored for machine learning applications. A system integration framework is designed, incorporating advanced super-feature assembly techniques under graph structures, time-series models, and dynamic mechanisms. The proposed framework enables seamless system integration, thereby supporting the decision-making process in the context of carbon finance.

In response to the second challenge of data scarcity, we introduce a mechanism-driven learning and expert system strategy based on multi-domain knowledge assembly. By constructing a knowledge base and implementing a rule engine, this approach utilizes existing experience and theoretical frameworks to provide reliable decision support even in the absence of sufficient data. This ensures that scientifically sound and reasonable decisions can still be made despite data limitations.

The third challenge, limited computing resources, is addressed through the integration of the Kolmogorov-Arnold Representation-based knowledge assembly computing framework with neural networks tailored for the carbon finance domain. This framework enables efficient learning and reasoning with reduced computational resources, shorter

processing times, and higher accuracy, thereby enhancing intelligent decision-making capabilities in resource-constrained environments.

For the fourth challenge of bias and decision consistency, we designed an adaptive decision fusion framework that utilizes statistical consistency as a key mechanism. By establishing an optimal decision fusion process, the framework ensures that decision-making results exhibit the highest possible consistency, even when different preferences and perspectives are involved in the decision process.

The intelligent knowledge reconstruction decision support system proposed in this study not only effectively addresses the challenges of data processing and knowledge reconstruction but also offers practical insights for the application of carbon finance in specific fields. This system provides significant theoretical contributions and technical pathways for the research, development, and future application of intelligent decision-making systems.

8.3 Limitations and Future Work

While this thesis has made significant strides in advancing the understanding of carbon finance and decision-making systems, several limitations and areas for future research merit consideration. Acknowledging these limitations provides a framework for continued exploration and innovation in this critical field.

8.3.1 Expanding Data Sources and Types

One limitation of the current study is the reliance on specific datasets, which may not fully capture the complexity and variability of carbon markets. Future research could focus on incorporating diverse data sources, including real-time environmental data, socio-economic indicators, and user-generated content. By leveraging big data analytics and IoT technologies, researchers can enhance the robustness of decision support systems and improve their predictive capabilities.

8.3.2 Enhancing Model Generalizability

The models developed in this thesis were primarily tailored to specific contexts within carbon finance. Future investigations could aim to generalize these models across different geographical regions and regulatory frameworks. This would involve testing

the adaptability of the proposed systems in varying market conditions and regulatory environments, thereby validating their effectiveness and versatility.

8.3.3 Integrating Stakeholder Perspectives

While this research has addressed technical and analytical dimensions, the incorporation of stakeholder perspectives remains an area for improvement. Future work should emphasize qualitative research methodologies, such as interviews and focus groups, to capture the insights of various stakeholders involved in carbon finance, including policymakers, investors, and community representatives. This holistic approach would enrich the understanding of biases and disparities in decision-making processes, leading to more inclusive and effective solutions.

8.3.4 Exploring Behavioral Aspects of Decision-Making

Another avenue for future research is the exploration of behavioral economics within the context of carbon finance. Understanding how cognitive biases influence decision-making can inform the design of interventions aimed at promoting sustainable practices. Incorporating behavioral insights into decision support systems can enhance their effectiveness by aligning technological solutions with human behavior.

8.3.5 Investigating Advanced Computational Techniques

The thesis has introduced several advanced computational methodologies, such as transformed graph attention computing and Kolmogorov-Arnold representation. Future research could delve deeper into the development and optimization of these techniques, exploring their applications beyond carbon finance. Investigating their potential in other interdisciplinary contexts could yield valuable insights and innovations that transcend traditional boundaries.

8.3.6 Addressing Ethical and Regulatory Implications

As the field of carbon finance continues to evolve, it is essential to consider the ethical and regulatory implications of emerging technologies and methodologies. Future research should address questions of accountability, transparency, and fairness in automated decision-making processes. Developing frameworks that align technological advance-

ments with ethical standards will be crucial in ensuring that decision support systems contribute positively to societal and environmental goals.

8.3.7 Longitudinal Studies and Impact Assessment

Finally, conducting longitudinal studies to assess the long-term impacts of the proposed systems on carbon finance and environmental sustainability is vital. Such studies would provide empirical evidence on the effectiveness of decision support mechanisms over time, allowing for continuous improvement and adaptation of strategies in response to changing conditions.

8.3.8 Summary

While this thesis contributes significantly to the understanding and management of carbon dynamics and decision-making processes, it also opens numerous avenues for future research. By addressing the identified limitations and pursuing these research directions, scholars can further enhance the field of carbon finance, leading to more effective and equitable solutions in the fight against climate change. The ongoing evolution of technologies and methodologies presents an exciting opportunity for future inquiry, with the potential to transform both academic and practical approaches to sustainable development.

BIBLIOGRAPHY

[1] A. ABADIE, S. CHOWDHURY, S. K. MANGLA, AND S. MALIK, *Impact of carbon offset perceptions on greenwashing: Revealing intentions and strategies through an experimental approach*, Industrial Marketing Management, 117 (2024), pp. 304–320.

[2] A. ABELS, T. LENAERTS, V. TRIANNI, AND A. NOWÉ, *Dealing with expert bias in collective decision-making*, Artificial Intelligence, 320 (2023), p. 103921.

[3] Y. ACHDOU AND O. PIRONNEAU, *Computational methods for option pricing*, SIAM, 2005.

[4] J. ADAMKIEWICZ, E. KOCHAŃSKA, I. ADAMKIEWICZ, AND R. M. ŁUKASIK, *Greenwashing and sustainable fashion industry*, Current Opinion in Green and Sustainable Chemistry, 38 (2022), p. 100710.

[5] S. ADHIKARI, E. MOON, J. PAZ-FERREIRO, AND W. TIMMS, *Comparative analysis of biochar carbon stability methods and implications for carbon credits*, Science of the Total Environment, 914 (2024), p. 169607.

[6] F. M. ALOTAIBI AND V. G. VASSILAKIS, *Toward an sdn-based web application firewall: Defending against sql injection attacks*, Future Internet, 15 (2023), p. 170.

[7] N. ALSHATRI AND F. K. HUSSAIN, *Data driven approach of external factors influencing carbon credit prices: A systematic literature review*, Available at SSRN 4602609, (2024).

[8] N. ALSHATRI, L. ISMAIL, AND F. K. HUSSAIN, *A systematic review of the external influence factors in multifactor analysis and the prediction of carbon credit prices*, in International Conference on Complex, Intelligent, and Software Intensive Systems, Springer, 2024, pp. 1–13.

[9] E. I. ALTMAN AND H. A. RIJKEN, *The added value of rating outlooks and rating reviews to corporate bond ratings*, in financial management association meeting, Barcelona, 2007.

[10] N. AMELI, P. DRUMMOND, A. BISARO, M. GRUBB, AND H. CHENET, *Climate finance and disclosure for institutional investors: why transparency is not enough*, Climatic Change, 160 (2020), pp. 565–589.

[11] S. AN, B. LI, D. SONG, AND X. CHEN, *Green credit financing versus trade credit financing in a supply chain with carbon emission limits*, European Journal of Operational Research, 292 (2021), pp. 125–142.

[12] K. ANAND, B. CRAIG, AND G. VON PETER, *Filling in the blanks: Network structure and interbank contagion*, Quantitative Finance, 15 (2015), pp. 625–636.

[13] S. ANAND AND K. MISHRA, *Identifying potential millennial customers for financial institutions using svm*, Journal of Financial Services Marketing, (2022), pp. 1–11.

[14] E. ANGELINI, G. DI TOLLO, AND A. ROLI, *A neural network approach for credit risk evaluation*, The quarterly review of economics and finance, 48 (2008), pp. 733–755.

[15] S. ANGILELLA AND S. MAZZÙ, *The financing of innovative smes: A multicriteria credit rating model*, European Journal of Operational Research, 244 (2015), pp. 540–554.

[16] J. R. ARONSON AND J. R. MARSDEN, *Duplicating moody's municipal credit ratings*, Public Finance Quarterly, 8 (1980), pp. 97–106.

[17] M. ASADNABIZADEH AND E. MOE, *A review of global carbon markets from kyoto to paris and beyond: The persistent failure of implementation*, Frontiers in Environmental Science, 12 (2024), p. 1368105.

[18] Y. BAI, T. CHAOLU, AND S. BILIGE, *The application of improved physics-informed neural network (ipinn) method in finance*, Nonlinear Dynamics, 107 (2022), pp. 3655–3667.

[19] G. BAKSHI, C. CAO, AND Z. CHEN, *Empirical performance of alternative option pricing models*, The Journal of finance, 52 (1997), pp. 2003–2049.

[20] S. BANSAL, M. MUKHOPADHYAY, AND S. MAURYA, *Strategic drivers for sustainable implementation of carbon trading in india*, Environment, Development and Sustainability, 25 (2023), pp. 4411–4435.

[21] W. BAO AND Q. ZHAO, *A structure-preserving parametric finite element method for surface diffusion*, SIAM Journal on Numerical Analysis, 59 (2021), pp. 2775–2799.

[22] S. BAROUMAND, A. ZAMAN, AND L. MIHAYLOVA, *Attack detection and fault-tolerant control of interconnected cyber-physical systems against simultaneous replayed time-delay and false-data injection attacks*, IET Control Theory & Applications, 17 (2023), pp. 527–541.

[23] N. BASHIR, D. IRWIN, AND P. SHENOY, *On the promise and pitfalls of optimizing embodied carbon*, ACM SIGENERGY Energy Informatics Review, 4 (2024), pp. 94–99.

[24] D. S. BATES, *20 testing option pricing models*, Handbook of statistics, 14 (1996), pp. 567–611.

[25] R. BAUER, K. GÖDKER, P. SMEETS, AND F. ZIMMERMANN, *Mental models in financial markets: How do experts reason about the pricing of climate risk?*, European Corporate Governance Institute–Finance Working Paper, (2024).

[26] M. BEHZADIAN, R. B. KAZEMZADEH, A. ALBADVI, AND M. AGHDASI, *Promethee: A comprehensive literature review on methodologies and applications*, European journal of Operational research, 200 (2010), pp. 198–215.

[27] Y. Z. BERGMAN, B. D. GRUNDY, AND Z. WIENER, *Theory of Rational Option Pricing: II*, Rodney L. White Center for Financial Research, 1995.

[28] J. BERNARDO, J. BERGER, A. DAWID, A. SMITH, ET AL., *Regression and classification using gaussian process priors*, Bayesian statistics, 6 (1998), p. 475.

[29] V. BERTHET, *The impact of cognitive biases on professionals‚Äô decision-making: A review of four occupational areas*, Frontiers in psychology, 12 (2022), p. 802439.

[30] H. BI AND T. D. ABHAYAPALA, *Point neuron learning: A new physics-informed neural network architecture*, arXiv preprint arXiv:2408.16969, (2024).

[31] C. M. BISHOP, *Training with noise is equivalent to tikhonov regularization*, Neural computation, 7 (1995), pp. 108–116.

[32] F. BLACK AND M. SCHOLES, *The pricing of options and corporate liabilities*, Journal of political economy, 81 (1973), pp. 637–654.

[33] S. BLANC, C. ACCASTELLO, E. BIANCHI, F. LINGUA, G. VACCHIANO, A. MOSSO, AND F. BRUN, *An integrated approach to assess carbon credit from improved forest management*, Journal of Sustainable Forestry, 38 (2019), pp. 31–45.

[34] S. BOCK, J. GOPPOLD, AND M. WEISS, *An improvement of the convergence proof of the adam-optimizer*, arXiv preprint arXiv:1804.10587, (2018).

[35] M. BOLDERMAN, D. FAN, M. LAZAR, AND H. BUTLER, *Generalized feedforward control using physics,Äîinformed neural networks*, IFAC-PapersOnLine, 55 (2022), pp. 148–153.

[36] M. BOSS, H. ELSINGER, M. SUMMER, AND S. THURNER 4, *Network topology of the interbank market*, Quantitative finance, 4 (2004), pp. 677–684.

[37] J.-P. BRANS, P. VINCKE, AND B. MARESCHAL, *How to select and how to rank projects: The promethee method*, European journal of operational research, 24 (1986), pp. 228–238.

[38] J. S. BUTLER AND B. SCHACHTER, *Unbiased estimation of the black/scholes formula*, Journal of Financial Economics, 15 (1986), pp. 341–357.

[39] S. CAI AND J. ZHANG, *Exploration of credit risk of p2p platform based on data mining technology*, Journal of Computational and Applied Mathematics, 372 (2020), p. 112718.

[40] D. CHAKRABORTY, H. BAŞAĞAOĞLU, AND J. WINTERLE, *Interpretable vs. non-interpretable machine learning models for data-driven hydro-climatological process modeling*, Expert Systems with Applications, 170 (2021), p. 114498.

[41] S. CHAKRABORTY, R. TOMSETT, R. RAGHAVENDRA, D. HARBORNE, M. ALZANTOT, F. CERUTTI, M. SRIVASTAVA, A. PREECE, S. JULIER, R. M. RAO, ET AL., *Interpretability of deep learning models: A survey of results*, in 2017 IEEE smartworld, ubiquitous intelligence & computing, advanced & trusted computed, scalable computing & communications, cloud & big data computing, Internet

of people and smart city innovation (smartworld/SCALCOM/UIC/ATC/CBDcom/IOP/SCI), IEEE, 2017, pp. 1–6.

[42] C.-C. CHEN AND S.-T. LI, *Credit rating with a monotonicity-constrained support vector machine model*, Expert Systems with Applications, 41 (2014), pp. 7235–7247.

[43] H. CHEN, H. WU, T. KAN, J. ZHANG, AND H. LI, *Low-carbon economic dispatch of integrated energy system containing electric hydrogen production based on vmd-gru short-term wind power prediction*, International Journal of Electrical Power & Energy Systems, 154 (2023), p. 109420.

[44] Y. CHENG, N. ZHANG, Y. WANG, J. YANG, C. KANG, AND Q. XIA, *Modeling carbon emission flow in multiple energy systems*, IEEE Transactions on Smart Grid, 10 (2018), pp. 3562–3574.

[45] V. CHERIAN AND M. BINDU, *Heart disease prediction using naive bayes algorithm and laplace smoothing technique*, Int. J. Comput. Sci. Trends Technol, 5 (2017), pp. 68–73.

[46] G. CIMINI AND M. SERRI, *Entangling credit and funding shocks in interbank markets*, PloS one, 11 (2016), p. e0161642.

[47] M. COLLINS, R. E. SCHAPIRE, AND Y. SINGER, *Logistic regression, adaboost and bregman distances*, Machine Learning, 48 (2002), pp. 253–285.

[48] T. CONG, X. HE, Y. SHEN, AND Y. ZHANG, *Test-time poisoning attacks against test-time adaptation models*, in 2024 IEEE Symposium on Security and Privacy (SP), IEEE, 2024, pp. 1306–1324.

[49] C. A. D. CUADRO, M. C. VANZULLI, AND P. A. GALIONE, *Exploring the capability of pinns for solving material identification problems*, Mecánica Computacional, 40 (2023), pp. 1183–1194.

[50] S. CUOMO, V. S. DI COLA, F. GIAMPAOLO, G. ROZZA, M. RAISSI, AND F. PICCIALLI, *Scientific machine learning through physics–informed neural networks: Where we are and what,Äôs next*, Journal of Scientific Computing, 92 (2022), p. 88.

[51] R. A. DA CUNHA, L. A. D. RANGEL, C. A. RUDOLF, AND L. DOS SANTOS, *A decision support approach employing the promethee method and risk factors for critical supply assessment in large-scale projects*, Operations Research Perspectives, 9 (2022), p. 100238.

[52] J. DAI, J. YANG, Y. WANG, AND Y. XU, *Blockchain-enabled cyber-resilience enhancement framework of microgrid distributed secondary control against false data injection attacks*, IEEE Transactions on Smart Grid, 15 (2023), pp. 2226–2236.

[53] P. DELACOTE, T. L,ÄôHORTY, A. KONTOLEON, T. A. WEST, A. CRETI, B. FILEWOD, G. LEVELLY, A. GUIZAR-COUTIÑO, B. GROOM, AND M. ELIAS, *Strong transparency required for carbon credit mechanisms*, Nature Sustainability, (2024), pp. 1–8.

[54] N. J. DELANEY AND S. CHATTERJEE, *Use of the bootstrap and cross-validation in ridge regression*, Journal of Business & Economic Statistics, 4 (1986), pp. 255–262.

[55] D. DEMEKAS AND P. GRIPPA, *Walking a tightrope: Financial regulation, climate change, and the transition to a low-carbon economy*, Journal of financial regulation, 8 (2022), pp. 203–229.

[56] S. DEMIRALAY, H. G. GENCER, AND S. BAYRACI, *Carbon credit futures as an emerging asset: Hedging, diversification and downside risks*, Energy Economics, 113 (2022), p. 106196.

[57] S. DENG, C. WANG, M. WANG, AND Z. SUN, *A gradient boosting decision tree approach for insider trading identification: An empirical model evaluation of china stock market*, Applied Soft Computing, 83 (2019), p. 105652.

[58] A. DHIMAN AND Y. HU, *Physics informed neural network for option pricing*, arXiv preprint arXiv:2312.06711, (2023).

[59] V. B. DJEUNDJE, J. CROOK, R. CALABRESE, AND M. HAMID, *Enhancing credit scoring with alternative data*, Expert Systems with Applications, 163 (2021), p. 113766.

[60] G. DONG, L. LIANG, L. WEI, J. XIE, AND G. YANG, *Optimization model of trade credit and asset-based securitization financing in carbon emission reduction supply chain*, Annals of Operations Research, (2023), pp. 1–50.

[61] P. DORAISWAMY, G. MCCARTY, E. HUNT JR, R. YOST, M. DOUMBIA, AND A. FRANZLUEBBERS, *Modeling soil carbon sequestration in agricultural lands of mali*, Agricultural Systems, 94 (2007), pp. 63–74.

[62] H. DU, Z. ZHAO, H. CHENG, J. YAN, AND Q. HE, *Modeling density-driven flow in porous media by physics-informed neural networks for co2 sequestration*, Computers and Geotechnics, 159 (2023), p. 105433.

[63] Y. Y. DUMAS, *Carbon credit incentives for agroforestry*.

[64] G. DZIUK AND C. M. ELLIOTT, *Finite element methods for surface pdes*, Acta Numerica, 22 (2013), pp. 289–396.

[65] B. ENKE, U. GNEEZY, B. HALL, D. MARTIN, V. NELIDOV, T. OFFERMAN, AND J. VAN DE VEN, *Cognitive biases: Mistakes or missing stakes?*, Review of Economics and Statistics, 105 (2023), pp. 818–832.

[66] L. FEDI, *The monitoring, reporting and verification of ships‚Äô carbon dioxide emissions: A european substantial policy measure towards accurate and transparent carbon dioxide quantification*, Ocean Yearbook Online, 31 (2017), pp. 381–417.

[67] M. FERRARA, T. CIANO, C. R. NAVA, AND L. CANANÀ, *Multi-criteria decision analysis: Hesitant fuzzy methodology towards expert systems for analyzing financial markets dynamics*, Soft Computing, (2023), pp. 1–16.

[68] J. D. FINNERTY, C. D. MILLER, AND R.-R. CHEN, *The impact of credit rating announcements on credit default swap spreads*, Journal of Banking & Finance, 37 (2013), pp. 2011–2030.

[69] M. P. FITZGERALD, K. RUSSO DONOVAN, J. KEES, AND J. KOZUP, *How confusion impacts product labeling perceptions*, Journal of Consumer Marketing, 36 (2019), pp. 306–316.

[70] M. FLORES-SOSA, E. AVILÉS-OCHOA, J. M. MERIGÓ, AND J. KACPRZYK, *The owa operator in multiple linear regression*, Applied Soft Computing, 124 (2022), p. 108985.

[71] J. H. FRIEDMAN AND J. J. MEULMAN, *Multiple additive regression trees with application in epidemiology*, Statistics in medicine, 22 (2003), pp. 1365–1381.

[72] I. FURSOV, M. MOROZOV, N. KAPLOUKHAYA, E. KOVTUN, R. RIVERA-CASTRO, G. GUSEV, D. BABAEV, I. KIREEV, A. ZAYTSEV, AND E. BURNAEV, *Adversarial attacks on deep models for financial transaction records*, in Proceedings of the 27th ACM SIGKDD Conference on Knowledge Discovery & Data Mining, 2021, pp. 2868–2878.

[73] D. GALAI AND R. W. MASULIS, *The option pricing model and the risk factor of stock*, Journal of Financial economics, 3 (1976), pp. 53–81.

[74] H. GAO, X. WANG, K. WU, Y. ZHENG, Q. WANG, W. SHI, AND M. HE, *A review of building carbon emission accounting and prediction models*, Buildings, 13 (2023), p. 1617.

[75] Y. GAO, Y. LI, L. ZHU, D. WU, Y. JIANG, AND S.-T. XIA, *Not all samples are born equal: Towards effective clean-label backdoor attacks*, Pattern Recognition, 139 (2023), p. 109512.

[76] F. GATTA, V. S. DI COLA, F. GIAMPAOLO, F. PICCIALLI, AND S. CUOMO, *Meshless methods for american option pricing through physics-informed neural networks*, Engineering Analysis with Boundary Elements, 151 (2023), pp. 68–82.

[77] A. GILBERT-SAAD, F. SIEDLOK, AND R. B. MCNAUGHTON, *Decision and design heuristics in the context of entrepreneurial uncertainties*, Journal of Business Venturing Insights, 9 (2018), pp. 75–80.

[78] S. M. GLOVER, M. H. TAYLOR, Y.-J. WU, AND K. T. TROTMAN, *Mind the gap: Why do experts have differences of opinion regarding the sufficiency of audit evidence supporting complex fair value measurements?*, Contemporary Accounting Research, 36 (2019), pp. 1417–1460.

[79] M. S. GOCKENBACH, *Understanding and implementing the finite element method*, SIAM, 2006.

[80] P. GOLBAYANI, I. FLORESCU, AND R. CHATTERJEE, *A comparative study of forecasting corporate credit ratings using neural networks, support vector machines, and decision trees*, The North American Journal of Economics and Finance, 54 (2020), p. 101251.

[81] M. GOLDBLUM, A. SCHWARZSCHILD, A. PATEL, AND T. GOLDSTEIN, *Adversarial attacks on machine learning systems for high-frequency trading*, in Proceedings of the Second ACM International Conference on AI in Finance, 2021, pp. 1–9.

[82] G. H. GOLUB, P. C. HANSEN, AND D. P. O'LEARY, *Tikhonov regularization and total least squares*, SIAM journal on matrix analysis and applications, 21 (1999), pp. 185–194.

[83] J. W. GOODELL, C. GURDGIEV, S. KARIM, AND A. PALMA, *Carbon emissions and liquidity management*, International Review of Financial Analysis, 95 (2024), p. 103367.

[84] L. H. GOULDER, *Timing is everything: how economists can better address the urgency of stronger climate policy*, Review of Environmental Economics and Policy, (2020).

[85] S. GRAY, A. CHAN, D. CLARK, AND R. JORDAN, *Modeling the integration of stakeholder knowledge in social–ecological decision-making: Benefits and limitations to knowledge diversity*, Ecological Modelling, 229 (2012), pp. 88–96.

[86] M. GREGOR AND B. MICHAELI, *Board bias, information, and investment efficiency*, Review of Accounting Studies, (2024), pp. 1–31.

[87] P. GROHS, F. HORNUNG, A. JENTZEN, AND P. VON WURSTEMBERGER, *A proof that artificial neural networks overcome the curse of dimensionality in the numerical approximation of Black–Scholes partial differential equations*, vol. 284, American Mathematical Society, 2023.

[88] T. G. GROSSMANN, U. J. KOMOROWSKA, J. LATZ, AND C.-B. SCHÖNLIEB, *Can physics-informed neural networks beat the finite element method?*, IMA Journal of Applied Mathematics, (2024), p. hxae011.

[89] J. GU, B. YANG, M. BRAUER, AND K. M. ZHANG, *Enhancing the evaluation and interpretability of data-driven air quality models*, Atmospheric Environment, 246 (2021), p. 118125.

[90] F. K. GÜNDOĞDU, S. DULEBA, S. MOSLEM, AND S. AYDIN, *Evaluating public transport service quality using picture fuzzy analytic hierarchy process and linear assignment model*, Applied Soft Computing, 100 (2021), p. 106920.

[91] K. GURNEY, *An introduction to neural networks*, CRC press, 2018.

[92] R. HAFEZ AND Y. YOUSSRI, *Review on jacobi-galerkin spectral method for linear pdes in applied mathematics*, Contemporary Mathematics, (2024), pp. 2051–2088.

[93] D. HAINAUT, *Valuation of guaranteed minimum accumulation benefits (gmabs) with physics-inspired neural networks*, Annals of Actuarial Science, (2024), pp. 1–32.

[94] D. HAINAUT AND A. CASAS, *Option pricing in the heston model with physics inspired neural networks*, tech. rep., 2024.

[95] P. HÁJEK, *Credit rating analysis using adaptive fuzzy rule-based systems: an industry-specific approach*, Central European Journal of Operations Research, 20 (2012), pp. 421–434.

[96] D. T. HAMILTON AND R. CANTOR, *Rating transition and default rates conditioned on outlooks*, The Journal of Fixed Income, 14 (2004), pp. 54–70.

[97] P. L. HAMMER, A. KOGAN, AND M. A. LEJEUNE, *A logical analysis of banks‚Äô financial strength ratings*, Expert Systems with Applications, 39 (2012), pp. 7808–7821.

[98] K. HAN, S. HONG, J. H. CHEON, AND D. PARK, *Logistic regression on homomorphic encrypted data at scale*, in Proceedings of the AAAI Conference on Artificial Intelligence, vol. 33, 2019, pp. 9466–9471.

[99] B. B. HAZARIKA, D. GUPTA, AND P. BORAH, *An intuitionistic fuzzy kernel ridge regression classifier for binary classification*, Applied Soft Computing, 112 (2021), p. 107816.

[100] P. HENDERSON, J. HU, J. ROMOFF, E. BRUNSKILL, D. JURAFSKY, AND J. PINEAU, *Towards the systematic reporting of the energy and carbon footprints of machine learning*, Journal of Machine Learning Research, 21 (2020), pp. 1–43.

[101] R. HIRK, K. HORNIK, AND L. VANA, *Multivariate ordinal regression models: an analysis of corporate credit ratings*, Statistical Methods & Applications, 28 (2019), pp. 507–539.

[102] M. HOU, H. FU, Z. HU, J. WANG, Y. CHEN, AND Y. YANG, *Numerical solving of generalized black-scholes differential equation using deep learning based on blocked residual connection*, Digital Signal Processing, 126 (2022), p. 103498.

[103] T. HOWLEY AND M. G. MADDEN, *The genetic kernel support vector machine: Description and evaluation*, Artificial intelligence review, 24 (2005), pp. 379–395.

[104] K. HU AND Y. CHEN, *Equilibrium fuel supply and carbon credit pricing under market competition and environmental regulations: A california case study*, Applied Energy, 236 (2019), pp. 815–824.

[105] Z. HU, K. SHUKLA, G. E. KARNIADAKIS, AND K. KAWAGUCHI, *Tackling the curse of dimensionality with physics-informed neural networks*, Neural Networks, 176 (2024), p. 106369.

[106] S.-C. HUANG, *Using gaussian process based kernel classifiers for credit rating forecasting*, Expert Systems with Applications, 38 (2011), pp. 8607–8611.

[107] X. HUANG, X. LIU, AND Y. REN, *Enterprise credit risk evaluation based on neural network algorithm*, Cognitive Systems Research, 52 (2018), pp. 317–324.

[108] Y. HUANG, Z. ZHANG, AND X. ZHANG, *A direct-forcing immersed boundary method for incompressible flows based on physics-informed neural network*, Fluids, 7 (2022), p. 56.

[109] Z. HUANG, H. CHEN, C.-J. HSU, W.-H. CHEN, AND S. WU, *Credit rating analysis with support vector machines and neural networks: a market comparative study*, Decision support systems, 37 (2004), pp. 543–558.

[110] D. HUISINGH, Z. ZHANG, J. C. MOORE, Q. QIAO, AND Q. LI, *Recent advances in carbon emissions reduction: policies, technologies, monitoring, assessment and modeling*, Journal of cleaner production, 103 (2015), pp. 1–12.

[111] M. HUTZENTHALER, A. JENTZEN, T. KRUSE, T. ANH NGUYEN, AND P. VON WURSTEMBERGER, *Overcoming the curse of dimensionality in the numerical approximation of semilinear parabolic partial differential equations*, Proceedings of the Royal Society A, 476 (2020), p. 20190630.

[112] A. Q. IBRAHIM, S. GÖTSCHEL, AND D. RUPRECHT, *Parareal with a physics-informed neural network as coarse propagator*, in European Conference on Parallel Processing, Springer, 2023, pp. 649–663.

[113] S. JADHAV, H. HE, AND K. JENKINS, *Information gain directed genetic algorithm wrapper feature selection for credit rating*, Applied Soft Computing, 69 (2018), pp. 541–553.

[114] R. JHA, J. HAYASE, AND S. OH, *Label poisoning is all you need*, Advances in Neural Information Processing Systems, 36 (2023), pp. 71029–71052.

[115] L. JIANG, S. WANG, C. LI, AND L. ZHANG, *Structure extended multinomial naive bayes*, Information Sciences, 329 (2016), pp. 346–356.

[116] A. M. KARMINSKY AND E. KHROMOVA, *Modelling banks,Äô credit ratings of international agencies*, Eurasian Economic Review, 6 (2016), pp. 341–363.

[117] G. E. KARNIADAKIS, I. G. KEVREKIDIS, L. LU, P. PERDIKARIS, S. WANG, AND L. YANG, *Physics-informed machine learning*, Nature Reviews Physics, 3 (2021), pp. 422–440.

[118] V. KESWANI, M. LEASE, AND K. KENTHAPADI, *Towards unbiased and accurate deferral to multiple experts*, in Proceedings of the 2021 AAAI/ACM Conference on AI, Ethics, and Society, 2021, pp. 154–165.

[119] S. Y. KIM AND M. PANDELAERE, *Lay beliefs of the ethical decision quality advantage for diverse groups*, in Academy of Management Proceedings, vol. 2024, Academy of Management Valhalla, NY 10595, 2024, p. 12776.

[120] T. N. KIPF AND M. WELLING, *Semi-supervised classification with graph convolutional networks*, arXiv preprint arXiv:1609.02907, (2016).

[121] T. KLIEGR, Š. BAHNÍK, AND J. FÜRNKRANZ, *A review of possible effects of cognitive biases on interpretation of rule-based machine learning models*, Artificial Intelligence, 295 (2021), p. 103458.

[122] S. KODAMA, *A version of kolmogorov-arnold representation theorem for differentiable functions of several variables*, Journal of Nonlinear Analysis and Optimization: Theory & Applications (JNAO), 2 (2011), pp. 253–257.

[123] X.-Y. KONG AND G.-H. YANG, *An intrusion detection method based on self-generated coding technology for stealthy false data injection attacks in train-ground communication systems*, IEEE Transactions on Industrial Electronics, 70 (2022), pp. 8468–8476.

[124] M. KÖPPEN, *The curse of dimensionality*, in 5th online world conference on soft computing in industrial applications (WSC5), vol. 1, 2000, pp. 4–8.

[125] F. N. KOUTANAEI, H. SAJEDI, AND M. KHANBABAEI, *A hybrid data mining model of feature selection algorithms and ensemble learning classifiers for credit scoring*, Journal of Retailing and Consumer Services, 27 (2015), pp. 11–23.

[126] N. KREIBICH AND L. HERMWILLE, *Caught in between: credibility and feasibility of the voluntary carbon market post-2020*, Climate Policy, 21 (2021), pp. 939–957.

[127] H. KUMAR AND N. YADAV, *Deep learning algorithms for solving differential equations: a survey*, Journal of Experimental & Theoretical Artificial Intelligence, (2023), pp. 1–40.

[128] K. KUNISCH AND D. WALTER, *Semiglobal optimal feedback stabilization of autonomous systems via deep neural network approximation*, ESAIM: Control, Optimisation and Calculus of Variations, 27 (2021), p. 16.

[129] L. LANGFELDT, *Decision-making in expert panels evaluating research: Constraints, processes and bias*, NIFU, 2002.

[130] B. LAUTERBACH AND P. SCHULTZ, *Pricing warrants: an empirical study of the black-scholes model and its alternatives*, The Journal of Finance, 45 (1990), pp. 1181–1209.

[131] C.-C. LEE, X. LI, C.-H. YU, AND J. ZHAO, *The contribution of climate finance toward environmental sustainability: New global evidence*, Energy Economics, 111 (2022), p. 106072.

[132] Y.-C. LEE, *Application of support vector machines to corporate credit rating prediction*, Expert Systems with Applications, 33 (2007), pp. 67–74.

[133] D. LI, W. E. WONG, W. WANG, Y. YAO, AND M. CHAU, *Detection and mitigation of label-flipping attacks in federated learning systems with kpca and k-means*, in 2021 8th International Conference on Dependable Systems and Their Applications (DSA), IEEE, 2021, pp. 551–559.

[134] X. LI, F. LIN, H. WANG, X. ZHANG, H. MA, C. WEN, AND F. BLAABJERG, *Temporal modeling for power converters with physics-in-architecture recurrent neural network*, IEEE Transactions on Industrial Electronics, (2024).

[135] Y. LI, H. CHEN, S. XU, Y. GE, J. TAN, S. LIU, AND Y. ZHANG, *Fairness in recommendation: Foundations, methods, and applications*, ACM Transactions on Intelligent Systems and Technology, 14 (2023), pp. 1–48.

[136] Y. LI, Y. JIANG, Z. LI, AND S.-T. XIA, *Backdoor learning: A survey*, IEEE transactions on neural networks and learning systems, 35 (2022), pp. 5–22.

[137] Y. LI, X. LI, D. MA, AND W. GONG, *Exploring green building certification credit selection: A model based on explainable machine learning*, Journal of Building Engineering, 95 (2024), p. 110279.

[138] Y. LI, S. V. UKKUSURI, AND J. FAN, *Managing congestion and emissions in transportation networks with dynamic carbon credit charge scheme*, Computers & Operations Research, 99 (2018), pp. 90–108.

[139] P. P. LIANG, C. WU, L.-P. MORENCY, AND R. SALAKHUTDINOV, *Towards understanding and mitigating social biases in language models*, in International Conference on Machine Learning, PMLR, 2021, pp. 6565–6576.

[140] A. LIAW, M. WIENER, ET AL., *Classification and regression by randomforest*, R news, 2 (2002), pp. 18–22.

[141] C. Z. LIU, K. CAO, Y. ZHANG, AND L. QIN, *Adaptive bias fusion using kappa-ordered weight to address multi-expert disparity*, in 2025 IEEE 20th Conference on Industrial Electronics and Applications (ICIEA), IEEE, 2025, pp. 1–6.

[142] C. Z. LIU, D. CHENG, Y. ZHANG, AND L. QIN, *Adversarial backdoor attacks on machine learning with covert false data injection-part a: Modeling*, in 2025 IEEE 20th Conference on Industrial Electronics and Applications (ICIEA), IEEE, 2025, pp. 1–6.

[143] C. Z. LIU, S. XIANG, D. CHENG, J. LIU, Y. ZHANG, AND L. QIN, *Transformed graph attention for credit rating*, in 2023 IEEE 18th Conference on Industrial Electronics and Applications (ICIEA), IEEE, 2023, pp. 1011–1016.

[144] H. LIU, Z. LIU, C. ZHANG, AND T. LI, *Transformational insurance and green credit incentive policies as financial mechanisms for green energy transitions and low-carbon economic development*, Energy Economics, 126 (2023), p. 107016.

[145] H. LIU AND L. SHEN, *Forecasting carbon price using empirical wavelet transform and gated recurrent unit neural network*, Carbon Management, 11 (2020), pp. 25–37.

[146] S. LIU AND E. DOBRIBAN, *Ridge regression: Structure, cross-validation, and sketching*, arXiv preprint arXiv:1910.02373, (2019).

[147] Y. LIU, L. TIAN, H. SUN, X. ZHANG, AND C. KONG, *Option pricing of carbon asset and its application in digital decision-making of carbon asset*, Applied Energy, 310 (2022), p. 118375.

[148] Z. LIU, Y. WANG, S. VAIDYA, F. RUEHLE, J. HALVERSON, M. SOLJAČIĆ, T. Y. HOU, AND M. TEGMARK, *Kan: Kolmogorov-arnold networks*, arXiv preprint arXiv:2404.19756, (2024).

[149] S. LO, *Finite element mesh generation and adaptive meshing*, Progress in Structural Engineering and Materials, 4 (2002), pp. 381–399.

[150] P. LOUIS, E. VAN LAERE, AND B. BAESENS, *Understanding and predicting bank rating transitions using optimal survival analysis models*, Economics Letters, 119 (2013), pp. 280–283.

[151] F. LU, L. QI, X. JIANG, G. LIU, Y. LIU, B. CHEN, Y. PANG, AND X. HU, *Nnw-gridstar: interactive structured mesh generation software for aircrafts*, Advances in Engineering Software, 145 (2020), p. 102803.

[152] H. LUO, C. WANG, C. LI, X. MENG, X. YANG, AND Q. TAN, *Multi-scale carbon emission characterization and prediction based on land use and interpretable machine learning model: A case study of the yangtze river delta region, china*, Applied Energy, 360 (2024), p. 122819.

[153] Z. LV, N. WANG, R. LOU, Y. TIAN, AND M. GUIZANI, *Towards carbon neutrality: Prediction of wave energy based on improved gru in maritime transportation*, Applied Energy, 331 (2023), p. 120394.

[154] J. D. MACBETH AND L. J. MERVILLE, *An empirical examination of the black-scholes call option pricing model*, The journal of finance, 34 (1979), pp. 1173–1186.

[155] ——, *Tests of the black-scholes and cox call option valuation models*, The Journal of Finance, 35 (1980), pp. 285–301.

[156] J. MACLURE, *Ai, explainability and public reason: The argument from the limitations of the human mind*, Minds and Machines, 31 (2021), pp. 421–438.

[157] A. MAHI-AL-RASHID, F. HOSSAIN, A. ANWAR, AND S. AZAM, *False data injection attack detection in smart grid using energy consumption forecasting*, Energies, 15 (2022), p. 4877.

[158] A. MAO, M. MOHRI, AND Y. ZHONG, *Regression with multi-expert deferral*, arXiv preprint arXiv:2403.19494, (2024).

[159] S. MARKIDIS, *From complexity to simplicity: Brain-inspired modularization of pinn solvers*, arXiv preprint arXiv:2401.15661, (2024).

[160] O. R. MASERA, J. GARZA-CALIGARIS, M. KANNINEN, T. KARJALAINEN, J. LISKI, G. NABUURS, A. PUSSINEN, B. H. DE JONG, AND G. MOHREN, *Modeling carbon sequestration in afforestation, agroforestry and forest management projects: the co2fix v. 2 approach*, Ecological modelling, 164 (2003), pp. 177–199.

[161] V. MASSON-DELMOTTE, P. ZHAI, A. PIRANI, S. L. CONNORS, C. PÉAN, S. BERGER, N. CAUD, Y. CHEN, L. GOLDFARB, M. GOMIS, ET AL., *Climate change 2021: the physical science basis*, Contribution of working group I to the sixth assessment report of the intergovernmental panel on climate change, 2 (2021), p. 2391.

[162] J. MAYER, A. DUGAN, G. BACHNER, AND K. W. STEININGER, *Is carbon pricing regressive? insights from a recursive-dynamic cge analysis with heterogeneous households for austria*, Energy Economics, 104 (2021), p. 105661.

[163] G. H. MENDONÇA, F. G. FERREIRA, R. T. CARDOSO, AND F. V. MARTINS, *Multi-attribute decision making applied to financial portfolio optimization problem*, Expert Systems with Applications, 158 (2020), p. 113527.

[164] M. MERCADIER AND J.-P. LARDY, *Credit spread approximation and improvement using random forest regression*, European Journal of Operational Research, 277 (2019), pp. 351–365.

[165] J. M. MERIGÓ AND A. M. GIL-LAFUENTE, *The induced generalized owa operator*, Information Sciences, 179 (2009), pp. 729–741.

[166] R. C. MERTON, *Theory of rational option pricing*, The Bell Journal of economics and management science, (1973), pp. 141–183.

[167] M. E. MERZA, S. H. HUSSEIN, AND Q. I. ALI, *Identification scheme of false data injection attack based on deep learning algorithms for smart grids*, Indonesian Journal of Electrical Engineering and Computer Science, 30 (2023), pp. 219–228.

[168] K. MIAO, M. ZHANG, F. GUO, R. LU, AND X. GUAN, *Detection of false data injection attacks in smart grids: An optimal transport-based reliable self-training approach*, IEEE Transactions on Information Forensics and Security, (2024).

[169] S. H. MOHAMMED, M. S. J. SINGH, A. AL-JUMAILY, M. T. ISLAM, M. S. ISLAM, A. M. ALENEZI, AND M. S. SOLIMAN, *Dual-hybrid intrusion detection system to detect false data injection in smart grids*, PLoS One, 20 (2025), p. e0316536.

[170] M. M. MOUSAVI AND J. LIN, *The application of promethee multi-criteria decision aid in financial decision making: Case of distress prediction models evaluation*, Expert Systems with Applications, 159 (2020), p. 113438.

[171] A. S. MUSLEH, G. CHEN, AND Z. Y. DONG, *A survey on the detection algorithms for false data injection attacks in smart grids*, IEEE Transactions on Smart Grid, 11 (2019), pp. 2218–2234.

[172] A. J. MYLES, R. N. FEUDALE, Y. LIU, N. A. WOODY, AND S. D. BROWN, *An introduction to decision tree modeling*, Journal of Chemometrics: A Journal of the Chemometrics Society, 18 (2004), pp. 275–285.

[173] M. A. NABIAN, R. J. GLADSTONE, AND H. MEIDANI, *Efficient training of physics-informed neural networks via importance sampling*, Computer-Aided Civil and Infrastructure Engineering, 36 (2021), pp. 962–977.

[174] L. NEDOVIĆ AND V. DEVEDŽIĆ, *Expert systems in finance‚Äîa cross-section of the field*, Expert Systems with Applications, 23 (2002), pp. 49–66.

[175] M. A. NETO, A. AMARO, L. ROSEIRO, J. CIRNE, AND R. LEAL, *Engineering computation of structures: the finite element method*, Springer, 2015.

[176] Q. NGUYEN, I. DIAZ-RAINEY, AND D. KURUPPUARACHCHI, *Predicting corporate carbon footprints for climate finance risk analyses: a machine learning approach*, Energy Economics, 95 (2021), p. 105129.

[177] W. S. NOBLE, *What is a support vector machine?*, Nature biotechnology, 24 (2006), pp. 1565–1567.

[178] A. O'HAGAN, C. E. BUCK, A. DANESHKHAH, J. R. EISER, P. H. GARTHWAITE, D. J. JENKINSON, J. E. OAKLEY, AND T. RAKOW, *Uncertain judgements: eliciting experts' probabilities*, (2006).

[179] H. OZTURK, E. NAMLI, AND H. I. ERDAL, *Modelling sovereign credit ratings: The accuracy of models in a heterogeneous sample*, Economic Modelling, 54 (2016), pp. 469–478.

[180] S. E. PAGE, *Making the difference: Applying a logic of diversity*, Academy of Management Perspectives, 21 (2007), pp. 6–20.

[181] J. PAJUKOSKI, *Predicting credit rating change using machine learning and natural lan*, Nature Methods, 15, pp. 233–234.

[182] O. PEREZ, *Judicial strategies for reviewing conflicting expert evidence: Biases, heuristics, and higher-order evidence*, The American Journal of Comparative Law, 64 (2016), pp. 75–120.

[183] M. PERRELLA, S. GERBINO, AND R. CITARELLA, *Bem in biomechanics: Modeling advances and limitations*, in Numerical Methods and Advanced Simulation in Biomechanics and Biological Processes, Elsevier, 2018, pp. 145–167.

[184] K. PETRIDIS, I. TAMPAKOUDIS, G. DROGALAS, AND N. KIOSSES, *A support vector machine model for classification of efficiency: An application to m&a*, Research in International Business and Finance, 61 (2022), p. 101633.

[185] A. S. PFAFF, S. KERR, R. F. HUGHES, S. LIU, G. A. SANCHEZ-AZOFEIFA, D. SCHIMEL, J. TOSI, AND V. WATSON, *The kyoto protocol and payments for tropical forest:: An interdisciplinary method for estimating carbon-offset supply and increasing the feasibility of a carbon market under the cdm*, Ecological Economics, 35 (2000), pp. 203–221.

[186] A. POLAR AND M. POLUEKTOV, *A deep machine learning algorithm for construction of the kolmogorov–arnold representation*, Engineering Applications of Artificial Intelligence, 99 (2021), p. 104137.

[187] W. P. POON, M. FIRTH, AND H.-G. FUNG, *A multivariate analysis of the determinants of moody‚Äôs bank financial strength ratings*, Journal of International Financial Markets, Institutions and Money, 9 (1999), pp. 267–283.

[188] J. QIU, C. LI, L. WANG, H. TANG, H. LI, AND E. VAN RANST, *Modeling impacts of carbon sequestration on net greenhouse gas emissions from agricultural soils in china*, Global Biogeochemical Cycles, 23 (2009).

[189] J. QUINONERO-CANDELA AND C. E. RASMUSSEN, *A unifying view of sparse approximate gaussian process regression*, The Journal of Machine Learning Research, 6 (2005), pp. 1939–1959.

[190] M. RAISSI, P. PERDIKARIS, AND G. E. KARNIADAKIS, *Physics-informed neural networks: A deep learning framework for solving forward and inverse problems involving nonlinear partial differential equations*, Journal of Computational physics, 378 (2019), pp. 686–707.

[191] A. A. RAMABATHIRAN AND P. RAMACHANDRAN, *Spinn: sparse, physics-based, and partially interpretable neural networks for pdes*, Journal of Computational Physics, 445 (2021), p. 110600.

[192] C. RAMSTEIN, G. DOMINIONI, S. ETTEHAD, L. LAM, M. QUANT, J. ZHANG, L. MARK, S. NIEROP, T. BERG, P. LEUSCHNER, ET AL., *State and trends of carbon pricing 2019*, The World Bank, 2019.

[193] K. RANDHAWA, C. K. LOO, M. SEERA, C. P. LIM, AND A. K. NANDI, *Credit card fraud detection using adaboost and majority voting*, IEEE access, 6 (2018), pp. 14277–14284.

[194] C. RAO, M. LIU, M. GOH, AND J. WEN, *2-stage modified random forest model for credit risk assessment of p2p network lending to ‚Äúthree rurals‚Äù borrowers*, Applied Soft Computing, 95 (2020), p. 106570.

[195] C. RAO, H. SUN, AND Y. LIU, *Physics-informed deep learning for incompressible laminar flows*, Theoretical and Applied Mechanics Letters, 10 (2020), pp. 207–212.

[196] S. REBAI, M. N. AZAIEZ, AND D. SAIDANE, *A multi-attribute utility model for generating a sustainability index in the banking sector*, Journal of Cleaner Production, 113 (2016), pp. 835–849.

[197] I. RISH ET AL., *An empirical study of the naive bayes classifier*, in IJCAI 2001 workshop on empirical methods in artificial intelligence, vol. 3, 2001, pp. 41–46.

[198] C. T. ROBERTSON, *Biased advice*, Emory LJ, 60 (2010), p. 653.

[199] L. ROJAS-SUAREZ, *Rating banks in emerging markets: What credit rating agencies should learn from financial indicators*, in Ratings, rating agencies and the global financial system, Springer, 2002, pp. 177–201.

[200] J.-Á. ROMÁN-GALLEGO, M.-L. PÉREZ-DELGADO, M. L. VIÑUELA, AND M.-C. VEGA-HERNÁNDEZ, *Artificial intelligence web application firewall for advanced detection of web injection attacks*, Expert Systems, 42 (2025), p. e13505.

[201] P. K. ROY, *Enriching the green economy through sustainable investments: An esg-based credit rating model for green financing*, Journal of Cleaner Production, 420 (2023), p. 138315.

[202] C. RUDIN AND Y. SHAPOSHNIK, *Globally-consistent rule-based summary-explanations for machine learning models: application to credit-risk evaluation*, Journal of Machine Learning Research, 24 (2023), pp. 1–44.

[203] M. RYO, *Explainable artificial intelligence and interpretable machine learning for agricultural data analysis*, Artificial Intelligence in Agriculture, 6 (2022), pp. 257–265.

[204] M. SAITO AND S. YAMANAKA, *Performance evaluation of least-squares probabilistic classifier for corporate credit rating classification problem*, JSIAM Letters, 13 (2021), pp. 9–12.

[205] C. SANTOS, A. COELHO, AND A. MARQUES, *A systematic literature review on greenwashing and its relationship to stakeholders: state of art and future research agenda*, Management Review Quarterly, 74 (2024), pp. 1397–1421.

[206] D. D. S. SANTOS AND T. A. E. FERREIRA, *Neural network learning of black-scholes equation for option pricing*, arXiv preprint arXiv:2405.05780, (2024).

[207] F. SANTOSO AND A. FINN, *A data-driven cyber–physical system using deep-learning convolutional neural networks: Study on false-data injection attacks in an unmanned ground vehicle under fault-tolerant conditions*, IEEE Transactions on Systems, Man, and Cybernetics: Systems, 53 (2022), pp. 346–356.

[208] U. R. SAXENA AND T. ALAM, *Provisioning trust-oriented role-based access control for maintaining data integrity in cloud*, International Journal of System Assurance Engineering and Management, 14 (2023), pp. 2559–2578.

[209] ——, *Role-based access using partial homomorphic encryption for securing cloud data*, International Journal of System Assurance Engineering and Management, 14 (2023), pp. 950–966.

[210] J. SCHMIDT-HIEBER, *The kolmogorov–arnold representation theorem revisited*, Neural networks, 137 (2021), pp. 119–126.

[211] K.-M. SCHNEIDER, *A comparison of event models for naive bayes anti-spam e-mail filtering*, in 10th Conference of the European Chapter of the Association for Computational Linguistics, 2003.

[212] T. SCHNEIDER, Y. HU, X. GAO, J. DUMAS, D. ZORIN, AND D. PANOZZO, *A large-scale comparison of tetrahedral and hexahedral elements for solving elliptic pdes with the finite element method*, ACM Transactions on Graphics (TOG), 41 (2022), pp. 1–14.

[213] M. R. SEGAL, *Machine learning benchmarks and random forest regression*, (2004).

[214] Y.-H. SHAO, W.-J. CHEN, AND N.-Y. DENG, *Nonparallel hyperplane support vector machine for binary classification problems*, Information Sciences, 263 (2014), pp. 22–35.

[215] R. SHARMA AND V. SHANKAR, *Accelerated training of physics-informed neural networks (pinns) using meshless discretizations*, Advances in Neural Information Processing Systems, 35 (2022), pp. 1034–1046.

[216] S. J. SIDDIQI, B. TAHIR, M. A. JAN, AND M. TARIQ, *Multichain-assisted lightweight security for code mutated false data injection attacks in connected autonomous vehicles*, IEEE Transactions on Intelligent Transportation Systems, 25 (2024), pp. 11000–11010.

[217] D. SILVA, A. CERQUEIRA, AND E. BRANDÃO, *Does investors‚Äô divergence of opinion affect stock mispricing?*, ACRN Journal of Finance and Risk Perspectives, 10 (2021).

[218] J. SINGH, *The role of disciplinary, interdisciplinary, and transdisciplinary education in sustainability science: Experiences from my professional journey*, in Research Journeys to Net Zero, Routledge, 2024, pp. 23–34.

[219] Y. SINGH, M. ADIL, AND S. I. HAQUE, *Personality traits and behaviour biases: the moderating role of risk-tolerance*, Quality & Quantity, 57 (2023), pp. 3549–3573.

[220] N. SINGHAL AND H. GUPTA, *Carbon Credit Currency for the Future*, Springer, 2011.

[221] D. SLEEMAN, L. MOSS, A. AIKEN, M. HUGHES, J. KINSELLA, AND M. SIM, *Detecting and resolving inconsistencies between domain experts‚Äô different perspectives on (classification) tasks*, Artificial intelligence in medicine, 55 (2012), pp. 71–86.

[222] C. W. SMITH JR, *Option pricing: A review*, Journal of Financial Economics, 3 (1976), pp. 3–51.

[223] J. SONG AND D. WU, *Modeling forest carbon sink trading with carbon credit using stochastic differential game*, Environmental Science and Pollution Research, 30 (2023), pp. 68934–68950.

[224] M. SOUI, I. GASMI, S. SMITI, AND K. GHÉDIRA, *Rule-based credit risk assessment model using multi-objective evolutionary algorithms*, Expert systems with applications, 126 (2019), pp. 144–157.

[225] B. SPOORTHI, S. S. KUMAR, A. P. RODRIGUES, R. FERNANDES, AND N. BALAJI, *Comparative analysis of bank loan defaulter prediction using machine learning techniques*, in 2021 IEEE International Conference on Distributed Computing, VLSI, Electrical Circuits and Robotics (DISCOVER), IEEE, 2021, pp. 24–29.

[226] K. E. STANOVICH AND R. F. WEST, *On the relative independence of thinking biases and cognitive ability.*, Journal of personality and social psychology, 94 (2008), p. 672.

[227] N. STERN, J. STIGLITZ, AND C. TAYLOR, *The economics of immense risk, urgent action and radical change: towards new approaches to the economics of climate change*, Journal of Economic Methodology, 29 (2022), pp. 181–216.

[228] J. STOKLASOVÁ, T. TALÁŠEK, AND J. STOKLASA, *Attitude-based multi-expert evaluation of design*, in Intelligent Systems and Applications in Business and Finance, Springer, 2022, pp. 1–16.

[229] N. SUKUMAR AND A. SRIVASTAVA, *Exact imposition of boundary conditions with distance functions in physics-informed deep neural networks*, Computer Methods in Applied Mechanics and Engineering, 389 (2022), p. 114333.

[230] H. TAO, S. ZHUANG, R. XUE, W. CAO, J. TIAN, AND Y. SHAN, *Environmental finance: an interdisciplinary review*, Technological Forecasting and Social Change, 179 (2022), p. 121639.

[231] R. TAO, M. UMAR, A. NASEER, AND U. RAZI, *The dynamic effect of eco-innovation and environmental taxes on carbon neutrality target in emerging seven (e7) economies*, Journal of Environmental Management, 299 (2021), p. 113525.

[232] P. TEMBHEKAR, J. N. A. MALAIYAPPAN, AND L. SHANMUGAM, *Cross-domain applications of mlops: From healthcare to finance*, Journal of Knowledge Learning and Science Technology ISSN: 2959-6386 (online), 2 (2023), pp. 581–598.

[233] C.-F. TSAI AND M.-L. CHEN, *Credit rating by hybrid machine learning techniques*, Applied soft computing, 10 (2010), pp. 374–380.

[234] T. TSOKA, X. YE, Y. CHEN, D. GONG, AND X. XIA, *Explainable artificial intelligence for building energy performance certificate labelling classification*, Journal of Cleaner Production, 355 (2022), p. 131626.

[235] C. A. TU, E. RASOULINEZHAD, AND T. SARKER, *Investigating solutions for the development of a green bond market: Evidence from analytic hierarchy process*, Finance Research Letters, 34 (2020), p. 101457.

[236] D. B. UNSAL, T. S. USTUN, S. S. HUSSAIN, AND A. ONEN, *Enhancing cybersecurity in smart grids: False data injection and its mitigation*, Energies, 14 (2021), p. 2657.

[237] B. D. UPADHYAY, S. S. SONIGRA, AND S. D. DAXINI, *Numerical analysis perspective in structural shape optimization: A review post 2000*, Advances in Engineering Software, 155 (2021), p. 102992.

[238] O. S. VAIDYA AND S. KUMAR, *Analytic hierarchy process: An overview of applications*, European Journal of operational research, 169 (2006), pp. 1–29.

[239] J. VAISSALO, A. DUTTA, E. BOURI, AND N. AZOURY, *Carbon emission allowances and nordic electricity markets: Linkages and hedging analysis*, Energy Reports, 12 (2024), pp. 2845–2854.

[240] C. VENTURES, *2019 official annual cybercrime report*, in Recuperado el, 2019.

[241] R. VERMA, D. BARREJÓN, AND E. NALISNICK, *Learning to defer to multiple experts: Consistent surrogate losses, confidence calibration, and conformal ensembles*, in International Conference on Artificial Intelligence and Statistics, PMLR, 2023, pp. 11415–11434.

[242] A. VEZHNEVETS AND V. VEZHNEVETS, *Modest adaboost-teaching adaboost to generalize better*, in Graphicon, vol. 12, 2005, pp. 987–997.

[243] L. VIGNEAU AND C. A. ADAMS, *The failure of transparency as self-regulation*, Sustainability Accounting, Management and Policy Journal, 14 (2023), pp. 852–876.

[244] J. P. VILLARINO, Á. LEITAO, AND J. G. RODRÍGUEZ, *Boundary-safe pinns extension: Application to non-linear parabolic pdes in counterparty credit risk*, Journal of Computational and Applied Mathematics, 425 (2023), p. 115041.

[245] A. G. VITUSHKIN, *A proof of the existence of analytic functions of several variables not representable by linear superpositions of continuously differentiable functions of fewer variables*, in Dokl. Akad. Nauk SSSR, vol. 156, 1964, p. 3.

[246] Q. WAN, J. QIAN, A. BAGHIRLI, AND A. AGHAYEV, *Green finance and carbon reduction: implications for green recovery*, Economic Analysis and Policy, 76 (2022), pp. 901–913.

[247] N. WANDEL, M. WEINMANN, M. NEIDLIN, AND R. KLEIN, *Spline-pinn: Approaching pdes without data using fast, physics-informed hermite-spline cnns*, in Proceedings of the AAAI conference on artificial intelligence, vol. 36, 2022, pp. 8529–8538.

[248] M. WANG AND H. KU, *Utilizing historical data for corporate credit rating assessment*, Expert Systems with Applications, 165 (2021), p. 113925.

[249] Q. WANG, W. TAI, Y. TANG, AND M. NI, *Review of the false data injection attack against the cyber-physical power system*, IET Cyber-Physical Systems: Theory & Applications, 4 (2019), pp. 101–107.

[250] X. WANG, J. LI, AND J. LI, *A deep learning based numerical pde method for option pricing*, Computational economics, 62 (2023), pp. 149–164.

[251] Z. WANG, J. MA, X. WANG, J. HU, Z. QIN, AND K. REN, *Threats to training: A survey of poisoning attacks and defenses on machine learning systems*, ACM Computing Surveys, 55 (2022), pp. 1–36.

[252] J. WARTH, H. A. VON DER GRACHT, AND I.-L. DARKOW, *A dissent-based approach for multi-stakeholder scenario development,Äîthe future of electric drive vehicles*, Technological Forecasting and Social Change, 80 (2013), pp. 566–583.

[253] S. WATSON, *Multi-attribute utility theory for measuring safety*, European Journal of Operational Research, 10 (1982), pp. 77–81.

[254] L. WEI, C. HUANG, Z. WANG, Z. WANG, X. ZHOU, AND L. CAO, *Monitoring of urban black-odor water based on nemerow index and gradient boosting decision tree regression using uav-borne hyperspectral imagery*, Remote Sensing, 11 (2019), p. 2402.

[255] X. WEI, *A method of enterprise financial risk analysis and early warning based on decision tree model*, Security and Communication Networks, 2021 (2021).

[256] C. K. WILLIAMS AND C. E. RASMUSSEN, *Gaussian processes for machine learning*, vol. 2, MIT press Cambridge, MA, 2006.

[257] J. WOO, A. T. ASUTOSH, J. LI, W. D. RYOR, C. J. KIBERT, AND A. SHOJAEI, *Blockchain: a theoretical framework for better application of carbon credit acquisition to the building sector*, in Construction Research Congress 2020, American Society of Civil Engineers Reston, VA, 2020, pp. 885–894.

[258] J. WOO, R. FATIMA, C. J. KIBERT, R. E. NEWMAN, Y. TIAN, AND R. S. SRINIVASAN, *Applying blockchain technology for building energy performance measurement, reporting, and verification (mrv) and the carbon credit market: A review of the literature*, Building and Environment, 205 (2021), p. 108199.

[259] R. G. WOOD, *Carbon finance and pro-poor co-benefits: The Gold Standard and Climate, Community and Biodiversity Standards*, vol. 4, IIED, 2011.

[260] Y. WU, Q. WANG, N. GUO, Y. TIAN, F. LI, AND X. SU, *Efficient multi-source self-attention data fusion for fdia detection in smart grid*, Symmetry, 15 (2023), p. 1019.

[261] P. XIA, Z. NI, H. XIAO, X. ZHU, AND P. PENG, *A novel spatiotemporal prediction approach based on graph convolution neural networks and long short-term memory for money laundering fraud*, Arabian Journal for Science and Engineering, (2021), pp. 1–17.

[262] Y. XIA, C. LIU, Y. LI, AND N. LIU, *A boosted decision tree approach using bayesian hyper-parameter optimization for credit scoring*, Expert Systems with Applications, 78 (2017), pp. 225–241.

[263] B. XIE, H. CHANG, X. WANG, T. BIAN, S. ZHOU, D. WANG, Z. ZHANG, AND W. ZHU, *Revisiting adversarial attacks on graph neural networks for graph classification*, arXiv preprint arXiv:2208.06651, (2022).

[264] Y. XIE, Y. MA, AND Y. WANG, *Automatic boundary fitting framework of boundary dependent physics-informed neural network solving partial differential equation with complex boundary conditions*, Computer Methods in Applied Mechanics and Engineering, 414 (2023), p. 116139.

[265] Z. XIE AND Z. WU, *Distributed fault-tolerant secondary control for dc microgrids against false data injection attacks*, International Journal of Electrical Power & Energy Systems, 144 (2023), p. 108599.

[266] X. XIONG, S. HU, D. SUN, S. HAO, H. LI, AND G. LIN, *Detection of false data injection attack in power information physical system based on svm–gab algorithm*, Energy Reports, 8 (2022), pp. 1156–1164.

[267] B. XU, N. WANG, T. CHEN, AND M. LI, *Empirical evaluation of rectified activations in convolutional network*, arXiv preprint arXiv:1505.00853, (2015).

[268] C. XU, F. ZHENG, AND G. GUO, *Stealthy false data injection attacks in multi-channel vehicular communication: White-box and gray-box strategies*, IEEE Transactions on Vehicular Technology, (2025).

[269] H. XU, R. WANG, L. RAIZMAN, AND Z. RABINOVICH, *Transferable environment poisoning: Training-time attack on reinforcement learning*, in Proceedings of the 20th international conference on autonomous agents and multiagent systems, 2021, pp. 1398–1406.

[270] L. XU, Y. A. SOLANGI, AND R. WANG, *Evaluating and prioritizing the carbon credit financing risks and strategies for sustainable carbon markets in china*, Journal of Cleaner Production, 414 (2023), p. 137677.

[271] L. XU AND J. YANG, *Carbon pricing policies and renewable energy development: Analysis based on cross-country panel data*, Journal of Environmental Management, 366 (2024), p. 121784.

[272] Z. XU, *An overview of methods for determining owa weights*, International journal of intelligent systems, 20 (2005), pp. 843–865.

[273] Z. XU, K. ZHAO, J. WANG, AND M. BASHIR, *Physics-informed probabilistic deep network with interpretable mechanism for trustworthy mechanical fault diagnosis*, Advanced Engineering Informatics, 62 (2024), p. 102806.

[274] V. YADAV, G. P. MALANSON, E. BEKELE, AND C. LANT, *Modeling watershed-scale sequestration of soil organic carbon for carbon credit programs*, Applied Geography, 29 (2009), pp. 488–500.

[275] Y. YAN, *Integrate carbon dynamic models in analyzing carbon sequestration impact of forest biomass harvest*, Science of the Total Environment, 615 (2018), pp. 581–587.

[276] Z. YANG, T. T. H. NGUYEN, H. N. NGUYEN, T. T. N. NGUYEN, AND T. T. CAO, *Greenwashing behaviours: Causes, taxonomy and consequences based on a systematic literature review*, Journal of business economics and management, 21 (2020), pp. 1486–1507.

[277] S. YAO, X. YU, S. YAN, AND S. WEN, *Heterogeneous emission trading schemes and green innovation*, Energy Policy, 155 (2021), p. 112367.

[278] D. YE AND T.-Y. ZHANG, *Summation detector for false data-injection attack in cyber-physical systems*, IEEE transactions on cybernetics, 50 (2019), pp. 2338–2345.

[279] C. YING, T. CAI, S. LUO, S. ZHENG, G. KE, D. HE, Y. SHEN, AND T.-Y. LIU, *Do transformers really perform bad for graph representation?*, arXiv preprint arXiv:2106.05234, (2021).

[280] B. YU, C. LI, N. MIRZA, AND M. UMAR, *Forecasting credit ratings of decarbonized firms: Comparative assessment of machine learning models*, Technological Forecasting and Social Change, 174 (2022), p. 121255.

[281] R. YU, D. ZHANG, X. ZHANG, AND X. HUANG, *Machine learning for data verification in emissions trading system*, Resources, Conservation and Recycling, 199 (2023), p. 107239.

[282] L. YUAN, Y.-Q. NI, X.-Y. DENG, AND S. HAO, *A-pinn: Auxiliary physics informed neural networks for forward and inverse problems of nonlinear integro-differential equations*, Journal of Computational Physics, 462 (2022), p. 111260.

[283] S. YUN, M. JEONG, R. KIM, J. KANG, AND H. J. KIM, *Graph transformer networks*, Advances in Neural Information Processing Systems, 32 (2019), pp. 11983–11993.

[284] M. ZADSAR, A. ABAZARI, A. AMELI, J. YAN, AND M. GHAFOURI, *Prevention and detection of coordinated false data injection attacks on integrated power and gas systems*, IEEE Transactions on Power Systems, (2022).

[285] M. ZAYERNOURI, M. AINSWORTH, AND G. E. KARNIADAKIS, *A unified petrov–galerkin spectral method for fractional pdes*, Computer Methods in Applied Mechanics and Engineering, 283 (2015), pp. 1545–1569.

[286] J. ZHAN, K. ZHANG, AND W.-Z. WU, *An investigation on wu-leung multi-scale information systems and multi-expert group decision-making*, Expert Systems with Applications, 170 (2021), p. 114542.

[287] C. ZHANG AND B. LIN, *Assessing and interpreting carbon market efficiency based on an interpretable machine learning*, Process Safety and Environmental Protection, 179 (2023), pp. 822–834.

[288] Q.-S. ZHANG AND S.-C. ZHU, *Visual interpretability for deep learning: a survey*, Frontiers of Information Technology & Electronic Engineering, 19 (2018), pp. 27–39.

[289] S. ZHANG, X. LI, M. ZONG, X. ZHU, AND D. CHENG, *Learning k for knn classification*, ACM Transactions on Intelligent Systems and Technology (TIST), 8 (2017), pp. 1–19.

[290] S. ZHANG, X. LI, M. ZONG, X. ZHU, AND R. WANG, *Efficient knn classification with different numbers of nearest neighbors*, IEEE transactions on neural networks and learning systems, 29 (2017), pp. 1774–1785.

[291] Y. ZHANG AND M. UMAIR, *Examining the interconnectedness of green finance: an analysis of dynamic spillover effects among green bonds, renewable energy, and carbon markets*, Environmental Science and Pollution Research, 30 (2023), pp. 77605–77621.

[292] Y. ZHANG, R. WANG, P. HUANG, X. WANG, AND S. WANG, *Risk evaluation of large-scale seawater desalination projects based on an integrated fuzzy comprehensive evaluation and analytic hierarchy process method*, Desalination, 478 (2020), p. 114286.

[293] Z. ZHANG AND C. SUN, *Structural damage identification via physics-guided machine learning: a methodology integrating pattern recognition with finite element model updating*, Structural Health Monitoring, 20 (2021), pp. 1675–1688.

[294] S. ZHAO, L. A. TUAN, J. FU, J. WEN, AND W. LUO, *Exploring clean label backdoor attacks and defense in language models*, IEEE/ACM transactions on audio, speech, and language processing, 32 (2024), pp. 3014–3024.

[295] Y. ZHAO, *Research on personal credit evaluation of internet finance based on blockchain and decision tree algorithm*, EURASIP Journal on Wireless Communications and Networking, 2020 (2020), pp. 1–12.

[296] Z. ZHAO, Y. HUANG, Z. ZHEN, AND Y. LI, *Data-driven false data-injection attack design and detection in cyber-physical systems*, IEEE Transactions on Cybernetics, 51 (2020), pp. 6179–6187.

[297] J. ZHOU, *Analysis and countermeasures of green finance development under carbon peaking and carbon neutrality goals*, Open Journal of Social Sciences, 10 (2022), pp. 147–154.

[298] B. ZHU, S. YE, P. WANG, J. CHEVALLIER, AND Y.-M. WEI, *Forecasting carbon price using a multi-objective least squares support vector machine with mixture kernels*, Journal of Forecasting, 41 (2022), pp. 100–117.

[299] G. ZIRKLE, R. LAL, AND B. AUGUSTIN, *Modeling carbon sequestration in home lawns*, HortScience, 46 (2011), pp. 808–814.